Univerzita Karlova v Praze

1. lékařská fakulta

Study program: Doctoral program in biomedicine

Study field: Biology and pathology of the cell

MUDr. Jan Philipp Novotný

Evolučně zachovalé mechanismy regulace genové exprese jadernými receptory

Conserved mechanisms of gene expression regulation by nuclear receptors

PhD Thesis

Supervisor: MUDr. Zdeněk Kostrouch, CSc.

Praha, 2018

Prohlášení:

Prohlašuji, že jsem závěrečnou práci zpracoval samostatně a že jsem řádně uvedl a citoval všechny použité prameny a literaturu. Současně prohlašuji, že práce nebyla využita k získání jiného nebo stejného titulu

Souhlasím s trvalým uložením elektronické verze mé práce v databázi systému mezi-univerzitního projektu Theses.cz za účelem soustavné kontroly podobnosti kvalifikačních prací.

Praha, 14.02.2018

Jan Philipp NOVOTNÝ

Identifikační záznam:

NOVOTNÝ, Jan Philipp. Evolučně zachovalé mechanismy regulace genové exprese jadernými receptory (Conserved mechanisms of gene expression regulation by nuclear receptors). Praha, 2018. 100s. 2 příl. Disertační práce. Univerzita Karlova v Praze, 1. lékařská fakulta, BIOCEV. Vedoucí práce Zdeněk Kostrouch.

Acknowledgements

I would like to express my appreciation to everybody involved in this fascinating journey and especially to my supervisor Zdeněk Kostrouch for the opportunities and guidance I was given. I would like to thank the whole lab for the great time we spent together.

Table of Contents

Abbreviations

9-*cis*-RA	9-*cis* retinoic acid
AF-1/2	Activator function 1/2
AKT	RAC-alpha serine/threonine-protein kinase
AMP	Adenosine monophosphate
APC	Adenomatous polyposis coli
AR	Androgen receptor
AT-RA	All-*trans* retinoic acid
Ch	*Chlorella sp.*
CHAPS	3-[(3-Cholamidopropyl)dimethylammonio]-1-propanesulfonate hydrate
COUP-TF	Chicken ovalbumin upstream promoter-transcription factor
cWNT	canonical WNT pathway
DBD	DNA binding domain
ddPCR	Digital droplet PCR
DEC	Dorsal epithelial cells
ECM	Extracellular matrix
ER	Estrogen receptor
FLAG	Polypeptide protein tag
FOX	Forkhead box proteins
GFP	Green fluorescent protein
GSK3B	Glycogen synthase kinase 3b
GST	Glutathione-S-transferase
HNF4	Hepatocyte nuclear factor 4
IPTG	Isopropyl-β-D-thiogalactopyranosid

JAK/STAT	The Janus kinase/signal transducers and activators of transcription
LBD	Ligand binding domain
MC	Multicellular
MED	Mediator complex
ME	*T. adhaerens* closest putative homologue and likely orthologue of L-malate-NADPC oxidoreductase (EC1.1.1.40).
MR	Mineralocorticoid receptor
NRs	Nuclear receptors
PCR	Polymerase chain reaction
Po	*Porphyridium cruentum*
PPAR	Peroxisome proliferator-activated receptor
PR	Progesterone receptor
qRT-PCR	Quantitative reverse-transcription polmyerase chain reaction
Rh	*Rhodomonas salina*
RTKs	Receptor tyrosine kinases
RXR	Retinoic X receptor
SMART	Simple Modular Architecture Research Tool
SMRT	Nuclear Receptor Corepressor 2
TaRXR	*Trichoplax adhaerens* retinoid X receptor
TF	Transcription factor
TGF	Transforming growth factor
TR	Thyroid hormone receptor
UC	Unicellular
VDR	Vitamin D receptor

Abstract

With the first appearance of life on Earth, organisms had to adapt to an ever-changing surrounding environment in order to survive. Since the emergence of metazoan multicellularity, subsets of cells could adapt to perform specific biological tasks beneficial to the whole organism, necessitating not only spatiotemporal regulation of gene expression during development, but also integration of tissue specific needs with overall organismal status. Within the set of evolutionary conserved regulatory systems, the family of nuclear receptor (NR) transcription factors stands out due to its high degree of evolutionary conservation, plasticity and uniqueness to the metazoan kingdom, regulating gene expression in response to, or in the absence of a ligand by genomic and non-genomic actions. With an increasing number of different compounds being recognized as ligands to NRs, it is now thought that ancient NRs were probably characterized by low ligand binding specificity, eventually serving as environmental sensors, integrating nutrient availability and gene expression at the base of metazoan evolution. Characterization of the NR network in one of the simplest metazoan organisms, *Trichoplax adhaerens*, revealed not only a functional network and sub-specialization of NR dependent gene regulation, but also exceptional sensitivity to 9-*cis* retinoic acid. Viewed together, these results suggest that the family of NRs not only expanded and subspecialized during the course of evolution, but also took part in the formation of new regulatory layers eventually attenuating previously established ones.

Abstrakt

Od samého počátku života na planetě Zemi se organismy, k tomu, aby přežily, musely adaptovat měnícím se podmínkám prostředí. S výskytem metazoické mnohobuněčnosti se skupiny buněk mohly adaptovat k tomu, aby vykonávaly specifickou biologickou funkci, ze které těží celý organismus. To vyžadovalo nejen časoprostorovou regulaci exprese genů během vývoje, ale i integraci specifických požadavků tkání s celkovým stavem organismu. V rámci souboru vývojově zachovaných regulačních systémů vyčnívá rodina transkripčních faktorů jaderných receptorů (NR). Důvodem je její vysoký stupeň evoluční konzervace, plasticita a jedinečnost ve vztahu k živočišné říši a účast při regulaci exprese genů v odezvě na ligand, či jeho nepřítomnost, genomovými a negenomovými mechanismy. Se zvyšujícím se počtem molekul, které jsou považovány za ligandy těchto receptorů, se dnes předpokládá, že původní receptory byly pravděpodobně charakterizovány nízkou specifičností vazby ligandu a eventuálně sloužily jako environmentální senzory, které integrovaly dostupnost živin a expresi genů na samém začátku evoluce Metazoa. Charakteristika sítě NR v jednom z nejjednodušších metazoických organismů, *Trichoplax adhaerens*, odhalila nejen funkční síť a sub-specializaci genové regulace závisející na NR, ale i výjimečnou citlivost na 9-*cis* kyselinu retinovou. S ohledem na tyto poznatky výsledky naznačují, že rodina jaderných receptorů se nejenže během evoluce rozšířila a sub-specializovala, ale také se podílela na tvorbě nových regulačních vrstev, které v důsledku tlumí vrstvy, které se vyvinuly dříve.

Thesis statements, goals, hypotheses

In this dissertation, I want to provide evidence supporting the hypothesis that increasingly complex regulation of gene expression by NRs is, at least to some extent, achieved by formation of new regulatory layers that eventually override/attenuate regulatory functions of a preexisting NR network.

To test this hypothesis, the following goals were set:

- Characterize NRs in one of the simplest and basal metazoan species, *Trichoplax adhaerens*.
- Search and characterize NR-ligand response at the base of metazoan evolution.
- Provide evidence for specific gene regulation by NRs that, during the course of evolution, was taken over by a new regulatory layer.
- Search and characterize evidence for regulatory mechanisms integrating cellular and general organismal status with gene expression that are likely to evolve at the base of metazoan evolution.

Introduction

From eukaryotic unicellularity to multicellularity

Evolution of multicellular life on Earth started around 700-1000 million years ago (Ma) in the proterozoic eon (2500-542Ma) (Knoll et al., 2006) and cumulated in the appearance of the first metazoan organisms about 750-800Ma (Erwin, 2015). It was, however, not until the Cambrian explosion (580-500Ma) that a wide variety of animals (Metazoa) appeared on Earth, which was probably linked ecological changes, such as the increase in atmospheric oxygen levels that allowed for higher metabolic activity (Knoll, 1996, Knoll and Carroll, 1999). In contrast to the metazoan fossil record, paleontological data regarding the first eukaryotic cells are scarce with estimates placing their first appearance to a timeframe of about 1866-1679 million years ago (Parfrey et al., 2011). Comparative molecular studies, however, revealed an astonishing amount of genes coding for cellular system components probably of bacterial and/or archaeal origin (Koonin, 2010), suggesting that the last common eukaryotic ancestor was already in possession of a cellular organization and gene complement of key systems such as RNA polymerase subunits that can be traced to archaeal origins (Makarova et al., 2005, Cox et al., 2008, Yutin et al., 2008, Blombach et al., 2009). Evidence thus indicates that core components of transcriptional gene regulation were already present before the appearance of modern eukaryotic organisms and probably evolved as defense mechanism against parasitic nucleic acids capable of hijacking the hosts ribosomes in order to replicate (Madhani, 2013). One of these defenses, the Mediator complex (MED) (Kornberg, 2005, Madhani, 2013), is found in all eukaryotic kingdoms (Allen and Taatjes, 2015, Nagulapalli et al., 2016) and represents a key regulatory element for class II gene expression by interacting with RNA Polymerase II and DNA bound transcription factors

(Malik and Roeder, 2010, Yin and Wang, 2014, Poss et al., 2013, Kim and Lis, 2005). The Mediator complex is conserved across species (Bourbon, 2008) and increased complexity was probably built upon an ancient four-module complex (Bourbon, 2008), allowing for specific gene expression by distinct Mediator subunits (Linder et al., 2008, Holstege et al., 1998, van de Peppel et al., 2005, Uwamahoro et al., 2012). In accordance with that, overexpression of the allegedly metazoan specific MED28 (Harper and Taatjes, 2017) was shown to repress smooth muscle differentiation (Beyer et al., 2007) and leads to cellular proliferation in different human cell lines (Lu et al., 2005). Thus, the presence of a set of allegedly metazoan-specific subunits (e.g. MED23, MED25, MED26, MED28 and MED30) might indicate specialized MED functions restricted to metazoan organisms (Conaway and Conaway, 2011).

Indeed, metazoan multicellularity differs from other multicellular arrangements that can be observed in prokaryotes, such as aggregates or filaments found with different bacterial or archaeal species (Lyons and Kolter, 2015, Frols, 2013, Mayerhofer et al., 1992) and is characterized by higher complexity when compared to non-metazoan multicellular eukaryotes, such as volvocine algae.

Even though multicellularity was invented multiple times during the course of evolution (Bonner, 1998a, Bonner, 1998b), it is thought to have occurred only once for Metazoa hundreds of million years ago (Herron et al., 2009, Grosberg and Strathmann, 2007). One of oldest fossil records of a multicellular eukaryote known to date are filaments belonging to the bangiacean red algae *Bangiomorpha pubescens* within Hunting formation in arctic Canada that were dated back to about 1200Ma (Butterfield, 2000). Within the primordial ocean, multicellularity probably provided benefits like avoiding predation (Labarbera, 1988) or better homeostasis (Michod and Roze, 2001), thereby increasing the organisms fitness. True multicellularity with differentiated cells perform-

ing specific tasks beneficial to the whole organism, however, is not possible without the transition from cellular autonomy to cooperation, which requires, amongst other events, changes in gene regulation (Simpson, 2012, Kirk, 2005). Keeping in mind that ancestral organisms probably went through a mobile and reproductive state, multicellularity thus represents a tradeoff between mobility and reproduction (Michod and Roze, 2001), in which the specialization of cells into germ and soma is necessary to form a new individual from a complex of cells (Michod, 2007). This cooperation among cells, which results in division of labor and synergism, however, needs mediation to reduce the conflict between cells in order to export fitness from a lower to a higher level (Michod, 2007). Hence kinship and altruism is a prerequisite for true multicellularity (Szathmary and Smith, 1995, Ihara, 1999) and if cooperation fails, it leads to the death of the organism (Merlo et al., 2006). True multicellularity therefore represents a state in which cells decrease their individual fitness to increase the overall fitness of the organism by the so-called covariance effect (Michod, 2006, Michod, 2007). This, however, implies that once individual cells become fitness components of the organism they can't survive on their own (Michod, 2006) so that not only processes like asymmetric cell division or incomplete cytokinesis had to evolve (Kirk, 2005), but also regulatory networks that integrate overall organismal homeostasis, individual cell status and environmental cues. Failure to properly mediate conflict between cells leads to loss of altruism and, eventually, to regainment of a self-sustaining ability at the expense of the whole organism (Arnal et al., 2015). In animals, this process can be observed in case of cancer, which shares striking features with the evolution of species (Lowe et al., 2004) and probably represents a disease as ancient as multicellularity itself (Domazet-Loso and Tautz, 2010). As such, tumor-suppressive mechanisms were imperative for the emergence of true multicellularity (Lowe et al., 2004) by preventing rogue growth of individual cells

(Casas-Selves and Degregori, 2011). These mechanisms include various pathways leading to apoptosis (Hipfner and Cohen, 2004, Lowe et al., 2004), DNA repair (Hoeijmakers, 2009), as well as maintenance of DNA integrity by telomere capping (Sharpless and DePinho, 2004, Chan and Blackburn, 2004), a process that shows co-evolution with body mass (Gorbunova and Seluanov, 2009). In addition to these intrinsic surveillance mechanisms, a number of metazoan organisms evolved an adaptive immune system able to actively detect rogue cells (Robert, 2010).

Furthermore, the role of the microenvironment in tumor suppression is increasingly recognized (Bissell and Hines, 2011). With many regulatory mechanisms in place, cancer cells thus have to alter several key pathways for evasion and subsequent uncontrolled growth to happen.

With systems activated to mediate conflict between cells on one side and autonomous growth of cells on the other, there exists a tight link between cancer and evolution of metazoan multicellularity. Dissection of core regulatory pathways in basal metazoan species, which in phylogenetically recent organisms are probably obscured by additional regulatory layers, might therefore shed light on the interplay allowing for cancer growth and possible therapeutic targets.

As described above, the mediator complex represents a highly conserved core system integrating various biological signals, such as those transmitted by nuclear receptors and cellular status, with gene expression. Of the signaling pathways unique to and conserved across metazoan species, the regulation of cellular proliferation and differentiation by the NR-MED signaling axis is of particular importance, because it is a pathway without an extensive intermediary signaling cascade.

Increasing evidence suggests that the first nuclear receptors showed low ligand specificity and eventually also functioned as environmental sensors (thereby eventually convey-

ing a pro-proliferation signal), which later-on adapted to serve more specialized functions that are seen in vertebrates, for example (Holzer et al., 2017). This was probably enabled by several rounds of gene duplications, which allowed for emergence of new functions by mutations during the course of evolution (Baker, 2005) and finally the presence of an endocrine system in vertebrates in which nuclear receptors play a pivotal role in organismal homeostasis. The NR-MED axis can thus be thought of a system of mediators that together perform the task of integrating not only environmental cues to specific gene expression, but also tissue specific demands that allowed for more complex animal evolution by addition of several regulatory layers within increasingly complex animals.

Regulation of gene expression in the context of metazoan evolution

Altruistic features of individual cells within a metazoan organism require strict regulation at cellular, as well as organismal level. Since the Cambrian explosion, the body plans of animals range from as simple as that of *Trichoplax adhaerens*, with only six described cell types, to complex organisms in possession of specialized endocrine tissues. Despite the range of complexity, only seven signaling pathways are essential for metazoan development (TGF-ß, WNT, RTKs, NRs, Notch-Delta pathway, Hedgehog and JAK/STAT pathway) (Pires-daSilva and Sommer, 2003, Gerhart, 1999), of which three evolved in the stem metazoan (Babonis and Martindale, 2017). They are highly conserved, transmit extracellular signaling into regulation of gene expression and may represent the ancient mechanism that permitted altruism by allowing differentiation of cells (Babonis and Martindale, 2017).

Receptor Tyrosine Kinase (RTK) signaling

RTKs are membrane bound receptors with an extracellular ligand binding site, a transmembrane helix and a cytosolic protein tyrosine kinase domain. Briefly, upon binding of a membrane-bound or soluble peptide or protein hormone, its extracellular domain changes confirmation, promoting dimerization of the extracellular domains, thereby causing approximation of their transmembrane and cytosolic domains and cross-phosphorylation, leading to activation of certain signal transduction pathways. The importance of proper conformation is highlighted in case of the insulin receptor, which can form disulfide-linked dimers in the absence of a ligand, but activation of the kinase domain is eventually achieved upon ligand binding. They are involved in numerous processes such as differentiation or cell-cell communication (Schlessinger, 2000) and overexpression is implicated with cancer (e.g. HER2 in breast cancer).

While not found in prokaryotic organisms and previously being thought to be metazoan specific, RTKs are now known to have appeared before the split of multicellular and unicellular eukaryotes (Manning et al., 2008, Miller, 2012), sharing a significant amount of features, such as autophosphorylation (Schultheiss et al., 2013).

JAK/STAT signaling

The Janus kinase-signal transducer and activator of transcription (JAK/STAT) pathway is activated upon binding of a ligand to a cytokine receptor, which results in conformational changes, dimerization and activation of the associated intracellular Janus kinases (JAKs). This leads to phosphorylation of signaling proteins that dimerize and translocate to the nucleus. In contrast to RTKs, this pathway involves receptors and kinases

encoded by different genes. The exact appearence of the JAK/STAT pathway in the course of evolution is, however, still debated (King et al., 2008).

Hedgehog signaling

Initially identified in *Drosophila melanogaster* (Nusslein-Volhard and Wieschaus, 1980), the hedgehog pathway is a key regulator in many processes, including cellular differentiation and tissue differentiation. In animals, the hedgehog protein is composed of a signaling domain at its N-terminal (Hedge) and a C-terminal domain responsible for autocatalytic protein cleavage (Hog). Even though a Hog-domain has been identified in choanoflagellates, the association with a Hedge domain represents a metazoan innovation (Ingham et al., 2011), whilst the identification of other components (such as a Hedge domain or dispatched and patched genes) in the choanoflagellate *Monosiga ovata* indicates that components of the Hedgehog pathway were already present in the last common ancestor of animals and choanoflaggelates (King et al., 2008).

Notch/Delta signaling

Orthologues of the Notch type I transmembrane receptor have been found in all Parahoxoans [Placozoa (Srivastava et al., 2008), Porifera (Riesgo et al., 2014), Ctenophora (Ryan et al., 2013), Cnidaria (Technau et al., 2005) and Bilateria (Gazave et al., 2009)] and the paracrine Notch signaling pathway represents a major system in controlling gene expression with regard to cellular identity, differentiation and apoptosis (Greenwald, 1998, Artavanis-Tsakonas et al., 1999, Mumm and Kopan, 2000, Baron, 2003, Kadesch, 2000, Kadesch, 2004). The mechanism of action includes binding of the transmembrane ligand Delta to Notch and subsequent proteolytic cleavage of the intra-

cellular Notch domain by a set of proteases, which then enables translocation of the Notch intracellular domain into the nucleus to affect transcription of target genes (Oswald et al., 2001). Due to the nature of a membrane-bound ligand, signaling is initiated by direct cell-cell contact thus behaving as a juxtacrine signaling system allowing for promotion of cell identity of adjacent cells. While all components of the Notch pathway are found in most Bilaterians and most in basal metazoans such as *Trichoplax adhaerens* or *Amphimedon queenslandica*, the absence of some components (*SMRT, Furin, Numb and Neuralized*) suggests evolutionary adaptions of this pathway in bilaterian species (Gazave et al., 2009). Furthermore, even though only metazoans possess a fully functional Notch signaling cascade, many of the components could be traced to other, unicellular, eukaryotic species (Gazave et al., 2009).

Transforming growth factor ß (TGF-ß) pathway

TGF-ß signaling is one of the fundamental signal transduction pathways found only within the animal kingdom and seems to be associated with the appearance early metazoan species, probably to allow for control of multicellular life (Huminiecki et al., 2009). As such, it has important regulatory functions in development, stem cell control, organogenesis, immunity, as well as in the context of disease (Massague and Gomis, 2006, Heldin et al., 1997, Dijke and Heldin, 2007). Orthologues can be found only across metazoan species, including *Trichoplax adhaerens*, (King et al., 2008, Suga et al., 2013), suggesting that the TGF-ß cytokine pathway is a metazoan innovation (Huminiecki et al., 2009).

By binding to and approximating type I and type II receptor serine/threonine kinases on the cell membrane, signaling is initiated through a TGF-ß ligand. The proximity of the

kinases then allows for phosphorylation of the type I receptor kinase by the type II receptor kinase. Phosphorylation of the type I receptor kinase subsequently results in signal transduction through a complement of eight different SMAD proteins representing three functional classes (receptor regulated SMAD, co-mediator SMAD and inhibitory SMAD). Activation of the SMAD proteins by phosphorylation subsequently leads to translocation of activated multiunit SMAD complexes (Massague and Wotton, 2000) into the cell nucleus and leads to activation or repression of transcription (Shi and Massague, 2003). While the full complement of the TGF-ß cascade is only found in metazoan species, the lack of pathway antagonists and intracellular cofactors in basal metazoans, such as ctenophores and sponges, indicates TGF-ß pathway modulation to have appeared during the course of evolution, adopting new functions in addition to the presumed integration of maternally derived signaling molecules for axis specification (Babonis and Martindale, 2017). The presence of tissue specific regulation of gene expression of the same gene by TGF-ß, such as the transcriptional repression of inhibitor of differentiation 1 (*ID1*) in mammary epithelial cells (Kang et al., 2003) and induction of the same gene in metastatic breast cancer cells (Padua et al., 2008), as well as stimulation or inhibition of cellular proliferation within a wound depending on cell differentiation (Ashcroft et al., 1999), highlights the contextual dependency of TGF-ß action. SMAD complexes can recognize CAGAC DNA sequences, but with an affinity that is probably too low for unassisted binding under physiological conditions (Shi et al., 1998). Binding of activated SMAD complexes to their target DNA sequence is therefore probably assisted by cofactors with the ability to bind to R-SMAD and a specific DNA sequence simultaneously (Massague and Wotton, 2000). It is by these cell type and cellular context specific cofactors that the biological inputs to TGF-ß pathway are translated into a variety and sometimes opposite responses (Massague and Wotton, 2000).

WNT signaling pathway

By regulating embryogenesis and cellular differentiation in different animals, the WNT pathway is responsible for primary (dorso-ventral) axis determination in several metazoan species (Petersen and Reddien, 2009, Holstein, 2012). Even though components of the WNT pathway were identified in several protozoans (Holstein, 2012), no unicellular organism analyzed to date was shown to encode for the full WNT signaling pathway. In addition to its role in axis determination, the original function of the WNT pathway was probably in defining the site of primitive streak formation (Arkell et al., 2013, Babonis and Martindale, 2017).

Briefly, pathway activation occurs after binding of a WNT ligand to the cysteine rich domain (CRD) of Frizzled receptors (Fzd) (Rao and Kuhl, 2010) that, together with low-density lipoprotein-related receptors, form a ternary complex (Tamai et al., 2000, Wehrli et al., 2000, Pinson et al., 2000). This in turn activates the ß-catenin/T cell factor signaling pathway, which is enabled by inactivation of the destruction complex compromised of Axin, glycogen synthase kinase 3b (GSK3B), Adenomatosis polyposis coli (APC) and Casein kinase I (CK1) that normally targets ß-catenin for proteosomal degradation by phosphorylation and sequestration of ß-catenin (van Amerongen and Nusse, 2009). Despite the division of downstream pathways into canonical and non-canonical, cellular responses after activation of the WNT signaling cascade are largely context and cell type specific (van Amerongen and Nusse, 2009). In the evolutionary context the presence of Wnt genes in basal metazoans and the importance of the pathway shows its essentiality for proper metazoan development (van Amerongen and Nusse, 2009). The presence of a full Wnt complement in Cnidaria, which possess blastoporal signaling center similar to that of deuterostomes and protostomes (Holstein, 2012), indicates evolutionary adapations of this pathway.

Nuclear receptors

The third signaling pathway unique to metazoans (with TGF-ß and WNT being the other two) is executed by nuclear receptors. NRs are highly conserved transcription factors sharing a common Bauplan (Pawlak et al., 2012) and are, in contrast to the other signaling pathways discussed, capable of directly translating ligand binding into regulation of gene expression. As such they provide a direct link between stimulus and biological response without the need for an extensive signaling cascade, which eases evolution (Babonis and Martindale, 2017), a hypothesis that is supported by the huge expansion of NRs in nematodes (Taubert et al., 2011). Even though fragments of NR domains have been found in prokaryotic organisms, evidence suggests that full sized NRs are a metazoan innovation. In accordance with that, genome sequence analysis of the presumably closest relative to the metazoan kingdom, Choanoflaggelates, did not reveal any genes coding for NRs (King et al., 2008). Despite the high sequence similarity of NRs across metazoan species, NRs show a considerable heterogeneity with regards to their number and function, with only four NRs present in the basal metazoan *Trichoplax adhaerens* to over 280 NRs found in *Caenorhabditis elegans* (Kostrouchova and Kostrouch, 2015). The evolutionary implication of such relatively simple and plastic signal transduction system is exemplified by the independent invention of transcription factors that are surprisingly similar to metazoan NRs in fungi (Shalchian-Tabrizi et al., 2008) and probably evolved for regulation of metabolism and as response to xenobiotics (Naar and Thakur, 2009, Thakur et al., 2008). Indeed, as more data are emerging regarding NR ligands, such as the rather promiscuous binding of PPARs to a variety of compounds (Issemann and Green, 1990), the historical view of specific high affinity ligand binding by NRs is challenged in the evolutionary context. The current concept therefore implies a soft key-lock model in which ancestral NRs were characterized by

low ligand affinity and specificity (Holzer et al., 2017) and later-on acquired high-affinity binding to a certain set of ligands as regulators in different species (Escriva et al., 2000, Markov and Laudet, 2011). Furthermore, the increasing number of non-hormonal substances recognized as NR ligands (Holzer et al., 2017), points towards a metabolic or environmental origin of NR ligands. Adoption of new and more specialized functions was then granted to the NR-ligand couple during the course of evolution. Thus, it is not surprising to see binding of different ligands to an orthologous NR exerting similar biological effect as it is the case for Triac and T_3 in the cephalochordate amphioxus and vertebrates, respectively (Paris et al., 2008).

Since the introduction of a unified system of NR nomenclature in 1999, the NR superfamily is divided into 7 subfamilies (Nuclear Receptors Nomenclature, 1999) and is based upon sequence homology (Laudet, 1997) of the evolutionary conserved DBDs, as well as LBDs that are consistent with the evolutionary scheme based upon a large number of sequenced genomes (King-Jones and Thummel, 2005, Reitzel and Tarrant, 2009, Srivastava et al., 2008, Bridgham et al., 2010) and is depicted in Table 1. Of these seven subfamilies, six can already be found before the split of Protostomia and Deuterostomia (Escriva et al., 1997, Escriva et al., 2002). In basal metazoan species the NR complement ranges from two in *Amphimedon queenslandica (Bridgham et al., 2010)*, to four in *Trichoplax adhaerens* and 17 in *Nematostella vectensis* (Reitzel and Tarrant, 2009) mostly related to the NR2 subfamily, indicating that the ancestral NR probably was probably most closely related to the NR2 subfamily of nuclear receptors (Holzer et al., 2017). The differences of the NR complement in various species, however, can only be explained partially by whole genome duplications that happened twice in vertebrates (Escriva et al., 2002), rather it seems to reflect the NR regulatory and evolutionary po-

tential (Kostrouchova and Kostrouch, 2015) leading to multiplied NRs within subfamilies and probably sub-specialization of function.

Nuclear receptor subfamily	**Nuclear receptor group**	**Nomenclative name**	**Common name**	***T. adhaerens***	***N. vectensis***	***A. queenslandica***
NR1	1A Thyroid hormone receptors	NR1A1	TRA			
		NR1A2	TRB			
	1B Retinoic acid receptors	NR1B1	RARA			
		NR1B2	RARB			
		NR1B3	RARG			
	1C Peroxisome prolferator activated receptors	NR1C1	PPARA			
		NR1C2	PPARD			
		NR1C3	PPARG			
	1D Rev-Erb receptors	NR1D1	Rev-Erb-alpha			
		NR1D2	Rev-Erb-beta			
	1F RAR related orphan receptors	NR1F1	RORA			
		NR1F2	RORB			
		NR1F3	RORG			
	1H Liver X receptor-like receptors	NR1H1	LXRB			
		NR1H2	LXRA			
		NR1H3	FXRA			
		NR1H5	FXRB			
	1I Vitamin D recep-	NR1I1	VDR			
		NR1I2	PXR			

	tor-like receptors	NR1I3	CAR			
NR2	2A Hepatocyte nuclear factor 4 receptors	NR2A1	HNF4A			
		NR2A2	HNF4G			
	2B Retinoid X receptors	NR2B1	RXRA		*	
		NR2B2	RXRB			
		NR2B3	RXRG			
	2C Testicular receptors	NR2C1	TR2			
		NR2C2	TR4			
	2E Tailless-like receptors	NR2E1	TLX			
		NR2E2	PNR			
	2F COUP-TF like receptors	NR2F1	COUP-TF1			
		NR2F2	COUP-TF2			
		NR2F3	EAR-2			
NR3	3A Estrogen receptors	NR3A1	ESR1			
		NR3A2	ESR2			
	3B Estrogen related receptors	NR3B1	ESRRA			
		NR3B2	ESRRB			
		NR3B3	ESRRG			
	3C 3-Ketosteroid receptors	NR3C1	GR			
		NR3C2	MR			
		NR3C3	PR			
		NR3C4	AR			
NR4	4A Nerve growth factor IB like-receptors	NR4A1	NGFIB			
		NR4A2	NURR1			
		NR4A3	NOR1			

NR5	5A Fushi tarazu F1-like receptors	NR5A1	SF1			
		NR5A2	LRH-1			
NR6	6A GCNF receptors	NR6A1	GCNF			
NR0	0B DAX-like receptors	NR0B1	DAX1			
		NR0B2	SHP			

Table 1: Classification of NRs according to the current classification system. The NR complement of three basal metazoan species - Placozoa (*T. adhaerens*), Cnidaria (*Nematostella vectensis*) and Porifera (*Amphimedon queenslandica*) - is indicated by black color. * Probable secondary loss of RXR in *N. vectensis*. Table modified and expanded according to (Germain et al., 2006, Reitzel and Tarrant, 2009, Bridgham et al., 2010, Srivastava et al., 2008).

Another classification system takes into account the dimerization capabilities of NRs and DNA binding capabilities, dividing the superfamily into four classes (Mangelsdorf et al., 1995). In this classification system, Class I receptors are recognized by their ability to bind as homodimers to inverted DNA repeats, while Class II receptors heterodimerize with retinoic acid receptor (RXR), binding to direct repeats (with exceptions). Class III and IV receptors bind as homodimers to direct repeats and extended core sites as monomers, respectively (Mangelsdorf et al., 1995).

Examples of Class I receptors include the glucocorticoid receptors (GRs), estrogen receptors (ERs), progesterone receptors (PRs), mineralocorticoid receptors (MRs) and androgen receptors (ARs), which, when unliganded, are complexed to chaperones (e.g. Hsp70) in the cytosol and dissociate into the nucleus to affect gene expression after lig-

and-induced allosteric change has occurred (Beato and Klug, 2000). NR action is then executed depending on the set of associated proteins (Hermanson et al., 2002, Kraus and Wong, 2002), such as co-activators (Cosma, 2002) and co-repressors (Privalsky, 2004), as well as chromatin structure by managing access of the transcriptional machinery to specific gene sequences (Khorasanizadeh, 2004).

In contrast to Class I receptors, Class II receptors not only bind as RXR heterodimers, but are also located within the nucleus complexed with co-repressors in their cognate state, repressing transcription. After ligand binding induced conformational change, histone acetylase complexes are recruited, reversing the repressive effects and assembly of the preinitiation complex is started by binding to the Mediator complex (Chen and Roeder, 2011). Repression is maintained by NCoR and SMRT co-repressor complexes (Chen and Evans, 1995, Horlein et al., 1995) associated with histone deacetylases (Watson et al., 2012). Cell-autonomous feedback with several NRs in Class II is observed, because they bind ligands produced in the same cell (Sever and Glass, 2013). This class of receptors includes e.g. retinoic X receptor (RXR), thyroid hormone receptor (TR) and vitamin D receptor (VDR).

Class III NRs function similarily as Class I NRs, with homodimers binding commonly to direct repeats (e.g. HNF4, COUP-TF, RXR) (Rastinejad et al., 2015a). Class IV NRs compromise a group of NR monomers binding to single DNA half-sites (e.g. ROR, NURR family) (Rastinejad et al., 2015a, Mangelsdorf et al., 1995)

Nuclear receptor structure

NR overall structure can be divided into a N-terminal regulatory (A/B) domain, containing the activation function 1 (AF-1), a DNA binding domain (DBD or C domain) containing a repeat of the C_4 zinc-finger motif, a hinge region (D domain), followed by a

ligand binding domain (LBD) containing the AF-2 domain (E domain) and a C-terminal domain (or F domain) (**Figure 1**) (Bain et al., 2007, Rastinejad et al., 2015a). NRs represent dynamic structures in which binding to e.g. the DBD or LBD leads to allosteric changes and transmission of information across the NR (Rastinejad et al., 2015a).

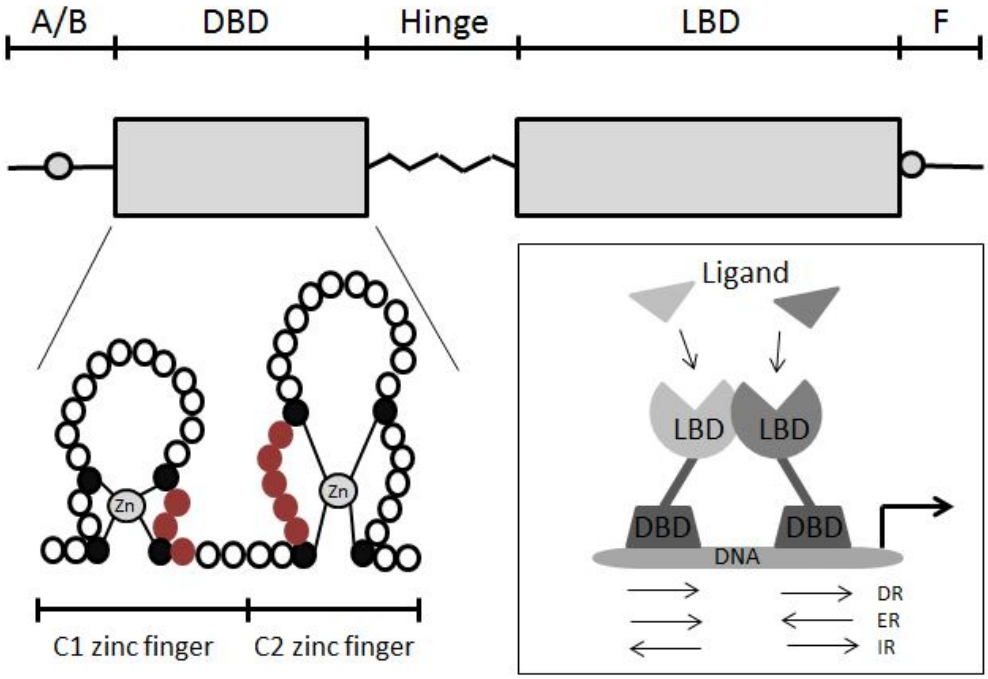

Figure 1: Schematic representation of NR structure. AF-1 and AF-2 are delineated by circles at the N-terminal and C-terminal, respectively. The zinc finger motif structure of the DBD is depicted in the lower left corner. Black circles represent cysteine residues associated with zinc atoms. P-box and D-box residues are highlighted in red within the C1 and C2 zinc finger, respectively. The lower right corner shows a NR dimer bound to DNA. Arrows depict the orientation of response elements as direct repeat (DR), everted repeat (ER) and inverted repeat (IR). The picture was adapted from (Pawlak et al., 2012, Tsai and O'Malley, 1994, Jonker et al., 2009, Vogeler et al., 2014).

The N-terminal domain (A/B)

The A/B domain is highly mobile and its sequence very variable in between NRs. It contains the activation function-1 (AF-1), which is a target of post-translational modifications that confer tissue specific properties to NR signaling (van der Steen et al., 2013, Becares et al., 2017, Berrabah et al., 2011).

The DNA binding domain (C)

The DBD of the glucocorticoid receptor is among the most studied and representative of DBD structure across the NR superfamily. Its structure is composed of two nonequivalent zinc finger domains, as well as two alpha helixes (**Figure 1**). Of these, the N-terminal helix (helix 1) makes contact with the major groove of the DNA within the response element (the critical residues required for binding make up the P-box), while the second helix (helix 2) at the C-terminal is involved in structure stabilization and is oriented in a perpendicular fashion towards helix 1. After binding to its response element, interactions of the P-box with the DNA half-site lead to a conformational change of the dimerization interface called D-box, which is located within the C-terminal zinc finger and represents the residues required for dimerization after allosteric structural changes upon binding to the response element. While the general structure of class I and class II NRs is similar, heterodimerization with RXR seems to be dependent upon helical unfolding within the C-terminal extension of the DBD, with two helices called T- and A-box playing important roles in the process of heterodimerization of the thyroid receptor (Bain et al., 2007) and DNA binding (Rastinejad et al., 2000, Zhao et al., 2000).

The NR response elements are, in the majority of cases, composed of two hexameric sequences that are oriented as direct, inverted or everted repeats and separated by a spacer of variable length (**Figure 1**) (Helsen and Claessens, 2014). They are mostly found in enhancer regions far away from the transcriptional start site (Carroll et al., 2006). The DBD determines the recognition of a receptor to a certain response element, while the hinge region (also known as the DBD C-terminal extension) plays a crucial role in allosterically allowing the correct positioning of the receptors (Pawlak et al., 2012).

The hinge region (D)

The hinge region is evolutionary far less conserved than DBD or LBD, but plays an important role by providing flexibility to the NR, specifying the relative orientation of the DBD and LBD (Pawlak et al., 2012). It contains sites for post-translational modifications such as phosphorylation, methylation, acetylation and sumoylation (Clinckemalie et al., 2012, Anbalagan et al., 2012).

The ligand binding domain (E)

The LBD is found only within the superfamily of NRs (Moras et al., 2015). It contains the activation function 2 (AF-2), which is responsible for ligand independent recruitment of transcriptional activators (Huang et al., 2010), and is composed of about 12 alpha helices (Wurtz et al., 1996) that form a hydrophobic pocket that is shaped by residues of helices 3,7, and 10 (Nagy and Schwabe, 2004, Li et al., 2003, Wurtz et al., 1996). The mode of ligand activation is still discussed (Rastinejad et al., 2015b, Moras et al., 2015) and two models of action are proposed. The first model of activation supports a ‘mousetrap mechanism’ in which helix-12 entraps the ligand after binding the

LBD pocket (Renaud et al., 1995) and binding of an antagonist leads to a different repositioning of helix-12, which can result in binding of co-repressors (Heldring et al., 2007). In contrast to that, the helix-12 dynamic stabilization model proposes an unstructured and highly mobile helix-12 in the apo-state (unliganded state), which transits into a stable helical formation upon ligand binding (Kallenberger et al., 2003). Besides the ongoing discussion regarding the exact mechanism of ligand activation, the activation function-2 contained within helix-12 plays an important role in co-activator binding via LXXLL sequences and co-repressor segments with LXXXLXXX[I/L] sequence (L =leucine, I= isoleucine, X= any amino acid), whose interaction is dependent upon ligand occupation (Darimont et al., 1998, Webb et al., 2000, Rastinejad et al., 2015a). While binding of NRs to their specific response element represents a key event, association of NRs with co-regulators is needed for specific execution of their regulatory function (Xu et al., 1999). These can be functionally divided into co-activators and co-repressors, of which more than 350 have been identified (Millard et al., 2013, Lonard and O'Malley, 2012). These co-regulator complexes lead to activation or repression of target genes by histone tail modifications (McKenna et al., 1999) or local chromatin remodeling (Glass et al., 1997) and possess enzymatic activity (Wolf et al., 2008). In case of co-activators gene expression is enhanced (Onate et al., 1995). While the size of the LBD pocket varies considerably (Huang et al., 2010) with some NRs also functioning as metabolic sensors recognizing diverse ligands such as phospholipids, heme and different metabolites (Chawla et al., 2001, Ingraham and Redinbo, 2005, Itoh et al., 2008, Raghuram et al., 2007, Yin et al., 2007, Pardee et al., 2009) and ERR binding different types of ligands (Brzozowski et al., 1997, Shiau et al., 1998), the absence of a ligand binding pocket in human monomeric Nurr1 (Ingraham and Redinbo, 2005) and an impeded LXXLL binding of co-factors as a result (Wang et al., 2003) represents an

exception. Despite the different kinds of NR ligands they all share a lipophilic nature, which allows them to diffuse through cells and bind to the hydrophobic LBD pocket (Huang et al., 2010), thereby circumventing the need of cell surface receptors (Sever and Glass, 2013).

C-terminal domain (F)

The F domain shows large variability in sequence and is poorly defined. Functional studies showed that it is dispensable for ligand binding and transcriptional activity. It seems, however, to be involved in interaction with co-factors (Kim et al., 2003) and modification of DNA binding affinity via post-translational modifications (Jiang and Hart, 1997).

Quarternary structure of NRs

Quarternary structures of NR dimers show a lot of domain-domain interactions, such as DBD-LBD communication (Helsen et al., 2012, Zhang et al., 2011, Hall et al., 2002, Meijsing et al., 2009), most of which is dependent upon DNA binding (except LBD-LBD interaction) and binding of the dimer complex to different response elements results in overall different quarternary structures, which have influence on recruitment of co-factors and further modifications (Rastinejad et al., 2015a), eventually leading to the recruitment of RNA polymerase II or other components of the transcription initiation complex (Acevedo and Kraus, 2004). Furthermore, in case of ER, ligand binding influences the DNA binding capability (Deegan et al., 2011, Margeat et al., 2003) and signals are reciprocally transmitted across the NR structure (Zhang et al., 2011)

Post-transcriptional modifications of NRs

Altered post-translational modifications of NRs have been linked to several human diseases and can be divided into two broad categories: reversible modifications (phosphorylation, acetylation, methylation) and modifications involving polypeptide linkage (sumoylation and ubiquitination) (Anbalagan et al., 2012), which can influence transcriptional activity (Choi et al., 2006, Sentis et al., 2005, Lin et al., 2003, Lin et al., 2001). As such, post-translational modifications provide another regulatory layer of NR function.

Major phosphorylation sites are located within the A/B region, but can also be found in the conserved DBD and LBD regions (Rochette-Egly et al., 1995) and affect, for example, ligand responsiveness of NRs (Delmotte et al., 1999) or influence NR localization (Sun et al., 2007). This regulatory potential results in several ligand-independent functions by post-translational modifications, which include NR activation (Mani, 2001, Weigel and Zhang, 1998, Berrabah et al., 2011) and degradation (Hashiguchi et al., 2016). Examples include phosphorylation (Lin et al., 2001), as well as acetylation (Fu et al., 2003) and sumoylation (Poukka et al., 2000, Bawa-Khalfe et al., 2007) of the androgen receptor (AR) in prostate cancer. Thus, post-translational modifications are increasingly recognized as the cause or result of pathological mechanisms underlying human diseases (Anbalagan et al., 2012). Furthermore, tissue specific regulatory effects are provided by modification of the AF-1 domain in the case of ligand dependent NRs, such as the mineralocorticoid receptor, in which a nuclear localization signal is coded that can be phosphorylated and thereby influences NR localization (Walther et al., 2005) and palmitoylation of the E domain promotes localization of steroid receptors (Class I) to the plasma membrane (Pedram et al., 2007).

Non-genomic actions of NRs

Nuclear receptors exert their action primarily by altering gene expression. It is, however, increasingly recognized that NRs do not function through their DNA binding capability only. This is in unison with the rapid effects of e.g. glucocorticoids that are incompatible with the genomic action of steroids due to latency (Wehling, 1997). Examples include cyclic AMP generation upon stimulation with estrogen in uterine epithelial cells (Szego and Davis, 1967), which suggested that estrogen induced activity might be exerted at the cell membrane, rather than the nucleus (Pietras and Szego, 1977) and has been subsequently shown to hold true for several NRs, such as AR, ER and PR or (truncated) TR, which can be found at the cell membrane (Levin and Hammes, 2016). Localization of NRs to the plasma membrane can therefore not only activate cytosolic signals, protein kinases or G-protein signaling, but also engage in regulation of gene transcription by the effects of membrane-initiated signaling targeting transcription factors, such as phosphorylation (Levin and Hammes, 2016). With this potentially broad range of effects, non-genomic actions of NRs are involved in a wide variety of cellular processes and play an important role not only in the physiological state, but also in diseases such as breast cancer, in which glucose uptake and subsequent glycolysis was shown to be enhanced through AKT by membrane bound ER signaling (O'Mahony et al., 2012).

Signaling through the mediator complex

Signaling by NRs converges at the mediator complex, a large, multi-subunit complex encompassing 25 to 30 subunits (yeast and human, respectively) (Bourbon, 2008) with an overall molecular weight of >1MDa (Thompson et al., 1993). It is tightly associated with the general transcriptional machinery by making contact with RNA polymerase II and interacting with transcription factors and is thus regarded a general transcription

factor (Takagi and Kornberg, 2006). As such, it is, together with TFIIA, TFIIB, TFIID, TFIIE, TFIIF, TFIIH and RNA polymerase II, part of the pre-initiation complex (Hahn, 2004, Thomas and Chiang, 2006), but is not required for transcription "*per se"* (Poss et al., 2013). The mediator complex can be structurally divided into 4 modules: Head, middle, tail, as well as kinase. Whether the core mediator complex is formed by the head, middle and tail modules (Ansari and Morse, 2013), held together by the mediator subunit Med14 (Tsai et al., 2014, Tsai et al., 2017, Robinson et al., 2015, Nozawa et al., 2017) or by the middle and head modules only, is a matter of debate. Studies show, however, that the tail module is not needed for recruitment of mediator to the pre-initiation complex (Jeronimo et al., 2016, Petrenko et al., 2016, Lacombe et al., 2013). Contact with RNA polymerase II is made via the head and middle modules, while sequence specific TFs associate with the tail (Jeronimo and Robert, 2017). Consistent with that, deletion of tail subunits did not affect viability, but resulted in changed expression of a specific subset of genes (Ansari et al., 2012). Furthermore, it has been shown that the mediator complex can exist as "heterogeneous subcomplexes" (Weber and Garabedian, 2017) lacking certain subunits (Cevher et al., 2014, Baidoobonso et al., 2007, Zhang et al., 2005) and it is thought that Mediator is capable of altering its subunit composition, eventually promoting malignancy through changes in gene expression (Weber and Garabedian, 2017).

Other functions apart from transcription initiation include elongation (Conaway and Conaway, 2013), chromatin looping (Park et al., 2005) and histone modification (Meyer et al., 2008), evidencing the wide and complex regulatory potential of the mediator complex, of which much is yet to be understood. The possibility of post-translational modifications of mediator subunits resulting in alteration of their activity (Nagalingam

et al., 2012) adds an additional layer of regulation of gene expression at the level of the mediator complex as the endpoint of signaling cascades (Jiang et al., 1998).

Keeping in mind the evolutionary conservation of this multi-protein complex in eukaryotes, it seems not surprising that it is involved in regulation of homeostatic systems, such as metabolic gene expression and that mediator subunits, such as MED25 are needed for proper signal transduction by (e.g. metabolic) nuclear receptors (e.g. HNF4) (Rana et al., 2011). Furthermore, a dual function of MED28 has been recognized recently. It functions as mediator complex subunit in the nucleus (Sato et al., 2004, Beyer et al., 2007) and interacts with the cytoskeleton in the cytoplasm (Wiederhold et al., 2004, Lu et al., 2006, Huang et al., 2012), thereby potentially being able to integrate cellular status with gene expression.

Cancer and multicellularity

True complex multicellularity requires altruistic behavior of single cells within an organism. Loss of such behavior leads to e.g. uncontrolled cellular proliferation within an animal, eventually causing death of the whole animal by destruction of its environment.

As such, cancer could be defined as the result of processes leading to deterioration of regulatory functions enabling altruistic behavior. As a result of failed mediation, cancer can be found in nearly all multicellular eukaryotes, ranging from animals to plants and fungi (even though in the latter two the occurrences are lower) (Miller and Torday, 2017, Madsen T, 2017). And, indeed, core signaling pathways required for multicellularity in metazoans (such as NRs or WNT) (Rokas, 2008) are frequently deregulated (Rubin and de Sauvage, 2006, Baek and Kim, 2014, Doan et al., 2017, Weinberg,

2007). Furthermore, cancer cells are autonomous, that is, they can survive if isolated, thereby representing an indispensable tool in cancer research.

It is a matter of rather vivid controversy what underlying mechanisms lead to the abortion of altruistic behavior. Several hypotheses have been proposed to explain this process, ranging from random, unpredictable mutations (Heng et al., 2010) to sequential gene mutations conferring an advantage by Darwinian selection (Vogelstein et al., 2013). Furthermore, an atavistic model has been proposed in the light of increasing analysis from an evolutionary biology point of view and will be discussed in the following due to its implications and thematic relation to the hypothesis proposed.

The atavistic model roots itself in evolutionary connections of eukaryotic unicellular and metazoan life. It is based on the presence of more-recently evolved regulatory mechanisms that suppress ancestral genetic traits (Davies and Lineweaver, 2011) or restrict them to specific contexts (Bussey et al., 2017), examples of which include the development of tails, webbed feet or supernumerary nipples in humans (Le Page, 2007). Metazoan cells thus possess a "toolkit for the survival, maintenance and propagation of non-differentiated or weakly-differentiated cells" (Davies and Lineweaver, 2011) needed by unicellular (UC) eukaryotic cells to survive. During the course of metazoan evolution this toolkit was then suppressed, where and when needed, by new layers of regulatory systems allowing for complex multicellularity (MC). Assuming this hypothesis is correct, higher expression of genes conserved in unicellular organisms should therefore be observed in cancer cells when compared to normal tissue. In line with this, a recent study by Trigos et al. (Trigos et al., 2017) showed that tumors not only preferentially express genes conserved in unicellular species, but that these genes are limited to specific cellular processes (e.g. cell death), while genes associated with multicellular processes (e.g. cell differentiation) are downregulated. Furthermore, the percentage of UC

genes in transcriptomes was shown to increase with progression to higher cancer grades (Trigos et al., 2017) (**Figure 2)** and drug resistance to be associated with up-regulation of UC genes rather than mutations (Wu et al., 2015). Taken together, this evidence supports the atavistic theory and indicates breakdown of evolutionary more recent regulatory layers in cancer, providing new insights for possible treatment strategies (Bussey et al., 2017).

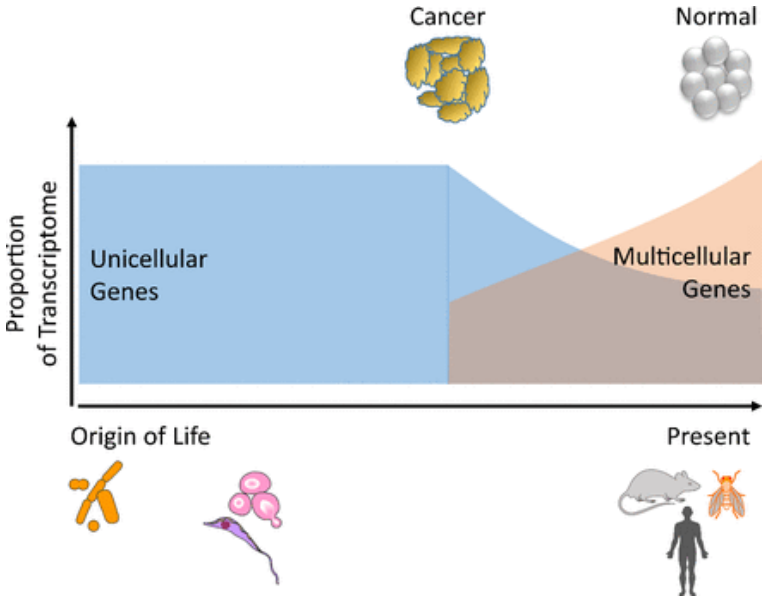

Figure 2: Graphical representation showing the repression of unicellular genes by multicellular genes in the course of evolution. According to the atavistic theory, cancer results from the reactivation of an ancient toolkit that is suppressed in metazoan organisms. Reprinted from Bussey, Kimberly J., et al. "Ancestral gene regulatory networks drive cancer." Proceedings of the National Academy of Sciences 114.24 (2017): 6160-6162.

Trichoplax adhaerens as a model organism

Trichoplax adhaerens, the only named species of the phylum Placozoa so far, is considered to be morphologically one of the simplest metazoan organisms (Ringrose et al., 2013) and is composed of only six cell types and no mesenchymal tissue (Smith et al., 2014). Even though there is only one named species to date, 19 placozoan species lineages have been reported (Eitel et al., 2013) of which the H13 lineage might represent a new species (Eitel et al., 2017). Placozoa can be found in coastal waters (Eitel and Schierwater, 2010) within a temperature range between 32°C and > 10°C (Tomassetti et al., 2005) and exhibit a seasonal pattern with higher abundance during the summer (Maruyama, 2004, Paknia and Schierwater, 2015).

Previously raised notions of *Trichoplax adhaerens* representing a secondarily simplified organism, thus being a triploblastic, rather than diploblastic species, could not be supported by mitochondrial, as well as whole genome data (Ender and Schierwater, 2003, Srivastava et al., 2008). Together with Porifera, Ctenophora, Cnidaria and Bilateria, Placozoa represents one of the five major metazoan lineages (Collins et al., 2005). Despite numerous efforts, the exact phylogenetic relationships of these lineages, however, is still a matter of debate and several conflicting scenarios have been published (Nosenko et al., 2013) (Lanna, 2015), such as the "Ctenophora-first" scenario (Ryan et al., 2013). Nevertheless, analysis of all available data identified Placozoa as the most basal diploblast group (Schierwater et al., 2009b) (**Figure 3**) and placozoan morphology (disk-shaped and lacking symmetry) fits the placula hypothesis of metazoan evolution proposed by Otto Bütschli in 1884, requiring only minor differentiation processes (Schierwater et al., 2009a).

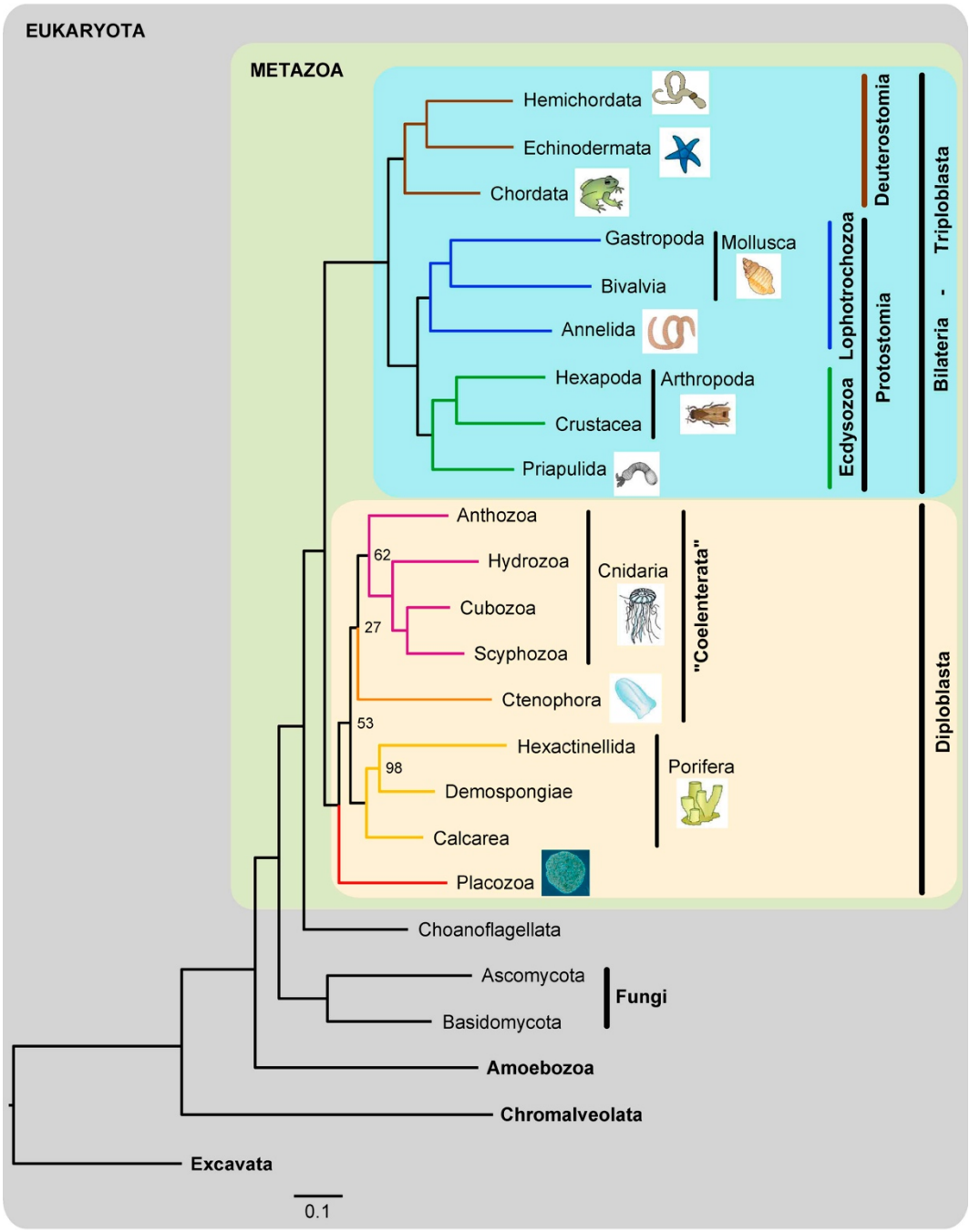

Figure 3: Maximum Likelihood Phylogenetic Tree of Metazoan Relationships Using the Concatenated Data Matrix by Schierwater B et al. Reprinted from: Concatenated Analysis Sheds Light on Early Metazoan Evolution and Fuels a Modern "Urmetazoon" Hypothesis. Schierwater B et al. PLoS Biol 7(1). 2009. doi:10.1371/journal.pbio.1000020 under the Creative Commons Attribution (CC BY) license.

Placozoan morphology has recently been shown to be built by six different cell types (Smith et al., 2014) that make up a small disk-shaped animal, which locomotes by ciliary gliding (**Figures 4 and 5**). Its body plan can be divided into a ventral plate made up of ventral ciliated epithelial cells with microvilli (Ruthmann et al., 1986), cells containing large lipophilic inclusions (lipophil cells) and gland cells. The dorsal epithelium is composed of ciliated dorsal epithelial cells that, together with the ventral plate, surround crystal cells containing birefringent crystals. Fiber cells make contact with other cell types through their branching processes (Smith et al., 2014). Escaping morphological evidence so far, stem cells are thought to be present around the margin (Martinelli and Spring, 2004, Jakob et al., 2004). Furthermore, shiny spheres that can sometimes be observed as dark granules, are probably found in dorsal cells and might represent lipid inclusions, but also seem be involved in predator defense (Jackson and Buss, 2009).

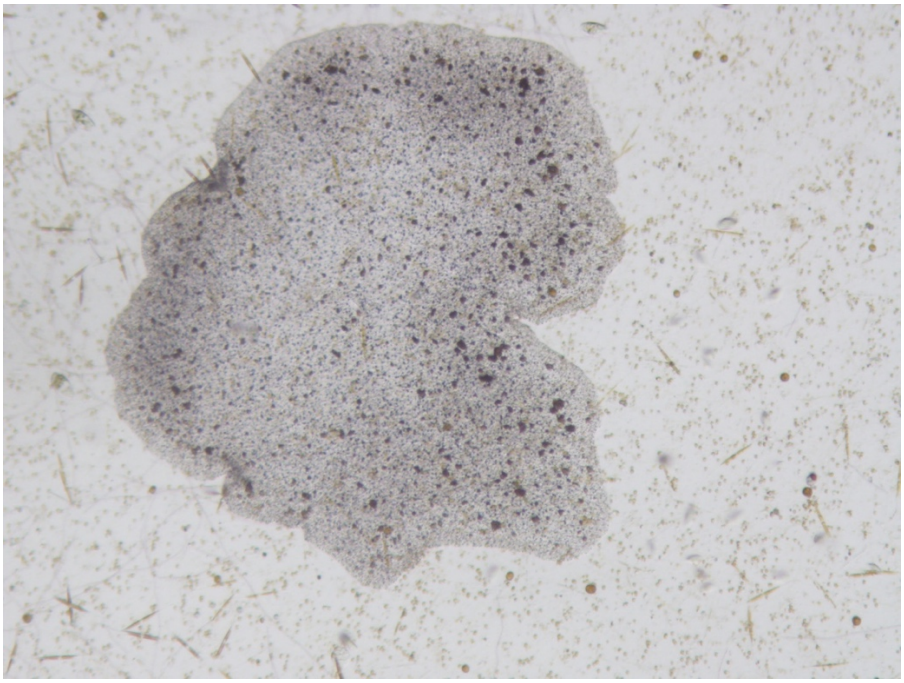

Figure 4: Typical *Trichoplax adhaerens* cultured in petri dish with unspecified food sources. An irregular rim, as well as multiple shiny spheres (dark granules) can be observed.

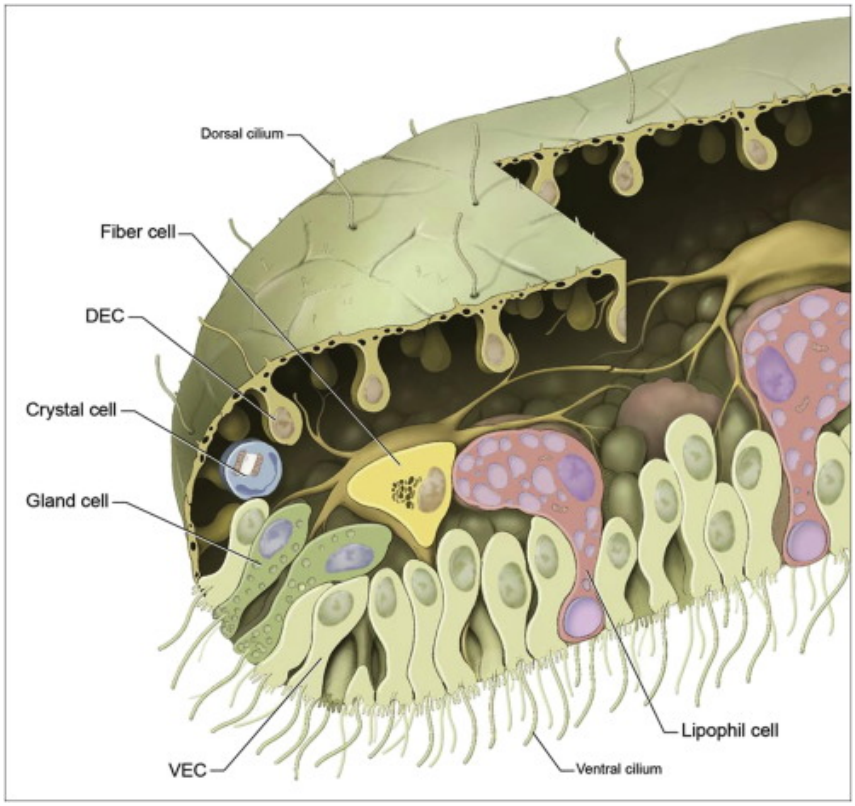

Figure 5: Drawing of *Trichoplax adhaerens* body plan. Shiny spheres are not depicted and are probably located in dorsal epithelial cells (DEC). Ventral epithelial cells (VEC) are ciliated and possess numerous microvilli. Reprinted from Current Biology, 24.14, Smith, Carolyn L., et al., "Novel cell types, neurosecretory cells, and body plan of the early-diverging metazoan *Trichoplax adhaerens*.", 1565-1572., Copyright (2014), with permission from Elsevier.

Compared to the amount of genomic information, little is known about the functions of described cell types. Because *T. adhaerens* feeds by external digestion underneath its ventral plate, ventral epithelial cells are thought to be engaged in nutrient uptake and, due to their microvilli, are thought to resemble cells of the digestive track (Halanych, 2004). Previously assumed to secrete digestive enzymes (Halanych, 2004), gland cells are now proposed to be neurosecretory (Smith et al., 2014). This is in line with results showing positive neuropeptide immunolabeling of these cells (Schuchert, 1993), but

further functional characterization is pending. Also, the assumption that contractions of fiber cells result in the frequently observed shape changes could not be verified morphologically because their processes lack myofibrils and probably also adhesive contacts (Smith et al., 2014).

Under laboratory conditions *T. adhaerens* usually reproduces by binary fission, but development of embryos until a certain stage has been observed (Eitel et al., 2011). Even though sexual reproduction has never been observed, molecular analysis revealed allele shuffling, indicating sexual reproduction in this species (Signorovitch et al., 2005).

The *Trichoplax adhaerens* genome contains only approximately 98 million base pairs with over 11 000 protein coding genes (Srivastava et al., 2008). As such, the genome size is comparable to *Caenorhabditis elegans* and *Drosophila*, which underwent secondary reduction. Interestingly, genome analysis revealed large blocks of conserved synteny relative to vertebrate genomes and an extensive set of transcription factors associated with metazoan development (e.g. patterning), as well as differentiation and cell type specification, such as all essential components of TGF-ß signaling or GATA family zinc-finger transcription factors that are involved in cardiac and blood cell fates (Srivastava et al., 2008). Furthermore, despite an extracellular matrix (ECM) was not identified to date, the genome contains several genes coding for putative ECM proteins. Interestingly, taken together, the placozoan genome codes for and transcribes several factors associated with 'higher' animals without apparent correlate in *Trichoplax* morphology (Schierwater et al., 2009a).

Study strategy and reasoning

To answer the goals set to support our hypothesis we chose to study nuclear receptors in the probably most basal metazoan species known today, *Trichoplax adhaerens*. Characterization of the NR complement in one of the simplest animals would allow answers to several key questions associated with the hypothesis. That is, it would provide insights about whether NRs at the base of metazoan evolution are functional, whether they can form a network, what their ligands might be and last, but not least, enable insights about the ancestral regulation of specific gene expression by NRs, which according to our hypothesis formed new and overrode preexisting regulatory layers during the course of metazoan evolution.

Secondly, to show integration of NR signaling (and thereby organismal/environmental status) with overall cellular status, we chose to study the downstream regulatory pathway of NRs. We did so by characterization of a key component of the mediator complex, whose composition has been shown to be cell type specific to a certain extent (D'Alessio et al., 2011). Because of its dual nature, being a mediator complex subunit in the nucleus (Sato et al., 2004, Beyer et al., 2007) and interacting with the cytoskeleton in the cytoplasm (Wiederhold et al., 2004, Lu et al., 2006, Huang et al., 2012), we identified the mediator subunit MDT-28 in *C. elegans* as a likely candidate for integration of cellular status with overall organismal (or environmental) status signaled by NRs. Due to its properties, detailed descriptions of phenotypical abnormalities and wealth of established protocols we then identified the previously incorrectly annotated orthologue of MED28 in *Caenorhabditis elegans* (MDT-28) and characterized its functions, localizations and interactions with other proteins (Kostrouchova et al., 2017).

Interestingly, the previously incorrectly annotated orthologue of MDT-28 turned out to be an orthologue of Perilipin (*plin-1*) (Chughtai et al., 2015), which is involved in lipid

droplet regulation. The high sequence identity with MED28 furthermore raises the question of a possible dual role of *plin-1*.

METHODS

PART I – Characterization of NRs in *T. adhaerens*

The following methods (part I) section was reprinted and modified under the Creative Commons CC-BY 4.0 license from Novotný et al. (2017), *Trichoplax adhaerens* reveals a network of nuclear receptors sensitive to *9-cis*-retinoic acid at the base of metazoan evolution. PeerJ 5:e3789; DOI 10.7717/peerj.3789

Bioinformatics and cloning of RXR

The predicted RXR gene models on jgi (http://jgi.doe.gov/) (Nordberg et al., 2014) were screened for the characteristic molecular signature of the DNA binding domain (C-X2-C-Xl3-C-X2-C-X15-C-X5-C-X9-C-X2-C-X4-C-X4-M) (Kostrouch et al., 1995) and the appropriate predicted gene model (protein ID 53515) was selected for further use.

The alignment of different RXRs was performed by Clustal Omega (http://www.ebi.ac.uk/Tools/msa/clustalo/) (Sievers et al., 2011) and adjusted/exported as an image file using Jalview (http://www.jalview.org). Protein domain characterization was performed with SMART (Letunic et al., 2015, Schultz et al., 1998). Analysis of HNF4, ERR and COUP-TF was done similarly. Phylogenetic analysis was performed on RXR ClustalO alignment using PhyMLv3.1 (Guindon et al., 2010) implemented in SeaView v4.6.1 with a 100 bootstrap analysis and SPR distance computation. The tree was then visualized using FigTree v1.4.3.

T. adhaerens total RNA was obtained from 50-100 pooled individual animals and extracted using TRIZOL® reagent (Invitrogen, Carlsbad, CA, USA) according to the protocol supplied by the manufacturer.

Subsequently, cDNA was prepared with random hexamers and SuperScript III (Invitrogen™) according to the manufacturer's protocol.

Several RXR transcripts were then amplified by PCR with primers covering the starting sequence ((GCGGATCC)ATGGAGGACAGATCGTTTAAAAAA), starting at 32 bp 5' of ATG (TCTACCAATGTTTATCGCATCGGTTA) and starting at 97 bp 5' of ATG (TTAAGGCTTAACTGATGATGTTGTGAATG) with a common reverse primer covering the last 24 bp of the predicted gene sequence ((CGGAATTC)TTAAGAACTGCCTGTTTCCAGCAT).

Each PCR product was then ligated into pCR®2.1-TOPO® or pCR®4-TOPO® vector with the classic TA Cloning Kit and TOPO TA Cloning Kit (Invitrogen™), respectively. The ligated products were then transformed using One Shot® TOP10 Chemically Competent *E. coli* and cultured on LB Agar plates containing 100 µg/ml ampicillin. Plasmid DNA was extracted from obtained colonies and screened for mutations by sequencing using vector specific M13 forward and reverse primers. Only non-mutated sequences were used in subsequent experiments.

The RXR fragments were then restricted and inserted into pGEX-2T vector system for bacterial expression (Addgene, Cambridge, MA, USA). Proper insertion was verified by sequencing.

Protein expression

BL21 pLysS bacteria were transformed with previously described RXR mRNA inserted into pGEX-2T vector. Stocks of transformed bacteria were stored in 8% glycerol according to the Novagen pET System Manual (11th edition) (http://kirschner.med.harvard.edu/files/protocols/Novagen_petsystem.pdf). For protein expression, bacteria were scraped from stock and incubated in Liquid Broth (LB) with

ampicillin (100 µg/ml) and chloramphenicol (34 µg/ml) overnight. The culture was then used to inoculate 100 ml of LB + antibiotics and grown to OD600 = 0.6-0.8 at 37 ºC, then induced with 100 µl 1M IPTG (isopropyl-D-thiogalactopyranoside) (Sigma-Aldrich, St. Louis, MO, USA) and moved to 25 ºC (RT) for 5 h. The culture was then spun at 9000 xg for 15 min and the supernatant discarded. The bacterial pellet was re-suspended in 10 ml GST binding buffer (25 mM Tris pH 7.5, 150 mM NaCl, 1 mM EDTA + protease inhibitor (S8820 Sigma Fast, Sigma-Aldrich, St. Louis, MO, USA or cOmplete™, EDTA-free Protease Inhibitor Cocktail, Roche, Basel, Switzerland). Bacteria were then lysed by 6 x 20 s ultrasonication on ice (50 watts, 30kHz, highest setting – 100%) (Ultrasonic Processor UP50H, (Hielscher Ultrasonics GmbH, Teltow, Germany) and subsequently incubated with 15-20 mg glutathione agarose beads (Sigma-Aldrich®) prepared according to manufacturer's instructions. Incubation took place at 4 ºC for about 10 h after which the beads were washed according to instructions, re-suspended in regeneration buffer (50mM Tris-HCl pH7.4, 1mM EDTA, 120 mM KCl, 5 mM DTT, 8% glycerol (v/v)) or 50mM TRIS–HCl pH 7.4 + 9% (v/v) glycerol for subsequent thrombin (bovine plasma, Sigma-Aldrich®) cleavage, if performed, and then adjusted for regeneration buffer conditions. GST-TaRXR was eluted from glutathione agarose beads using 10 mM reduced glutathione (Sigma-Aldrich, StLouis, Mo, USA) in 50 mM Tris-HCl buffer pH 8.0. The size of the GST-TaRXR fusion protein was checked by polyacrylamide gel electrophoresis. Thrombin cleavage was performed at RT for 4 h and the quality of the purified protein was assessed by polyacrylamide gel electrophoresis.

Radioactive 9-*cis-RA* binding assay

Radioactive ^{3}H-labelled 9-*cis-RA* and ^{3}H-labelled AT-RA were purchased from PerkinElmer (Waltham, MA, USA). Binding was performed in 100 µl binding buffer (50mM Tris-HCl pH7.4, 1mM EDTA, 120 mM KCl, 5 mM DTT, 8% glycerol (v/v), 0.3% to 0.5% (w/v) CHAPS (3-[(3-Cholamidopropyl)dimethylammonio]-1-propanesulfonate hydrate, Sigma-Aldrich) for 2 h on wet ice in a dark environment. The protein used for binding was either GST-RXR fusion protein on beads with about 375 ng/assay and thrombin-cleaved RXR. For estimation of specific binding, 200x excess of either 9-*cis*-RA or AT-RA (Sigma-Aldrich) was used. In case of GST-RXR fusion protein, 50 µl of the supernatant was removed after 30 s at 1300 g and washed 3x with 1000 µl wash buffer (50 mM Tris-HCl pH7.4, 1 mM EDTA, 120 mM KCl, 5 mM DTT, 8% (v/v) glycerol, 0.5% (w/v) CHAPS) removing 900 µl after each wash. For cleaved RXR protein 10 µl hydroxyapatite slurry (AG-1 XB Resin, Bio-Rad, Hercules, CA, USA) suspended in binding buffer (12.7 mg/100µl) were added to the assay and mixed twice, collecting the apatite slurry by centrifugation (15 s at 600 g). 95 µl of the supernatant was removed and the slurry washed twice with 1 ml of wash buffer, removing 900 µl after each wash. Work with retinoids was done under indirect illumination with a 60W, 120V yellow light bulb (BugLite, General Electric Co, Nela Parc, Cleveland OH, USA) as described (Cahnmann, 1995). The radioactivity of the GST-fusion protein and cleaved protein was measured using Packard Tri-Carb 1600TR Liquid Scintillation Analyzer (Packard, A Canberra Company, Canberra Industries, Meriden, CT, USA) and Ultima Gold Scintillation Fluid (PerkinElmer, Waltham, MA, USA). The fraction of bound ^{3}H-labelled 9-*cis*-RA and ^{3}H-labelled all-*trans*-RA was determined as a ratio of the bound radioactivity of precipitated GST-TaRXR / total radioactivity used at the particular condition (determined as the sum of bound radioactivity and the total radioactivi-

ty of collected wash fluids) in the absence of non-radioactive competitors or 200 fold excess of 9-*cis*-RA and all-*trans*-RA in the case of ^{3}H-labelled 9-*cis*-RA and 40 fold excess of non-radioactive competitors in the case of ^{3}H-labelled all-*trans*-RA (to compensate for the higher affinity of 9-*cis*-RA compared to all-*trans*-RA in binding to TaRXR).

Culture of *T. adhaerens* and algae

Trichoplax adhaerens was cultured in Petri dishes containing filtered artificial seawater (Instant Ocean, Spectrum Brands, Blacksburg, VA, USA) with a salinity of approx. 38-40 ppt. *Rhodomonas salina* (strain CCAP 978/27), *Chlorella sp*., *Porphyridium cruentum* (UTEX B637) and other non-classified algae, as well as aquarium milieu established in the laboratory by mixing salt water obtained from a local aquarium shop were used to maintain the stock. The cultures were kept at approx. 23°C and an automated illumination for 12 h/day was used with a conventional light bulb on a daylight background from late spring to mid-summer in the laboratory located at 50.07031N, 14.42934E with laboratory windows oriented eastward. The natural illumination included almost direct morning light from 8 AM to 10.30 AM, indirect sunlight for most of the daytime and sunlight reflected from a building across the street from 1 PM to 6 PM. Algae were maintained as described (Kana et al., 2014, Kana et al., 2012). The experiments were performed predominantly during sunny weather.

Treatment of *T. adhaerens* with retinoic acids

Incubation of the animals was done overnight in the absence of light. Each batch within an experiment was derived from similar cultures and fed with similar amounts and composition of algae. All experiments were started in a dark room with indirect

yellow light illumination (similarly as in the case of the ligand binding studies) and further incubations were done in the dark for 24 hours. In experiments aimed at the visualization of 9-*cis*-RA effect on *T. adhaerens* response to feeding conditions, parallel cultures were set and fed with *P. cruentum.* Large animals of approximately the same size were individually transferred to new control and experimental cultures and fed with *P. cruentum* algal cells. After 6 hours of incubation under natural indirect illumination, all animals in both control and experimental cultures were photographed (max. magnification on Olympus SZX7 with Olympus E-410 camera) and the final volume of cultures was adjusted to 50 ml (determined by the weight of cultures in 110 mm glass Petri dishes). Next, the room was darkened and further manipulations were done under indirect illumination with yellow light. Five µl of vehicle (1% DMSO in ethanol) or vehicle containing 9-*cis*-RA was added into 50 ml of final volume to the final concentration of 9-*cis*-RA 3.3 nM. Similarly, parallel sub-cultures were prepared from slowly growing cultures fed by microorganisms covering glass slides in an equilibrated 25 l laboratory aquarium and fed by *Chlorella sp*. Cultures were incubated in the dark for 24 h and all animals were counted under microscope and photographed again. The cultures were then left under natural illumination and cultured for an additional two or three weeks. Animals fed by *P. cruentum* were measured again at 72, 90 and 450 h and those fed by *Chlorella sp*. at 72, 90 and 378 h.

Quantitative PCR

Droplet digital PCR was performed on a QX100 Droplet Digital PCR System (Bio-Rad Laboratories, Hercules, CA, USA). For this, *T. adhaerens* was cultured according to culture conditions described and 4-10 animals removed per 100µl TRIZol

reagent (Invitrogen, Carlsbad, CA, USA). Total RNA was measured by a UV spectrophotometer and used as a reference for normalization.

Reverse transcription was performed with SuperScript III Reverse Transcriptase (ThermoFisher, Waltham, MA, USA) according to manufacturer's instructions. The cDNA (corresponding to 100-500 ng of RNA) was then mixed with ddPCR Supermix (Bio-Rad, Hercules, CA, USA) according to the manufacturer's instructions and analyzed. PCR primers were designed using the UPL online ProbeFinder (Roche) software and were as follows:

TaRXR

left:tctgcaagttggtatgaagca, right: agttggtgtgctattctttacgc

TaHNF4 (ref|XM_002115774.1|):

left: ggaatgatttgattttacctcgac, right: tacgacaagcgatacgagca

TaCOUP-TF (ref|XM_002109770.1):

left: attttgaatgctgcccaatg, right: ttactggttgtggagtatggaaac

TaSoxB1 (ref|XM_002111308.1|):

left: tgtcagatgcggataaacga, right: ggatgttccttcatgtgtaatgc

TaTrox-2 (ref|XM_002118165.1|):

left: gcctatagtcgatcctgccata, right: ttggtgatgatggttgtcca

TaPaxB1 (gb|DQ022561.1):

left: tcaaacgggttctgttagcc, right: ggtgttgccaccttaggc

TaERR (nuclear receptor 3, gb|KC261632.1):

left: ttacgcatgtgatatggttatgg, right: agcgtgcctatttatttcgtct

Results were subsequently analyzed using the Bio-Rad ddPCR software. Manual correction of the cut off was performed when automated analysis was not possible. To

visualize changes in nuclear receptor expression in the absence of a reliable housekeeping gene as a reference, we considered the absolute quantity of each nuclear receptor as a percentage of the overall nuclear receptor expression and subsequently visualized the change of receptor expression by subtraction of the percentage of the control experiment. Absolute copy numbers of the proposed malic enzyme orthologue in *T. adhaerens* have been normalized to overall RNA quantity for expressional analysis.

Experiments with quantification by qRT-PCR were performed on a Roche LightCycler II with OneTaq polymerase and the same probes as for ddPCR.

For the estimation of the relative expression of NRs in small (< 0.5 mm) versus big animals (>1 mm), 20 to 30 animals from the same culture were used for each paired experiment.

Identification of *T. adhaerens* orthologue of malic enzyme

P48163 (MAOX_HUMAN) protein sequence was used as the query sequence and searched against *T. adhaerens* database with BLASTP on http://blast.ncbi.nlm.nih.gov/Blast.cgi using standard algorithm parameters. The best hit was a hypothetical protein TRIADDRAFT_50795 with a sequence identity of 57% and a query coverage of 93% and was assumed to be *T. adhaerens* closest orthologue of vertebrate L-malate-$NADP^+$ oxidoreductase.

Microscopy and image analysis

Observation of *T. adhaerens* was done with an Olympus SZX10 microscope equipped with DF Plan 2x objective and Olympus DP 73 camera operated by CellSens Dimension computer program (kindly provided by Olympus, Prague, Czech Republic)

or Olympus CKX41 or SZX7 with Olympus E-410 camera and QuickPhoto Micro 3.1 program.

Circularity was calculated by establishing the area (A) and perimeter (p) of *T. adhaerens* using ImageJ (https://imagej.nih.gov/ij/) and then calculated with the isoperimetric quotient $Q = \frac{4\pi A}{p^2}$, (A – Area, p – perimeter). GraphPad Prism 5 (or higher) was used for graphical representation and calculations of the confidence intervals with p = 0.05.

PART II – Characterization of MDT-28

Detailed descriptions of the methods and results can be found in the paper 'The nematode homologue of Mediator complex subunit 28, F28F8.5, is a critical regulator of *C. elegans* development' (Kostrouchova et al., 2017).

Briefly, MED28 orthologue sequences were searched in UniProtKB (uniprot.org) and NCBI (ncbi.nlm.nih.gov) with BLAST, PSI-BLAST (Altschul et al., 1997), HHblits (Remmert et al., 2011) and HHpred (Soding et al., 2005). The obtained mammalian and insect sequences were aligned using T-coffee (Notredame et al., 2000, Di Tommaso et al., 2011), as well as PROMALS (Pei et al., 2008, Pei et al., 2007, Pei and Grishin, 2007) and secondary structure predictions performed with PSIPRED (Jones, 1999, McGuffin et al., 2000, Cuff and Barton, 2000).

RNA of cultured worms was isolated by phenol-chloroform extraction, precipitated with ethanol and subsequently treated with DNase (Promega, Fitchburg, WI, USA). Complementary DNA was prepared with SuperScript III (Invitrogen, Carlsbad, CA, USA).

The detailed protocol was described in (Kostrouchova et al., 2017) and (Zima et al., 2015).

Transgenic animals were either prepared by PCR fusion (Hobert, 2002) by constructing a fusion product of the F28F8.5 gene sequence and GFP derived from pPD95.75 containing its 3' UTR at the C-terminal, which was then injected into the gonads of young adult hermaphrodites or by genome editing using CRISPR/Cas9 according to (Dickinson and Goldstein, 2016, Ward, 2015, Dickinson et al., 2015, Dickinson et al., 2013). In this case, the F28F8.5 gene was edited by insertion of a construct coding for GFP, *sqt-1(d)* within a self-excising cassette (leading to a rolling phenotype), *hs::Cre* (heat shock inducible Cre recombinase) and a hygR (hygromycin resistance) gene. Induction of heat-shock then lead to removal of the self-excising cassette and N-terminal GFP tagged F28F8.5, which was disrupted prior to heat-shock.

RNA interference was performed by dsRNA microinjection of previously linearized F28F8.5 cDNA containing pCRII(Topo) plasmid (Invitrogen, Carlsbad, Ca, USA) transcribed *in vitro* using SP6/T7 Riboprobe® in vitro Transcription Systems (Promega, Madison, WI, USA).

For distinguishing GFP-specific fluorescence and auto-fluorescence, fluorescence-lifetime imaging microscopy was performed additionally to Nomarski optics, fluorescence and confocal microscopy.

Classical polymerase chain reaction (PCR) was performed for single nematode PCR, while a protocol adopted from Ly et al. (Ly et al., 2015) was used for quantitative reverse transcription-PCR.

For binding studies, ^{35}S Methionine (Institute of Isotopes, Budapest, Hungary) labeled mdt-6 was translated using the rabbit reticulocyte TNT-system (Promega, Madison, WI, USA). GST-labeled F28F8.5 was obtained by expressing recombinant pGEX-2T in

BL21 *E. coli* after induction with isopropyl β-D-1-thiogalactopyranoside (IPTG) (Sigma-Aldrich, St. Louis, MO, USA). Similarly, FLAG-labeled MDT-30 was expressed from pET28(+) in BL21 *E. coli* after induction with IPTG. Proteins were then incubated and isolated using glutathione-agarose beads (Sigma-Aldrich, St. Louis, MO, USA). Samples were then separated by polyacrylamide gel electrophoresis and radioactively labeled protein detected using a TRI-CARB 1600TR Liquid Scintillation Analyzer (Packard, Meriden, CT, USA) or by autoradiography. FLAG-labeled MDT-30 was visualized by anti-FLAG antibody.

Previously incorrectly annotated as MDT-28, W01A8.1 was shown to be an orthologue of the perilipin family (Chughtai et al., 2015). Association with lipid droplets and co-localization of GFP fused *plin-1* with transgenic lines expressing human PLIN1, 2 and 3 were performed using the CRISPR/Cas9 gene editing method and subsequent fluorescence microscopy in *C. elegans*. Lipid droplets were either visualized with lipid staining LipidTox after formaldehyde fixation or with Coherent Anti-Stokes Raman microscopy (CARS) *in vivo*. Functional analysis was performed by RNA interference by microinjections and subsequent phenotypical analysis, as well as visualization of lipid droplets. Detailed descriptions of the methods can be found in the publication 'Perilipin-related protein regulates lipid metabolism in *C. elegans*' (Chughtai et al., 2015).

Results

Results of part I

Supplementary files and figures referenced to in this section can be accessed online.

T. adhaerens retinoid X receptor shows high cross-species sequence identity

By using the ab initio model of the JGI *Trichoplax* database as a reference, we screened the *Trichoplax* JGI database for RXR orthologues with a complete DBD and LBD sequence and were able to obtain, as well as verify, a full length RXR transcript previously not annotated as the 'best model'. Blastp analysis showed a high sequence similarity to human, as well as mouse RXR with 66% overall sequence identity to human RXR alpha.

SMART analysis of the proposed TaRXR sequence showed a zinc finger DNA binding domain (amino acid residues 16-87) and a ligand binding domain (amino acid residues 155-342) with E values $<10^{-40}$. Blast analysis of the zinc finger DNA binding and ligand binding domains revealed a sequence identity of 81% and 70% to human RXR alpha, respectively. Both domains contained the predicted molecular pattern characteristic for each domain. The heptad repeat LLLRLPAL proposed for dimerization activity (Forman and Samuels, 1990b, Forman and Samuels, 1990a, Kiefer, 2006) as well as the LBD signature for 9-*cis*-RA binding Q-x(33)-L-x(3)-F-x(2)-R-x(9)-L-x(44)-R-x(63)-H (Egea et al., 2000) were present (**Fig. 6**). From 11 amino acid residues

shown to be critical for 9-*cis*-RA binding (A271, A272, Q 275, L 309, F 313, R 316, L 326, A 327, R 371, C 432, H 435), 9 are conserved, while the remaining two amino acids are substituted [A327S, and C432T (C432A in *Tripedalia cystophora*)]. Due to the high sequence identity, we proposed a 9-*cis*-retinoic acid binding capability of the hypothesized TaRXR sequence, as well as DNA binding capability. Phylogenetic analysis using PhyML algorithm indicates that TaRXR is likely to precede branching of RXRs in cubomedusae and scyphomedusae and clusters with RXRs in Bilateria**.**

The remaining three NRs identified in the *T. adhaerens* genome show also very high overall sequence identity with vertebrate orthologues.

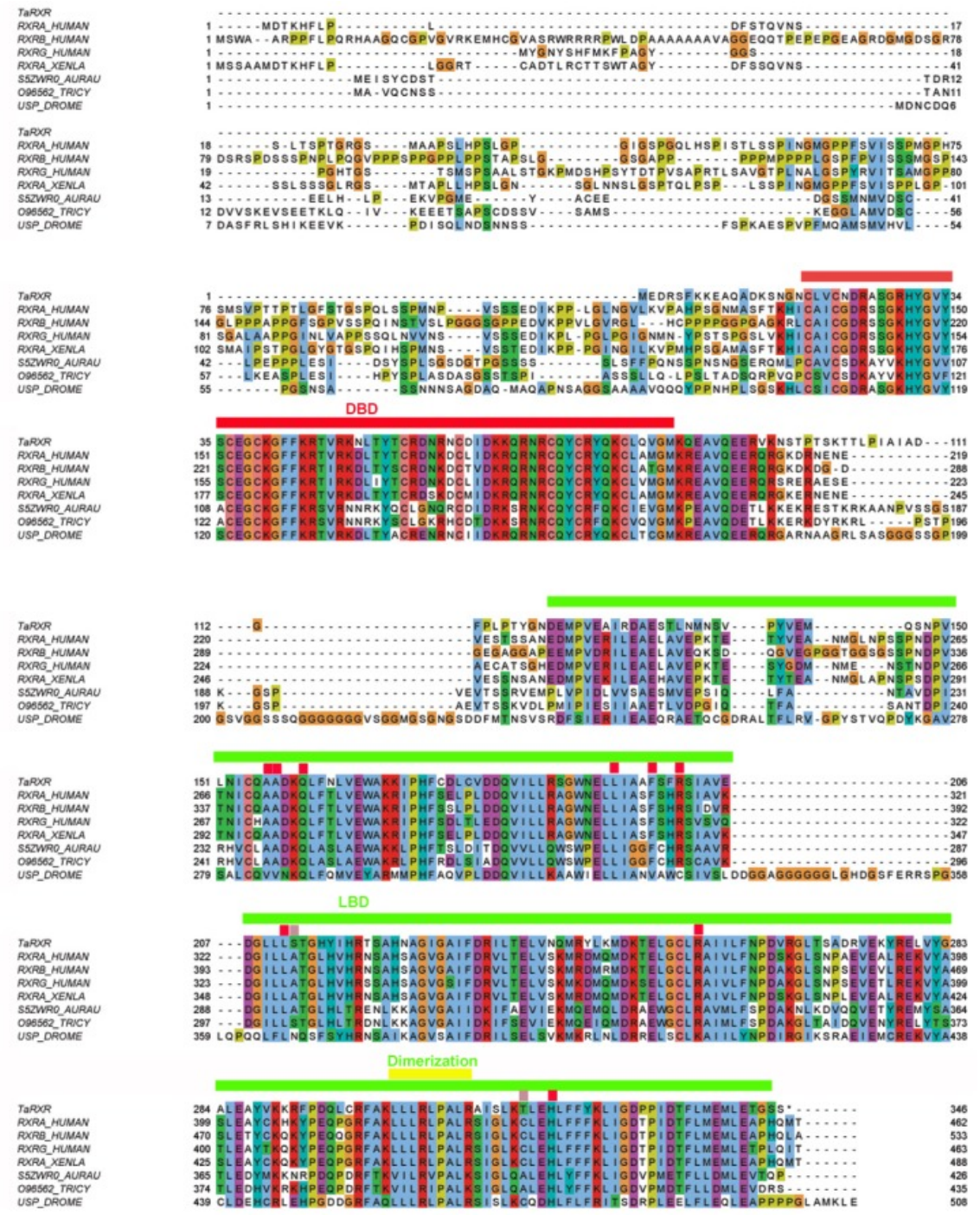

Figure 6: Aligned with ClustalO, amino acid residue types colored according to Clustal scheme in Jalview. Sequences from top to bottom (organism, identifier): *Trichoplax adhaerens*, TaRXR ID 53515; *Homo sapiens*, sp|P19793|RXRA_HUMAN; *Homo sapiens*, sp|P28702|RXRB_HUMAN; *Homo sapiens*, sp|P48443|RXRG_HUMAN; *Xenopus laevis*, RXR alpha, sp|P51128|RXRA_XENLA; *Aurelia aurita*, RXR, tr|S5ZWR0|S5ZWR0_AURAU Retinoid X receptor; *Tripedalia cystophora*, RXR,

tr|O96562|O96562_TRICY Retinoic acid X receptor; *Drosophila melanogaster*, USP, sp|P20153|USP_DROME. DNA binding domain (DBD, red line), Ligand binding domain (LBD, green line), dimerization domain (yellow line) and amino acid residues critical for 9-*cis*-RA binding (conserved—red rectangles, not conserved—pink rectangles) are indicated.

TaRXR shows preferential binding affinity to 9-*cis*-retinoic acid over all-*trans*-retinoic acid

In order to analyze the binding properties of TaRXR, we expressed TaRXR as a GST-fusion protein (GST-TaRXR) in bacteria which was then purified as GST-fusion protein and used directly for binding studies or cleaved by thrombin and eluted as TaRXR. The binding of ^{3}H-labelled 9-*cis*-RA or ^{3}H-labelled all-*trans*-RA was determined by measuring total bound radioactivity and the radioactivity displaceable by 200 fold excess of nonradioactive competitors. Consistent with the high conservation of the LBD, the experiments showed that TaRXR prepared as thrombin cleaved TaRXR or GST-TaRXR binds 9-*cis*-RA with high affinity and specificity (**Fig. 7 A and B**). The 9-*cis*-RA binding assay showed high affinity binding to GST-TaRXR with a saturation plateau from 5 nM to 10 nM (**Fig. 7 C**). In contrast, all-*trans*-retinoic acid did not show high affinity binding to TaRXR of GST-TaRXR.

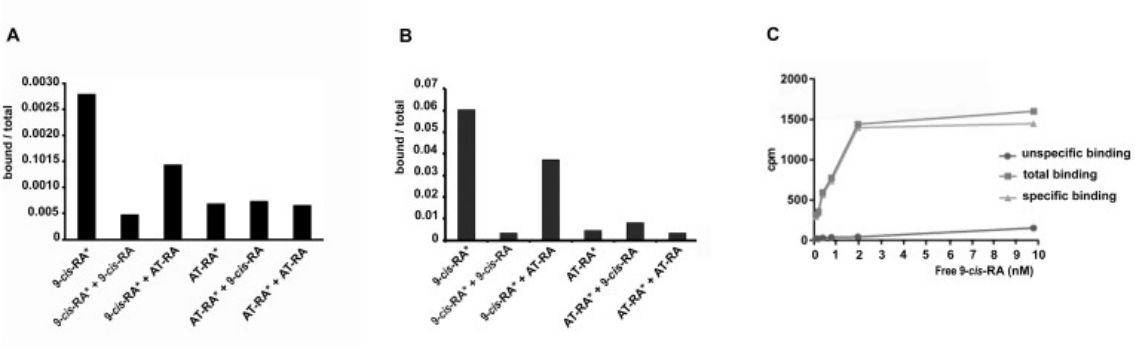

Figure 7: (A) Single point analysis of binding preference of *T. adhaerens* RXR (thrombin cleaved) to ^{3}H-labelled 9-*cis*-RA over all-*trans*-RA. Radioactive 9-*cis*-RA (9-*cis*-RA*) binds at a concentration of 4 nM to 200 nanograms of *T. adhaerens* RXR. 200-fold excess of unlabeled *9-cis*-RA displaces more than 80% of labeled *9-cis*-RA from binding to *T. adhaerens* RXR (9-*cis*-RA* + 9-*cis*-RA) while the same molar excess of all-*trans*-RA (9-*cis*-RA* + AT-RA) which is likely to contain approximately 1% spontaneously isomerized 9-*cis*- RA, competes away less than 50 % of bound ^{3}H-labeled 9-*cis*-RA. Radioactive ^{3}H-labeld all-*trans*-RA (AT-RA*) at identical conditions binds only slightly more than the observed non-specific binding. This interaction is not displaced by the excess of non-labeled 9-*cis*-RA (AT-RA* + 9-*cis*-RA) nor non-labeled all-*trans*-RA (AT-RA* + AT-RA). Results are expressed as a ratio of the radioactivity bound to TaRXR/total radioactivity used for the binding at the given condition. (B) Analysis of binding properties of *T. adhaerens* RXR (in the form of GST-TaRXR) to ^{3}H-labelled 9-*cis*-RA and ^{3}H-labelled all-*trans*-RA. The experiment differs from the experiment shown in A in 5-fold greater amount of radioactive all-*trans*-RA (and therefore only 40-fold excess of non-radioactive competitors). The experiment shows identical binding properties of GST-TaRXR as those observed with thrombin cleaved TaRXR. (C) Kinetic analysis of binding of ^{3}H-labeled 9-*cis*-RA to *T. adhaerens* RXR prepared as GST-fusion protein (GST-TaRXR). The plateau is reached at around 3 to 5 × 10^{-9} M.

9-*cis*-retinoic acid induces malic enzyme gene expression at nanomolar concentrations

Next, we searched whether 9-*cis*-RA has observable biological effects on *T. adharens* at nanomolar concentrations. We hypothesized that TaRXR is likely to be involved in the regulation of metabolic events. In vertebrates, RXR is a dimerization partner of TR and together, these two NRs are regulating a wide range of metabolic pathways. We, therefore, searched for an orthologue of vertebrate L-malate-$NADP^+$ oxidoreductase (EC 1.1.1.40) in *T. adhaerens* genome since this enzyme is an established reporter of the state of thyroid hormone dependent regulation (see Discussion).

The sequence of the *T. adhaerens* likely orthologue of vertebrate L-malate-$NADP^+$ oxidoreductase was retrieved from the *Trichoplax* genomic database together with its presumed promoter based on the predicted sequence.

Droplet digital PCR showed an increased transcription of the predicted L-malate-$NADP^+$ oxidoreductase gene after incubation of *T. adhaerens* with 9-*cis*-RA, but not with all-*trans*-RA **(Fig. 8)**. In repeated experiments, we observed that the level of induction was higher at 9-*cis*-RA concentrations in the range of 1 to 10 nM, than above 10 nM. We also noticed that the level of the induction slightly varied based on the actual *T. adhaerens* cultures and the algal food composition of the *T. adhaerens* cultures.

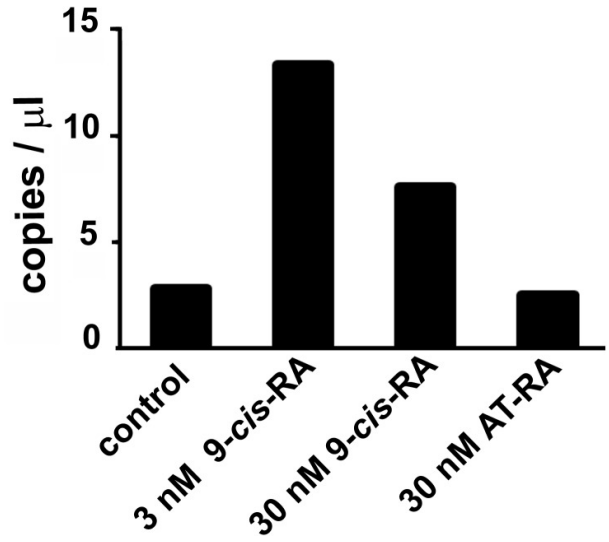

Figure 8: Ten to fifteen animals were cultured in the dark overnight with indicated ligands or in medium containing only the solvent used for ligand solutions. Total RNA and cDNA were prepared using identical conditions and diluted to the same working concentration suitable for ddPCR. In repeated experiments, incubation with 3 nM 9-*cis*-RA induced expression of the putative *T. adhaerens* L-malate-$NADP^+$ oxidoreductase more than four times. Incubation with 30 nM 9-*cis*-RA induced enzyme expression also, but to a lesser extent and 30 nM all-*trans*-RA (AT-RA) did not upregulate the expression of the predicted L-malate-$NADP^+$oxidoreductase.

Changes in the culture environment alter the expression pattern of the nuclear receptor complement in *T. adhaerens*

From the experience we gained by culturing *T. adhaerens*, as well as from the previous experiments we knew that the culture conditions could dramatically influence phenotype. Having the possible developmental functions of the ancestral NRs in mind, we raised the question whether the expression patterns of the NRs reflect changes in phenotype.

Firstly, we assayed the relative expression of RXR against all three other NRs in small versus big animals (<0.5 mm or >1mm). The relative proportion of the RXR expression compared to the remaining NRs was found to be higher in big animals (33%) than in small animals (24%). The treatment by 3.3 nM 9-*cis*-RA led to a dramatic increase of the relative expression of RXR in comparison to the rest of the NR complement (51%), indicating that phenotypic changes are connected with differential expression of NRs and that 9-*cis*-RA affects the expression of RXR.

In order to see the effect of 9-*cis*-RA on all NRs, we sampled and extracted RNA from cultures containing the same number of big and small animals treated with different concentrations of 9-*cis*-RA. The experimental cultures were started from the same original cultures and during incubation were fed with *Chlorella sp.* only since this algal food showed to have the least effect on *T. adhaerens* cultures. All four *T. adhaerens* NRs were quantified by either qRT-PCR or ddPCR.

Analysis of NR expression pattern in animals incubated with different concentrations of 9-*cis*-RA revealed a relative increase in RXR expression at low nanomolar concentrations (<10 nM) in repeated experiments. In contrast, further increase of 9-*cis*-RA resulted in smaller changes compared to the expression pattern of NRs in control animals or even reverted the values observed in low nanomolar conditions (**Fig. 9**).

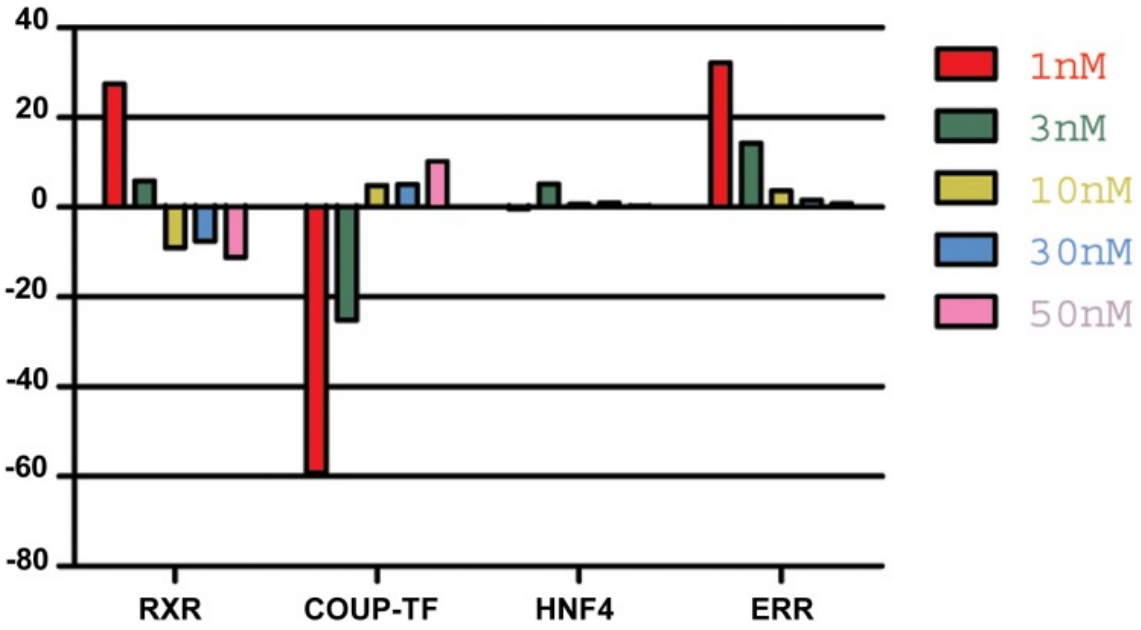

Figure 9: A representative experiment of the expression of *T. adhaerens* NRs in animals exposed to various concentrations of 9-*cis*-RA expressed as a ratio of obtained values compared to the control using ddPCR. One and 3 nM 9-*cis*-RA upregulate RXR and ERR, but downregulate COUP-TF. The expression of *T. adhaerens* HNF4 is not affected by 9-*cis*-RA. The effect of the exposure to 9-*cis*-RA is stronger in the case of 1 nM 9-*cis*-RA compared to 3 nM 9-*cis*-RA. The exposure to 30 nM, as well as 50 nM concentrations of 9-*cis*-RA reverse the effect of 9-*cis*-RA on the expression of RXR and COUP-TF, but do not influence the expression of ERR. The level of expression of HNF4 is not changed by exposure of *T. adhaerens* to various concentrations of 9-*cis*-RA. The data suggest that a network sensitive to nanomolar concentrations of 9-*cis*-RA at the expressional level is formed by RXR, COUP-TF and ERR. All four NRs have conserved P-box (regions responsible for binding to response elements (RE) in gene promoters) and are likely to bind overlapping REs and to form a functional network.

Food composition dramatically changes the phenotype and the reproduction rate of *T. adhaerens*

T. adhaerens retrieved from laboratory aquariums used for the stock cultures were relatively similar in appearance and included small round animals containing approximately 50 cells and grew to animals with an approximate diameter of 0.2 mm and rarely were bigger. Their rate of multiplication when transferred to Petri dishes was doubling in one month or even one week, depending on whether the glass was covered by microbial and algal films established during culturing in aquariums. We attempted to use several defined algae as artificial food. They included *Pyrrenomonas helgolandii*, *Picocystis salinarium*, *Tetraselmis subcoriformis*, *Rhodomonas salina*, *Phaeodactylum tricornutum*, *Porphyridium cruentum* and *Chlorella sp*. Individual subcultures of *T. adhaerens* differed in the rate of propagation and appearance as well as colors that were varying from greenish to brown and reddish taints depending on the food that was used as singular species food or mixtures (**Figure 10**). Also, contaminants from the original algal food, which prevailed in some cultures, had an influence on *T. adhaerens* growth and behavior. In controlled experiments, it became clear that some food components or their metabolites are influencing growth and appearance of *T. adherens* more than food availability. When *T. adhaerens* were fed with equal amounts of algal cells (although they differed in size and expected digestibility), the addition of algae containing red pigments - Cryptophytes (*Pyrrenomonas helgolandii* and *Rhodomonas salina*) or Rhodophyta (*Porphyridium cruentum*) - had a strong positive effect on *T. adhaerens* growth, especially in combination with the green algae *Chlorella sp.* (**Figure 11**).

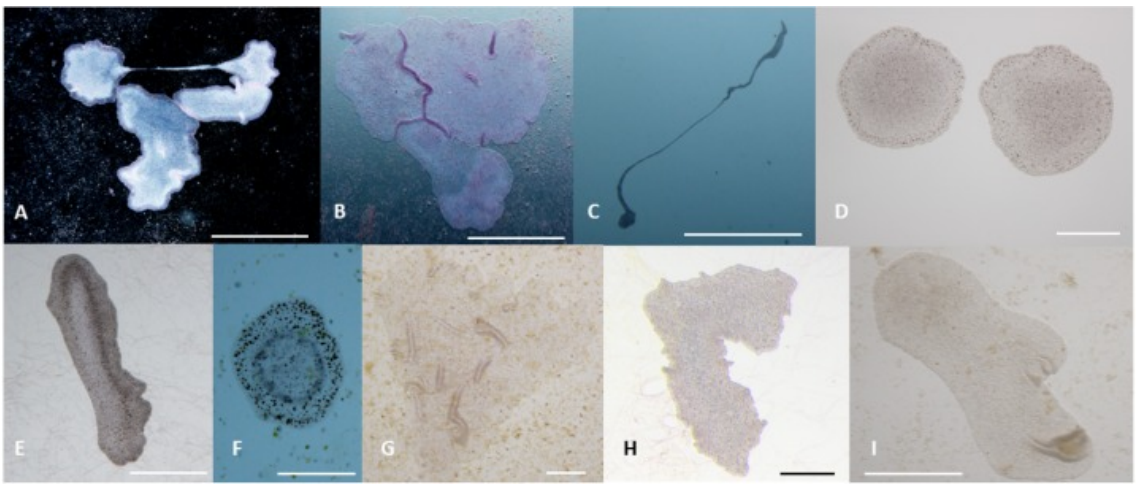

Figure 10: *T. adhaerens* acquires various body shapes in individual cultures dependent on food availability and composition. At conditions maintained in stable and biologically equilibrated stock aquariums, *T. adhaerens*is usually small and pale with diameter varying from 50 µm to 400 µm while cultures with added algae contain large flat animals with diameter reaching up to 1 mm (A and B). In some cultures, animals grow as long stretching structures, reaching a length exceeding one or even several centimeters (C). The algal food makes the animals greenish, reddish, rusty or brown with variable proportion of prominent dark cells. Animal shapes also vary from flat and round with smooth circumference, to curved or ruffled circumference or animals with long projections. Bars represent 1 mm in (A, B, I), 1 cm in C, 250 µm in (D), 500 µm in (E and H), 200 µm in (F), and 100 µm in (G).

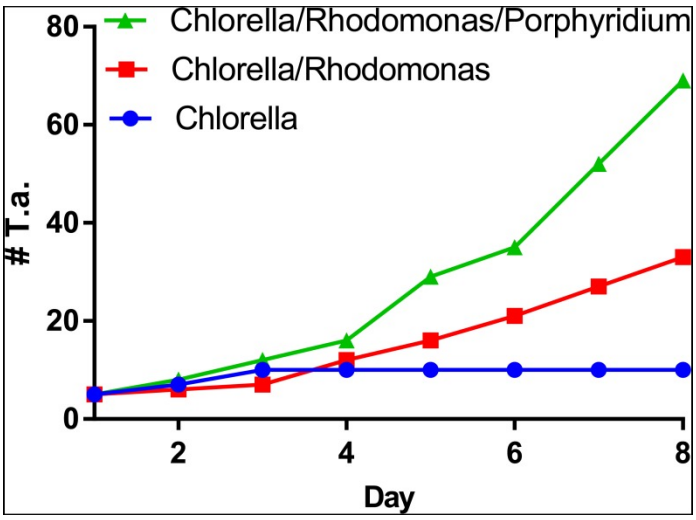

Figure 11: Three cultures of five large animals in each were established and fed with the same number of algal cells consisting of *Chlorella sp.*, *Chlorella sp.* and *Rhodomonas salina* and *Chlorella sp.*, *Rhodomonas salina* and *Porphyridium cruentum*. While the culture fed with *Chlorella sp.* only doubled in the number of animals within a period of one week, cultures with red pigment containing algae multiplied more than five times and 10 times within the same time period.

Furthermore, the addition of *Porphyridium cruentum* to *Chlorella sp.* resulted in a significant change in circularity, while feeding *T. adhaerens* with 'triple food' containing *Chlorella*, *Rhodomonas* and *Porphyridium* showed the most pronounced effect. Culturing *T. adhaerens* on either of the single foods showed similar isoperimetric values (**Figure 12).**

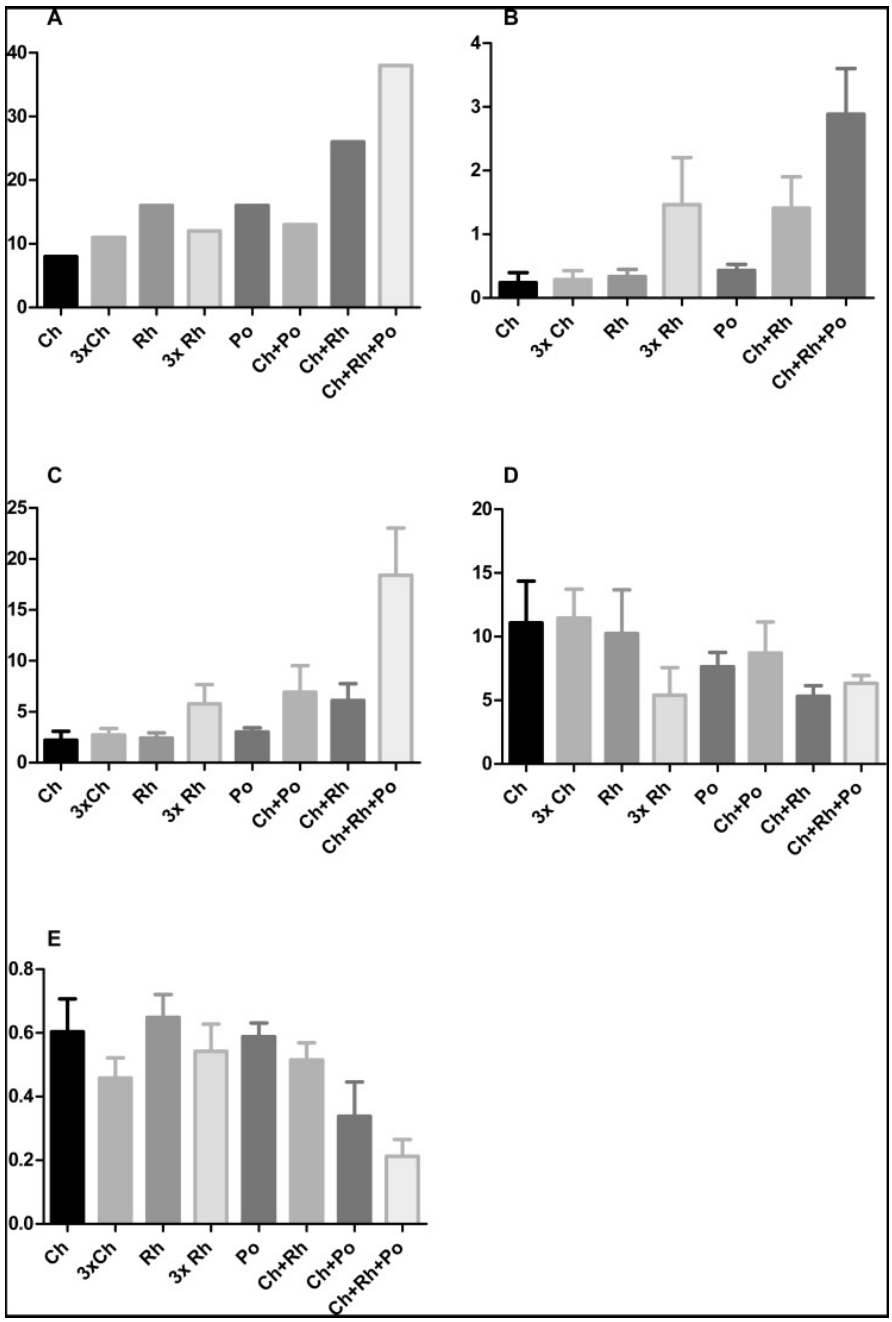

Figure 12: *T. adhaerens* was cultured similarly as shown in figure 6 and all animals were photographed and analyzed using ImageJ program for their number (A), mean area (B), mean perimeter (C), mean perimeter/area ratio (D) and mean isometric quotient (E) after one week. Ch—stands for feeding with *Chlorella sp.*, Rh—*Rhodomonas salina*, Po—*Porphyridium cruentum*, and their combinations. 3Rh stands for a culture with three times higher concentration of *Rhodomonas salina* and 3Ch for three times higher concentration of *Chlorella sp.* (A) shows that addition of *Rhodomonas salina* (Ch + Rh)

greatly increases the number of animals observed after one week of culture. This effect is even more pronounced in cultures containing all three algae, while three times bigger concentration of only one type of algae (Ch and Rh) has little or no effect. This is even more pronounced when the area and perimeter are determined (B and C). Determination of the isoperimetric quotient in individual cultures indicates that cultures with *Rhodomonas salina* have a significantly smaller ratio, suggesting higher proliferative rate of structures at the animal circumference (E). Bars represent 95% confidence interval.

9-*cis*-RA interferes with *T. adhaerens* growth response to specific algal food

In order to see the effect of 9-*cis*-RA on *T. adhaerens* in cultures, we exposed cultures kept in a naturally established laboratory microenvironment or fed by specific algal foods to 3, 5 and 10 nM 9-*cis*-RA. The slowly growing cultures kept in naturally established laboratory microenvironment did not show any gross morphological changes even in 10 nM 9-*cis*-RA during the period of one week. Contrary to that, cultures fed with mixed algal food incubated in the presence of 3 and 5 nM 9-*cis*-RA ceased propagation and most animals developed a balloon-like phenotype, and later darkened and decomposed.

For controlled experiments, cultures fed by *P. cruentum* or *Chlorella sp*. were incubated in the presence of vehicle (DMSO/ethanol) or vehicle containing 9-*cis*-RA at 3.3 nM final concentration. After 24 hours of incubation in the dark, control cultures fed by *P. cruentum* propagated normally while animals fed by *P. cruentum* and incubated with 9-*cis*-RA decreased their area and perimeter (**Figure 13 A**). At 72 h of incubation, all animals fed by *P. cruentum* and treated by 3.3 nM 9-*cis*-RA developed the balloon-like phenotype and none of them survived 90 hours of exposure to 9-*cis*-RA (**Figure 13**

B). Animals transferred from stationary cultures grown in a naturally established laboratory microenvironment and subsequently fed by *Chlorella sp*. suffered initial loses at 24 h of incubation despite that their appearance seemed to be normal and well adopted to the new culture condition at time 0 (regarding feeding with algal food and immediately prior to addition of vehicle or 9-*cis*-RA to the culture and 6 h after the transfer from the parent cultures). Animals that survived the transfer and adopted to feeding by *Chlorella sp*., were not inhibited by exposure to 3.3 nM 9-*cis*-RA for 24 h (**Figure 13 C**) and even showed a slight statistically not significant increase in their area and perimeter. Nevertheless, the isoperimetric values of animals incubated for 24 h with 9-cis-RA showed a significant increase indicating a decrease of growth or exhaustion of peripheral area, that is likely to contain stem cells that further differentiate into the specialized cell types (Jakob et al., 2004). In contrary to animals fed by *P. cruentum,* exposure of animals fed by *Chlorella sp.* to 9-*cis*-RA was not associated with the development of the balloon-like phenotype and animals survived more than 250 h. In contrast to control animals which started to proliferate after 100 h, animals exposed to 9-*cis*-RA did not proliferate between 90 and 280 h of subsequent culture (**Figure 13 D**) suggesting that 9-*cis*-RA interferes with animal response to specific food and processes necessary for animal growth and propagation. The growth arrest of *T. adhaerens* caused by 9-*cis*-RA was reverted by addition of *Porphyridium cruentum* indicating that a specific food constituent rather than food availability interferes with 9-*cis*-RA regulatory potential (**Figure 14**).

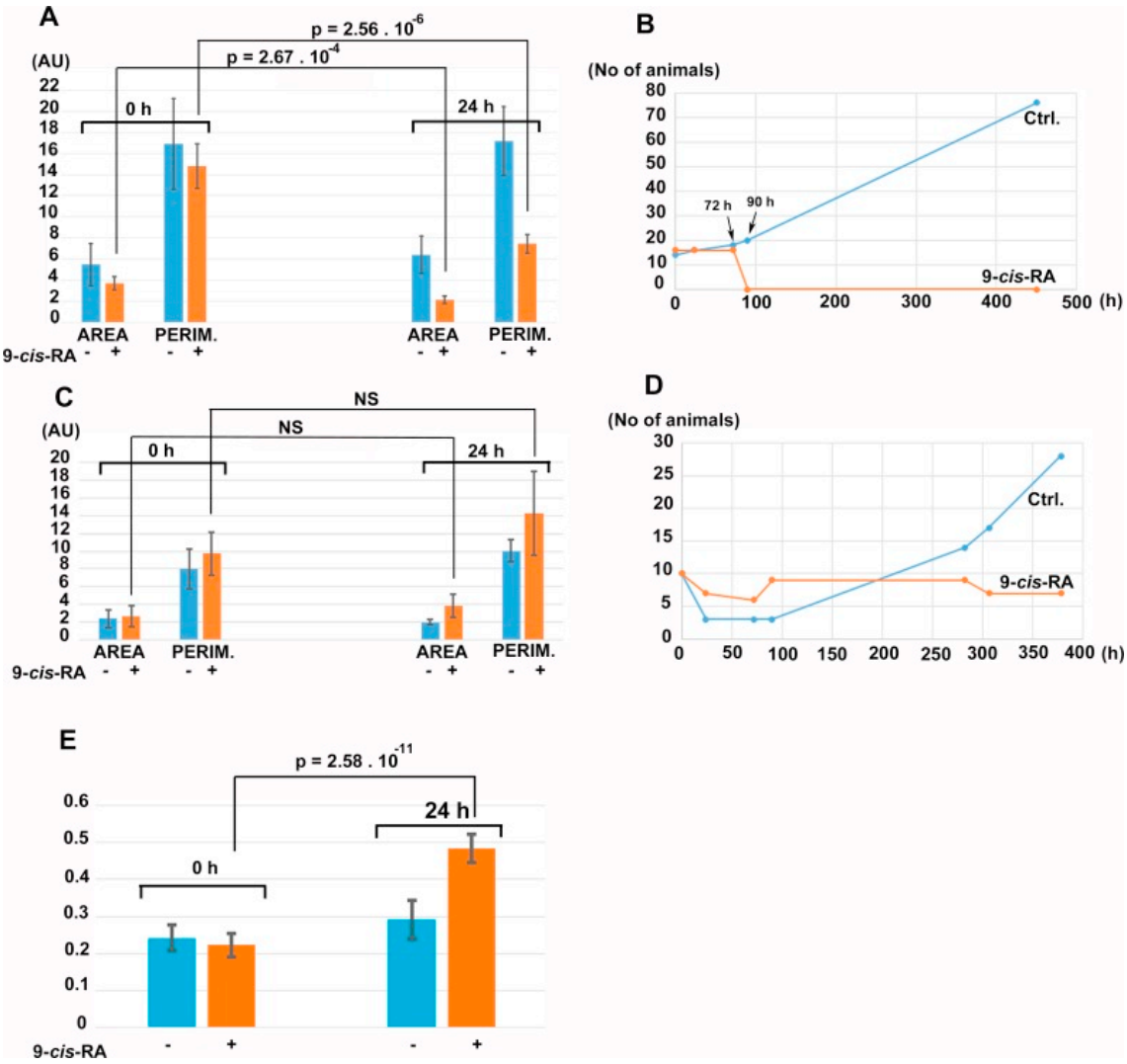

Figure 13: (A) shows the comparison of the total area and total perimeter of control *T. adhaerens* and *T. adhaerens* treated by 9-*cis*-RA for 24 h expressed as arbitrary units derived from pixel measurements obtained at 24 h and compared to values obtained immediately prior to incubation. The data indicates that animals incubated in 3.3 nM 9-*cis*-RA decreased their area and perimeter to approximately 50% in comparison to control animals. (B) shows the development of cultures over a three-week period. The animals treated by 9-*cis*-RA developed a balloon-like phenotype at 72 h of incubation and died at 90 h of incubation. (C and D) show the data obtained with *T. adhaerens* originating from cultures fed by naturally established biofilms in laboratory aquariums, fed by *Chlorella sp*. and treated similarly as shown in (A and B). (E) shows

the analysis of circularity of animals presented in (A) and documents that animals treated by 9-*cis*-RA increased their circularity already at 24 h of exposure suggesting arrest of growth of animal peripheral tissues.

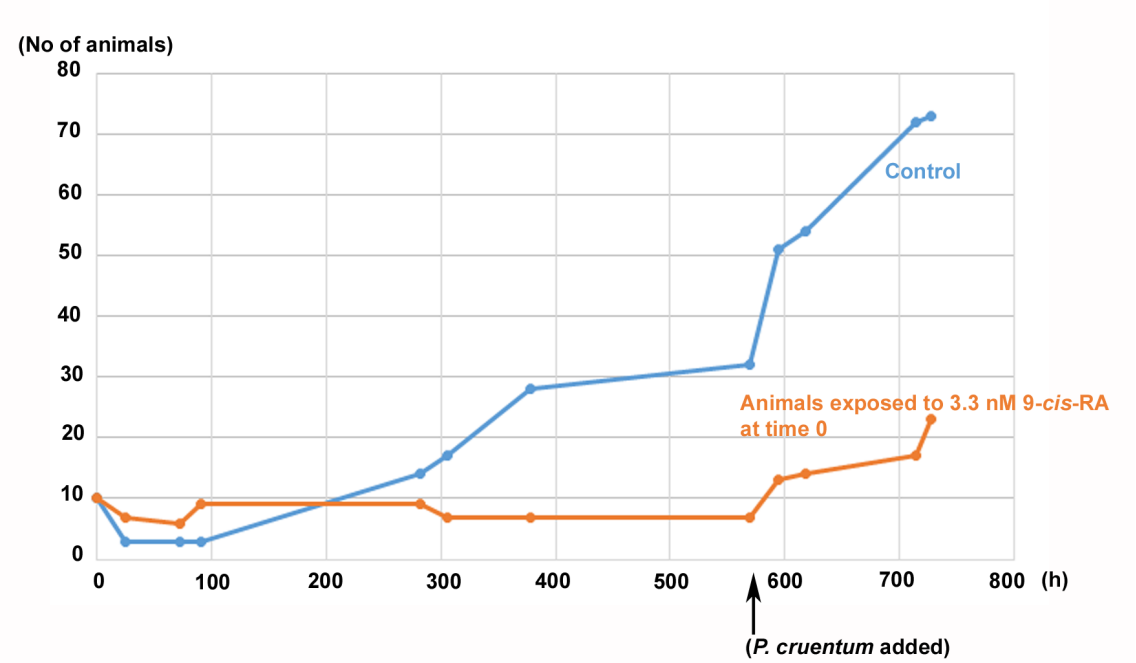

Figure 14: Continuation of the experiment shown in Fig. 13D. The animal cultures (started from stationary cultures fed by a naturally established milieu in a laboratory aquarium) were transferred to new Petri dishes and left for 6h to settle down. The cultures were photographed for measuring the surface and perimeter of the animals, subsequently fed with a suspension of *Chlorella sp*., and exposed to 3.3 nM 9-*cis*-RA or hormone-free vehicle; here the time was set as 'time 0'. The cultures were incubated for 24 h in the dark, photographed again for the surface and perimeter measurements and cultivated for an additional ~24 days at natural illumination in the laboratory (location: 49.98167N, 14.48725E with windows oriented WbS (azimuth 260°)). The slow growth visible in the control culture between 380 h and approximately 550 h corresponded to cloudy days and the faster growth corresponded to sunny days. After 24 days of incuba-

tion the cultures received additional feeding with *Porphyridium cruentum* which stimulated growth of both, the control culture and the culture exposed to 9-*cis*-RA (without a change of the culture medium). The experiment shows that animals arrested by the treatment with 9-*cis*-RA were arrested in growth but retained the potential to proliferate in response to feeding by *P. cruentum*. It has to be taken into account that several uncontrolled factors are likely to influence the growth of both cultures such as degradation or isomerization of 9-*cis*-RA in the experimental culture, or the possible growth of additional microorganisms in prolonged cultures. Natural illumination is also variable despite that external and internal lamellar window blinds were used for prevention of direct exposure of cultures to afternoon sunshine.

Results of part II

We recognized the previously falsely annotated orthologue of MED28 in *C. elegans* as orthologue of perilipin, now named plin-1. We did so by showing its localization and co-localization with transgenic human perilipin orthologues on the surface of lipid droplets that were visualized using LipidTox staining *in vitro* or by *in vivo* CARS microscopy. Furthermore, we provided a functional analysis by gene knock-down and knock-out studies, which resulted in differential intracellular distribution of lipid droplets. Routine sequence analysis did not reveal homology and identification of the perilipin orthologue in *C. elegans* required extensive statistical analysis of hidden Markov profiles in a various number of diverse sequences. Intriguingly, the striking sequence similarity between *plin-1* and *mdt-28* raises the question about a possible overlap in function.

Further sequence analysis then revealed F28F8.5 as the most likely orthologue of MED28 in *C. elegans* (now named MDT-28). We showed localization of GFP-tagged

MDT-28 within the cytoplasm and nucleus. Using a radioactive binding assay, we confirmed interaction of MDT-28 with mediator subunit 6 and 30. Functionally, *mdt-28* knockdown resulted in developmental defects with embryonic and larval arrest in the majority of cases. Animals with complete knockout showed defective development most pronounced in later larval stages.

Discussion

Nuclear receptor signaling is one of the essential regulatory pathways unique to metazoan species. The structure and function of nuclear receptors allow for direct response in the presence or absence of a ligand without the need for an intermediary cascade. Thereby, it represents a regulatory system highly adaptive to evolutionary changes that is not only subject to mutations involving its genes, but also with regards to evolution of ligands and downstream regulatory units such as the Mediator complex. This is exemplified by tissue specific NR function (Pak et al., 2005) and the existence species specific high affinity ligands for receptor orthologues executing similar functions. In vertebrates, the endocrine system regulates various key aspects of cellular and organismal homeostasis. As such, it is not only e.g. directly influencing the reproductive cycle by orchestrating the development of the oocyte and enabling, as well as maintaining, a favorable environment after fertilization, but it is also involved in homeostasis of the somatic tissue. Even though, by definition, an endocrine system can only be present in an organism possessing a vascular system and ligands that are distributed by it, responsive NR networks can be found in a variety of invertebrate species and the appearance of specialized endocrine gland tissue reflects the importance and evolutionary plasticity of

NR signaling. Keeping in mind this high plasticity of NR signaling it is therefore necessary to integrate evolutionary and functionalistic aspects in order to gain a better understanding of NR regulated gene expression. Analysis of NR function in different species by comparative endocrinology could thus eventually reveal previously unrecognized pathological mechanisms of NRs in human diseases such as cancer. In line with this, studying NR networks in basal metazoan species might unravel the most basal functions of NRs, which adapted during the course of evolution to form new regulatory layers allowing for increasingly complex metazoan organisms.

***Trichoplax adhaerens* codes for a functional, ligand responsive NR complement**

Whole genome sequencing revealed the presence of a four NR complement in *Trichoplax adhaerens*. Of those, COUP-TF, HNF4 and RXR belong to the NR2 subfamily of nuclear receptors that is thought to be the most ancient NR subfamily, because members of it are found in all basal metazoan species (e.g.Porifera or Cnidaria, see **Table 1**), while NRs of the other subfamilies probably evolved during two waves of gene duplication (Escriva et al., 2004). Analysis of the TaRXR gene sequence revealed high sequence identity with human RXR, suggesting not only structural, but also functional relatedness. In line with that, it shows similar nanomolar affinity to 9-*cis*-RA as cnidarian jRXR (Kostrouch et al., 1998) and vertebrate RXR (Allenby et al., 1993a), clearly identifying TaRXR as an orthologue of vertebrate RXR. With regards to its proposed position within the phylogenetic tree, placozoan TaRXR thus probably represents the most basal liganded nuclear receptor known to date.

Since autoregulation, as well as cross-regulation by their ligands has been shown for a large number of NRs (Tata, 1994), we searched whether 9-*cis*-RA affects the expression of TaRXR relative to the other *T. adhaerens* NRs. Our results showed not only effects

on specific gene expression in response to very low concentrations of 9-*cis*-RA (at 1 or 3 nM), but also an additional dose-dependent reverse effect of higher concentrations. Even though it cannot be ruled out that higher ligand concentrations might affect any of the remaining NRs, the results are most likely in line with our binding experiments that suggested an additional, low affinity, but high affinity binding site. Furthermore, 9-*cis*-RA was shown to increase RXR protein turnover by protein degradation in mammalian cell lines (Nomura et al., 1999). Although it is not clear if 9-*cis*-RA is the natural ligand for RXRs (Wolf, 2006, Ruhl et al., 2015) conserved in all metazoan phyla studied to date, we show not only that 9-*cis*-RA binds TaRXR with nanomolar affinity but also positively regulates its expression, which resembles auto-activation of several NRs in vertebrates [e.g. ER and TR (Tata, 1994, Bagamasbad and Denver, 2011)].

Furthermore, three out of four NRs constituting the NR complement in *T. adhaerens* respond to treatment by 9-*cis*-RA at transcriptional level. Two NRs, RXR itself and ERR respond positively to nanomolar concentrations of 9-*cis*-RA, while COUP-TF, which often acts as an inhibitor of specific gene expression (Tran et al., 1992), is regulated negatively by 9-*cis*-RA. Interestingly, COUP-TF was recently shown to be inactivated by small hydrophobic molecules (Le Guevel et al., 2017). The regulatory connections of *T. adhaerens* NRs places the autoregulation and cross-regulation of NRs to the base of metazoan evolution.

Transcriptional regulation of malic enzyme subspecialized during evolution

The retinoid acid receptor is a dimerization partner for numerous NRs and, together with the thyroid hormone receptor regulates expression of malic enzyme in mammals (Dozin et al., 1985a, Dozin et al., 1985b, Petty et al., 1990, Petty et al., 1989). Cell-type specific differences of this regulation have been associated with expression levels of

RXRα (Fang and Hillgartner, 2000, Hillgartner et al., 1992), suggesting regulation of malic enzyme expression by RXR has been conserved during evolution at least partially. This is in line with our experimental data showing probably RXR mediated induction of malic enzyme by nanomolar concentrations of 9-*cis*-RA *in vivo*. These results indicate that RXR dependent regulation of malic enzyme was present at the base of metazoan evolution and that additional regulation by TR represents an innovation of triploblastic species (Bilateria), indicating attenuation of RXR dependent regulation of gene expression through additional regulatory layers.

Ancestral NRs probably sensed environmental and food derived ligands

In our feeding assay we showed that food composition is more important for *T. adhaerens* growth and propagation than its quantity, indicating that specific food constituents are required for development and reproduction. Alteration of development and reproduction rates were readily observed after addition of red pigment containing algae as an additional food source, while the effect of 9-*cis*-RA on *T. adhaerens* culture was dependent upon algal food composition, eventually leading to growth arrest, morphological changes and an increase in isoperimetric value as a measure of circularity. These observations indicate that a specific food constituent present in red pigment containing algae is interfering with the 9-*cis*-RA regulatory potential. The increase in isoperimetric value and growth arrest suggest 9-*cis*-RA, as well as food constituent mediated regulation of stem cells within the peripheral area of *T. adhaerens*, eventually stimulating differentiation into specialized cell types. Considering the high affinity of TaRXR to 9-*cis*-RA and the dynamically functioning NR network, this regulation is probably mediated through TaRXR within this network, which is supported by the relative changes of the

NR complement observed in differently sized animals, even though an effect on the remaining NRs cannot be excluded.

It seems likely that very low concentrations of natural ligands including 9-*cis*-RA or similarly shaped molecules or other molecules present in the algal food or produced from algal food as metabolites in *T. adhaerens* regulate the gene expression via RXR in *T. adhaerens*. This may be connected with *T. adhaerens* strong response to light exposure visible as coordinated relocations of animals inside laboratory culture containers and a strong influence of annual seasons on *T. adhaerens* propagation rates observed in laboratories localized in temperate geographical zones. The 9-*cis* conformation of RA is not only sensitive to light exposure with its reversal to all-*trans* conformation, but it can also be formed by specific UV irradiation from all-*trans* conformation up to 10% as shown by Dr. Hans Cahnmann (Cahnmann, 1995).

Furthermore, the chlorophyll hydrophobic side chain, which anchors the molecule to the chloroplast thylakoid membrane is metabolized to phytol that was shown to act as an RXR agonist (Kitareewan et al., 1996). Other molecules called rexinoids, which often contain aromatic rings in their structure, act as RXR agonists or antagonists (Dawson and Xia, 2012). Lately, another group of ligands called organotins was shown to affect regulation by RXR (le Maire et al., 2009). It has been proposed that RXRs can bind a larger group of polyunsaturated fatty acids (docosahexaenoic acid and arachidonic acid) and act as their sensor (de Urquiza et al., 2000, Lengqvist et al., 2004).

The high sensitivity of *T. adhaerens* to 9-*cis*-RA might be explained by several scenarios. The activation of RXR by 9-*cis*-RA or similar compounds has been documented in vertebrates (Allenby et al., 1993b, Ruhl et al., 2015, de Lera et al., 2016) and the observation of 9-*cis*-RA induced growth arrest is similar as data reported on mammalian cells (e.g. (Wente et al., 2007)). However, the concentration of 9-*cis*-RA used in

our experiments is approximately 30 to 3000 times lower than the levels reported in most mammalian systems. Furthermore, the exceptionally high sensitivity of *T. adhaerens* to 9-*cis*-RA implies the possibility that the originally very strong regulation mediated by NRs might have been softened or inhibited by additionally evolved mechanisms. To our knowledge, there are no reports of 100% lethal effects of exposure to low nanomolar levels of 9-*cis*-RA in any metazoan organism. It can thus be speculated whether these mechanisms were likely to evolve to modulate 9-*cis*-RA's or similar ligand's regulatory potential further and might involve stronger regulations by heterodimerization partners of RXR and enzymatic or transport mechanisms regulating the availability of ligands in cells and tissues of phylogenetically more recent metazoan species. Although our experimental data regarding the reversal of 9-*cis*-RA induced growth arrest upon feeding *T. adhaerens* with *Porphyridium cruentum* (**Figure 14**) cannot with certainty show that constituents of *Porphyridium* are involved in modifying 9-*cis*-RA action, they indicate a direct or indirect counter-mechanism.

NR conveyed signals are integrated with cellular status through the mediator complex in Metazoa

While ancestral NRs and other regulatory pathways were needed to allow for complex multicellularity, other mechanisms capable of communicating the cell status towards the transcriptional machinery and thereby enabling integration of cell specific with overall organismal homeostasis had to evolve concomitantly. Previous work already established a possible connection between proteome status and gene expression by SKP-1 and BIR in *C. elegans* through interaction with various nuclear and cytoplasmic proteins (e.g. transcription factors and cytoskeletal proteins)(Kostrouch et al., 2014). Similarly, the mediator subunit 28 was also localized in the cytoplasm and probably serves dual func-

tion (Kostrouchova et al., 2017). Keeping in mind the modular structure of the mediator complex allowing for cell type specific transcriptional regulation and the presence of metazoan specific MED28, it can thus be hypothesized that orthologues of MED28 are capable of linking cellular structural status with gene expression in Metazoa. Such regulatory mechanism has been shown to be exerted by several, primarily cytoplasmic structural proteins, such as those interacting with steroid receptors (George et al., 2009), FOX transcription factors (Gan et al., 2005, Wang et al., 2015) and also BIR-1/Survivin (Kostrouch et al., 2014). Signals conveyed by NRs are thus probably modified at the level of the transcriptional core machinery allowing for cell type specific gene regulation that was also shown to be mediated by NR cofactors.

Conclusion

Gene expression is already tightly regulated in unicellular organisms, but true multicellularity requires tight homeostasis not only on a single cell, but also on an organismal level in which cells have to lose fitness by performing specialized functions in order to increase fitness of the whole organism.

By characterization of the NR complement in *T. adhaerens* we showed that functional and liganded NRs can be placed at the base of metazoan evolution. Furthermore, our results suggest that NRs probably served as environmental sensors. Our experimental data support the concept that regulation of gene expression by NRs subspecialized and new regulatory layers appeared during the course of evolution, while ancestral regulation attenuated over time, and that the adaptations of gene expression by NRs reflect the evolution of increasingly complex metazoans, which is in line with the breakdown of regulatory layers in cancer cells according to the atavistic theory. Our results are in line with the notion that these environmental and, later-on, endocrine cues are probably

modified by structural proteins signaling structural cell status to the transcriptional core machinery in metazoans, thereby providing a link between environmental/organismal, as well as cell structural status.

In essence, our work provides new insights regarding the adaptations of regulatory layers involved in gene expression during the course of animal evolution which might help to understand the consequences of mediatory loss that occurs in cancer.

References

ACEVEDO, M. L. & KRAUS, W. L. 2004. Transcriptional activation by nuclear receptors. *Essays Biochem,* 40**,** 73-88.

ALLEN, B. L. & TAATJES, D. J. 2015. The Mediator complex: a central integrator of transcription. *Nat Rev Mol Cell Biol,* 16**,** 155-66.

ALLENBY, G., BOCQUEL, M. T., SAUNDERS, M., KAZMER, S., SPECK, J., ROSENBERGER, M., LOVEY, A., KASTNER, P., GRIPPO, J. F., CHAMBON, P. & ET AL. 1993a. Retinoic acid receptors and retinoid X receptors: interactions with endogenous retinoic acids. *Proc Natl Acad Sci U S A,* 90**,** 30-4.

ALLENBY, G., BOCQUEL, M. T., SAUNDERS, M., KAZMER, S., SPECK, J., ROSENBERGER, M., LOVEY, A., KASTNER, P., GRIPPO, J. F., CHAMBON, P. & LEVIN, A. A. 1993b. Retinoic acid receptors and retinoid X receptors: interactions with endogenous retinoic acids. *Proc Natl Acad Sci U S A,* 90**,** 30-4.

ALTSCHUL, S. F., MADDEN, T. L., SCHAFFER, A. A., ZHANG, J., ZHANG, Z., MILLER, W. & LIPMAN, D. J. 1997. Gapped BLAST and PSI-BLAST: a new generation of protein database search programs. *Nucleic Acids Res,* 25**,** 3389-402.

ANBALAGAN, M., HUDERSON, B., MURPHY, L. & ROWAN, B. G. 2012. Post-translational modifications of nuclear receptors and human disease. *Nucl Recept Signal,* 10**,** e001.

ANSARI, S. A., GANAPATHI, M., BENSCHOP, J. J., HOLSTEGE, F. C., WADE, J. T. & MORSE, R. H. 2012. Distinct role of Mediator tail module in regulation of SAGA-dependent, TATA-containing genes in yeast. *EMBO J,* 31**,** 44-57.

ANSARI, S. A. & MORSE, R. H. 2013. Mechanisms of Mediator complex action in transcriptional activation. *Cell Mol Life Sci,* 70**,** 2743-56.

ARKELL, R. M., FOSSAT, N. & TAM, P. P. 2013. Wnt signalling in mouse gastrulation and anterior development: new players in the pathway and signal output. *Curr Opin Genet Dev,* 23**,** 454-60.

ARNAL, A., UJVARI, B., CRESPI, B., GATENBY, R. A., TISSOT, T., VITTECOQ, M., EWALD, P. W., CASALI, A., DUCASSE, H., JACQUELINE, C., MISSE, D., RENAUD, F., ROCHE, B. & THOMAS, F. 2015. Evolutionary perspective of cancer: myth, metaphors, and reality. *Evol Appl,* 8**,** 541-4.

ARTAVANIS-TSAKONAS, S., RAND, M. D. & LAKE, R. J. 1999. Notch signaling: cell fate control and signal integration in development. *Science,* 284**,** 770-6.

ASHCROFT, G. S., YANG, X., GLICK, A. B., WEINSTEIN, M., LETTERIO, J. L., MIZEL, D. E., ANZANO, M., GREENWELL-WILD, T., WAHL, S. M., DENG, C. & ROBERTS, A. B. 1999. Mice lacking Smad3 show accelerated wound healing and an impaired local inflammatory response. *Nat Cell Biol,* 1**,** 260-6.

BABONIS, L. S. & MARTINDALE, M. Q. 2017. Phylogenetic evidence for the modular evolution of metazoan signalling pathways. *Philos Trans R Soc Lond B Biol Sci,* 372.

BAEK, S. H. & KIM, K. I. 2014. Emerging roles of orphan nuclear receptors in cancer. *Annu Rev Physiol,* 76**,** 177-95.

BAGAMASBAD, P. & DENVER, R. J. 2011. Mechanisms and significance of nuclear receptor auto- and cross-regulation. *Gen Comp Endocrinol,* 170**,** 3-17.

BAIDOOBONSO, S. M., GUIDI, B. W. & MYERS, L. C. 2007. Med19(Rox3) regulates Intermodule interactions in the Saccharomyces cerevisiae mediator complex. *J Biol Chem,* 282**,** 5551-9.

BAIN, D. L., HENEGHAN, A. F., CONNAGHAN-JONES, K. D. & MIURA, M. T. 2007. Nuclear receptor structure: implications for function. *Annu Rev Physiol,* 69**,** 201-20.

BAKER, M. E. 2005. Xenobiotics and the evolution of multicellular animals: emergence and diversification of ligand-activated transcription factors. *Integr Comp Biol,* 45**,** 172-8.

BARON, M. 2003. An overview of the Notch signalling pathway. *Semin Cell Dev Biol,* 14**,** 113-9.

BAWA-KHALFE, T., CHENG, J., WANG, Z. & YEH, E. T. 2007. Induction of the SUMO-specific protease 1 transcription by the androgen receptor in prostate cancer cells. *J Biol Chem,* 282**,** 37341-9.

BEATO, M. & KLUG, J. 2000. Steroid hormone receptors: an update. *Hum Reprod Update,* 6**,** 225-36.

BECARES, N., GAGE, M. C. & PINEDA-TORRA, I. 2017. Posttranslational Modifications of Lipid-Activated Nuclear Receptors: Focus on Metabolism. *Endocrinology,* 158**,** 213-225.

BERRABAH, W., AUMERCIER, P., LEFEBVRE, P. & STAELS, B. 2011. Control of nuclear receptor activities in metabolism by post-translational modifications. *FEBS Lett,* 585**,** 1640-50.

BEYER, K. S., BEAUCHAMP, R. L., LEE, M. F., GUSELLA, J. F., NAAR, A. M. & RAMESH, V. 2007. Mediator subunit MED28 (Magicin) is a repressor of smooth muscle cell differentiation. *J Biol Chem,* 282**,** 32152-7.

BISSELL, M. J. & HINES, W. C. 2011. Why don't we get more cancer? A proposed role of the microenvironment in restraining cancer progression. *Nat Med,* 17**,** 320-9.

BLOMBACH, F., MAKAROVA, K. S., MARRERO, J., SIEBERS, B., KOONIN, E. V. & VAN DER OOST, J. 2009. Identification of an ortholog of the eukaryotic RNA polymerase III subunit RPC34 in Crenarchaeota and Thaumarchaeota suggests specialization of RNA polymerases for coding and non-coding RNAs in Archaea. *Biol Direct,* 4**,** 39.

BONNER, J. T. 1998a. The origins of multicellularity. *Integrative Biology: Issues, News, and Reviews,* 1**,** 27-36.

BONNER, J. T. 1998b. Volvox: Molecular-Genetic Origins of Multicellularity and Cellular Differentiation. David L. Kirk. *The Quarterly Review of Biology,* 73**,** 506-506.

BOURBON, H. M. 2008. Comparative genomics supports a deep evolutionary origin for the large, four-module transcriptional mediator complex. *Nucleic Acids Res,* 36**,** 3993-4008.

BRIDGHAM, J. T., EICK, G. N., LARROUX, C., DESHPANDE, K., HARMS, M. J., GAUTHIER, M. E., ORTLUND, E. A., DEGNAN, B. M. & THORNTON, J. W. 2010. Protein evolution by molecular tinkering: diversification of the nuclear receptor superfamily from a ligand-dependent ancestor. *PLoS Biol,* 8.

BRZOZOWSKI, A. M., PIKE, A. C., DAUTER, Z., HUBBARD, R. E., BONN, T., ENGSTROM, O., OHMAN, L., GREENE, G. L., GUSTAFSSON, J. A. & CARLQUIST, M. 1997. Molecular basis of agonism and antagonism in the oestrogen receptor. *Nature,* 389**,** 753-8.

BUSSEY, K. J., CISNEROS, L. H., LINEWEAVER, C. H. & DAVIES, P. C. W. 2017. Ancestral gene regulatory networks drive cancer. *Proc Natl Acad Sci U S A,* 114**,** 6160-6162.

BUTTERFIELD, N. J. 2000. Bangiomorpha pubescens n. gen., n. sp.: implications for the evolution of sex, multicellularity, and the Mesoproterozoic/Neoproterozoic radiation of eukaryotes. *Paleobiology,* 26**,** 386-404.

CAHNMANN, H. J. 1995. A fast photoisomerization method for the preparation of tritium-labeled 9-cis-retinoic acid of high specific activity. *Anal Biochem,* 227**,** 49-53.

CARROLL, J. S., MEYER, C. A., SONG, J., LI, W., GEISTLINGER, T. R., EECKHOUTE, J., BRODSKY, A. S., KEETON, E. K., FERTUCK, K. C., HALL, G. F., WANG, Q., BEKIRANOV, S., SEMENTCHENKO, V., FOX, E. A., SILVER, P. A., GINGERAS, T. R., LIU, X. S. & BROWN, M. 2006. Genome-wide analysis of estrogen receptor binding sites. *Nat Genet,* 38**,** 1289-97.

CASAS-SELVES, M. & DEGREGORI, J. 2011. How cancer shapes evolution, and how evolution shapes cancer. *Evolution (N Y),* 4**,** 624-634.

CEVHER, M. A., SHI, Y., LI, D., CHAIT, B. T., MALIK, S. & ROEDER, R. G. 2014. Reconstitution of active human core Mediator complex reveals a critical role of the MED14 subunit. *Nat Struct Mol Biol,* 21**,** 1028-34.

CHAN, S. R. & BLACKBURN, E. H. 2004. Telomeres and telomerase. *Philos Trans R Soc Lond B Biol Sci,* 359**,** 109-21.

CHAWLA, A., REPA, J. J., EVANS, R. M. & MANGELSDORF, D. J. 2001. Nuclear receptors and lipid physiology: opening the X-files. *Science,* 294**,** 1866-70.

CHEN, J. D. & EVANS, R. M. 1995. A transcriptional co-repressor that interacts with nuclear hormone receptors. *Nature,* 377**,** 454-7.

CHEN, W. & ROEDER, R. G. 2011. Mediator-dependent nuclear receptor function. *Semin Cell Dev Biol,* 22**,** 749-58.

CHOI, S. J., CHUNG, S. S., RHO, E. J., LEE, H. W., LEE, M. H., CHOI, H. S., SEOL, J. H., BAEK, S. H., BANG, O. S. & CHUNG, C. H. 2006. Negative modulation of RXRalpha transcriptional activity by small ubiquitin-related modifier (SUMO) modification and its reversal by SUMO-specific protease SUSP1. *J Biol Chem,* 281**,** 30669-77.

CHUGHTAI, A. A., KASSAK, F., KOSTROUCHOVA, M., NOVOTNY, J. P., KRAUSE, M. W., SAUDEK, V., KOSTROUCH, Z. & KOSTROUCHOVA, M. 2015. Perilipin-related protein regulates lipid metabolism in C. elegans. *PeerJ,* 3**,** e1213.

CLINCKEMALIE, L., VANDERSCHUEREN, D., BOONEN, S. & CLAESSENS, F. 2012. The hinge region in androgen receptor control. *Mol Cell Endocrinol,* 358**,** 1-8.

COLLINS, A. G., CARTWRIGHT, P., MCFADDEN, C. S. & SCHIERWATER, B. 2005. Phylogenetic context and Basal metazoan model systems. *Integr Comp Biol,* 45**,** 585-94.

CONAWAY, R. C. & CONAWAY, J. W. 2011. Origins and activity of the Mediator complex. *Semin Cell Dev Biol,* 22**,** 729-34.

CONAWAY, R. C. & CONAWAY, J. W. 2013. The Mediator complex and transcription elongation. *Biochim Biophys Acta,* 1829**,** 69-75.

COSMA, M. P. 2002. Ordered recruitment: gene-specific mechanism of transcription activation. *Mol Cell,* 10**,** 227-36.

COX, C. J., FOSTER, P. G., HIRT, R. P., HARRIS, S. R. & EMBLEY, T. M. 2008. The archaebacterial origin of eukaryotes. *Proc Natl Acad Sci U S A,* 105**,** 20356-61.

CUFF, J. A. & BARTON, G. J. 2000. Application of multiple sequence alignment profiles to improve protein secondary structure prediction. *Proteins,* 40**,** 502-11.

D'ALESSIO, J. A., NG, R., WILLENBRING, H. & TJIAN, R. 2011. Core promoter recognition complex changes accompany liver development. *Proc Natl Acad Sci U S A,* 108**,** 3906-11.

DARIMONT, B. D., WAGNER, R. L., APRILETTI, J. W., STALLCUP, M. R., KUSHNER, P. J., BAXTER, J. D., FLETTERICK, R. J. & YAMAMOTO, K. R. 1998. Structure and specificity of nuclear receptor-coactivator interactions. *Genes Dev,* 12**,** 3343-56.

DAVIES, P. C. & LINEWEAVER, C. H. 2011. Cancer tumors as Metazoa 1.0: tapping genes of ancient ancestors. *Phys Biol,* 8**,** 015001.

DAWSON, M. I. & XIA, Z. B. 2012. The retinoid X receptors and their ligands. *Biochimica Et Biophysica Acta-Molecular and Cell Biology of Lipids,* 1821**,** 21-56.

DE LERA, A. R., KREZEL, W. & RUHL, R. 2016. An Endogenous Mammalian Retinoid X Receptor Ligand, At Last! *ChemMedChem,* 11**,** 1027-37.

DE URQUIZA, A. M., LIU, S., SJOBERG, M., ZETTERSTROM, R. H., GRIFFITHS, W., SJOVALL, J. & PERLMANN, T. 2000. Docosahexaenoic acid, a ligand for the retinoid X receptor in mouse brain. *Science,* 290**,** 2140-4.

DEEGAN, B. J., BHAT, V., SELDEEN, K. L., MCDONALD, C. B. & FAROOQ, A. 2011. Genetic variations within the ERE motif modulate plasticity and energetics of binding of DNA to the ERalpha nuclear receptor. *Arch Biochem Biophys,* 507**,** 262-70.

DELMOTTE, M.-H., TAHAYATO, A., FORMSTECHER, P. & LEFEBVRE, P. 1999. Serine 157, a retinoic acid receptor α residue phosphorylated by protein kinase C in vitro, is involved in RXR· RARα heterodimerization and transcriptional activity. *Journal of Biological Chemistry,* 274**,** 38225-38231.

DI TOMMASO, P., MORETTI, S., XENARIOS, I., OROBITG, M., MONTANYOLA, A., CHANG, J. M., TALY, J. F. & NOTREDAME, C. 2011. T-Coffee: a web server for the multiple sequence alignment of protein and RNA sequences using structural information and homology extension. *Nucleic Acids Res,* 39**,** W13-7.

DICKINSON, D. J. & GOLDSTEIN, B. 2016. CRISPR-Based Methods for Caenorhabditis elegans Genome Engineering. *Genetics,* 202**,** 885-901.

DICKINSON, D. J., PANI, A. M., HEPPERT, J. K., HIGGINS, C. D. & GOLDSTEIN, B. 2015. Streamlined Genome Engineering with a Self-Excising Drug Selection Cassette. *Genetics,* 200**,** 1035-49.

DICKINSON, D. J., WARD, J. D., REINER, D. J. & GOLDSTEIN, B. 2013. Engineering the Caenorhabditis elegans genome using Cas9-triggered homologous recombination. *Nat Methods,* 10**,** 1028-34.

DIJKE, P. & HELDIN, C.-H. 2007. *Smad signal transduction: Smads in proliferation, differentiation and disease*, Springer.

DOAN, T. B., GRAHAM, J. D. & CLARKE, C. L. 2017. Emerging functional roles of nuclear receptors in breast cancer. *J Mol Endocrinol,* 58**,** R169-R190.

DOMAZET-LOSO, T. & TAUTZ, D. 2010. Phylostratigraphic tracking of cancer genes suggests a link to the emergence of multicellularity in metazoa. *BMC Biol,* 8**,** 66.

DOZIN, B., CAHNMANN, H. J. & NIKODEM, V. M. 1985a. Identification of thyroid hormone receptors in rat liver nuclei by photoaffinity labeling with L-thyroxine and triiodo-L-thyronine. *Biochemistry,* 24**,** 5197-202.
DOZIN, B., MAGNUSON, M. A. & NIKODEM, V. M. 1985b. Tissue-specific regulation of two functional malic enzyme mRNAs by triiodothyronine. *Biochemistry,* 24**,** 5581-6.
EGEA, P. F., KLAHOLZ, B. P. & MORAS, D. 2000. Ligand-protein interactions in nuclear receptors of hormones. *FEBS letters,* 476**,** 62-7.
EITEL, M., FRANCIS, W., OSIGUS, H.-J., KREBS, S., VARGAS, S., BLUM, H., WILLIAMS, G. A., SCHIERWATER, B. & WÖRHEIDE, G. 2017. A taxogenomics approach uncovers a new genus in the phylum Placozoa. *bioRxiv*.
EITEL, M., GUIDI, L., HADRYS, H., BALSAMO, M. & SCHIERWATER, B. 2011. New insights into placozoan sexual reproduction and development. *PLoS One,* 6**,** e19639.
EITEL, M., OSIGUS, H. J., DESALLE, R. & SCHIERWATER, B. 2013. Global diversity of the Placozoa. *PLoS One,* 8**,** e57131.
EITEL, M. & SCHIERWATER, B. 2010. The phylogeography of the Placozoa suggests a taxon-rich phylum in tropical and subtropical waters. *Mol Ecol,* 19**,** 2315-27.
ENDER, A. & SCHIERWATER, B. 2003. Placozoa Are Not Derived Cnidarians: Evidence from Molecular Morphology. *Molecular Biology and Evolution,* 20**,** 130-134.
ERWIN, D. H. 2015. Early metazoan life: divergence, environment and ecology. *Philos Trans R Soc Lond B Biol Sci,* 370.
ESCRIVA, H., BERTRAND, S. & LAUDET, V. 2004. The evolution of the nuclear receptor superfamily. *Essays Biochem,* 40**,** 11-26.
ESCRIVA, H., DELAUNAY, F. & LAUDET, V. 2000. Ligand binding and nuclear receptor evolution. *Bioessays,* 22**,** 717-27.
ESCRIVA, H., HOLLAND, N. D., GRONEMEYER, H., LAUDET, V. & HOLLAND, L. Z. 2002. The retinoic acid signaling pathway regulates anterior/posterior patterning in the nerve cord and pharynx of amphioxus, a chordate lacking neural crest. *Development,* 129**,** 2905-16.
ESCRIVA, H., SAFI, R., HANNI, C., LANGLOIS, M. C., SAUMITOU-LAPRADE, P., STEHELIN, D., CAPRON, A., PIERCE, R. & LAUDET, V. 1997. Ligand binding was acquired during evolution of nuclear receptors. *Proc Natl Acad Sci U S A,* 94**,** 6803-8.
FANG, X. & HILLGARTNER, F. B. 2000. Alterations in retinoid X receptor-alpha expression contribute to cell-type dependent differences in thyroid hormone regulation of malic enzyme transcription. *Mol Cell Endocrinol,* 164**,** 41-52.
FORMAN, B. M. & SAMUELS, H. H. 1990a. Dimerization among nuclear hormone receptors. *New Biol,* 2**,** 587-94.
FORMAN, B. M. & SAMUELS, H. H. 1990b. Interactions among a subfamily of nuclear hormone receptors: the regulatory zipper model. *Mol Endocrinol,* 4**,** 1293-301.
FROLS, S. 2013. Archaeal biofilms: widespread and complex. *Biochem Soc Trans,* 41**,** 393-8.
FU, M., RAO, M., WANG, C., SAKAMAKI, T., WANG, J., DI VIZIO, D., ZHANG, X., ALBANESE, C., BALK, S., CHANG, C., FAN, S., ROSEN, E., PALVIMO, J. J., JANNE, O. A., MURATOGLU, S., AVANTAGGIATI, M. L. & PESTELL, R. G. 2003. Acetylation of androgen receptor enhances coactivator binding and promotes prostate cancer cell growth. *Mol Cell Biol,* 23**,** 8563-75.

GAN, L., ZHENG, W., CHABOT, J. G., UNTERMAN, T. G. & QUIRION, R. 2005. Nuclear/cytoplasmic shuttling of the transcription factor FoxO1 is regulated by neurotrophic factors. *J Neurochem,* 93**,** 1209-19.
GAZAVE, E., LAPEBIE, P., RICHARDS, G. S., BRUNET, F., ERESKOVSKY, A. V., DEGNAN, B. M., BORCHIELLINI, C., VERVOORT, M. & RENARD, E. 2009. Origin and evolution of the Notch signalling pathway: an overview from eukaryotic genomes. *BMC Evol Biol,* 9**,** 249.
GEORGE, A. A., SCHILTZ, R. L. & HAGER, G. L. 2009. Dynamic access of the glucocorticoid receptor to response elements in chromatin. *Int J Biochem Cell Biol,* 41**,** 214-24.
GERHART, J. 1999. 1998 Warkany lecture: signaling pathways in development. *Teratology,* 60**,** 226-39.
GERMAIN, P., STAELS, B., DACQUET, C., SPEDDING, M. & LAUDET, V. 2006. Overview of nomenclature of nuclear receptors. *Pharmacol Rev,* 58**,** 685-704.
GLASS, C. K., ROSE, D. W. & ROSENFELD, M. G. 1997. Nuclear receptor coactivators. *Curr Opin Cell Biol,* 9**,** 222-32.
GORBUNOVA, V. & SELUANOV, A. 2009. Coevolution of telomerase activity and body mass in mammals: from mice to beavers. *Mech Ageing Dev,* 130**,** 3-9.
GREENWALD, I. 1998. LIN-12/Notch signaling: lessons from worms and flies. *Genes Dev,* 12**,** 1751-62.
GROSBERG, R. K. & STRATHMANN, R. R. 2007. The Evolution of Multicellularity: A Minor Major Transition? *Annual Review of Ecology, Evolution, and Systematics,* 38**,** 621-654.
GUINDON, S., DUFAYARD, J. F., LEFORT, V., ANISIMOVA, M., HORDIJK, W. & GASCUEL, O. 2010. New algorithms and methods to estimate maximum-likelihood phylogenies: assessing the performance of PhyML 3.0. *Syst Biol,* 59**,** 307-21.
HAHN, S. 2004. Structure and mechanism of the RNA polymerase II transcription machinery. *Nat Struct Mol Biol,* 11**,** 394-403.
HALANYCH, K. M. 2004. Invertebrates; Invertebrate Zoology: A Functional Evolutionary Approach. *Systematic Biology,* 53**,** 662-664.
HALL, J. M., MCDONNELL, D. P. & KORACH, K. S. 2002. Allosteric regulation of estrogen receptor structure, function, and coactivator recruitment by different estrogen response elements. *Mol Endocrinol,* 16**,** 469-86.
HARPER, T. M. & TAATJES, D. J. 2017. The complex structure and function of Mediator. *J Biol Chem*.
HASHIGUCHI, T., ARAKAWA, S., TAKAHASHI, S., GONZALEZ, F. J., SUEYOSHI, T. & NEGISHI, M. 2016. Phosphorylation of Farnesoid X Receptor at Serine 154 Links Ligand Activation With Degradation. *Mol Endocrinol,* 30**,** 1070-1080.
HELDIN, C. H., MIYAZONO, K. & TEN DIJKE, P. 1997. TGF-beta signalling from cell membrane to nucleus through SMAD proteins. *Nature,* 390**,** 465-71.
HELDRING, N., PAWSON, T., MCDONNELL, D., TREUTER, E., GUSTAFSSON, J. A. & PIKE, A. C. 2007. Structural insights into corepressor recognition by antagonist-bound estrogen receptors. *J Biol Chem,* 282**,** 10449-55.
HELSEN, C. & CLAESSENS, F. 2014. Looking at nuclear receptors from a new angle. *Mol Cell Endocrinol,* 382**,** 97-106.
HELSEN, C., DUBOIS, V., VERFAILLIE, A., YOUNG, J., TREKELS, M., VANCRAENENBROECK, R., DE MAEYER, M. & CLAESSENS, F. 2012.

Evidence for DNA-binding domain--ligand-binding domain communications in the androgen receptor. *Mol Cell Biol,* 32**,** 3033-43.
HENG, H. H., STEVENS, J. B., BREMER, S. W., YE, K. J., LIU, G. & YE, C. J. 2010. The evolutionary mechanism of cancer. *J Cell Biochem,* 109**,** 1072-84.
HERMANSON, O., GLASS, C. K. & ROSENFELD, M. G. 2002. Nuclear receptor coregulators: multiple modes of modification. *Trends Endocrinol Metab,* 13**,** 55-60.
HERRON, M. D., HACKETT, J. D., AYLWARD, F. O. & MICHOD, R. E. 2009. Triassic origin and early radiation of multicellular volvocine algae. *Proc Natl Acad Sci U S A,* 106**,** 3254-8.
HILLGARTNER, F. B., CHEN, W. & GOODRIDGE, A. G. 1992. Overexpression of the alpha-thyroid hormone receptor in avian cell lines. Effects on expression of the malic enzyme gene are selective and cell-specific. *J Biol Chem,* 267**,** 12299-306.
HIPFNER, D. R. & COHEN, S. M. 2004. Connecting proliferation and apoptosis in development and disease. *Nat Rev Mol Cell Biol,* 5**,** 805-15.
HOBERT, O. 2002. PCR fusion-based approach to create reporter gene constructs for expression analysis in transgenic C. elegans. *Biotechniques,* 32**,** 728-30.
HOEIJMAKERS, J. H. 2009. DNA damage, aging, and cancer. *N Engl J Med,* 361**,** 1475-85.
HOLSTEGE, F. C., JENNINGS, E. G., WYRICK, J. J., LEE, T. I., HENGARTNER, C. J., GREEN, M. R., GOLUB, T. R., LANDER, E. S. & YOUNG, R. A. 1998. Dissecting the regulatory circuitry of a eukaryotic genome. *Cell,* 95**,** 717-28.
HOLSTEIN, T. W. 2012. The evolution of the Wnt pathway. *Cold Spring Harb Perspect Biol,* 4**,** a007922.
HOLZER, G., MARKOV, G. V. & LAUDET, V. 2017. Evolution of Nuclear Receptors and Ligand Signaling: Toward a Soft Key-Lock Model? *Curr Top Dev Biol,* 125**,** 1-38.
HORLEIN, A. J., NAAR, A. M., HEINZEL, T., TORCHIA, J., GLOSS, B., KUROKAWA, R., RYAN, A., KAMEI, Y., SODERSTROM, M., GLASS, C. K. & ET AL. 1995. Ligand-independent repression by the thyroid hormone receptor mediated by a nuclear receptor co-repressor. *Nature,* 377**,** 397-404.
HUANG, C. Y., CHOU, Y. H., HSIEH, N. T., CHEN, H. H. & LEE, M. F. 2012. MED28 regulates MEK1-dependent cellular migration in human breast cancer cells. *J Cell Physiol,* 227**,** 3820-7.
HUANG, P., CHANDRA, V. & RASTINEJAD, F. 2010. Structural overview of the nuclear receptor superfamily: insights into physiology and therapeutics. *Annu Rev Physiol,* 72**,** 247-72.
HUMINIECKI, L., GOLDOVSKY, L., FREILICH, S., MOUSTAKAS, A., OUZOUNIS, C. & HELDIN, C. H. 2009. Emergence, development and diversification of the TGF-beta signalling pathway within the animal kingdom. *BMC Evol Biol,* 9**,** 28.
IHARA, J. 1999. Darwinian dynamics: Evolutionary transitions in fitness and individuality by Richard E. Michod. *Complexity,* 5**,** 42-43.
INGHAM, P. W., NAKANO, Y. & SEGER, C. 2011. Mechanisms and functions of Hedgehog signalling across the metazoa. *Nat Rev Genet,* 12**,** 393-406.
INGRAHAM, H. A. & REDINBO, M. R. 2005. Orphan nuclear receptors adopted by crystallography. *Curr Opin Struct Biol,* 15**,** 708-15.
ISSEMANN, I. & GREEN, S. 1990. Activation of a member of the steroid hormone receptor superfamily by peroxisome proliferators. *Nature,* 347**,** 645-50.

ITOH, T., FAIRALL, L., AMIN, K., INABA, Y., SZANTO, A., BALINT, B. L., NAGY, L., YAMAMOTO, K. & SCHWABE, J. W. 2008. Structural basis for the activation of PPARgamma by oxidized fatty acids. *Nat Struct Mol Biol,* 15**,** 924-31.

JACKSON, A. M. & BUSS, L. W. 2009. Shiny spheres of placozoans (Trichoplax) function in anti-predator defense. *Invertebrate Biology,* 128**,** 205-212.

JAKOB, W., SAGASSER, S., DELLAPORTA, S., HOLLAND, P., KUHN, K. & SCHIERWATER, B. 2004. The Trox-2 Hox/ParaHox gene of Trichoplax (Placozoa) marks an epithelial boundary. *Dev Genes Evol,* 214**,** 170-5.

JERONIMO, C., LANGELIER, M. F., BATAILLE, A. R., PASCAL, J. M., PUGH, B. F. & ROBERT, F. 2016. Tail and Kinase Modules Differently Regulate Core Mediator Recruitment and Function In Vivo. *Mol Cell,* 64**,** 455-466.

JERONIMO, C. & ROBERT, F. 2017. The Mediator Complex: At the Nexus of RNA Polymerase II Transcription. *Trends Cell Biol,* 27**,** 765-783.

JIANG, M. S. & HART, G. W. 1997. A subpopulation of estrogen receptors are modified by O-linked N-acetylglucosamine. *J Biol Chem,* 272**,** 2421-8.

JIANG, Y. W., VESCHAMBRE, P., ERDJUMENT-BROMAGE, H., TEMPST, P., CONAWAY, J. W., CONAWAY, R. C. & KORNBERG, R. D. 1998. Mammalian mediator of transcriptional regulation and its possible role as an end-point of signal transduction pathways. *Proc Natl Acad Sci U S A,* 95**,** 8538-43.

JONES, D. T. 1999. Protein secondary structure prediction based on position-specific scoring matrices. *J Mol Biol,* 292**,** 195-202.

JONKER, J. W., STEDMAN, C. A., LIDDLE, C. & DOWNES, M. 2009. Hepatobiliary ABC transporters: physiology, regulation and implications for disease. *Front Biosci (Landmark Ed),* 14**,** 4904-20.

KADESCH, T. 2000. Notch signaling: a dance of proteins changing partners. *Exp Cell Res,* 260**,** 1-8.

KADESCH, T. 2004. Notch signaling: the demise of elegant simplicity. *Curr Opin Genet Dev,* 14**,** 506-12.

KALLENBERGER, B. C., LOVE, J. D., CHATTERJEE, V. K. & SCHWABE, J. W. 2003. A dynamic mechanism of nuclear receptor activation and its perturbation in a human disease. *Nat Struct Biol,* 10**,** 136-40.

KANA, R., KOTABOVA, E., LUKES, M., PAPACEK, S., MATONOHA, C., LIU, L. N., PRASIL, O. & MULLINEAUX, C. W. 2014. Phycobilisome Mobility and Its Role in the Regulation of Light Harvesting in Red Algae. *Plant Physiol,* 165**,** 1618-1631.

KANA, R., KOTABOVA, E., SOBOTKA, R. & PRASIL, O. 2012. Non-photochemical quenching in cryptophyte alga Rhodomonas salina is located in chlorophyll a/c antennae. *PloS one,* 7**,** e29700.

KANG, Y., CHEN, C. R. & MASSAGUE, J. 2003. A self-enabling TGFbeta response coupled to stress signaling: Smad engages stress response factor ATF3 for Id1 repression in epithelial cells. *Mol Cell,* 11**,** 915-26.

KHORASANIZADEH, S. 2004. The nucleosome: from genomic organization to genomic regulation. *Cell,* 116**,** 259-72.

KIEFER, J. C. 2006. Emerging developmental model systems. *Dev Dyn,* 235**,** 2895-9.

KIM, K., THU, N., SAVILLE, B. & SAFE, S. 2003. Domains of estrogen receptor alpha (ERalpha) required for ERalpha/Sp1-mediated activation of GC-rich promoters by estrogens and antiestrogens in breast cancer cells. *Mol Endocrinol,* 17**,** 804-17.

KIM, Y. J. & LIS, J. T. 2005. Interactions between subunits of Drosophila Mediator and activator proteins. *Trends Biochem Sci,* 30**,** 245-9.
KING, N., WESTBROOK, M. J., YOUNG, S. L., KUO, A., ABEDIN, M., CHAPMAN, J., FAIRCLOUGH, S., HELLSTEN, U., ISOGAI, Y., LETUNIC, I., MARR, M., PINCUS, D., PUTNAM, N., ROKAS, A., WRIGHT, K. J., ZUZOW, R., DIRKS, W., GOOD, M., GOODSTEIN, D., LEMONS, D., LI, W., LYONS, J. B., MORRIS, A., NICHOLS, S., RICHTER, D. J., SALAMOV, A., SEQUENCING, J. G., BORK, P., LIM, W. A., MANNING, G., MILLER, W. T., MCGINNIS, W., SHAPIRO, H., TJIAN, R., GRIGORIEV, I. V. & ROKHSAR, D. 2008. The genome of the choanoflagellate Monosiga brevicollis and the origin of metazoans. *Nature,* 451**,** 783-8.
KING-JONES, K. & THUMMEL, C. S. 2005. Nuclear receptors--a perspective from Drosophila. *Nat Rev Genet,* 6**,** 311-23.
KIRK, D. L. 2005. A twelve-step program for evolving multicellularity and a division of labor. *Bioessays,* 27**,** 299-310.
KITAREEWAN, S., BURKA, L. T., TOMER, K. B., PARKER, C. E., DETERDING, L. J., STEVENS, R. D., FORMAN, B. M., MAIS, D. E., HEYMAN, R. A., MCMORRIS, T. & WEINBERGER, C. 1996. Phytol metabolites are circulating dietary factors that activate the nuclear receptor RXR. *Mol Biol Cell,* 7**,** 1153-66.
KNOLL, A. H. 1996. Breathing room for early animals. *Nature,* 382**,** 111-2.
KNOLL, A. H. & CARROLL, S. B. 1999. Early animal evolution: emerging views from comparative biology and geology. *Science,* 284**,** 2129-37.
KNOLL, A. H., JAVAUX, E. J., HEWITT, D. & COHEN, P. 2006. Eukaryotic organisms in Proterozoic oceans. *Philos Trans R Soc Lond B Biol Sci,* 361**,** 1023-38.
KOONIN, E. V. 2010. The origin and early evolution of eukaryotes in the light of phylogenomics. *Genome Biol,* 11**,** 209.
KORNBERG, R. D. 2005. Mediator and the mechanism of transcriptional activation. *Trends Biochem Sci,* 30**,** 235-9.
KOSTROUCH, D., KOSTROUCHOVA, M., YILMA, P., CHUGHTAI, A. A., NOVOTNY, J. P., NOVAK, P., KOSTROUCHOVA, V., KOSTROUCHOVA, M. & KOSTROUCH, Z. 2014. SKIP and BIR-1/Survivin have potential to integrate proteome status with gene expression. *J Proteomics,* 110**,** 93-106.
KOSTROUCH, Z., KOSTROUCHOVA, M., LOVE, W., JANNINI, E., PIATIGORSKY, J. & RALL, J. E. 1998. Retinoic acid X receptor in the diploblast, Tripedalia cystophora. *Proc Natl Acad Sci U S A,* 95**,** 13442-7.
KOSTROUCH, Z., KOSTROUCHOVA, M. & RALL, J. E. 1995. Steroid/thyroid hormone receptor genes in Caenorhabditis elegans. *Proc Natl Acad Sci U S A,* 92**,** 156-9.
KOSTROUCHOVA, M., KOSTROUCH, D., CHUGHTAI, A. A., KASSAK, F., NOVOTNY, J. P., KOSTROUCHOVA, V., BENDA, A., KRAUSE, M. W., SAUDEK, V., KOSTROUCHOVA, M. & KOSTROUCH, Z. 2017. The nematode homologue of Mediator complex subunit 28, F28F8.5, is a critical regulator of C. elegans development. *PeerJ,* 5**,** e3390.
KOSTROUCHOVA, M. & KOSTROUCH, Z. 2015. Nuclear receptors in nematode development: Natural experiments made by a phylum. *Biochim Biophys Acta,* 1849**,** 224-37.
KRAUS, W. L. & WONG, J. 2002. Nuclear receptor-dependent transcription with chromatin. Is it all about enzymes? *Eur J Biochem,* 269**,** 2275-83.

LABARBERA, M. 1988. The Evolution of Individuality. Leo W. Buss. Princeton University Press, Princeton, NJ, 1988. xvi, 203 pp., illus. $40; paper, $12.95. *Science,* 240**,** 1073-4.
LACOMBE, T., POH, S. L., BARBEY, R. & KURAS, L. 2013. Mediator is an intrinsic component of the basal RNA polymerase II machinery in vivo. *Nucleic Acids Res,* 41**,** 9651-62.
LANNA, E. 2015. Evo-devo of non-bilaterian animals. *Genet Mol Biol,* 38**,** 284-300.
LAUDET, V. 1997. Evolution of the nuclear receptor superfamily: early diversification from an ancestral orphan receptor. *J Mol Endocrinol,* 19**,** 207-26.
LE GUEVEL, R., OGER, F., MARTINEZ-JIMENEZ, C. P., BIZOT, M., GHEERAERT, C., FIRMIN, F., PLOTON, M., KRETOVA, M., PALIERNE, G., STAELS, B., BARATH, P., TALIANIDIS, I., LEFEBVRE, P., EECKHOUTE, J. & SALBERT, G. 2017. Inactivation of the Nuclear Orphan Receptor COUP-TFII by Small Chemicals. *ACS Chem Biol*.
LE MAIRE, A., GRIMALDI, M., ROECKLIN, D., DAGNINO, S., VIVAT-HANNAH, V., BALAGUER, P. & BOURGUET, W. 2009. Activation of RXR-PPAR heterodimers by organotin environmental endocrine disruptors. *EMBO Rep,* 10**,** 367-73.
LE PAGE, M. 2007. The ancestor within. *New Scientist,* 193**,** 28-33.
LENGQVIST, J., MATA DE URQUIZA, A., BERGMAN, A. C., WILLSON, T. M., SJOVALL, J., PERLMANN, T. & GRIFFITHS, W. J. 2004. Polyunsaturated fatty acids including docosahexaenoic and arachidonic acid bind to the retinoid X receptor alpha ligand-binding domain. *Mol Cell Proteomics,* 3**,** 692-703.
LETUNIC, I., DOERKS, T. & BORK, P. 2015. SMART: recent updates, new developments and status in 2015. *Nucleic Acids Res,* 43**,** D257-60.
LEVIN, E. R. & HAMMES, S. R. 2016. Nuclear receptors outside the nucleus: extranuclear signalling by steroid receptors. *Nat Rev Mol Cell Biol,* 17**,** 783-797.
LI, Y., LAMBERT, M. H. & XU, H. E. 2003. Activation of nuclear receptors: a perspective from structural genomics. *Structure,* 11**,** 741-6.
LIN, H. K., HU, Y. C., YANG, L., ALTUWAIJRI, S., CHEN, Y. T., KANG, H. Y. & CHANG, C. 2003. Suppression versus induction of androgen receptor functions by the phosphatidylinositol 3-kinase/Akt pathway in prostate cancer LNCaP cells with different passage numbers. *J Biol Chem,* 278**,** 50902-7.
LIN, H. K., YEH, S., KANG, H. Y. & CHANG, C. 2001. Akt suppresses androgen-induced apoptosis by phosphorylating and inhibiting androgen receptor. *Proc Natl Acad Sci U S A,* 98**,** 7200-5.
LINDER, T., RASMUSSEN, N. N., SAMUELSEN, C. O., CHATZIDAKI, E., BARAZNENOK, V., BEVE, J., HENRIKSEN, P., GUSTAFSSON, C. M. & HOLMBERG, S. 2008. Two conserved modules of Schizosaccharomyces pombe Mediator regulate distinct cellular pathways. *Nucleic Acids Res,* 36**,** 2489-504.
LONARD, D. M. & O'MALLEY, B. W. 2012. Nuclear receptor coregulators: modulators of pathology and therapeutic targets. *Nat Rev Endocrinol,* 8**,** 598-604.
LOWE, S. W., CEPERO, E. & EVAN, G. 2004. Intrinsic tumour suppression. *Nature,* 432**,** 307-15.
LU, M., ZHANG, L., MAUL, R. S., SARTIPPOUR, M. R., NORRIS, A., WHITELEGGE, J., RAO, J. Y. & BROOKS, M. N. 2005. The novel gene EG-1 stimulates cellular proliferation. *Cancer Res,* 65**,** 6159-66.

LU, M., ZHANG, L., SARTIPPOUR, M. R., NORRIS, A. J. & BROOKS, M. N. 2006. EG-1 interacts with c-Src and activates its signaling pathway. *Int J Oncol,* 29**,** 1013-8.
LY, K., REID, S. J. & SNELL, R. G. 2015. Rapid RNA analysis of individual Caenorhabditis elegans. *MethodsX,* 2**,** 59-63.
LYONS, N. A. & KOLTER, R. 2015. On the evolution of bacterial multicellularity. *Curr Opin Microbiol,* 24**,** 21-8.
MADHANI, H. D. 2013. The frustrated gene: origins of eukaryotic gene expression. *Cell,* 155**,** 744-9.
MADSEN T, A. A., VITTECOQ M, BERNEX F, ET AL. 2017. Cancer in the animal kingdom. *In:* UJVARI B, R. B., THOMAS F (ed.) *Ecology and Evolution of Cancer.* Academic Press.
MAKAROVA, K. S., WOLF, Y. I., MEKHEDOV, S. L., MIRKIN, B. G. & KOONIN, E. V. 2005. Ancestral paralogs and pseudoparalogs and their role in the emergence of the eukaryotic cell. *Nucleic Acids Res,* 33**,** 4626-38.
MALIK, S. & ROEDER, R. G. 2010. The metazoan Mediator co-activator complex as an integrative hub for transcriptional regulation. *Nat Rev Genet,* 11**,** 761-72.
MANGELSDORF, D. J., THUMMEL, C., BEATO, M., HERRLICH, P., SCHUTZ, G., UMESONO, K., BLUMBERG, B., KASTNER, P., MARK, M., CHAMBON, P. & EVANS, R. M. 1995. The nuclear receptor superfamily: the second decade. *Cell,* 83**,** 835-9.
MANI, S. 2001. Ligand-independent activation of progestin receptors in sexual receptivity. *Horm Behav,* 40**,** 183-90.
MANNING, G., YOUNG, S. L., MILLER, W. T. & ZHAI, Y. 2008. The protist, Monosiga brevicollis, has a tyrosine kinase signaling network more elaborate and diverse than found in any known metazoan. *Proc Natl Acad Sci U S A,* 105**,** 9674-9.
MARGEAT, E., BOURDONCLE, A., MARGUERON, R., POUJOL, N., CAVAILLES, V. & ROYER, C. 2003. Ligands differentially modulate the protein interactions of the human estrogen receptors alpha and beta. *J Mol Biol,* 326**,** 77-92.
MARKOV, G. V. & LAUDET, V. 2011. Origin and evolution of the ligand-binding ability of nuclear receptors. *Mol Cell Endocrinol,* 334**,** 21-30.
MARTINELLI, C. & SPRING, J. 2004. Expression pattern of the homeobox gene Not in the basal metazoan Trichoplax adhaerens. *Gene Expr Patterns,* 4**,** 443-7.
MARUYAMA, Y. K. 2004. Occurrence in the field of a long-term, year-round, stable population of placozoans. *Biol Bull,* 206**,** 55-60.
MASSAGUE, J. & GOMIS, R. R. 2006. The logic of TGFbeta signaling. *FEBS Lett,* 580**,** 2811-20.
MASSAGUE, J. & WOTTON, D. 2000. Transcriptional control by the TGF-beta/Smad signaling system. *EMBO J,* 19**,** 1745-54.
MAYERHOFER, L. E., MACARIO, A. J. & CONWAY DE MACARIO, E. 1992. Lamina, a novel multicellular form of Methanosarcina mazei S-6. *J Bacteriol,* 174**,** 309-14.
MCGUFFIN, L. J., BRYSON, K. & JONES, D. T. 2000. The PSIPRED protein structure prediction server. *Bioinformatics,* 16**,** 404-5.
MCKENNA, N. J., LANZ, R. B. & O'MALLEY, B. W. 1999. Nuclear receptor coregulators: cellular and molecular biology. *Endocr Rev,* 20**,** 321-44.

MEIJSING, S. H., PUFALL, M. A., SO, A. Y., BATES, D. L., CHEN, L. & YAMAMOTO, K. R. 2009. DNA binding site sequence directs glucocorticoid receptor structure and activity. *Science,* 324**,** 407-10.
MERLO, L. M., PEPPER, J. W., REID, B. J. & MALEY, C. C. 2006. Cancer as an evolutionary and ecological process. *Nat Rev Cancer,* 6**,** 924-35.
MEYER, K. D., DONNER, A. J., KNUESEL, M. T., YORK, A. G., ESPINOSA, J. M. & TAATJES, D. J. 2008. Cooperative activity of cdk8 and GCN5L within Mediator directs tandem phosphoacetylation of histone H3. *EMBO J,* 27**,** 1447-57.
MICHOD, R. E. 2006. The group covariance effect and fitness trade-offs during evolutionary transitions in individuality. *Proc Natl Acad Sci U S A,* 103**,** 9113-7.
MICHOD, R. E. 2007. Evolution of individuality during the transition from unicellular to multicellular life. *Proc Natl Acad Sci U S A,* 104 Suppl 1**,** 8613-8.
MICHOD, R. E. & ROZE, D. 2001. Cooperation and conflict in the evolution of multicellularity. *Heredity (Edinb),* 86**,** 1-7.
MILLARD, C. J., WATSON, P. J., FAIRALL, L. & SCHWABE, J. W. 2013. An evolving understanding of nuclear receptor coregulator proteins. *J Mol Endocrinol,* 51**,** T23-36.
MILLER, W. B., JR. & TORDAY, J. S. 2017. A systematic approach to cancer: evolution beyond selection. *Clin Transl Med,* 6**,** 2.
MILLER, W. T. 2012. Tyrosine kinase signaling and the emergence of multicellularity. *Biochim Biophys Acta,* 1823**,** 1053-7.
MORAS, D., BILLAS, I. M., ROCHEL, N. & KLAHOLZ, B. P. 2015. Structure-function relationships in nuclear receptors: the facts. *Trends Biochem Sci,* 40**,** 287-90.
MUMM, J. S. & KOPAN, R. 2000. Notch signaling: from the outside in. *Dev Biol,* 228**,** 151-65.
NAAR, A. M. & THAKUR, J. K. 2009. Nuclear receptor-like transcription factors in fungi. *Genes Dev,* 23**,** 419-32.
NAGALINGAM, A., TIGHIOUART, M., RYDEN, L., JOSEPH, L., LANDBERG, G., SAXENA, N. K. & SHARMA, D. 2012. Med1 plays a critical role in the development of tamoxifen resistance. *Carcinogenesis,* 33**,** 918-30.
NAGULAPALLI, M., MAJI, S., DWIVEDI, N., DAHIYA, P. & THAKUR, J. K. 2016. Evolution of disorder in Mediator complex and its functional relevance. *Nucleic Acids Res,* 44**,** 1591-612.
NAGY, L. & SCHWABE, J. W. 2004. Mechanism of the nuclear receptor molecular switch. *Trends Biochem Sci,* 29**,** 317-24.
NOMURA, Y., NAGAYA, T., HAYASHI, Y., KAMBE, F. & SEO, H. 1999. 9-cis-retinoic acid decreases the level of its cognate receptor, retinoid X receptor, through acceleration of the turnover. *Biochem Biophys Res Commun,* 260**,** 729-33.
NORDBERG, H., CANTOR, M., DUSHEYKO, S., HUA, S., POLIAKOV, A., SHABALOV, I., SMIRNOVA, T., GRIGORIEV, I. V. & DUBCHAK, I. 2014. The genome portal of the Department of Energy Joint Genome Institute: 2014 updates. *Nucleic Acids Res,* 42**,** D26-31.
NOSENKO, T., SCHREIBER, F., ADAMSKA, M., ADAMSKI, M., EITEL, M., HAMMEL, J., MALDONADO, M., MULLER, W. E., NICKEL, M., SCHIERWATER, B., VACELET, J., WIENS, M. & WORHEIDE, G. 2013. Deep metazoan phylogeny: when different genes tell different stories. *Mol Phylogenet Evol,* 67**,** 223-33.

NOTREDAME, C., HIGGINS, D. G. & HERINGA, J. 2000. T-Coffee: A novel method for fast and accurate multiple sequence alignment. *J Mol Biol,* 302**,** 205-17.
NOZAWA, K., SCHNEIDER, T. R. & CRAMER, P. 2017. Core Mediator structure at 3.4 A extends model of transcription initiation complex. *Nature,* 545**,** 248-251.
NUCLEAR RECEPTORS NOMENCLATURE, C. 1999. A unified nomenclature system for the nuclear receptor superfamily. *Cell,* 97**,** 161-3.
NUSSLEIN-VOLHARD, C. & WIESCHAUS, E. 1980. Mutations affecting segment number and polarity in Drosophila. *Nature,* 287**,** 795-801.
O'MAHONY, F., RAZANDI, M., PEDRAM, A., HARVEY, B. J. & LEVIN, E. R. 2012. Estrogen modulates metabolic pathway adaptation to available glucose in breast cancer cells. *Mol Endocrinol,* 26**,** 2058-70.
ONATE, S. A., TSAI, S. Y., TSAI, M. J. & O'MALLEY, B. W. 1995. Sequence and characterization of a coactivator for the steroid hormone receptor superfamily. *Science,* 270**,** 1354-7.
OSWALD, F., TAUBER, B., DOBNER, T., BOURTEELE, S., KOSTEZKA, U., ADLER, G., LIPTAY, S. & SCHMID, R. M. 2001. p300 acts as a transcriptional coactivator for mammalian Notch-1. *Mol Cell Biol,* 21**,** 7761-74.
PADUA, D., ZHANG, X. H., WANG, Q., NADAL, C., GERALD, W. L., GOMIS, R. R. & MASSAGUE, J. 2008. TGFbeta primes breast tumors for lung metastasis seeding through angiopoietin-like 4. *Cell,* 133**,** 66-77.
PAK, T. R., CHUNG, W. C., LUND, T. D., HINDS, L. R., CLAY, C. M. & HANDA, R. J. 2005. The androgen metabolite, 5alpha-androstane-3beta, 17beta-diol, is a potent modulator of estrogen receptor-beta1-mediated gene transcription in neuronal cells. *Endocrinology,* 146**,** 147-55.
PAKNIA, O. & SCHIERWATER, B. 2015. Global Habitat Suitability and Ecological Niche Separation in the Phylum Placozoa. *PLoS One,* 10**,** e0140162.
PARDEE, K. I., XU, X., REINKING, J., SCHUETZ, A., DONG, A., LIU, S., ZHANG, R., TIEFENBACH, J., LAJOIE, G., PLOTNIKOV, A. N., BOTCHKAREV, A., KRAUSE, H. M. & EDWARDS, A. 2009. The structural basis of gas-responsive transcription by the human nuclear hormone receptor REV-ERBbeta. *PLoS Biol,* 7**,** e43.
PARFREY, L. W., LAHR, D. J., KNOLL, A. H. & KATZ, L. A. 2011. Estimating the timing of early eukaryotic diversification with multigene molecular clocks. *Proc Natl Acad Sci U S A,* 108**,** 13624-9.
PARIS, M., ESCRIVA, H., SCHUBERT, M., BRUNET, F., BRTKO, J., CIESIELSKI, F., ROECKLIN, D., VIVAT-HANNAH, V., JAMIN, E. L., CRAVEDI, J. P., SCANLAN, T. S., RENAUD, J. P., HOLLAND, N. D. & LAUDET, V. 2008. Amphioxus postembryonic development reveals the homology of chordate metamorphosis. *Curr Biol,* 18**,** 825-30.
PARK, S. W., LI, G., LIN, Y. P., BARRERO, M. J., GE, K., ROEDER, R. G. & WEI, L. N. 2005. Thyroid hormone-induced juxtaposition of regulatory elements/factors and chromatin remodeling of Crabp1 dependent on MED1/TRAP220. *Mol Cell,* 19**,** 643-53.
PAWLAK, M., LEFEBVRE, P. & STAELS, B. 2012. General molecular biology and architecture of nuclear receptors. *Curr Top Med Chem,* 12**,** 486-504.
PEDRAM, A., RAZANDI, M., SAINSON, R. C., KIM, J. K., HUGHES, C. C. & LEVIN, E. R. 2007. A conserved mechanism for steroid receptor translocation to the plasma membrane. *J Biol Chem,* 282**,** 22278-88.
PEI, J. & GRISHIN, N. V. 2007. PROMALS: towards accurate multiple sequence alignments of distantly related proteins. *Bioinformatics,* 23**,** 802-8.

PEI, J., KIM, B. H. & GRISHIN, N. V. 2008. PROMALS3D: a tool for multiple protein sequence and structure alignments. *Nucleic Acids Res,* 36**,** 2295-300.
PEI, J., KIM, B. H., TANG, M. & GRISHIN, N. V. 2007. PROMALS web server for accurate multiple protein sequence alignments. *Nucleic Acids Res,* 35**,** W649-52.
PETERSEN, C. P. & REDDIEN, P. W. 2009. Wnt signaling and the polarity of the primary body axis. *Cell,* 139**,** 1056-68.
PETRENKO, N., JIN, Y., WONG, K. H. & STRUHL, K. 2016. Mediator Undergoes a Compositional Change during Transcriptional Activation. *Mol Cell,* 64**,** 443-454.
PETTY, K. J., DESVERGNE, B., MITSUHASHI, T. & NIKODEM, V. M. 1990. Identification of a thyroid hormone response element in the malic enzyme gene. *J Biol Chem,* 265**,** 7395-400.
PETTY, K. J., MORIOKA, H., MITSUHASHI, T. & NIKODEM, V. M. 1989. Thyroid hormone regulation of transcription factors involved in malic enzyme gene expression. *J Biol Chem,* 264**,** 11483-90.
PIETRAS, R. J. & SZEGO, C. M. 1977. Specific binding sites for oestrogen at the outer surfaces of isolated endometrial cells. *Nature,* 265**,** 69-72.
PINSON, K. I., BRENNAN, J., MONKLEY, S., AVERY, B. J. & SKARNES, W. C. 2000. An LDL-receptor-related protein mediates Wnt signalling in mice. *Nature,* 407**,** 535-8.
PIRES-DASILVA, A. & SOMMER, R. J. 2003. The evolution of signalling pathways in animal development. *Nat Rev Genet,* 4**,** 39-49.
POSS, Z. C., EBMEIER, C. C. & TAATJES, D. J. 2013. The Mediator complex and transcription regulation. *Crit Rev Biochem Mol Biol,* 48**,** 575-608.
POUKKA, H., KARVONEN, U., JANNE, O. A. & PALVIMO, J. J. 2000. Covalent modification of the androgen receptor by small ubiquitin-like modifier 1 (SUMO-1). *Proc Natl Acad Sci U S A,* 97**,** 14145-50.
PRIVALSKY, M. L. 2004. The role of corepressors in transcriptional regulation by nuclear hormone receptors. *Annu Rev Physiol,* 66**,** 315-60.
RAGHURAM, S., STAYROOK, K. R., HUANG, P., ROGERS, P. M., NOSIE, A. K., MCCLURE, D. B., BURRIS, L. L., KHORASANIZADEH, S., BURRIS, T. P. & RASTINEJAD, F. 2007. Identification of heme as the ligand for the orphan nuclear receptors REV-ERBalpha and REV-ERBbeta. *Nat Struct Mol Biol,* 14**,** 1207-13.
RANA, R., SURAPUREDDI, S., KAM, W., FERGUSON, S. & GOLDSTEIN, J. A. 2011. Med25 is required for RNA polymerase II recruitment to specific promoters, thus regulating xenobiotic and lipid metabolism in human liver. *Mol Cell Biol,* 31**,** 466-81.
RAO, T. P. & KUHL, M. 2010. An updated overview on Wnt signaling pathways: a prelude for more. *Circ Res,* 106**,** 1798-806.
RASTINEJAD, F., OLLENDORFF, V. & POLIKARPOV, I. 2015a. Nuclear receptor full-length architectures: confronting myth and illusion with high resolution. *Trends Biochem Sci,* 40**,** 16-24.
RASTINEJAD, F., OLLENDORFF, V. & POLIKARPOV, I. 2015b. Response to Moras et al. *Trends Biochem Sci,* 40**,** 290-2.
RASTINEJAD, F., WAGNER, T., ZHAO, Q. & KHORASANIZADEH, S. 2000. Structure of the RXR-RAR DNA-binding complex on the retinoic acid response element DR1. *EMBO J,* 19**,** 1045-54.

REITZEL, A. M. & TARRANT, A. M. 2009. Nuclear receptor complement of the cnidarian Nematostella vectensis: phylogenetic relationships and developmental expression patterns. *BMC Evol Biol,* 9**,** 230.
REMMERT, M., BIEGERT, A., HAUSER, A. & SODING, J. 2011. HHblits: lightning-fast iterative protein sequence searching by HMM-HMM alignment. *Nat Methods,* 9**,** 173-5.
RENAUD, J. P., ROCHEL, N., RUFF, M., VIVAT, V., CHAMBON, P., GRONEMEYER, H. & MORAS, D. 1995. Crystal structure of the RAR-gamma ligand-binding domain bound to all-trans retinoic acid. *Nature,* 378**,** 681-9.
RIESGO, A., FARRAR, N., WINDSOR, P. J., GIRIBET, G. & LEYS, S. P. 2014. The analysis of eight transcriptomes from all poriferan classes reveals surprising genetic complexity in sponges. *Mol Biol Evol,* 31**,** 1102-20.
RINGROSE, J. H., VAN DEN TOORN, H. W., EITEL, M., POST, H., NEERINCX, P., SCHIERWATER, B., ALTELAAR, A. F. & HECK, A. J. 2013. Deep proteome profiling of Trichoplax adhaerens reveals remarkable features at the origin of metazoan multicellularity. *Nat Commun,* 4**,** 1408.
ROBERT, J. 2010. Comparative study of tumorigenesis and tumor immunity in invertebrates and nonmammalian vertebrates. *Dev Comp Immunol,* 34**,** 915-25.
ROBINSON, P. J., TRNKA, M. J., PELLARIN, R., GREENBERG, C. H., BUSHNELL, D. A., DAVIS, R., BURLINGAME, A. L., SALI, A. & KORNBERG, R. D. 2015. Molecular architecture of the yeast Mediator complex. *Elife,* 4.
ROCHETTE-EGLY, C., OULAD-ABDELGHANI, M., STAUB, A., PFISTER, V., SCHEUER, I., CHAMBON, P. & GAUB, M. P. 1995. Phosphorylation of the retinoic acid receptor-alpha by protein kinase A. *Mol Endocrinol,* 9**,** 860-71.
ROKAS, A. 2008. The origins of multicellularity and the early history of the genetic toolkit for animal development. *Annu Rev Genet,* 42**,** 235-51.
RUBIN, L. L. & DE SAUVAGE, F. J. 2006. Targeting the Hedgehog pathway in cancer. *Nat Rev Drug Discov,* 5**,** 1026-33.
RUHL, R., KRZYZOSIAK, A., NIEWIADOMSKA-CIMICKA, A., ROCHEL, N., SZELES, L., VAZ, B., WIETRZYCH-SCHINDLER, M., ALVAREZ, S., SZKLENAR, M., NAGY, L., DE LERA, A. R. & KREZEL, W. 2015. 9-cis-13,14-Dihydroretinoic Acid Is an Endogenous Retinoid Acting as RXR Ligand in Mice. *PLoS Genet,* 11**,** e1005213.
RUTHMANN, A., BEHRENDT, G. & WAHL, R. 1986. The ventral epithelium of Trichoplax adhaerens (Placozoa): Cytoskeletal structures, cell contacts and endocytosis. *Zoomorphology,* 106**,** 115-122.
RYAN, J. F., PANG, K., SCHNITZLER, C. E., NGUYEN, A. D., MORELAND, R. T., SIMMONS, D. K., KOCH, B. J., FRANCIS, W. R., HAVLAK, P., PROGRAM, N. C. S., SMITH, S. A., PUTNAM, N. H., HADDOCK, S. H., DUNN, C. W., WOLFSBERG, T. G., MULLIKIN, J. C., MARTINDALE, M. Q. & BAXEVANIS, A. D. 2013. The genome of the ctenophore Mnemiopsis leidyi and its implications for cell type evolution. *Science,* 342**,** 1242592.
SATO, S., TOMOMORI-SATO, C., PARMELY, T. J., FLORENS, L., ZYBAILOV, B., SWANSON, S. K., BANKS, C. A., JIN, J., CAI, Y., WASHBURN, M. P., CONAWAY, J. W. & CONAWAY, R. C. 2004. A set of consensus mammalian mediator subunits identified by multidimensional protein identification technology. *Mol Cell,* 14**,** 685-91.

SCHIERWATER, B., DE JONG, D. & DESALLE, R. 2009a. Placozoa and the evolution of Metazoa and intrasomatic cell differentiation. *Int J Biochem Cell Biol,* 41**,** 370-9.
SCHIERWATER, B., EITEL, M., JAKOB, W., OSIGUS, H. J., HADRYS, H., DELLAPORTA, S. L., KOLOKOTRONIS, S. O. & DESALLE, R. 2009b. Concatenated analysis sheds light on early metazoan evolution and fuels a modern "urmetazoon" hypothesis. *PLoS Biol,* 7**,** e20.
SCHLESSINGER, J. 2000. Cell signaling by receptor tyrosine kinases. *Cell,* 103**,** 211-25.
SCHUCHERT, P. 1993. Trichoplax adhaerens (Phylum Placozoa) has Cells that React with Antibodies Against the Neuropeptide RFamide. *Acta Zoologica,* 74**,** 115-117.
SCHULTHEISS, K. P., CRADDOCK, B. P., TONG, M., SEELIGER, M. & MILLER, W. T. 2013. Metazoan-like signaling in a unicellular receptor tyrosine kinase. *BMC Biochem,* 14**,** 4.
SCHULTZ, J., MILPETZ, F., BORK, P. & PONTING, C. P. 1998. SMART, a simple modular architecture research tool: identification of signaling domains. *Proc Natl Acad Sci U S A,* 95**,** 5857-64.
SENTIS, S., LE ROMANCER, M., BIANCHIN, C., ROSTAN, M. C. & CORBO, L. 2005. Sumoylation of the estrogen receptor alpha hinge region regulates its transcriptional activity. *Mol Endocrinol,* 19**,** 2671-84.
SEVER, R. & GLASS, C. K. 2013. Signaling by nuclear receptors. *Cold Spring Harb Perspect Biol,* 5**,** a016709.
SHALCHIAN-TABRIZI, K., MINGE, M. A., ESPELUND, M., ORR, R., RUDEN, T., JAKOBSEN, K. S. & CAVALIER-SMITH, T. 2008. Multigene phylogeny of choanozoa and the origin of animals. *PLoS One,* 3**,** e2098.
SHARPLESS, N. E. & DEPINHO, R. A. 2004. Telomeres, stem cells, senescence, and cancer. *J Clin Invest,* 113**,** 160-8.
SHI, Y. & MASSAGUE, J. 2003. Mechanisms of TGF-beta signaling from cell membrane to the nucleus. *Cell,* 113**,** 685-700.
SHI, Y., WANG, Y. F., JAYARAMAN, L., YANG, H., MASSAGUE, J. & PAVLETICH, N. P. 1998. Crystal structure of a Smad MH1 domain bound to DNA: insights on DNA binding in TGF-beta signaling. *Cell,* 94**,** 585-94.
SHIAU, A. K., BARSTAD, D., LORIA, P. M., CHENG, L., KUSHNER, P. J., AGARD, D. A. & GREENE, G. L. 1998. The structural basis of estrogen receptor/coactivator recognition and the antagonism of this interaction by tamoxifen. *Cell,* 95**,** 927-37.
SIEVERS, F., WILM, A., DINEEN, D., GIBSON, T. J., KARPLUS, K., LI, W., LOPEZ, R., MCWILLIAM, H., REMMERT, M., SODING, J., THOMPSON, J. D. & HIGGINS, D. G. 2011. Fast, scalable generation of high-quality protein multiple sequence alignments using Clustal Omega. *Mol Syst Biol,* 7**,** 539.
SIGNOROVITCH, A. Y., DELLAPORTA, S. L. & BUSS, L. W. 2005. Molecular signatures for sex in the Placozoa. *Proc Natl Acad Sci U S A,* 102**,** 15518-22.
SIMPSON, C. 2012. The evolutionary history of division of labour. *Proc Biol Sci,* 279**,** 116-21.
SMITH, C. L., VAROQUEAUX, F., KITTELMANN, M., AZZAM, R. N., COOPER, B., WINTERS, C. A., EITEL, M., FASSHAUER, D. & REESE, T. S. 2014. Novel cell types, neurosecretory cells, and body plan of the early-diverging metazoan Trichoplax adhaerens. *Curr Biol,* 24**,** 1565-72.

SODING, J., BIEGERT, A. & LUPAS, A. N. 2005. The HHpred interactive server for protein homology detection and structure prediction. *Nucleic Acids Res,* 33**,** W244-8.

SRIVASTAVA, M., BEGOVIC, E., CHAPMAN, J., PUTNAM, N. H., HELLSTEN, U., KAWASHIMA, T., KUO, A., MITROS, T., SALAMOV, A., CARPENTER, M. L., SIGNOROVITCH, A. Y., MORENO, M. A., KAMM, K., GRIMWOOD, J., SCHMUTZ, J., SHAPIRO, H., GRIGORIEV, I. V., BUSS, L. W., SCHIERWATER, B., DELLAPORTA, S. L. & ROKHSAR, D. S. 2008. The Trichoplax genome and the nature of placozoans. *Nature,* 454**,** 955-60.

SUGA, H., CHEN, Z., DE MENDOZA, A., SEBE-PEDROS, A., BROWN, M. W., KRAMER, E., CARR, M., KERNER, P., VERVOORT, M., SANCHEZ-PONS, N., TORRUELLA, G., DERELLE, R., MANNING, G., LANG, B. F., RUSS, C., HAAS, B. J., ROGER, A. J., NUSBAUM, C. & RUIZ-TRILLO, I. 2013. The Capsaspora genome reveals a complex unicellular prehistory of animals. *Nat Commun,* 4**,** 2325.

SUN, K., MONTANA, V., CHELLAPPA, K., BRELIVET, Y., MORAS, D., MAEDA, Y., PARPURA, V., PASCHAL, B. M. & SLADEK, F. M. 2007. Phosphorylation of a conserved serine in the deoxyribonucleic acid binding domain of nuclear receptors alters intracellular localization. *Mol Endocrinol,* 21**,** 1297-311.

SZATHMARY, E. & SMITH, J. M. 1995. The major evolutionary transitions. *Nature,* 374**,** 227-232.

SZEGO, C. M. & DAVIS, J. S. 1967. Adenosine 3',5'-monophosphate in rat uterus: acute elevation by estrogen. *Proc Natl Acad Sci U S A,* 58**,** 1711-8.

TAKAGI, Y. & KORNBERG, R. D. 2006. Mediator as a general transcription factor. *J Biol Chem,* 281**,** 80-9.

TAMAI, K., SEMENOV, M., KATO, Y., SPOKONY, R., LIU, C., KATSUYAMA, Y., HESS, F., SAINT-JEANNET, J. P. & HE, X. 2000. LDL-receptor-related proteins in Wnt signal transduction. *Nature,* 407**,** 530-5.

TATA, J. R. 1994. Autoregulation and crossregulation of nuclear receptor genes. *Trends Endocrinol Metab,* 5**,** 283-90.

TAUBERT, S., WARD, J. D. & YAMAMOTO, K. R. 2011. Nuclear hormone receptors in nematodes: evolution and function. *Mol Cell Endocrinol,* 334**,** 49-55.

TECHNAU, U., RUDD, S., MAXWELL, P., GORDON, P. M., SAINA, M., GRASSO, L. C., HAYWARD, D. C., SENSEN, C. W., SAINT, R., HOLSTEIN, T. W., BALL, E. E. & MILLER, D. J. 2005. Maintenance of ancestral complexity and non-metazoan genes in two basal cnidarians. *Trends Genet,* 21**,** 633-9.

THAKUR, J. K., ARTHANARI, H., YANG, F., PAN, S. J., FAN, X., BREGER, J., FRUEH, D. P., GULSHAN, K., LI, D. K., MYLONAKIS, E., STRUHL, K., MOYE-ROWLEY, W. S., CORMACK, B. P., WAGNER, G. & NAAR, A. M. 2008. A nuclear receptor-like pathway regulating multidrug resistance in fungi. *Nature,* 452**,** 604-9.

THOMAS, M. C. & CHIANG, C. M. 2006. The general transcription machinery and general cofactors. *Crit Rev Biochem Mol Biol,* 41**,** 105-78.

THOMPSON, C. M., KOLESKE, A. J., CHAO, D. M. & YOUNG, R. A. 1993. A multisubunit complex associated with the RNA polymerase II CTD and TATA-binding protein in yeast. *Cell,* 73**,** 1361-75.

TOMASSETTI, P., VOIGT, O., COLLINS, A. G., PORRELLO, S., PEARSE, V. B. & SCHIERWATER, B. 2005. Placozoans (Trichoplax adhaerens Schulze 1883) in the Mediterranean sea. *Meiofauna Marina,* 14**,** 5-7.

TRAN, P., ZHANG, X. K., SALBERT, G., HERMANN, T., LEHMANN, J. M. & PFAHL, M. 1992. COUP orphan receptors are negative regulators of retinoic acid response pathways. *Mol Cell Biol,* 12**,** 4666-76.

TRIGOS, A. S., PEARSON, R. B., PAPENFUSS, A. T. & GOODE, D. L. 2017. Altered interactions between unicellular and multicellular genes drive hallmarks of transformation in a diverse range of solid tumors. *Proc Natl Acad Sci U S A,* 114**,** 6406-6411.

TSAI, K. L., TOMOMORI-SATO, C., SATO, S., CONAWAY, R. C., CONAWAY, J. W. & ASTURIAS, F. J. 2014. Subunit architecture and functional modular rearrangements of the transcriptional mediator complex. *Cell,* 157**,** 1430-44.

TSAI, K. L., YU, X., GOPALAN, S., CHAO, T. C., ZHANG, Y., FLORENS, L., WASHBURN, M. P., MURAKAMI, K., CONAWAY, R. C., CONAWAY, J. W. & ASTURIAS, F. J. 2017. Mediator structure and rearrangements required for holoenzyme formation. *Nature,* 544**,** 196-201.

TSAI, M. J. & O'MALLEY, B. W. 1994. Molecular mechanisms of action of steroid/thyroid receptor superfamily members. *Annu Rev Biochem,* 63**,** 451-86.

UWAMAHORO, N., QU, Y., JELICIC, B., LO, T. L., BEAUREPAIRE, C., BANTUN, F., QUENAULT, T., BOAG, P. R., RAMM, G., CALLAGHAN, J., BEILHARZ, T. H., NANTEL, A., PELEG, A. Y. & TRAVEN, A. 2012. The functions of Mediator in Candida albicans support a role in shaping species-specific gene expression. *PLoS Genet,* 8**,** e1002613.

VAN AMERONGEN, R. & NUSSE, R. 2009. Towards an integrated view of Wnt signaling in development. *Development,* 136**,** 3205-14.

VAN DE PEPPEL, J., KETTELARIJ, N., VAN BAKEL, H., KOCKELKORN, T. T., VAN LEENEN, D. & HOLSTEGE, F. C. 2005. Mediator expression profiling epistasis reveals a signal transduction pathway with antagonistic submodules and highly specific downstream targets. *Mol Cell,* 19**,** 511-22.

VAN DER STEEN, T., TINDALL, D. J. & HUANG, H. 2013. Posttranslational modification of the androgen receptor in prostate cancer. *Int J Mol Sci,* 14**,** 14833-59.

VOGELER, S., GALLOWAY, T. S., LYONS, B. P. & BEAN, T. P. 2014. The nuclear receptor gene family in the Pacific oyster, Crassostrea gigas, contains a novel subfamily group. *BMC Genomics,* 15**,** 369.

VOGELSTEIN, B., PAPADOPOULOS, N., VELCULESCU, V. E., ZHOU, S., DIAZ, L. A., JR. & KINZLER, K. W. 2013. Cancer genome landscapes. *Science,* 339**,** 1546-58.

WALTHER, R. F., ATLAS, E., CARRIGAN, A., ROULEAU, Y., EDGECOMBE, A., VISENTIN, L., LAMPRECHT, C., ADDICKS, G. C., HACHE, R. J. & LEFEBVRE, Y. A. 2005. A serine/threonine-rich motif is one of three nuclear localization signals that determine unidirectional transport of the mineralocorticoid receptor to the nucleus. *J Biol Chem,* 280**,** 17549-61.

WANG, W., LI, X., LEE, M., JUN, S., AZIZ, K. E., FENG, L., TRAN, M. K., LI, N., MCCREA, P. D., PARK, J. I. & CHEN, J. 2015. FOXKs promote Wnt/beta-catenin signaling by translocating DVL into the nucleus. *Dev Cell,* 32**,** 707-18.

WANG, Z., BENOIT, G., LIU, J., PRASAD, S., AARNISALO, P., LIU, X., XU, H., WALKER, N. P. & PERLMANN, T. 2003. Structure and function of Nurr1 identifies a class of ligand-independent nuclear receptors. *Nature,* 423**,** 555-60.

WARD, J. D. 2015. Rapid and precise engineering of the Caenorhabditis elegans genome with lethal mutation co-conversion and inactivation of NHEJ repair. *Genetics,* 199**,** 363-77.
WATSON, P. J., FAIRALL, L. & SCHWABE, J. W. 2012. Nuclear hormone receptor co-repressors: structure and function. *Mol Cell Endocrinol,* 348**,** 440-9.
WEBB, P., ANDERSON, C. M., VALENTINE, C., NGUYEN, P., MARIMUTHU, A., WEST, B. L., BAXTER, J. D. & KUSHNER, P. J. 2000. The nuclear receptor corepressor (N-CoR) contains three isoleucine motifs (I/LXXII) that serve as receptor interaction domains (IDs). *Mol Endocrinol,* 14**,** 1976-85.
WEBER, H. & GARABEDIAN, M. J. 2017. The Mediator Complex in Genomic and Non-Genomic Signaling in Cancer. *Steroids*.
WEHLING, M. 1997. Specific, nongenomic actions of steroid hormones. *Annu Rev Physiol,* 59**,** 365-93.
WEHRLI, M., DOUGAN, S. T., CALDWELL, K., O'KEEFE, L., SCHWARTZ, S., VAIZEL-OHAYON, D., SCHEJTER, E., TOMLINSON, A. & DINARDO, S. 2000. arrow encodes an LDL-receptor-related protein essential for Wingless signalling. *Nature,* 407**,** 527-30.
WEIGEL, N. L. & ZHANG, Y. 1998. Ligand-independent activation of steroid hormone receptors. *J Mol Med (Berl),* 76**,** 469-79.
WEINBERG, R. A. R. A. 2007. The biology of cancer.
WENTE, W., BRENNER, M. B., ZITZER, H., GROMADA, J. & EFANOV, A. M. 2007. Activation of liver X receptors and retinoid X receptors induces growth arrest and apoptosis in insulin-secreting cells. *Endocrinology,* 148**,** 1843-9.
WIEDERHOLD, T., LEE, M. F., JAMES, M., NEUJAHR, R., SMITH, N., MURTHY, A., HARTWIG, J., GUSELLA, J. F. & RAMESH, V. 2004. Magicin, a novel cytoskeletal protein associates with the NF2 tumor suppressor merlin and Grb2. *Oncogene,* 23**,** 8815-25.
WOLF, G. 2006. Is 9-cis-retinoic acid the endogenous ligand for the retinoic acid-X receptor? *Nutr Rev,* 64**,** 532-8.
WOLF, I. M., HEITZER, M. D., GRUBISHA, M. & DEFRANCO, D. B. 2008. Coactivators and nuclear receptor transactivation. *J Cell Biochem,* 104**,** 1580-6.
WU, A., ZHANG, Q., LAMBERT, G., KHIN, Z., GATENBY, R. A., KIM, H. J., POURMAND, N., BUSSEY, K., DAVIES, P. C., STURM, J. C. & AUSTIN, R. H. 2015. Ancient hot and cold genes and chemotherapy resistance emergence. *Proc Natl Acad Sci U S A,* 112**,** 10467-72.
WURTZ, J. M., BOURGUET, W., RENAUD, J. P., VIVAT, V., CHAMBON, P., MORAS, D. & GRONEMEYER, H. 1996. A canonical structure for the ligand-binding domain of nuclear receptors. *Nat Struct Biol,* 3**,** 206.
XU, L., GLASS, C. K. & ROSENFELD, M. G. 1999. Coactivator and corepressor complexes in nuclear receptor function. *Curr Opin Genet Dev,* 9**,** 140-7.
YIN, J. W. & WANG, G. 2014. The Mediator complex: a master coordinator of transcription and cell lineage development. *Development,* 141**,** 977-87.
YIN, L., WU, N., CURTIN, J. C., QATANANI, M., SZWERGOLD, N. R., REID, R. A., WAITT, G. M., PARKS, D. J., PEARCE, K. H., WISELY, G. B. & LAZAR, M. A. 2007. Rev-erbalpha, a heme sensor that coordinates metabolic and circadian pathways. *Science,* 318**,** 1786-9.
YUTIN, N., MAKAROVA, K. S., MEKHEDOV, S. L., WOLF, Y. I. & KOONIN, E. V. 2008. The deep archaeal roots of eukaryotes. *Mol Biol Evol,* 25**,** 1619-30.
ZHANG, J., CHALMERS, M. J., STAYROOK, K. R., BURRIS, L. L., WANG, Y., BUSBY, S. A., PASCAL, B. D., GARCIA-ORDONEZ, R. D., BRUNING, J.

B., ISTRATE, M. A., KOJETIN, D. J., DODGE, J. A., BURRIS, T. P. & GRIFFIN, P. R. 2011. DNA binding alters coactivator interaction surfaces of the intact VDR-RXR complex. *Nat Struct Mol Biol,* 18**,** 556-63.

ZHANG, X., KRUTCHINSKY, A., FUKUDA, A., CHEN, W., YAMAMURA, S., CHAIT, B. T. & ROEDER, R. G. 2005. MED1/TRAP220 exists predominantly in a TRAP/ Mediator subpopulation enriched in RNA polymerase II and is required for ER-mediated transcription. *Mol Cell,* 19**,** 89-100.

ZHAO, Q., CHASSE, S. A., DEVARAKONDA, S., SIERK, M. L., AHVAZI, B. & RASTINEJAD, F. 2000. Structural basis of RXR-DNA interactions. *J Mol Biol,* 296**,** 509-20.

ZIMA, V., SEBKOVA, K., SIMECKOVA, K., DVORAK, T., SAUDEK, V. & KOSTROUCHOVA, M. 2015. Prorenin Receptor Homologue VHA-20 is Critical for Intestinal pH Regulation, Ion and Water Management and Larval Development in C. elegans. *Folia Biol (Praha),* 61**,** 168-77.

Supplementary files

1. Novotný JP, Chughtai AA, Kostrouchová M, Kostrouchová V, Kostrouch D, Kaššák F, Kaňa R, Schierwater B, Kostrouchová M, Kostrouch Z. (2017) *Trichoplax adhaerens* reveals a network of nuclear receptors sensitive to 9-*cis*-retinoic acid at the base of metazoan evolution. *PeerJ*5:e3789 https://doi.org/10.7717/peerj.3789
2. Kostrouchová M, Kostrouch D, Chughtai AA, Kaššák F, Novotný JP, Kostrouchová V, Benda A, Krause MW, Saudek V, Kostrouchová M, Kostrouch Z. (2017) The nematode homologue of Mediator complex subunit 28, F28F8.5, is a critical regulator of *C. elegans* development. *PeerJ*5:e3390 https://doi.org/10.7717/peerj.3390

Trichoplax adhaerens reveals a network of nuclear receptors sensitive to 9-*cis*-retinoic acid at the base of metazoan evolution

Jan Philipp Novotný[1,2], Ahmed Ali Chughtai[1], Markéta Kostrouchová[1,3], Veronika Kostrouchová[1], David Kostrouch[1], Filip Kaššák[1], Radek Kaňa[4], Bernd Schierwater[5,6], Marta Kostrouchová[1] and Zdenek Kostrouch[1]

[1] Biocev, First Faculty of Medicine, Charles University, Vestec, Czech Republic
[2] Department of Medicine V., University of Heidelberg, Heidelberg, Germany
[3] Department of Pathology, Third Faculty of Medicine, Charles University, Prague, Czech Republic
[4] Institute of Microbiology, Laboratory of Photosynthesis, Czech Academy of Sciences, Třeboň, Czech Republic
[5] Institute for Animal Ecology and Cell Biology, University of Veterinary Medicine, Hannover, Germany
[6] Department of Ecology and Evolutionary Biology, Yale University, New Haven, CT, United States of America

ABSTRACT

Trichoplax adhaerens, the only known species of Placozoa is likely to be closely related to an early metazoan that preceded branching of Cnidaria and Bilateria. This animal species is surprisingly well adapted to free life in the World Ocean inhabiting tidal costal zones of oceans and seas with warm to moderate temperatures and shallow waters. The genome of *T. adhaerens* (sp. Grell) includes four nuclear receptors, namely orthologue of RXR (NR2B), HNF4 (NR2A), COUP-TF (NR2F) and ERR (NR3B) that show a high degree of similarity with human orthologues. In the case of RXR, the sequence identity to human RXR alpha reaches 81% in the DNA binding domain and 70% in the ligand binding domain. We show that *T. adhaerens* RXR (TaRXR) binds 9-*cis* retinoic acid (9-*cis*-RA) with high affinity, as well as high specificity and that exposure of *T. adhaerens* to 9-*cis*-RA regulates the expression of the putative *T. adhaerens* orthologue of vertebrate L-malate-NADP$^+$ oxidoreductase (EC 1.1.1.40) which in vertebrates is regulated by a heterodimer of RXR and thyroid hormone receptor. Treatment by 9-*cis*-RA alters the relative expression profile of *T. adhaerens* nuclear receptors, suggesting the existence of natural ligands. Keeping with this, algal food composition has a profound effect on *T. adhaerens* growth and appearance. We show that nanomolar concentrations of 9-*cis*-RA interfere with *T. adhaerens* growth response to specific algal food and causes growth arrest. Our results uncover an endocrine-like network of nuclear receptors sensitive to 9-*cis*-RA in *T. adhaerens* and support the existence of a ligand-sensitive network of nuclear receptors at the base of metazoan evolution.

Subjects Evolutionary Studies, Genomics, Molecular Biology, Diabetes and Endocrinology
Keywords *Trichoplax adhaerens*, RXR, 9-*cis* retinoic acid, Food, ERR, HNF4, COUP, Nuclear receptor

Submitted 21 April 2017
Accepted 18 August 2017
Published 29 September 2017

Corresponding author
Zdenek Kostrouch,
Zdenek.kostrouch@lf1.cuni.cz

Academic editor
Christopher Cooper

Additional Information and Declarations can be found on page 23

DOI **10.7717/peerj.3789**

How to cite this article Novotný et al. (2017), *Trichoplax adhaerens* reveals a network of nuclear receptors sensitive to 9-*cis*-retinoic acid at the base of metazoan evolution. **PeerJ 5:e3789; DOI 10.7717/peerj.3789**

INTRODUCTION

Life on Earth began 4.1 to 3.5 billion years ago (*Bell et al., 2015*) with the appearance of the first unicellular organisms that subsequently evolved, in part, to multicellular lifeforms forming the kingdom Metazoa that have specialized tissues for digestion, regulation of homeostasis, locomotion, perception, analysis of the environment and reproduction.

In contrast to unicellular organisms, metazoans are in need of regulatory mechanisms that provide the means of coordination between various tissues in a tight arrangement with cellular homeostasis. This coordination on the level of humoral signaling includes regulation by nuclear receptors (NRs), which respond to small, mostly hydrophobic molecules, including hormones produced by specific tissues, metabolites or even molecules present in the environment and transfer these signals to the nucleus, thus leading to a dynamically changing but adaptive gene expression (*Escriva, Bertrand & Laudet, 2004*).

NRs therefore play an important role in maintaining intra- and inter-cellular functions in multicellular organisms. Their overall structure is common in most nuclear receptors and consists of an A/B (N-terminal) domain, the DNA binding domain (DBD), a hinge region, the ligand binding domain (LBD) and the C-terminal domain (*Kumar & Thompson, 1999*; *Robinson-Rechavi, Escriva Garcia & Laudet, 2003*). The DBD and LBD of NRs exhibit an especially high degree of conservation and the changes that were acquired during evolution allow classification of the NR protein family into six subfamilies (*Laudet, 1997*; *Escriva et al., 1998*). NRs that evolved within these subfamilies show functional connections that include specialization of regulatory functions in time or cell type restriction, fortification of ancestral functions or their specific inhibition by newly evolved NRs (*Escriva, Bertrand & Laudet, 2004*; *Kostrouchova & Kostrouch, 2015*).

With the overall structure maintained across metazoan species, nuclear receptors show significant heterogeneity regarding their quantity and function, many of which have not yet been explored in e.g., *Caenorhabditis elegans* with over 280 nuclear receptors (reviewed in *Kostrouchova & Kostrouch, 2015*).

The evolutionary changes accumulated in diversified NRs allow functional subspecialization at the level of specific sequence binding within gene promoters (response elements), protein-protein interactions with functionally linked receptor interactors and adoption of new ligands as specific hormonal regulators. The evolution of hormonal ligands acquired by different species during evolution is well documented and indicates the potential of NRs to adopt new ligands as regulators (*Escriva, Delaunay & Laudet, 2000*; *Markov & Laudet, 2011*). Indeed, it is now thought that NRs evolved as environmental sensors that were able to sense a wide variety of compounds with low affinity and specificity, some of which later-on acquired higher affinity binding towards certain ligands that are products of metabolic pathways (*Holzer, Markov & Laudet, 2017*). This can be exemplified by the high affinity and specificity binding of certain receptors, such as the mineralocorticoid or androgen receptors, while the family of PPARs shows a rather promiscuous binding to a variety of different substances (*Issemann & Green, 1990*). Keeping in mind the metabolic origin of NR ligands, it is not completely surprising to see different ligands binding to

orthologues across species, such as Triac and T3 in the case of TR (*Paris et al., 2008*), thus changing in the course of evolution and adapting to new environments.

This is accompanied by the essential questions, to what degree the plasticity of ligand selection is a fundamental property of NRs and what the origin of specific ligand binding by NRs might be. It has been suggested that the original NR, which is the ancestral NR possessing gene regulatory capacity, may have been an unliganded molecular regulator (*Escriva et al., 1997*). However, it is now believed that the ancestral NR is most closely related to the NR2 subfamily, as members of this family can be found in basal metazoans and are sensors of fatty acids (*Holzer, Markov & Laudet, 2017*). More recently, it was proposed that the ligand binding and ligand-dependent regulatory potential of NRs is an inherent feature of the evolution of NRs (*Bridgham et al., 2010*). Due to their nature of fine tuning cellular responses in response to environmental changes without necessarily showing high affinity binding to a set of ligands, cross-species comparison of nuclear receptor networks might shed light on the details of the NR network function (*Holzer, Markov & Laudet, 2017*).

A search for NRs that may be closely related to an ancient ancestor of the NR family led to the discovery of an RXR orthologue in Cnidaria (*Kostrouch et al., 1998*). Surprisingly, this receptor showed not only extremely high degree of sequence identity with vertebrate RXRs, far surpassing the degree of conservation observed in insects but also by its ability to bind the same ligand as vertebrate RXRs, *9-cis*-retinoic acid (*9-cis*-RA), with an affinity close to that reported for vertebrate RXRs. Similarly, as vertebrate RXRs, the jellyfish RXR showed a specific binding preference for *9-cis*-RA over all-*trans*-retinoic acid (AT-RA) and was able to heterodimerize with vertebrate thyroid hormone receptor alpha. Recent genome sequencing projects confirmed the existence of highly conserved RXR across several metazoan species including insects (*Locusta migratoria* (*Nowickyj et al., 2008*)), that are evolutionarily older than species with a more diversified RXR orthologue such as Usp found in *Drosophila* (reviewed in *Gutierrez-Mazariegos, Schubert & Laudet, 2014*).

To date, the nuclear receptor network has mainly been studied in complex organisms already in possession of an extensive endocrine network. Albeit dissection of nuclear receptor networks in these organisms can outline functions and associated regulatory cascades, basal tasks might be obscured by the gain of further, more specialized functions. Genome analysis of the basal metazoan *Trichoplax adhaerens* by whole genome sequencing revealed four highly conserved nuclear receptors, namely orthologues of HNF4 (NR2A), RXR (NR2B), ERR (NR3B) and COUP-TF (NR2F) (*Baker, 2008*; *Srivastava et al., 2008*) and thus allows assessment of the most basal workings of nuclear receptors. Surprisingly, the degree of conservation of the predicted placozoan NRs with known vertebrate NRs is not only very high at the level of the predicted secondary structure, as can be expected for true NRs, but also at the level of the primary amino acid sequence. Especially the similarity of the placozoan RXR (TaRXR) to its vertebrate orthologues is high, as it is in the case of the cubomedusan RXR. *T. adhaerens,* which shows characteristics of a basal metazoan with only a few cell types (*Smith et al., 2014*) and a relatively simple 4 member NR complement, offers a unique model that may shed light on the evolution of gene regulation by NRs.

In this presented work, we attempted to study the placozoan RXR orthologue functionally. Our results show that *T. adhaerens* RXR binds 9-*cis*-RA with an affinity comparable to that of vertebrate and jellyfish RXRs and that *T. adhaerens* responds to nanomolar concentrations of 9-*cis*-RA with a transcriptional upregulation of the putative orthologue of a malic enzyme that is regulated by a heterodimer formed by liganded thyroid hormone receptor and RXR in vertebrates. We also show that 9-*cis*- RA affects the relative expression of the four NRs present in *T. adhaerens* genome suggesting that these NRs may form a regulatory network capable of responding to possible ligands present in these animals or their environment. In line with this, growth, multiplication and appearance of *T. adhaerens* are strongly affected by food composition, especially by red pigment containing algae suggesting that specific food components or their metabolites may be ligands involved in the ancestral regulatory network of NRs. In support of this, 3.3 nM 9-*cis*-RA interferes with *T. adhaerens* growth response to the feeding by *Porphyridium cruentum* and causes balloon-like phenotypes and death of animals while animals fed by *Chlorella sp*. are partially protected against the treatment by 3.3 nM 9-*cis*-RA, do not develop balloon-like phenotypes but are also arrested in their growth and propagation indicating that 9-*cis*-RA interferes with *T. adhaerens* growth and development.

METHODS

Bioinformatics and cloning of RXR

The predicted RXR gene models on jgi (http://jgi.doe.gov/) (*Nordberg et al., 2014*) were screened for the characteristic molecular signature of the DNA binding domain (C-X2-C-Xl3-C-X2-C-X15-C-X5-C-X9-C-X2-C-X4-C-X4-M) (*Kostrouch, Kostrouchova & Rall, 1995*) and the appropriate predicted gene model (protein ID 53515) was selected for further use.

The alignment of different RXRs was performed by Clustal Omega (http://www.ebi.ac.uk/Tools/msa/clustalo/) (*Sievers et al., 2011*) and adjusted/exported as an image file using Jalview (http://www.jalview.org). Protein domain characterization was performed with SMART (*Schultz et al., 1998*; *Letunic, Doerks & Bork, 2015*). Analysis of HNF4, ERR and COUP-TF was done similarly. Phylogenetic analysis was performed on RXR ClustalO alignment using PhyMLv3.1 (*Guindon et al., 2010*) implemented in SeaView v4.6.1 with a 100 bootstrap analysis and SPR distance computation. The tree was then visualized using FigTree v1.4.3.

T. adhaerens total RNA was obtained from 50-100 pooled individual animals and extracted using TRIZOL® reagent (Invitrogen, Carlsbad, CA, USA) according to the protocol supplied by the manufacturer.

Subsequently, cDNA was prepared with random hexamers and SuperScript III (Invitrogen™) according to the manufacturer's protocol. Several RXR transcripts were then amplified by PCR with primers covering the starting sequence ((GCG-GATCC)ATGGAGGACAGATCGTTTAAAAAA), starting at 32 bp 5′ of ATG (TCTACCAATGTTTATCGCATCGGTTA) and starting at 97 bp 5′ of ATG (TTAAGGCT-TAACTGATGATGTTGTGAATG) with a common reverse primer covering the last 24 bp of the predicted gene sequence ((CGGAATTC)TTAAGAACTGCCTGTTTCCAGCAT).

Each PCR product was then ligated into pCR®2.1-TOPO® or pCR®4-TOPO® vector with the classic TA Cloning Kit and TOPO TA Cloning Kit (Invitrogen™), respectively. The ligated products were then transformed using One Shot® TOP10 Chemically Competent *E. coli* and cultured on LB Agar plates containing 100 μg/ml ampicillin. Plasmid DNA was extracted from obtained colonies and screened for mutations by sequencing using vector specific M13 forward and reverse primers. Only non-mutated sequences were used in subsequent experiments. The RXR fragments were then restricted and inserted into pGEX-2T vector system for bacterial expression (Addgene, Cambridge, MA, USA). Proper insertion was verified by sequencing.

Protein expression

Bl21 pLysS bacteria were transformed with previously described RXR mRNA inserted into pGEX-2T vector. Stocks of transformed bacteria were stored in 8% glycerol according to the Novagen pET System Manual (11th edition) (https://www.google.cz/search?q=Novagen+pET+System+Manual+&ie=utf-8&oe=utf-8&client=firefox-b&gfe_rd=cr&ei=T9z1WMHJDsni8AfpmoGoCQ). For protein expression, bacteria were scraped from stock and incubated in Liquid Broth (LB) with ampicillin (100 μg/ml) and chloramphenicol (34 μg/ml) overnight. The culture was then used to inoculate 100 ml of LB + antibiotics and grown to OD600 = 0.6–0.8 at 37 °C, then induced with 100 μl 1M IPTG (isopropyl-D-thiogalactopyranoside) (Sigma-Aldrich, St. Louis, MO, USA) and moved to 25 °C (RT) for 5 h. The culture was then spun at 9,000 xg for 15 min and the supernatant discarded. The bacterial pellet was resuspended in 10 ml GST binding buffer (25 mM Tris pH 7.5, 150 mM NaCl, 1 mM EDTA) + protease inhibitor (S8820 Sigma Fast, Sigma-Aldrich, St. Louis, MO, USA or cOmplete™, EDTA-free Protease Inhibitor Cocktail, Roche, Basel, Switzerland). Bacteria were then lysed by 6 × 20 s ultrasonication on ice (50 watts, 30 kHz, highest setting—100%) (Ultrasonic Processor UP50H, Hielscher Ultrasonics GmbH, Teltow, Germany) and subsequently incubated with 15–20 mg glutathione agarose beads (Sigma-Aldrich®) prepared according to manufacturer's instructions. Incubation took place at 4 °C for about 10 h after which the beads were washed according to instructions, resuspended in regeneration buffer (50mM Tris–HCl pH7.4, 1mM EDTA, 120 mM KCl, 5 mM DTT, 8% glycerol (v/v)) or 50mM TRIS–HCl pH 7.4 + 9% (v/v) glycerol for subsequent thrombin (bovine plasma, Sigma-Aldrich®) cleavage, if performed, and then adjusted for regeneration buffer conditions. GST-TaRXR was eluted from glutathione agarose beads using 10 mM reduced glutathione (Sigma-Aldrich, StLouis, Mo, USA) in 50 mM Tris–HCl buffer pH 8.0. The size of the GST-TaRXR fusion protein was checked by polyacrylamide gel electrophoresis. Thrombin cleavage was performed at RT for 4 h and the quality of the purified protein was assessed by polyacrylamide gel electrophoresis.

Radioactive *9-cis RA* binding assay

Radioactive ^{3}H-labelled 9-*cis-RA* and ^{3}H-labelled AT-RA were purchased from PerkinElmer (Waltham, MA, USA). Binding was performed in 100 μl binding buffer (50mM Tris–HCl pH7.4, 1mM EDTA, 120 mM KCl, 5 mM DTT, 8% glycerol (v/v), 0.3%

to 0.5% (w/v) CHAPS (3-[(3-Cholamidopropyl)dimethylammonio]-1-propanesulfonate hydrate, Sigma-Aldrich)) for 2 h on wet ice in a dark environment. The protein used for binding was either GST-RXR fusion protein on beads with about 375 ng/assay and thrombin-cleaved RXR. For estimation of specific binding, 200x excess of either 9-*cis*- RA or AT-RA (Sigma-Aldrich) was used. In case of GST-RXR fusion protein, 50 µl of the supernatant was removed after 30 s at 1300 g and washed 3x with 1000 µl wash buffer (50 mM Tris–HCl pH7.4, 1 mM EDTA, 120 mM KCl, 5 mM DTT, 8% (v/v) glycerol, 0.5% (w/v) CHAPS) removing 900 µl after each wash. For cleaved RXR protein 10 µl hydroxyapatite slurry (AG-1 XB Resin, Bio-Rad, Hercules, CA, USA) suspended in binding buffer (12.7 mg/100 µl) were added to the assay and mixed twice, collecting the apatite slurry by centrifugation (15 s at 600 g). 95 µl of the supernatant was removed and the slurry washed twice with 1 ml of wash buffer, removing 900 µl after each wash. Work with retinoids was done under indirect illumination with a 60 W, 120 V yellow light bulb (BugLite, General Electric Co, Nela Parc, Cleveland Oh, USA) as described (*Cahnmann, 1995*). The radioactivity of the GST-fusion protein and cleaved protein was measured using Packard Tri-Carb 1600TR Liquid Scintillation Analyzer (Packard, A Canberra Company, Canberra Industries, Meriden, CT, USA) and Ultima Gold Scintillation Fluid (PerkinElmer, Waltham, MA, USA). The fraction of bound ^{3}H-labelled 9-cis-RA and ^{3}H-labelled all-*trans*-RA was determined as a ratio of the bound radioactivity of precipitated GST-TaRXR/total radioactivity used at the particular condition (determined as the sum of bound radioactivity and the total radioactivity of collected wash fluids) in the absence of non-radioactive competitors or 200 fold excess of 9-cis-RA and all-trans-RA in the case of ^{3}H-labelled 9-*cis*-RA and 40 fold excess of non-radioactive competitors in the case of ^{3}H-labelled all-*trans*-RA (to compensate for the higher affinity of 9-*cis*-RA compared to all-*trans*-RA in binding to TaRXR).

Culture of *T. adhaerens* and algae

Trichoplax adhaerens was cultured in Petri dishes containing filtered artificial seawater (Instant Ocean, Spectrum Brands, Blacksburg, VA, USA) with a salinity of approx. 38–40 ppt. *Rhodomonas salina* (strain CCAP 978/27), *Chlorella sp*., *Porphyridium cruentum* (UTEX B637) and other non-classified algae, as well as aquarium milieu established in the laboratory by mixing salt water obtained from a local aquarium shop were used to maintain the stock. The cultures were kept at approx. 23 °C and an automated illumination for 12 h/day was used with a conventional light bulb on a daylight background from late spring to mid-summer in the laboratory located at 50.07031N, 14.42934E with laboratory windows oriented eastward. The natural illumination included almost direct morning light from 8 AM to 10.30 AM, indirect sunlight for most of the daytime and sunlight reflected from a building across the street from 1 PM to 6 PM. Algae were maintained as described (*Kana et al., 2012*; *Kana et al., 2014*). The experiments were performed predominantly during sunny weather.

Treatment of *T. adhaerens* with retinoic acids

Incubation of the animals was done overnight in the absence of light. Each batch within an experiment was derived from similar cultures and fed with similar amounts and

composition of algae. All experiments were started in a dark room with indirect yellow light illumination (similarly as in the case of the ligand binding studies) and further incubations were done in the dark for 24 h. In experiments aimed at the visualization of 9-*cis*-RA effect on *T. adhaerens* response to feeding conditions, parallel cultures were set and fed with *P. cruentum*. Large animals of approximately the same size were individually transferred to new control and experimental cultures and fed with *P. cruentum* algal cells. After 6 h of incubation under natural indirect illumination, all animals in both control and experimental cultures were photographed (max. magnification on Olympus SZX7 with Olympus E-410 camera) and the final volume of cultures was adjusted to 50 ml (determined by the weight of cultures in 110 mm glass Petri dishes). Next, the room was darkened and further manipulations were done under indirect illumination with yellow light. Five μl of vehicle (1% DMSO in ethanol) or vehicle containing 9-*cis*-RA was added into 50 ml of final volume to the final concentration of 9-*cis*-RA 3.3 nM. Similarly, parallel sub-cultures were prepared from slowly growing cultures fed by microorganisms covering glass slides in an equilibrated 25 l laboratory aquarium and fed by *Chlorella sp*. Cultures were incubated in the dark for 24 h and all animals were counted under microscope and photographed again. The cultures were then left under natural illumination and cultured for an additional two or three weeks. Animals fed by *P. cruentum* were measured again at 72, 90 and 450 h and those fed by *Chlorella sp*. at 72, 90 and 378 h.

Quantitative PCR

Droplet digital PCR was performed on a QX100 Droplet Digital PCR System (Bio-Rad Laboratories, Hercules, CA, USA). For this, *T. adhaerens* was cultured according to culture conditions described and 4-10 animals removed per 100 μl TRIZol reagent (Invitrogen, Carlsbad, CA, USA). Total RNA was measured by a UV spectrophotometer and used as a reference for normalization.

Reverse transcription was performed with SuperScript III Reverse Transcriptase (ThermoFisher, Waltham, MA, USA) according to manufacturer's instructions. The cDNA (corresponding to 100–500 ng of RNA) was then mixed with ddPCR Supermix (Bio-Rad, Hercules, CA, USA) according to the manufacturer's instructions and analyzed. PCR primers were designed using the UPL online ProbeFinder (Roche) software and were as follows:

TaRXR—left:tctgcaagttggtatgaagca, right: agttggtgtgctattctttacgc
TaHNF4 ref|XM_002115774.1|:
left: ggaatgatttgattttacctcgac, right: tacgacaagcgatacgagca
TaCOUP-TF (ref|XM_002109770.1|):
left: attttgaatgctgcccaatg, right: ttactggttgtggagtatggaaac
TaSoxB1 (ref|XM_002111308.1|):
left: tgtcagatgcggataaacga, right: ggatgttccttcatgtgtaatgc
TaTrox-2 (ref|XM_002118165.1|):
left: gcctatagtcgatcctgccata, right: ttggtgatgatggttgtcca
TaPaxB1 (gb|DQ022561.1):
left: tcaaacgggttctgttagcc, right: ggtgttgccaccttaggc

TaERR (nuclear receptor 3, gb|KC261632.1):
left: ttacgcatgtgatatggttatgg, right: agcgtgcctatttatttcgtct

Results were subsequently analyzed using the Bio-Rad ddPCR software. Manual correction of the cut off was performed when automated analysis was not possible. To visualize changes in nuclear receptor expression in the absence of a reliable housekeeping gene as a reference, we considered the absolute quantity of each nuclear receptor as a percentage of the overall nuclear receptor expression and subsequently visualized the change of receptor expression by subtraction of the percentage of the control experiment. Absolute copy numbers of the proposed malic enzyme orthologue in *T. adhaerens* have been normalized to overall RNA quantity for expressional analysis.

Experiments with quantification by qRT-PCR were performed on a Roche LightCycler II with OneTaq polymerase and the same probes as for ddPCR.

For the estimation of the relative expression of NRs in small (<0.5 mm) versus big animals (>1 mm), 20 to 30 animals from the same culture were used for each paired experiment.

Identification of *T. adhaerens* orthologue of L-malate-NADP$^+$ oxidoreductase (EC 1.1.1.40)

P48163 (MAOX_HUMAN) protein sequence was used as the query sequence and searched against *T. adhaerens* database with BLASTP on http://blast.ncbi.nlm.nih.gov/Blast.cgi using standard algorithm parameters. The best hit was a hypothetical protein TRIADDRAFT_50795 with a sequence identity of 57% and a query coverage of 93% and was assumed to be *T. adhaerens* closest orthologue of vertebrate L-malate-NADP$^+$ oxidoreductase.

Microscopy and image analysis

Observation of *T. adhaerens* was done with an Olympus SZX10 microscope equipped with DF Plan 2x objective and Olympus DP 73 camera operated by CellSens Dimension computer program (kindly provided by Olympus, Prague, Czech Republic) or Olympus CKX41 or SZX7 with Olympus E-410 camera and QuickPhoto Micro 3.1 program.

Circularity was calculated by establishing the area (A) and perimeter (p) of *T. adhaerens* using ImageJ (https://imagej.nih.gov/ij/) and then calculated with the isoperimetric quotient $Q = \frac{4\pi A}{p^2}$, (A, Area; p, perimeter). GraphPad Prism 5 (or higher) was used for graphical representation and calculations of the confidence intervals with $p = 0.05$.

RESULTS

T. adhaerens retinoid X receptor shows high cross-species sequence identity

By using the ab initio model of the JGI *Trichoplax* database as a reference, we screened the *Trichoplax* JGI database for RXR orthologues with a complete DBD and LBD sequence and were able to obtain, as well as verify a full length RXR transcript previously not annotated as the 'best model'. Blastp analysis showed a high sequence similarity to human, as well as mouse RXR with 66% overall sequence identity to human RXR alpha.

SMART analysis of the proposed TaRXR sequence showed a zinc finger DNA binding domain (amino acid residues 16–87) and a ligand binding domain (amino acid residues 155–342) with E values $<10^{-40}$. Blast analysis of the zinc finger DNA binding and ligand binding domains revealed a sequence identity of 81% and 70% to human RXR alpha, respectively. Both domains contained the predicted molecular pattern characteristic for each domain. The heptad repeat LLLRLPAL proposed for dimerization activity (*Forman & Samuels, 1990b*; *Forman & Samuels, 1990a*; *Kiefer, 2006*) as well as the LBD signature for 9-*cis*-RA binding Q-x(33)-L-x(3)-F-x(2)-R-x(9)-L-x(44)-R-x(63)-H (*Egea, Klaholz & Moras, 2000*) were present (Fig. 1). From 11 amino acid residues shown to be critical for 9-*cis*-RA binding (A271, A272, Q 275, L 309, F 313, R 316, L 326, A 327, R 371, C 432, H 435), nine are conserved, while the remaining two amino acids are substituted (A327S, and C432T (C432A in *Tripedalia cystophora*)). Due to the high sequence identity, we propose a 9-*cis*-retinoic acid binding capability of the hypothesized TaRXR sequence, as well as DNA binding capability. Phylogenetic analysis using PhyML algorithm indicates that TaRXR is likely to precede branching of RXRs in cubomedusae and scyphomedusae and clusters with RXRs in bilateria Fig. S1).

The remaining three NRs identified in the *T. adhaerens* genome show also very high overall sequence identity with vertebrate orthologues. Alignments of *T. adhaerens* HNF4, COUP-TF and ERR with orthologues from selected species can be found in File S2.

TaRXR shows preferential binding affinity to *9-cis* retinoic acid over all-*trans*-retinoic acid

In order to analyze the binding properties of TaRXR, we expressed TaRXR as a GST-fusion protein (GST-TaRXR) in bacteria which was then purified as a GST-fusion protein and used directly for binding studies or cleaved by thrombin and eluted as TaRXR. The binding of ^{3}H-labelled 9-*cis*-RA or ^{3}H-labelled all-*trans*-RA was determined by measuring total bound radioactivity and the radioactivity displaceable by 200 fold excess of nonradioactive competitors. Consistent with the high conservation of the LBD, the experiments showed that TaRXR prepared as thrombin cleaved TaRXR or GST-TaRXR binds 9-*cis*-RA with high affinity and specificity (Figs. 2A and 2B). The 9-*cis*-RA binding assay showed high affinity binding to GST-TaRXR with a saturation plateau from 5 nM to 10 nM (Fig. 2C). In contrast, all-*trans*-retinoic acid did not show high affinity binding to TaRXR of GST-TaRXR.

9-cis-retinoic acid induces malic enzyme gene expression at nanomolar concentrations

Next, we searched whether 9-*cis*-RA has observable biological effects on *T. adharens* at nanomolar concentrations. We hypothesized that TaRXR is likely to be involved in the regulation of metabolic events. In vertebrates, RXR is a dimerization partner of TR and together these two NRs are regulating a wide range of metabolic pathways. We, therefore, searched for an orthologue of vertebrate L-malate-NADP^{+} oxidoreductase (EC 1.1.1.40) in *T. adhaerens* genome since this enzyme is an established reporter of the state of thyroid hormone dependent regulation (see 'Discussion').

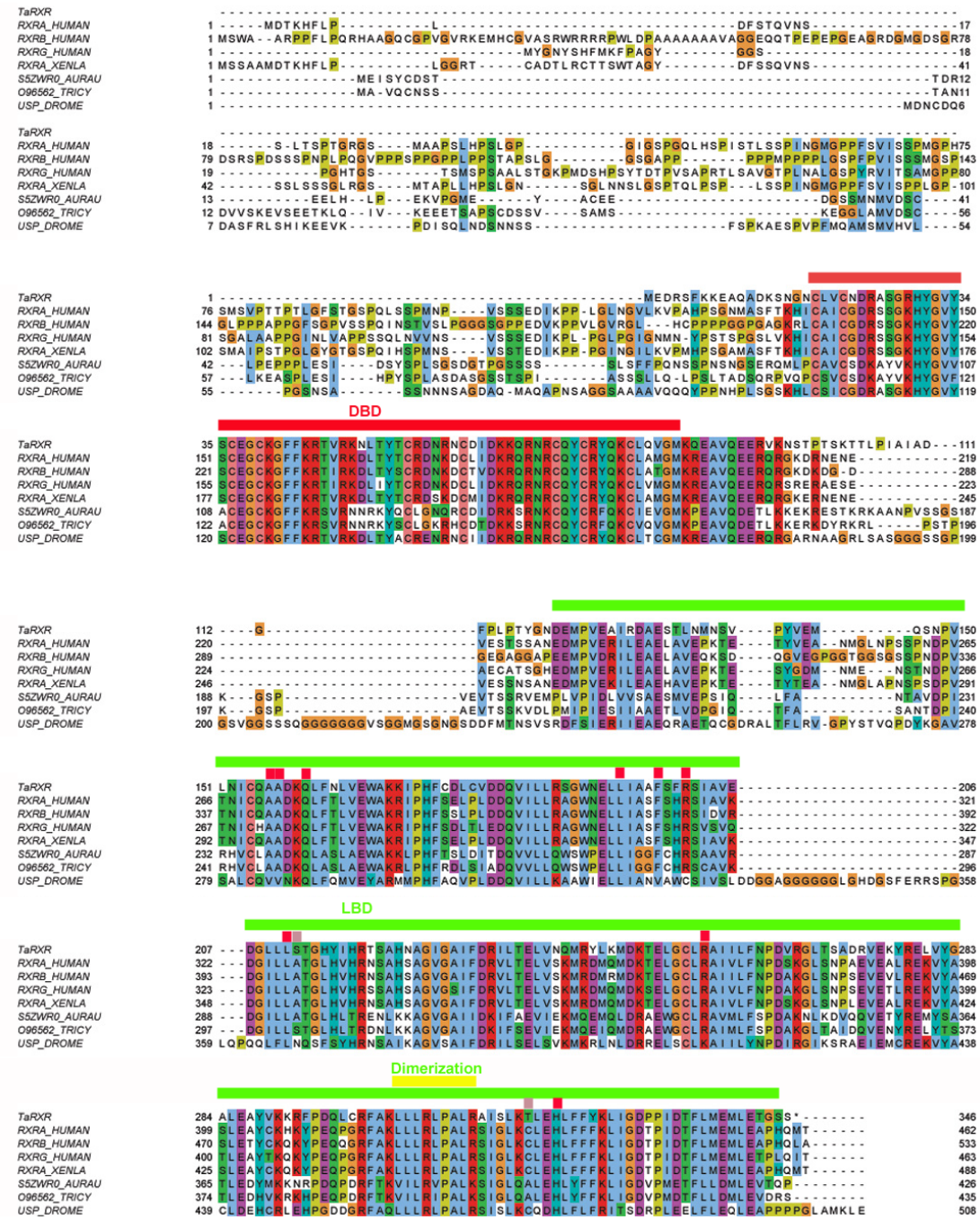

Figure 1 Multiple sequence alignment of selected metazoan homologues of RXR compared with TaRXR. Aligned with ClustalO, amino acid residue types colored according to Clustal scheme in Jalview, * indicates DBD footprint residues, # LBD footprint residues. Black box shows the DBD, red box represents the LBD. Sequences from top to bottom (organism, identifier): *Trichoplax adhaerens*, TaRXR ID 53515; *Homo sapiens*, sp|P19793|RXRA_HUMAN; *Homo sapiens*, sp|P28702|RXRB_HUMAN; *Homo sapiens*, sp|P48443|RXRG_HUMAN; *Xenopus laevis*, RXR alpha, sp|P51128|RXRA_XENLA; *Aurelia aurita*, RXR, tr|S5ZWR0|S5ZWR0_AURAU Retinoid X receptor; *Tripedalia cystophora*, RXR, tr|O96562|O96562_TRICY Retinoic acid X receptor; *Drosophila melanogaster*, USP, sp|P20153|USP_DROME. DNA binding domain (DBD, red line), Ligand binding domain (LBD, green line), dimerization domain (yellow line) and amino acid residues critical for 9-*cis*-RA binding (conserved—red rectangles, not conserved—pink rectangles) are indicated. Readers with specific color preferences may download the compared sequences (File S1) and create the Clustal scheme with different color specifications using the Jalview program (http://www.jalview.org/).

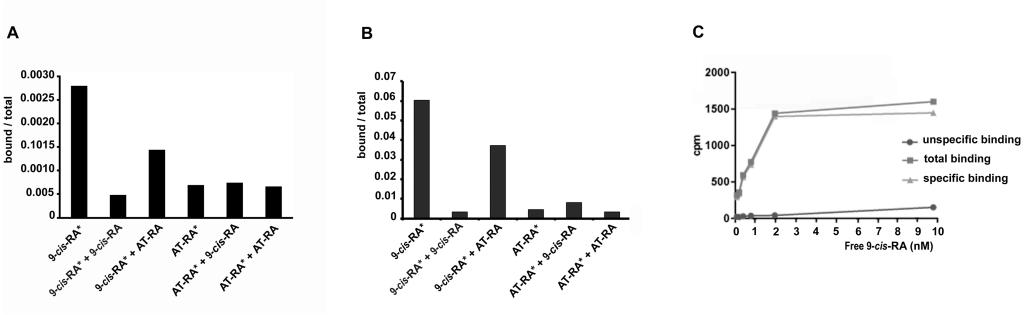

Figure 2 Binding of retinoic acids to TaRXR. (A) Single point analysis of binding preference of *T. adhaerens* RXR (thrombin cleaved) to ^{3}H-labelled 9-*cis*-RA over all-*trans*-RA. Radioactive 9-*cis*-RA (9-*cis*-RA*) binds at a concentration of 4 nM to 200 nanograms of *T. adhaerens* RXR. 200-fold excess of unlabeled *9-cis*-RA displaces more than 80% of labeled *9-cis*-RA from binding to *T. adhaerens* RXR (9-*cis*-RA* + 9-*cis*-RA) while the same molar excess of all-*trans*-RA (9-*cis*-RA*+ AT-RA) which is likely to contain approximately 1% spontaneously isomerized 9-*cis*- RA, competes away less than 50 % of bound ^{3}H-labeled 9-*cis*-RA. Radioactive ^{3}H-labeld all-*trans*-RA (AT-RA*) at identical conditions binds only slightly more than the observed non-specific binding. This interaction is not displaced by the excess of non-labeled 9-*cis*-RA (AT-RA* + 9-*cis*-RA) nor non-labeled all-*trans*-RA (AT-RA* + AT-RA). Results are expressed as a ratio of the radioactivity bound to TaRXR/total radioactivity used for the binding at the given condition. (B) Analysis of binding properties of *T. adhaerens* RXR (in the form of GST-TaRXR) to ^{3}H-labelled 9-*cis*-RA and ^{3}H-labelled all-*trans*-RA. The experiment differs from the experiment shown in A in 5-fold greater amount of radioactive all-*trans*-RA (and therefore only 40-fold excess of non-radioactive competitors). The experiment shows identical binding properties of GST-TaRXR as those observed with thrombin cleaved TaRXR. (C) Kinetic analysis of binding of ^{3}H-labeled 9-*cis*-RA to *T. adhaerens* RXR prepared as GST-fusion protein (GST-TaRXR). The plateau is reached at around 3 to 5×10^{-9} M.

The sequence of the *T. adhaerens* likely orthologue of vertebrate L-malate-NADP^{+} oxidoreductase was retrieved from the *Trichoplax* genomic database together with its presumed promoter based on the predicted sequence (File S3).

Droplet digital PCR showed an increased transcription of the predicted L-malate-NADP^{+} oxidoreductase gene after incubation of *T. adhaerens* with 9-*cis*-RA, but not with all-*trans*-RA (Fig. 3). In repeated experiments, we observed that the level of induction was higher at 9-*cis*-RA concentrations in the range of 1 to 10 nM, than above 10 nM. We also noticed that the level of the induction slightly varied based on the actual *T. adhaerens* cultures and the algal food composition of the *T. adhaerens* cultures.

Changes in the culture environment alter the expression pattern of the nuclear receptor complement in *T. adhaerens*

From the experience we gained by culturing *T. adhaerens*, as well as from the previous experiments we knew that the culture conditions could dramatically influence phenotype. Having the possible developmental functions of the ancestral NRs in mind, we raised the question whether the expression patterns of the NRs reflect changes in phenotype.

Firstly, we assayed the relative expression of RXR against all three other NRs in small versus big animals (<0.5 mm or >1 mm). The relative proportion of & expression compared to the remaining NRs was found to be higher in big animals (33%) than in small animals (24%). The treatment by 3.3 nM 9-*cis*-RA led to a dramatic increase of the relative

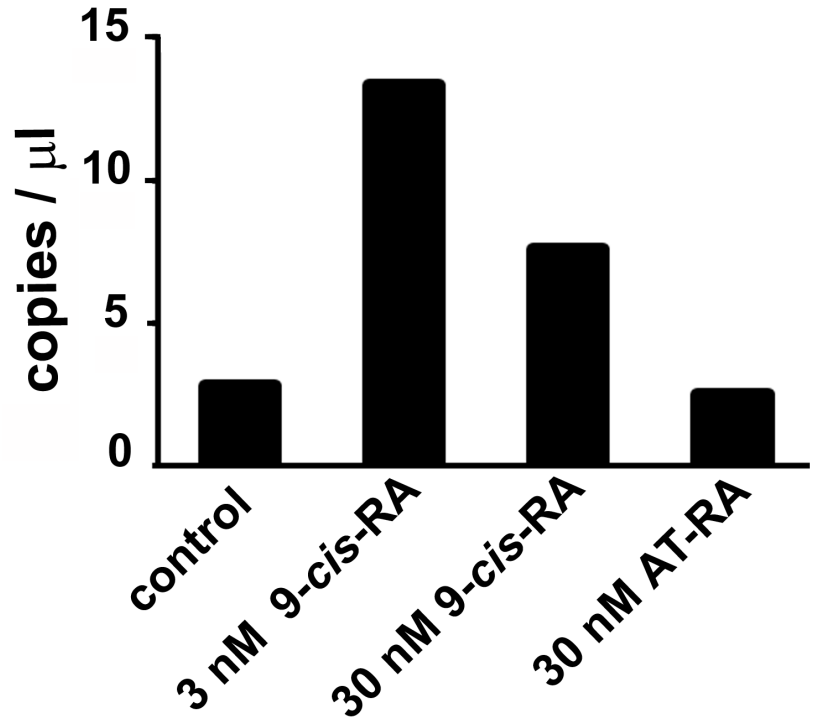

Figure 3 The effect of 9-*cis*-RA on the expression of the *T. adhaerens* closest putative homologue and likely orthologue of L-malate-NADP$^+$ oxidoreductase (EC1.1.1.40). Ten to fifteen animals were cultured in the dark overnight with indicated ligands or in medium containing only the solvent used for ligand solutions. Total RNA and cDNA were prepared using identical conditions and diluted to the same working concentration suitable for ddPCR. In repeated experiments, incubation with 3 nM 9-*cis*-RA induced expression of the putative *T. adhaerens* L-malate-NADP$^+$ oxidoreductase more than four times. Incubation with 30 nM 9-*cis*-RA induced enzyme expression also, but to a lesser extent and 30 nM all-*trans*-RA (AT-RA) did not upregulate the expression of the predicted L-malate-NADP$^+$ oxidoreductase.

expression of RXR in comparison to the rest of the NR complement (51%), indicating that phenotypic changes are connected with differential expression of NRs and that 9-*cis*- RA affects the expression of RXR.

In order to see the effect of 9-*cis*-RA on all NRs, we sampled and extracted RNA from cultures containing the same number of big and small animals treated with different concentrations of 9-*cis*-RA. The experimental cultures were started from the same original cultures and during incubation were fed with *Chlorella sp.* only since this algal food showed to have the least effect on *T. adhaerens* cultures. All four *T. adhaerens* NRs were quantified by either qRT-PCR or ddPCR.

Analysis of NR expression pattern in animals incubated with different concentrations of 9-*cis*-RA, revealed a relative increase in RXR expression at low nanomolar concentrations (<10 nM) in repeated experiments. In contrast, further increase of 9-*cis*-RA resulted in smaller changes compared to the expression pattern of NRs in control animals or even reverted the values observed in low nanomolar conditions (Fig. 4).

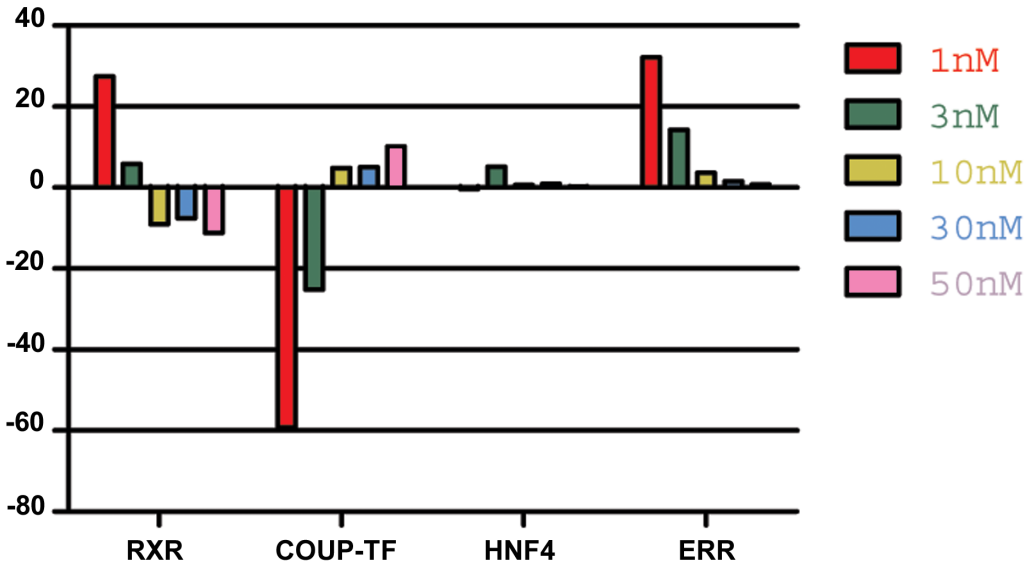

Figure 4 The effect of *9-cis*-RA on the expression of *T adhaerens* NRs. A representative experiment of the expression of *T. adhaerens* NRs in animals exposed to various concentrations of 9-*cis*-RA expressed as a ratio of obtained values compared to the control using ddPCR. One and 3 nM 9-*cis*-RA upregulate RXR and ERR, but downregulate COUP-TF. The expression of *T. adhaerens* HNF4 is not affected by 9-*cis*-RA. The effect of the exposure to 9-*cis*-RA is stronger in the case of 1 nM 9-*cis*-RA compared to 3 nM 9-*cis*-RA. The exposure to 30 nM, as well as 50 nM concentrations of 9-*cis*-RA reverse the effect of 9-*cis*-RA on the expression of RXR and COUP-TF, but do not influence the expression of ERR. The level of expression of HNF4 is not changed by exposure of *T. adhaerens* to various concentrations of 9-*cis*-RA. The data suggest that a network sensitive to nanomolar concentrations of 9-*cis*-RA at the expressional level is formed by RXR, COUP-TF and ERR. All four NRs have conserved P-box (regions responsible for binding to response elements (RE) in gene promoters) and are likely to bind overlapping REs and to form a functional network.

Food composition dramatically changes the phenotype and the reproduction rate of *T. adhaerens*

T. adhaerens retrieved from laboratory aquariums used for the stock cultures were relatively similar in appearance and included small round animals containing approximately 50 cells and grew to animals with an approximate diameter of 0.2 mm and rarely were bigger. Their rate of multiplication when transferred to Petri dishes was doubling in one month or even one week, depending on whether the glass was covered by microbial and algal films established during culturing in aquariums. We attempted to use several defined algae as artificial food. They included *Pyrrenomonas helgolandii*, *Picocystis salinarium*, *Tetraselmis subcoriformis*, *Rhodomonas salina*, *Phaeodactylum tricornutum*, *Porphyridium cruentum* and *Chlorella sp*. Individual subcultures of *T. adhaerens* differed in the rate of propagation and appearance as well as colors that were varying from greenish to brown and reddish taints depending on the food that was used as singular species food or mixtures (Fig. 5). Also, contaminants from the original algal food, which prevailed in some cultures, had an influence on *T. adhaerens* growth and behavior. In controlled experiments, it became clear that some food components or their metabolites are influencing growth and appearance of *T. adherens* more than food availability. When *T. adhaerens* were fed with

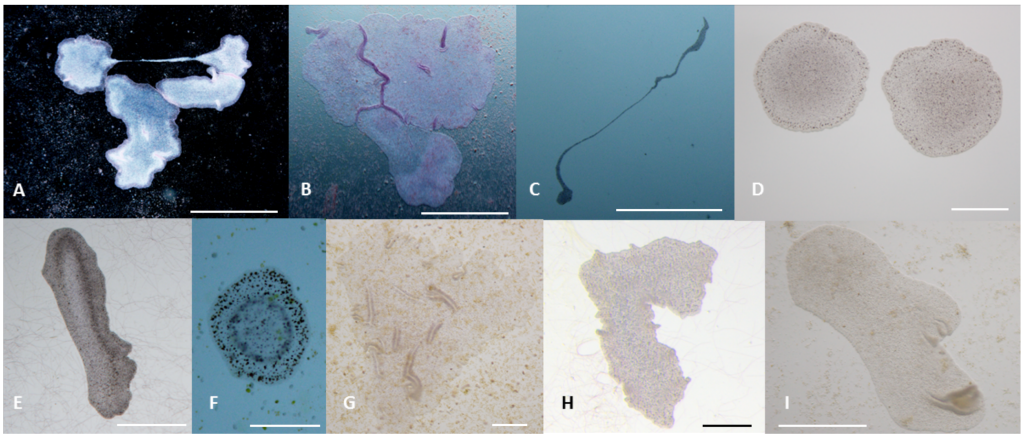

Figure 5 Phenotypes of *T. adhaerens* change at various feeding conditions. *T. adhaerens* acquires various body shapes in individual cultures dependent on food availability and composition. At conditions maintained in stable and biologically equilibrated stock aquariums, *T. adhaerens* is usually small and pale with diameter varying from 50 μm to 400 μm while cultures with added algae contain large flat animals with diameter reaching up to 1 mm (A and B). In some cultures, animals grow as long stretching structures, reaching a length exceeding one or even several centimeters (C). The algal food makes the animals greenish, reddish, rusty or brown with variable proportion of prominent dark cells. Animal shapes also vary from flat and round with smooth circumference, to curved or ruffled circumference or animals with long projections. Bars represent 1 mm in (A, B, I), 1 cm in C, 250 μm in (D), 500 μm in (E and H), 200 μm in (F) , and 100 μm in (G).

equal amounts of algal cells (although they differed in size and expected digestibility), the addition of algae containing red pigments—Cryptophytes (*Pyrrenomonas helgolandii* and *Rhodomonas salina*) or Rhodophyta (*Porphyridium cruentum*)—had a strong positive effect on *T. adhaerens* growth (Fig. 6), especially in combination with the green algae *Chlorella sp.* (Fig. 6).

Furthermore, the addition of *Porphyridium cruentum* to *Chlorella sp.* resulted in a significant change in circularity, while feeding *T. adhaerens* with 'triple food' containing *Chlorella*, *Rhodomonas* and *Porphyridium* showed the most pronounced effect. Culturing *T. adhaerens* on either of the single foods showed similar isoperimetric values (Fig. 7).

9-*cis*-RA interferes with *T. adhaerens* growth response to specific algal food

In order to see the effect of 9-*cis*-RA on *T. adhaerens* in cultures, we exposed cultures kept in a naturally established laboratory microenvironment or fed by specific algal foods to 3, 5 and 10 nM 9-*cis*-RA. The slowly growing cultures kept in naturally established laboratory microenvironment did not show any gross morphological changes even in 10 nM 9-*cis*-RA during the period of one week. Contrary to that, cultures fed with mixed algal food incubated in the presence of 3 and 5 nM 9-*cis*-RA ceased propagation and most animals developed a balloon-like phenotype, and later darkened and decomposed.

For controlled experiments, cultures fed by *P. cruentum* or *Chlorella sp*. were incubated in the presence of vehicle (DMSO/ethanol) or vehicle containing 9-*cis*-RA at 3.3 nM final concentration. After 24 h of incubation in the dark, control cultures fed by *P. cruentum*

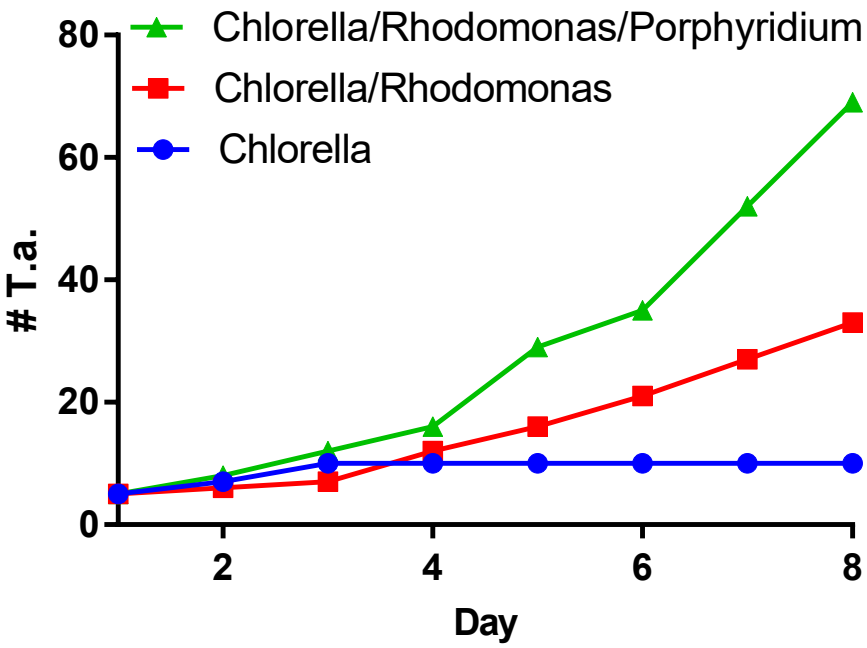

Figure 6 Propagation of *T. adhaerens* depends on algal food composition. Three cultures of five large animals in each were established and fed with the same number of algal cells consisting of *Chlorella sp.*, *Chlorella sp.* and *Rhodomonas salina* and *Chlorella sp.*, *Rhodomonas salina* and *Porphyridium cruentum*. While the culture fed with *Chlorella sp.* only doubled in the number of animals within a period of one week, cultures with red pigment containing algae multiplied more than five times and 10 times within the same time period.

propagated normally while animals fed by *P. cruentum* and incubated with 9-*cis*-RA decreased their area and perimeter (Fig. 8A). At 72 h of incubation, all animals fed by *P. cruentum* and treated by 3.3 nM 9-*cis*-RA developed the balloon-like phenotype and none of them survived 90 h of exposure to 9-*cis*-RA (Fig. 8B and Fig. S2). Animals transferred from stationary cultures grown in a naturally established laboratory microenvironment and subsequently fed by *Chlorella sp*. suffered initial loses at 24 h of incubation despite that their appearance seemed to be normal and well adopted to the new culture condition at time 0 (regarding feeding with algal food and immediately prior to addition of vehicle or 9-*cis*-RA to the culture and 6 h after the transfer from the parent cultures). Animals that survived the transfer and adopted to feeding by *Chlorella sp*., were not inhibited by exposure to 3.3 nM 9-*cis*-RA for 24 h (Fig. 8C) and even showed a slight statistically not significant increase in their area and perimeter. Nevertheless, the isoperimetric values of animals incubated for 24 h with 9-cis-RA showed a significant increase indicating a decrease of growth or exhaustion of peripheral area, that is likely to contain stem cells that further differentiate into the specialized cell types (*Jakob et al., 2004*). In contrary to animals fed by *P. cruentum,* exposure to 9-*cis*-RA was not associated with the development of the balloon-like phenotype and animals survived more than 250 h (Fig. S3). In contrast to control animals which started to proliferate after 100 h, animals exposed to 9-*cis*-RA did not proliferate between 90 and 280 h of subsequent culture (Fig. 8D) suggesting that

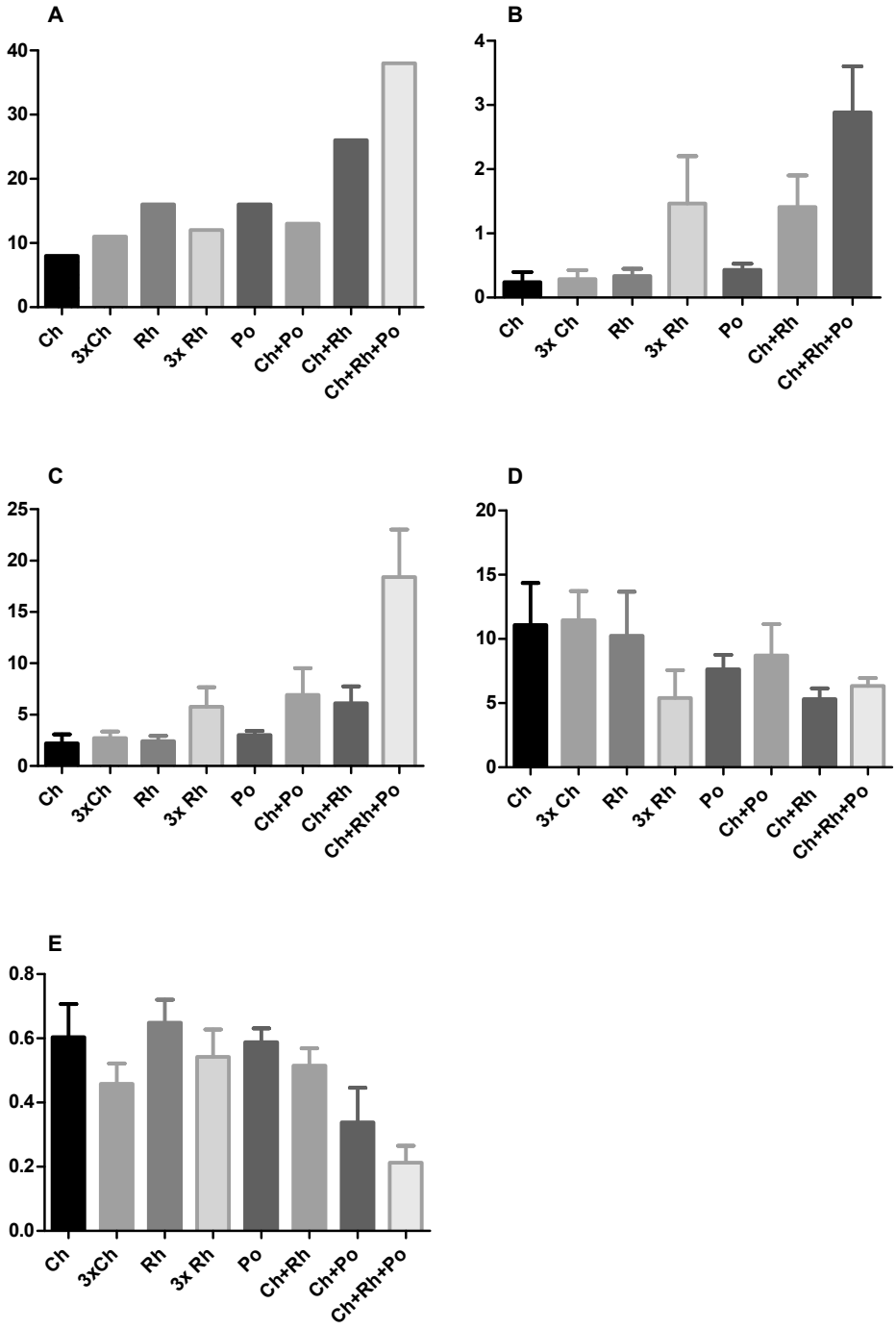

Figure 7 The effect of algal food composition on *T. adhaerens* growth and appearance. *T. adhaerens* was cultured similarly as shown in Fig. 6 and all animals were photographed and analyzed using ImageJ program for their number (A), mean area (B), mean perimeter (C), mean perimeter/area ratio (D) and mean isometric quotient (E) (continued on next page…)

Figure 7 (…continued)
after one week. Ch—stands for feeding with *Chlorella sp.*, Rh—*Rhodomonas salina*, Po—*Porphyridium cruentum*, and their combinations. 3Rh stands for a culture with three times higher concentration of *Rhodomonas salina* and 3Ch for three times higher concentration of *Chlorella sp.* (A) shows that addition of *Rhodomonas salina* (Ch + Rh) greatly increases the number of animals observed after one week of culture. This effect is even more pronounced in cultures containing all three algae, while three times bigger concentration of only one type of algae (Ch and Rh) has little or no effect. This is even more pronounced when the area and perimeter are determined (B and C). Determination of the isoperimetric quotient in individual cultures indicates that cultures with *Rhodomonas salina* have a significantly smaller ratio, suggesting higher proliferative rate of structures at the animal circumference (E). Bars represent 95% confidence interval. Raw data are provided as Files S5 and S6.

9-*cis*-RA interferes with animal response to specific food and processes necessary for animal growth and propagation. The growth arrest of *T. adhaerens* caused by 9-*cis*-RA was reverted by addition of *Porphyridium cruentum* indicating that a specific food constituent rather than food availability interferes with 9-*cis*-RA regulatory potential (Fig. S4).

DISCUSSION

T. adhaerens is probably the closest living species to basal metazoans with only four NRs

Trichoplax adhaerens is an especially interesting species from an evolutionary perspective. It shows the most primitive metazoan planar body arrangement known with a simple dorsal-ventral polarity, the establishment of which is one of the most ancient events in evolution of animal symmetries (*Smith et al., 1995*; *Stein & Stevens, 2014*). The Placozoa are disposed with only a few (probably six) morphologically recognizable cell types (*Jakob et al., 2004*; *Smith et al., 2014*).

In strong contrast to this, the *T. adhaerens* genome shows larger blocks of conserved synteny relative to the human genome than flies or nematodes (*Srivastava et al., 2008*). Genome analyses indicate that Placozoa are basal relative to Bilateria as well as all other diploblastic phyla (*Schierwater et al., 2009*), but all kinds of different views are also discussed (reviewed in *Schierwater et al., 2016*).

In concordance with this, its genome contains four (*Srivastava et al., 2008*) rather than 17 NRs, which can be found in the cnidarian *Nematostella vectensis* (*Reitzel & Tarrant, 2009*). Even though it has been proposed that Placozoa lost representatives of NR6 (SF1/GCNF), TR2/TR4 of the NR2 subfamily and invertebrate specific nuclear receptors (INR, clade of invertebrate-only nuclear receptors with no standard nomenclature) NR1/NR4 (*Bridgham et al., 2010*). The reasoning in this direction depends on the assumed phylogenic position of the phylum Placozoa.

The four NRs found in the genome of *T. adhaerens* are relatively highly related to their vertebrate counterparts, RXR (NR2B), HNF4 (NR2A), COUP-TF (NR2F) and ERR (NR3B) (*Srivastava et al., 2008*). Among them, *T. adhaerens* RXR and HNF4 show the highest degree of identity in protein sequence and the relatedness of *T. adhaerens* RXR (TaRXR) to human RXR is similar to that of *Tripedalia cystophora* RXR (jRXR) (*Kostrouch et al., 1998*), which has also been shown to bind 9-*cis*-RA at nanomolar concentrations. These results suggest that TaRXR is structurally and also functionally very closely related

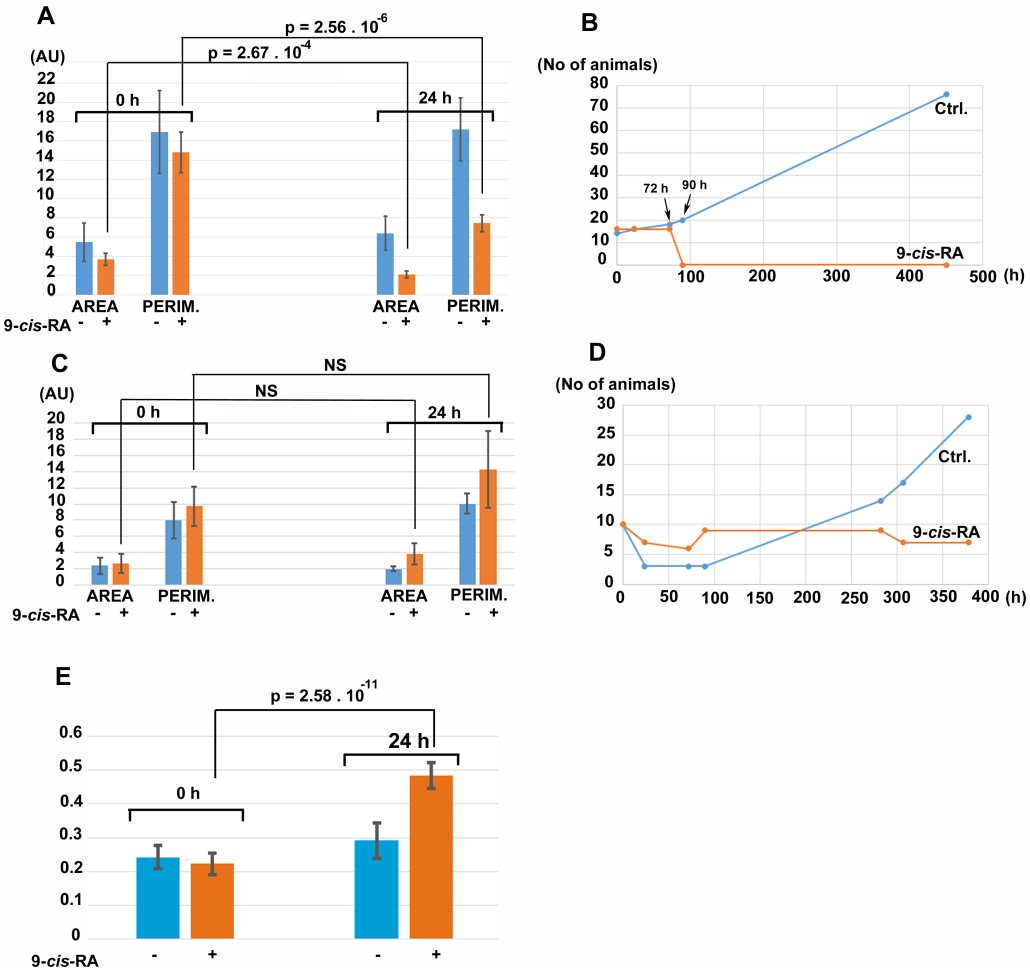

Figure 8 **The effect of 9-*cis*-RA on growth of *T. adhaerens* fed by *Porphyridium cruentum* or *Chlorella sp.*** (A) shows the comparison of the total area and total perimeter of control *T. adhaerens* and *T. adhaerens* treated by 9-*cis*-RA for 24 h expressed as arbitrary units derived from pixel measurements obtained at 24 h and compared to values obtained immediately prior to incubation. The data indicates that animals incubated in 3.3 nM 9-*cis*-RA decreased their area and perimeter to approximately 50% in comparison to control animals. (B) shows the development of cultures over a three-week period. The animals treated by 9-*cis*-RA developed a balloon-like phenotype at 72 h of incubation and died at 90 h of incubation. (C and D) show the data obtained with *T. adhaerens* originating from cultures fed by naturally established biofilms in laboraotory aquariums, fed by *Chlorella sp.* and treated similarly as shown in (A and B). (E) shows the analysis of circularity of animals presented in (A) and documents that animals treated by 9-*cis*-RA increased their circularity already at 24 h of exposure suggesting arrest of growth of animal peripheral tissues.

to its vertebrate counterparts, most probably representing the most basal liganded NR of all Metazoa known today.

T. adhaerens RXR binds preferentially 9-*cis*-RA

By using a radioactively labelled ligand, we could demonstrate that the RXR orthologue in *T. adhaerens* binds 9-*cis*-RA with very high affinity and shows a strong binding preference

to 9-*cis*-RA over all-*trans*-RA similarly, as is the case in vertebrate RXRs (*Allenby et al., 1993*) and the cnidarian TcRXR (*Kostrouch et al., 1998*).

9-*cis*-RA affects the expression of a *T. adhaerens* orthologue of a conserved metabolically active enzyme, L-malate-NADP$^+$ oxidoreductase

A biological role of 9-*cis*-RA binding with high affinity to the placozoan RXR receptor is supported by our *in vivo* experiments. In the search for genes that may be under the regulation of TaRXR, we identified a putative orthologue of vertebrate L-malate-NADP$^+$ oxidoreductase (EC 1.1.1.40) and analyzed the effect of 9-*cis*-RA or all-*trans*-RA on its expression. In agreement with our binding experiments, we observed induction of this enzyme's expression at low nanomolar concentrations of 9-cis-RA (1 to 10 nM). Interestingly, higher concentrations of 9-*cis*-RA (30 nM) had a smaller effect on expression and all-*trans*-RA had no effect up to 30 nM concentrations. A plausible explanation for this could be that 9-*cis*-RA also acts as a ligand for other *T. adhaerens* NRs which may have an opposite effect on the expression of L-malate-NADP$^+$ oxidoreductase. Furthermore, 9-*cis*-RA could act as a supranatural ligand and the continuous occupation of TaRXR by this high affinity ligand may interfere with the normal function of the receptor within the transcription initiation machinery.

In mammals, regulation of malic enzyme expression is mediated by a thyroid hormone receptor (TR)—RXR heterodimer (*Dozin, Cahnmann & Nikodem, 1985*; *Dozin, Magnuson & Nikodem, 1985*; *Petty et al., 1989*; *Petty et al., 1990*). By showing a 9-*cis*-RA dependent change in the expression of the likely placozoan malic enzyme orthologue *in vivo*, we provide indirect evidence of a conserved RXR mediated regulation of gene expression. Although the expression of L-malate-NADP$^+$ oxidoreductase in mammals is usually used as a factor reflecting regulation by thyroid hormone (*Dozin, Magnuson & Nikodem, 1986*), it has also been shown that its cell-type associated differences depend on the expression level of RXR alpha (*Hillgartner, Chen & Goodridge, 1992*; *Fang & Hillgartner, 2000*) suggesting that regulation by RXR has been conserved throughout metazoan evolution while additional regulation via thyroid hormone represents an innovation of Bilateria (*Wu, Niles & LoVerde, 2007*).

NRs form a network responding to 9-*cis*-RA

Since autoregulation and cross-regulation of NRs by their specific ligands is well documented for a large number of nuclear receptors (*Tata, 1994*), we searched if 9-*cis*-RA affects the expression of TaRXR mRNA relative to the other *T. adhaerens* NRs. Our *in vivo* experiments showed not only effects on specific gene expression in response to very low concentrations of 9-*cis*-RA (at 1 or 3 nM), but also an additional dose-dependent reverse effect of higher concentrations. This is likely to be in line with our binding experiments that suggested the possibility of an additional binding site or sites with higher capacity and lower affinity. We also cannot rule out that higher concentrations of 9-*cis*-RA affect some of the three remaining *T. adhaerens* NRs. Nevertheless, an inhibitory effect of 9-*cis*-RA on the expression of its cognate receptor at the protein level (through protein degradation) was reported (*Nomura et al., 1999*).

Although it is not clear if 9-*cis*-RA is the natural ligand for RXRs (*Wolf, 2006*; *Ruhl et al., 2015*) conserved in all metazoan phyla studied to date, we show not only that 9-*cis*-RA binds TaRXR with nanomolar affinity but also positively regulates its expression, which resembles auto-activation of several NRs in vertebrates (e.g., ER and TR (*Tata, 1994*; *Bagamasbad & Denver, 2011*)). Furthermore, three out of four NRs constituting the NR complement in *T. adhaerens* respond to treatment by 9-*cis*- RA at transcriptional level. Two NRs, RXR itself and ERR, respond positively to nanomolar concentrations of 9-*cis*-RA, while COUP-TF, which often acts as an inhibitor of specific gene expression (*Tran et al., 1992*), is regulated negatively by 9-*cis*-RA. COUP-TF was recently shown to be inactivated by small hydrophobic molecules (*Le Guevel et al., 2017*). The regulatory connections of *T. adhaerens* NRs places the autoregulation and cross-regulation of NRs to the base of metazoan evolution. The proposed regulatory network of *T. adhaerens* NRs is schematically represented in Fig. S5.

Food composition rather than quantity affects phenotype of *T. adhaerens*

At first glance, *T. adhaerens* seems to benefit from any source of biological material on surfaces that can be digested and absorbed by its digestive system (e.g., aquarium microorganisms and detritus). Feeding with certain live microorganisms in laboratory cultures, however, dramatically changes the dynamics of *T. adhaerens* cultures, such as shape, size, color, body transparency, growth and divisions of the animal. For example, we observed poor growth and reproduction rates of *T. adhaerens* fed solely on *Chlorella sp.* even at a relatively high density. In contrast, cultures fed with red pigment containing *Rhodomonas salina* showed much faster proliferation and led, in part, to the formation of giant animals, seeming to halt their division. Despite *Porphyridium cruentum* containing similar pigments as *Rhodomonas*, such as phycoerythrin, cultures grown with *Porphyridium* as the main nutrient source did not show phenotypical abnormalities but the addition of it to a culture with *Chlorella* and *Rhodomonas* resulted in an additive effect on reproduction rate.

Even though the growth of *T. adhaerens* seems to follow a simple program, it is likely to require strict regulatory mechanisms. Formation of specific cellular types is connected with phenotypic appearance of animals possessing larger proportions of certain cells, e.g., upper epithelium in balloon-like animals or larger proportion of peripheral regions containing stem cell-like cells in narrow or prolonged animals. Analysis of circularity as a measure of location specific cellular proliferation is in concordance with the observed culture characteristics and shows that lower isoperimetric values (less 'roundness') indicate higher reproduction rates.

Our experiments provide evidence that food composition is more important for *T. adhaerens* growth and propagation than its quantity, which is in line with the recent finding of phosphate and nitrate playing important roles determining the distribution of placozoans around the globe (*Paknia & Schierwater, 2015*). It indicates that food constituents, especially those present in the algae containing phycobilin based red pigments like *Rhodomonas salina* and *Porphyridium cruentum* might possess hormone-like molecules or molecules resulting in hormone-like metabolites in *T. adhaerens* that act through the

NR complement and, indeed, analysis of NRs in differently sized animals indicates impact of food composition on NR expression.

The high sensitivity of *T. adhaerens* to 9-*cis*-RA reflected by the transcriptional response to low nanomolar concentrations of 9-*cis*-RA but not all-*trans*-RA and the interference of 3.3 nM 9-*cis*-RA with the animal response to feeding together with the high affinity binding of 9-*cis*-RA by TaRXR suggests that the response of *T. adhaerens* to 9-*cis*-RA is mediated by TaRXR. It cannot be excluded that other *T. adhaerens* NRs, especially TaCOUP-TF and possibly also TaHNF4 may also be affected by 9-*cis*-RA. It seems possible that 9-*cis*-RA or similarly shaped molecules may be present in *T. adhaerens* food or can be formed from retinoids and other molecular components of food. Our data indicate that the sensitivity of *T. adhaerens* to 9-*cis*-RA depends on the actual feeding conditions and animal growth. There are several possible scenarios that may explain the high sensitivity of *T. adhaerens* to 9-*cis*-RA. The activation of RXR by 9-*cis*-RA or similar compounds has been documented in vertebrates (*Allenby et al., 1993*; *Ruhl et al., 2015*; *De Lera, Krezel & Ruhl, 2016*). The observation of 9-*cis*-RA induced growth arrest is similar as data reported on mammalian cells (e.g., *Wente et al., 2007*) however the concentration of 9-*cis*-RA used in our experiments is approximately 30 to 3,000 times lower than the levels reported in most mammalian systems. It seems likely that very low concentrations of natural ligands including 9-*cis*-RA or similarly shaped molecules or other molecules present in the algal food or produced from algal food as metabolites in *T. adhaerens* regulate the gene expression via RXR in *T. adhaerens*. This may be connected with *T. adhaerens* strong response to light exposure visible as coordinated relocations of animals inside laboratory culture containers and a strong influence of annual seasons on *T. adhaerens* propagation rates observed in laboratories localized in temperate geographical zones. The 9-*cis* conformation of RA is not only sensitive to light exposure with its reversal to all-trans conformation but it can also be formed by specific UV irradiation from all-trans conformation up to 10% as shown by Dr. Hans Cahnmann (*Cahnmann, 1995*).

Chlorophyll hydrophobic side chain which anchors the molecule to the chloroplast thylakoid membrane is metabolized to phytol that was shown to act as an RXR agonist (*Kitareewan et al., 1996*). Other molecules called rexinoids, which often contain aromatic rings in their structure act as RXR agonists or antagonists (*Dawson & Xia, 2012*). Lately, another group of ligands called organotins was shown to affect regulation by RXR (*Le Maire et al., 2009*). It has been proposed that RXRs can bind a larger group of polyunsaturated fatty acids (docosahexaenoic acid and arachidonic acid) and act as their sensors (*De Urquiza et al., 2000*; *Lengqvist et al., 2004*).

When viewed together, our work shows the presence of 9-*cis*- RA binding RXR in Placozoa and argues for the existence of ligand regulated NRs at the base of metazoan evolution. Our observations suggest the existence an endocrine-like regulatory network of NRs in *T. adhaerens* (schematically represented in Fig. S5). Endocrine, hormone-receptor regulations involving NRs may be viewed as specialized, very powerful yet not prevailing regulations transmitted by NRs. Increasingly larger numbers of non-hormonal ligands originating in environment, food or metabolism are emerging as regulatory molecules of NRs (*Holzer, Markov & Laudet, 2017*). Our data suggest that non-hormonal, environment

and food derived ligands are likely to be the first or very early ligands regulating the metazoan response to food availability and orchestrating growth of basal metazoans and necessary differentiation to specialized cell types. In this sense, NRs in *T. adhaerens* represent an endocrine-like system of ancestor NRs.

This work suggests that ligand regulated RXR is involved in the coordination of animal growth and development throughout the metazoan evolution. This also suggests that the regulation by liganded NRs evolved as an evolutionary need connected with heterotrophy and multicellularity.

In fact, despite fragments of NR domains being found in prokaryotes, no single full sized NR has been discovered in bacteria or archaea and the closest known relatives to metazoans, unicellular and colonial Choanoflagellates, lack nuclear receptors, as well as genes of several other regulatory pathways (*King et al., 2008*). On the other hand in fungi, the sister group of Holozoa, *Shalchian-Tabrizi et al., (2008)* transcription factors surprisingly similar to metazoan NRs evolved independently possibly for the regulation of metabolism and response to xenobiotics (*Thakur et al., 2008*; *Naar & Thakur, 2009*). Thus, the evolution of NRs seems to be associated with two key evolutionary features of metazoans: multicellularity and heterotrophy.

Ctenophores, a possible sister phylum to *Cnidaria*, do not contain classical NRs featuring both mechanistically critical domains of NRs, the DNA binding and ligand binding domains. Nevertheless, the ctenophore *Mnemiopsis* contains two orthologues of NR2A (HNF4) that lack the DNA binding domain (*Reitzel et al., 2011*).

Our observations of the exceptionally high sensitivity of *T. adhaerens* to 9-*cis*-RA imply the possibility that the originally very strong regulations mediated by NRs might have been softened or inhibited by additionally evolved mechanisms. To our knowledge, there are no reports of 100% lethal effects of exposure to low nanomolar levels of 9-*cis*-RA in any metazoan organism. It can be speculated that these mechanisms were likely to evolve to modulate 9-*cis*-RA's or similar ligand's regulatory potential further and might involve stronger regulations by heterodimerization partners of RXR and enzymatic or transport mechanisms regulating the availability of ligands in cells and tissues of more recent Metazoa.

In conclusion, the presence of functional nuclear receptors in *T. adhaerens* and their proposed regulatory network support the hypothesis of a basic regulatory mechanism by NRs, which may have been subspecialized with the appearance of new NRs in order to cope with new environmental and behavioral challenges during the course of early metazoan evolution and developmental regulatory needs of increasingly more complex metazoan species.

ACKNOWLEDGEMENTS

The databases of NCBI (*NCBI Resource Coordinators, 2017*) and Joint Genome Institute of United States Department of Energy (http://jgi.doe.gov/) (*Nordberg et al., 2014*) provided bioinformatics support for this study.

ADDITIONAL INFORMATION AND DECLARATIONS

Funding

The main funding sources were: 1/the European Regional Development Fund "BIOCEV—Biotechnology and Biomedicine Centre of the Academy of Sciences and Charles University in Vestec" (CZ.1.05/1.1.00/02.0109) (The Start-Up Grant to the group Structure and Function of Cells in Their Normal State and in Pathology—Integrative Biology and Pathology (5.1.10)); 2/ The grant PRVOUK-P27/LF1/1 from the Charles University; 3/The grants SVV 260377/2017, SVV260257/2016, SVV260149/2015 and SVV 260023/2014 from the Charles University. This work was supported by the research project PRVOUK—Oncology P27, awarded by Charles University in Prague and by the project OPPK No. CZ.2.16/3.1.00/24024, awarded by European Fund for Regional Development (Prague & EU—We invest for your future). PROGRES Q26/LF1. This work was also supported by the Ministry of Education, Youth and Sports of CR within the LQ1604 National Sustainability Program II (Project BIOCEV-FAR) and by the project "BIOCEV" (CZ.1.05/1.1.00/02.0109). The work of Radek Kaňa was further supported by GACR 16-10088S and by the institutional projects Algatech Plus (MSMT LO1416) and Algamic (CZ 1.05/2.1.00/19.0392) provided by the Ministry of Education, Youth and Sports of the Czech Republic. For getting the project started Bernd Schierwater received support from the German Science Foundation (DEG Schi 277/27-1 and Schi 277/29-1). Authors received monetary support of the work reported in this publication from MediCentrum Praha. Zdenek Kostrouch and Marta Kostrouchová contributed with personal funds to this work. The funders (except authors) had no role in study design, data collection and analysis, decision to publish, or preparation of the manuscript.

Grant Disclosures

The following grant information was disclosed by the authors:
European Regional Development Fund "BIOCEV—Biotechnology and Biomedicine Centre of the Academy of Sciences and Charles University in Vestec: CZ.1.05/1.1.00/02.0109.
Charles University: PRVOUK-P27/LF1/1, SVV 260377/2017, SVV260257/2016, SVV260149/2015, SVV 260023/2014.
PRVOUK—Oncology P27.
European Fund for Regional Development: OPPK No. CZ.2.16/3.1.00/24024.
Grant Agency of the Czech Republic: 16-10088S.
The Ministry of Education, Youth and Sports of the Czech Republic: CZ 1.05/2.1.00/19.0392.
German Science Foundation: DEG Schi 277/27-1 and Schi 277/29-1.

Competing Interests

Marta Kostrouchová is an Academic Editor for PeerJ. Authors declare there are no competing interests.

Author Contributions

- Jan Philipp Novotný, Ahmed Ali Chughtai, Markéta Kostrouchová, Veronika Kostrouchová and David Kostrouch conceived and designed the experiments, performed

the experiments, analyzed the data, wrote the paper, prepared figures and/or tables, reviewed drafts of the paper.

- Filip Kaššák conceived and designed the experiments, performed the experiments, analyzed the data, wrote the paper, reviewed drafts of the paper.
- Radek Kaňa conceived and designed the experiments, contributed reagents/materials/-analysis tools, wrote the paper, reviewed drafts of the paper.
- Bernd Schierwater analyzed the data, contributed reagents/materials/analysis tools, wrote the paper, reviewed drafts of the paper.
- Marta Kostrouchová and Zdenek Kostrouch conceived and designed the experiments, performed the experiments, analyzed the data, contributed reagents/materials/analysis tools, wrote the paper, prepared figures and/or tables, reviewed drafts of the paper, contributed with perosnal funds.

DNA Deposition

The following information was supplied regarding the deposition of DNA sequences:

The sequence has been deposited in GenBank (accession number: MF805762). The raw data has been submitted as Supplementary Files.

Data Availability

The following information was supplied regarding data availability:

The raw data has been submitted as Supplementary Files.

Supplemental Information

Supplemental information for this article can be found online at http://dx.doi.org/10.7717/peerj.3789#supplemental-information.

REFERENCES

Allenby G, Bocquel MT, Saunders M, Kazmer S, Speck J, Rosenberger M, Lovey A, Kastner P, Grippo JF, Chambon P, Levin AA. 1993. Retinoic acid receptors and retinoid X receptors: interactions with endogenous retinoic acids. *Proceedings of the National Academy of Sciences of the United States of America* **90**:30–34.

Bagamasbad P, Denver RJ. 2011. Mechanisms and significance of nuclear receptor auto- and cross-regulation. *General and Comparative Endocrinology* **170**:3–17 DOI 10.1016/j.ygcen.2010.03.013.

Baker ME. 2008. Trichoplax, the simplest known animal, contains an estrogen-related receptor but no estrogen receptor: implications for estrogen receptor evolution. *Biochemical and Biophysical Research Communications* **375**:623–627 DOI 10.1016/j.bbrc.2008.08.047.

Bell EA, Boehnke P, Harrison TM, Mao WL. 2015. Potentially biogenic carbon preserved in a 4.1 billion-year-old zircon. *Proceedings of the National Academy of Sciences of the United States of America* **112**:14518–14521 DOI 10.1073/pnas.1517557112.

Bridgham JT, Eick GN, Larroux C, Deshpande K, Harms MJ, Gauthier ME, Ortlund EA, Degnan BM, Thornton JW. 2010. Protein evolution by molecular tinkering:

diversification of the nuclear receptor superfamily from a ligand-dependent ancestor. *PLOS Biology* **8(10)**:e1000497 DOI 10.1371/journal.pbio.1000497.

Cahnmann HJ. 1995. A fast photoisomerization method for the preparation of tritium-labeled 9-cis-retinoic acid of high specific activity. *Analytical Biochemistry* **227**:49–53 DOI 10.1006/abio.1995.1251.

Dawson MI, Xia ZB. 2012. The retinoid X receptors and their ligands. *Biochimica et Biophysica Acta-Molecular and Cell Biology of Lipids* **1821**:21–56 DOI 10.1016/j.bbalip.2011.09.014.

De Lera AR, Krezel W, Ruhl R. 2016. An endogenous mammalian retinoid X receptor ligand, at last! *ChemMedChem* **11**:1027–1037 DOI 10.1002/cmdc.201600105.

De Urquiza AM, Liu S, Sjoberg M, Zetterstrom RH, Griffiths W, Sjovall J, Perlmann T. 2000. Docosahexaenoic acid, a ligand for the retinoid X receptor in mouse brain. *Science* **290**:2140–2144 DOI 10.1126/science.290.5499.2140.

Dozin B, Cahnmann HJ, Nikodem VM. 1985. Identification of thyroid hormone receptors in rat liver nuclei by photoaffinity labeling with L-thyroxine and triiodo-L-thyronine. *Biochemistry* **24**:5197–5202 DOI 10.1021/bi00340a036.

Dozin B, Magnuson MA, Nikodem VM. 1985. Tissue-specific regulation of two functional malic enzyme mRNAs by triiodothyronine. *Biochemistry* **24**:5581–5586 DOI 10.1021/bi00341a044.

Dozin B, Magnuson MA, Nikodem VM. 1986. Thyroid hormone regulation of malic enzyme synthesis. Dual tissue-specific control. *Journal of Biological Chemistry* **261**:10290–10292.

Egea PF, Klaholz BP, Moras D. 2000. Ligand-protein interactions in nuclear receptors of hormones. *FEBS Letters* **476**:62–67 DOI 10.1016/S0014-5793(00)01672-0.

Escriva H, Bertrand S, Laudet V. 2004. The evolution of the nuclear receptor superfamily. *Essays in Biochemistry* **40**:11–26 DOI 10.1042/bse0400011.

Escriva H, Delaunay F, Laudet V. 2000. Ligand binding and nuclear receptor evolution. *Bioessays* **22**:717–727 DOI 10.1002/1521-1878(200008)22:8<717::AID-BIES5>3.0.CO;2-I.

Escriva H, Langlois MC, Mendonca RL, Pierce R, Laudet V. 1998. Evolution and diversification of the nuclear receptor superfamily. *Annals of the New York Academy of Sciences* **839**:143–146.

Escriva H, Safi R, Hanni C, Langlois MC, Saumitou-Laprade P, Stehelin D, Capron A, Pierce R, Laudet V. 1997. Ligand binding was acquired during evolution of nuclear receptors. *Proceedings of the National Academy of Sciences of the United States of America* **94**:6803–6808.

Fang X, Hillgartner FB. 2000. Alterations in retinoid X receptor-alpha expression contribute to cell-type dependent differences in thyroid hormone regulation of malic enzyme transcription. *Molecular and Cellular Endocrinology* **164**:41–52.

Forman BM, Samuels HH. 1990a. Dimerization among nuclear hormone receptors. *New Biologist* **2**:587–594.

Forman BM, Samuels HH. 1990b. Interactions among a subfamily of nuclear hormone receptors: the regulatory zipper model. *Molecular Endocrinology* **4**:1293–1301 DOI 10.1210/mend-4-9-1293.

Guindon S, Dufayard JF, Lefort V, Anisimova M, Hordijk W, Gascuel O. 2010. New algorithms and methods to estimate maximum-likelihood phylogenies: assessing the performance of PhyML 3.0. *Systematic Biology* **59**:307–321 DOI 10.1093/sysbio/syq010.

Gutierrez-Mazariegos J, Schubert M, Laudet V. 2014. Evolution of retinoic acid receptors and retinoic acid signaling. *Subcellular Biochemistry* **70**:55–73 DOI 10.1007/978-94-017-9050-5_4.

Hillgartner FB, Chen W, Goodridge AG. 1992. Overexpression of the alpha-thyroid hormone receptor in avian cell lines. Effects on expression of the malic enzyme gene are selective and cell-specific. *Journal of Biological Chemistry* **267**:12299–12306.

Holzer G, Markov GV, Laudet V. 2017. Evolution of nuclear receptors and ligand signaling: toward a soft key-lock model? *Current Topics in Developmental Biology* **125**:1–38 DOI 10.1016/bs.ctdb.2017.02.003.

Issemann I, Green S. 1990. Activation of a member of the steroid hormone receptor superfamily by peroxisome proliferators. *Nature* **347**:645–650 DOI 10.1038/347645a0.

Jakob W, Sagasser S, Dellaporta S, Holland P, Kuhn K, Schierwater B. 2004. The Trox-2 Hox/ParaHox gene of Trichoplax (Placozoa) marks an epithelial boundary. *Development Genes and Evolution* **214**:170–175.

Kana R, Kotabova E, Lukes M, Papacek S, Matonoha C, Liu LN, Prasil O, Mullineaux CW. 2014. Phycobilisome mobility and its role in the regulation of light harvesting in red algae. *Plant Physiology* **165**:1618–1631 DOI 10.1104/pp.114.236075.

Kana R, Kotabova E, Sobotka R, Prasil O. 2012. Non-photochemical quenching in cryptophyte alga *Rhodomonas salina* is located in chlorophyll a/c antennae. *PLOS ONE* **7**:e29700 DOI 10.1371/journal.pone.0029700.

Kiefer JC. 2006. Emerging developmental model systems. *Developmental Dynamics* **235**:2895–2899 DOI 10.1002/dvdy.20900.

King N, Westbrook MJ, Young SL, Kuo A, Abedin M, Chapman J, Fairclough S, Hellsten U, Isogai Y, Letunic I, Marr M, Pincus D, Putnam N, Rokas A, Wright KJ, Zuzow R, Dirks W, Good M, Goodstein D, Lemons D, Li W, Lyons JB, Morris A, Nichols S, Richter DJ, Salamov A, Sequencing JG, Bork P, Lim WA, Manning G, Miller WT, McGinnis W, Shapiro H, Tjian R, Grigoriev IV, Rokhsar D. 2008. The genome of the choanoflagellate Monosiga brevicollis and the origin of metazoans. *Nature* **451**:783–788 DOI 10.1038/nature06617.

Kitareewan S, Burka LT, Tomer KB, Parker CE, Deterding LJ, Stevens RD, Forman BM, Mais DE, Heyman RA, McMorris T, Weinberger C. 1996. Phytol metabolites are circulating dietary factors that activate the nuclear receptor RXR. *Molecular Biology of the Cell* **7**:1153–1166.

Kostrouch Z, Kostrouchova M, Love W, Jannini E, Piatigorsky J, Rall JE. 1998. Retinoic acid X receptor in the diploblast, *Tripedalia cystophora*. *Proceedings of the National Academy of Sciences of the United States of America* **95**:13442–13447.

Kostrouch Z, Kostrouchova M, Rall JE. 1995. Steroid/thyroid hormone receptor genes in *Caenorhabditis elegans*. *Proceedings of the National Academy of Sciences of the United States of America* **92**:156–159.

Kostrouchova M, Kostrouch Z. 2015. Nuclear receptors in nematode development: natural experiments made by a phylum. *Biochimica et Biophysica Acta/General Subjects* **1849**:224–237 DOI 10.1016/j.bbagrm.2014.06.016.

Kumar R, Thompson EB. 1999. The structure of the nuclear hormone receptors. *Steroids* **64**:310–319 DOI 10.1016/S0039-128X(99)00014-8.

Laudet V. 1997. Evolution of the nuclear receptor superfamily: early diversification from an ancestral orphan receptor. *Journal of Molecular Endocrinology* **19**:207–226.

Le Guevel R, Oger F, Martinez-Jimenez CP, Bizot M, Gheeraert C, Firmin F, Ploton M, Kretova M, Palierne G, Staels B, Barath P, Talianidis I, Lefebvre P, Eeckhoute J, Salbert G. 2017. Inactivation of the nuclear orphan receptor COUP-TFII by small chemicals. *ACS Chemical Biology* DOI 10.1021/acschembio.6b00593.

Le Maire A, Grimaldi M, Roecklin D, Dagnino S, Vivat-Hannah V, Balaguer P, Bourguet W. 2009. Activation of RXR-PPAR heterodimers by organotin environmental endocrine disruptors. *EMBO Reports* **10**:367–373 DOI 10.1038/embor.2009.8.

Lengqvist J, Mata De Urquiza A, Bergman AC, Willson TM, Sjovall J, Perlmann T, Griffiths WJ. 2004. Polyunsaturated fatty acids including docosahexaenoic and arachidonic acid bind to the retinoid X receptor alpha ligand-binding domain. *Molecular & Cellular Proteomics* **3**:692–703 DOI 10.1074/mcp.M400003-MCP200.

Letunic I, Doerks T, Bork P. 2015. SMART: recent updates, new developments and status in 2015. *Nucleic Acids Research* **43**:D257–D260 DOI 10.1093/nar/gku949.

Markov GV, Laudet V. 2011. Origin and evolution of the ligand-binding ability of nuclear receptors. *Molecular and Cellular Endocrinology* **334**:21–30 DOI 10.1016/j.mce.2010.10.017.

Naar AM, Thakur JK. 2009. Nuclear receptor-like transcription factors in fungi. *Genes and Development* **23**:419–432 DOI 10.1101/gad.1743009.

NCBI Resource Coordinators. 2017. Database resources of the national center for biotechnology information. *Nucleic Acids Research* **45**:D12–D17 DOI 10.1093/nar/gkw1071.

Nomura Y, Nagaya T, Hayashi Y, Kambe F, Seo H. 1999. 9-cis-retinoic acid decreases the level of its cognate receptor, retinoid X receptor, through acceleration of the turnover. *Biochemical and Biophysical Research Communications* **260**:729–733 DOI 10.1006/bbrc.1999.0969.

Nordberg H, Cantor M, Dusheyko S, Hua S, Poliakov A, Shabalov I, Smirnova T, Grigoriev IV, Dubchak I. 2014. The genome portal of the Department of Energy Joint Genome Institute: 2014 updates. *Nucleic Acids Research* **42**:D26–D31 DOI 10.1093/nar/gkt1069.

Nowickyj SM, Chithalen JV, Cameron D, Tyshenko MG, Petkovich M, Wyatt GR, Jones G, Walker VK. 2008. Locust retinoid X receptors: 9-Cis-retinoic acid in embryos from a primitive insect. *Proceedings of the National Academy of Sciences of the United States of America* **105**:9540–9545 DOI 10.1073/pnas.0712132105.

Paknia O, Schierwater B. 2015. Global habitat suitability and ecological niche separation in the phylum placozoa. *PLOS ONE* **10**:e0140162 DOI 10.1371/journal.pone.0140162.

Paris M, Escriva H, Schubert M, Brunet F, Brtko J, Ciesielski F, Roecklin D, Vivat-Hannah V, Jamin EL, Cravedi JP, Scanlan TS, Renaud JP, Holland ND, Laudet V. 2008. Amphioxus postembryonic development reveals the homology of chordate metamorphosis. *Current Biology* **3;18(11)**:825–830 DOI 10.1016/j.cub.2008.04.078.

Petty KJ, Desvergne B, Mitsuhashi T, Nikodem VM. 1990. Identification of a thyroid hormone response element in the malic enzyme gene. *Journal of Biological Chemistry* **265**:7395–7400.

Petty KJ, Morioka H, Mitsuhashi T, Nikodem VM. 1989. Thyroid hormone regulation of transcription factors involved in malic enzyme gene expression. *Journal of Biological Chemistry* **264**:11483–11490.

Reitzel AM, Pang K, Ryan JF, Mullikin JC, Martindale MQ, Baxevanis AD, Tarrant AM. 2011. Nuclear receptors from the ctenophore Mnemiopsis leidyi lack a zinc-finger DNA-binding domain: lineage-specific loss or ancestral condition in the emergence of the nuclear receptor superfamily? *Evodevo* **2**:Article 3 DOI 10.1186/2041-9139-2-3.

Reitzel AM, Tarrant AM. 2009. Nuclear receptor complement of the cnidarian *Nematostella vectensis*: phylogenetic relationships and developmental expression patterns. *BMC Evolutionary Biology* **9**:Article 230 DOI 10.1186/1471-2148-9-230.

Robinson-Rechavi M, Escriva Garcia H, Laudet V. 2003. The nuclear receptor superfamily. *Journal of Cell Science* **116**:585–586 DOI 10.1242/jcs.00247.

Ruhl R, Krzyzosiak A, Niewiadomska-Cimicka A, Rochel N, Szeles L, Vaz B, Wietrzych-Schindler M, Alvarez S, Szklenar M, Nagy L, De Lera AR, Krezel W. 2015. 9-cis-13,14-dihydroretinoic acid is an endogenous retinoid acting as RXR ligand in mice. *PLOS Genetics* **11**:e1005213 DOI 10.1371/journal.pgen.1005213.

Schierwater, Holland PWH, Miller DJ, Stadler PF, Wiegmann BM, Wörheide G, Wray GA, DeSalle R. 2016. Never Ending Analysis of a Century Old Evolutionary Debate: "Unringing" the Urmetazoon Bell. *Frontiers in Ecology and Evolution* **4**:Article 5 DOI 10.3389/fevo.2016.00005.

Schierwater B, Kolokotronis SO, Eitel M, DeSalle R. 2009. The Diploblast-Bilateria Sister hypothesis: parallel revolution of a nervous systems may have been a simple step. *Communicative & Integrative Biology* **2**:403–405.

Schultz J, Milpetz F, Bork P, Ponting CP. 1998. SMART, a simple modular architecture research tool: identification of signaling domains. *Proceedings of the National Academy of Sciences of the United States of America* **95**:5857–5864.

Shalchian-Tabrizi K, Minge MA, Espelund M, Orr R, Ruden T, Jakobsen KS, Cavalier-Smith T. 2008. Multigene phylogeny of choanozoa and the origin of animals. *PLOS ONE* **3**:e2098 DOI 10.1371/journal.pone.0002098.

Sievers F, Wilm A, Dineen D, Gibson TJ, Karplus K, Li W, Lopez R, McWilliam H, Remmert M, Soding J, Thompson JD, Higgins DG. 2011. Fast, scalable generation of high-quality protein multiple sequence alignments using Clustal Omega. *Molecular Systems Biology* **7**:Article 539 DOI 10.1038/msb.2011.75.

Smith CL, Giordano H, Schwartz M, DeLotto R. 1995. Spatial regulation of Drosophila snake protease activity in the generation of dorsal-ventral polarity. *Development* **121**:4127–4135.

Smith CL, Varoqueaux F, Kittelmann M, Azzam RN, Cooper B, Winters CA, Eitel M, Fasshauer D, Reese TS. 2014. Novel cell types, neurosecretory cells, and body plan of the early-diverging metazoan *Trichoplax adhaerens*. *Current Biology* **24**:1565–1572 DOI 10.1016/j.cub.2014.05.046.

Srivastava M, Begovic E, Chapman J, Putnam NH, Hellsten U, Kawashima T, Kuo A, Mitros T, Salamov A, Carpenter ML, Signorovitch AY, Moreno MA, Kamm K, Grimwood J, Schmutz J, Shapiro H, Grigoriev IV, Buss LW, Schierwater B, Dellaporta SL, Rokhsar DS. 2008. The Trichoplax genome and the nature of placozoans. *Nature* **454**:955–960.

Stein DS, Stevens LM. 2014. Maternal control of the Drosophila dorsal-ventral body axis. *Wiley Interdisciplinary Reviews: Developmental Biology* **3**:301–330 DOI 10.1002/wdev.138.

Tata JR. 1994. Autoregulation and crossregulation of nuclear receptor genes. *Trends in Endocrinology and Metabolism* **5**:283–290.

Thakur JK, Arthanari H, Yang F, Pan SJ, Fan X, Breger J, Frueh DP, Gulshan K, Li DK, Mylonakis E, Struhl K, Moye-Rowley WS, Cormack BP, Wagner G, Naar AM. 2008. A nuclear receptor-like pathway regulating multidrug resistance in fungi. *Nature* **452**:604–609 DOI 10.1038/nature06836.

Tran P, Zhang XK, Salbert G, Hermann T, Lehmann JM, Pfahl M. 1992. COUP orphan receptors are negative regulators of retinoic acid response pathways. *Molecular and Cellular Biology* **12**:4666–4676.

Wente W, Brenner MB, Zitzer H, Gromada J, Efanov AM. 2007. Activation of liver X receptors and retinoid X receptors induces growth arrest and apoptosis in insulin-secreting cells. *Endocrinology* **148**:1843–1849 DOI 10.1210/en.2006-1247.

Wolf G. 2006. Is 9-cis-retinoic acid the endogenous ligand for the retinoic acid-X receptor? *Nutrition Reviews* **64**:532–538 DOI 10.1111/j.1753-4887.2006.tb00186.x.

Wu W, Niles EG, LoVerde PT. 2007. Thyroid hormone receptor orthologues from invertebrate species with emphasis on Schistosoma mansoni. *BMC Evolutionary Biology* **7**:150 DOI 10.1186/1471-2148-7-150.

The nematode homologue of Mediator complex subunit 28, F28F8.5, is a critical regulator of *C. elegans* development

Markéta Kostrouchová[1,2], David Kostrouch[1], Ahmed A. Chughtai[1], Filip Kaššák[1], Jan P. Novotný[1], Veronika Kostrouchová[1], Aleš Benda[3], Michael W. Krause[4], Vladimír Saudek[5], Marta Kostrouchová[1] and Zdeněk Kostrouch[1]

[1] Biocev, First Faculty of Medicine, Charles University, Prague, Czech Republic
[2] Department of Pathology, Third Faculty of Medicine, Charles University, Prague, Czech Republic
[3] Imaging Methods Core Facility, BIOCEV, Faculty of Science, Charles University, Prague, Czech Republic
[4] Laboratory of Molecular Biology, National Institute of Diabetes and Digestive and Kidney Diseases, National Institutes of Health, Bethesda, MD, USA
[5] Metabolic Research Laboratories, Wellcome Trust-Medical Research Council Institute of Metabolic Science, University of Cambridge, Cambridge, UK

ABSTRACT

The evolutionarily conserved Mediator complex is a critical player in regulating transcription. Comprised of approximately two dozen proteins, the Mediator integrates diverse regulatory signals through direct protein-protein interactions that, in turn, modulate the influence of Mediator on RNA Polymerase II activity. One Mediator subunit, MED28, is known to interact with cytoplasmic structural proteins, providing a potential direct link between cytoplasmic dynamics and the control of gene transcription. Although identified in many animals and plants, MED28 is not present in yeast; no bona fide MED28 has been described previously in *Caenorhabditis elegans*. Here, we identify bioinformatically F28F8.5, an uncharacterized predicted protein, as the nematode homologue of MED28. As in other Metazoa, F28F8.5 has dual nuclear and cytoplasmic localization and plays critical roles in the regulation of development. *F28F8.5* is a vital gene and its null mutants have severely malformed gonads and do not reproduce. F28F8.5 interacts on the protein level with the Mediator subunits MDT-6 and MDT-30. Our results indicate that F28F8.5 is an orthologue of MED28 and suggest that the potential to link cytoplasmic and nuclear events is conserved between MED28 vertebrate and nematode orthologues.

Subjects Cell Biology, Developmental Biology, Evolutionary Studies, Molecular Biology
Keywords Gene expression regulation, *Caenorhabditis elegans*, Development, Evolution, Mediator complex, MED28

INTRODUCTION

The Mediator complex is a multiprotein assembly that is capable of integrating cellular signals with the regulation of transcription through direct interaction with RNA Polymerase II (Pol II). The Mediator complex is found in all eukaryotic organisms.

Submitted 13 October 2016
Accepted 8 May 2017
Published 6 June 2017

Corresponding author
Zdeněk Kostrouch,
Zdenek.kostrouch@lf1.cuni.cz

Academic editor
Heather Etchevers

Additional Information and Declarations can be found on page 23

DOI **10.7717/peerj.3390**

The core Mediator complex is comprised of 21 protein subunits in yeast and a similar number (26) in mammals, all named MED followed by a unique numerical designation (*Poss, Ebmeier & Taatjes, 2013*; *Allen & Taatjes, 2015*). In addition to this core Mediator complex, four additional subunits comprising the CDK8 or kinase module can associate with the core (*Poss, Ebmeier & Taatjes, 2013*). The Mediator complex likely co-evolved with basal transcription factors with a level of conservation between different phyla that is relatively low (*Poss, Ebmeier & Taatjes, 2013*; *Allen & Taatjes, 2015*). While most Mediator subunits are present in similar molar ratios and comprise the core complex, some subunits were found to be present in variable amounts when complexes were isolated from tissue culture cells (*Kulak et al., 2014*). Quantification of proteomically analyzed Mediator subunits showed that distinct forms of the complex have variable transcriptional activity (*Paoletti et al., 2006*) and analysis of Mediator complex subunits in *Drosophila* indicated that some subunits are critical only for specific gene transcription from endogenous genes but not for transcription from synthetic promoters (*Kim et al., 2004*). This diversity of Mediator subunit function reflects distinct transcription factor interactions with Mediator components and with Pol II, greatly expanding its possible regulatory roles for Mediator. For example, some Mediator subunits are essential for the transcription of many different protein-coding genes, while other subunits are essential for only a subset of genes, translating cellular signaling pathways to the regulation of specific target gene sets (reviewed in *Grants, Goh & Taubert (2015)*).

One of the Mediator complex subunits, MED28, is only found in higher eukaryotes. MED28 was originally identified as a gene expressed in endothelial cells where it was named EG-1 (Endothelial-derived Gene-1) (*Liu et al., 2002*); it was later shown to be part of the Mediator complex and re-named MED28 (*Sato et al., 2004*; *Beyer et al., 2007*). In addition to its role in the Mediator complex, the MED28 subunit has several cytoplasmic-associated interactions. MED28 has been shown to associate with (1) the actin cytoskeleton and linked to the regulation of smooth muscle genes (*Wiederhold et al., 2004*), (2) several Src-family kinases and it is a target of their phosphorylation (*Lee et al., 2006*), and (3) the plasma membrane where it interacts with Grb2 and Merlin (also called Neurofibromin 2 or Schwannomin) (*Wiederhold et al., 2004*), membrane-cytoskeleton scaffolding proteins linking actin filaments to the cell membrane (*McClatchey & Giovannini, 2005*; *McClatchey & Fehon, 2009*). These many and diverse cytoplasmic interactions suggest that MED28 could function to transmit cytoskeletal signals to transcription in the nucleus (*Lee et al., 2006*).

Although conserved between insects and mammals, a bona fide MED28 homologue had yet to be identified in nematodes. The relatively low conservation of Mediator complex subunits between eukaryotic phyla (*Poss, Ebmeier & Taatjes, 2013*; *Allen & Taatjes, 2015*) makes the identification of orthologues in distant species difficult and some suggested orthologues may require re-classification. Our previous work showed that the protein previously identified as "MDT-28" (**Med**ia**t**or-28) in nematodes (*Bourbon, 2008*) is instead the nematode homologue of perilipin, a protein regulating lipid metabolism at the level of lipid droplets and is not related to MED28 (*Chughtai et al., 2015*). Thinking it was unlikely that a MED28 homologue would be absent in nematode

genomes, we searched for it using the conserved features of MED28 orthologues from various phyla. Herein we identify a previously uncharacterized protein, F28F8.5, as the closest MED28 homologue. We show that F28F8.5 localizes to both nuclear and cytoplasmic compartments in most, if not all, cells throughout development. Downregulation by RNAi, or disruption of *F28F8.5* by deletion, results in multiple developmental defects during embryonic and larval development. Our work indicates that the homologue of Mediator complex subunit 28 exists in nematodes and suggests that the potential to link cytoplasmic and nuclear events is conserved between vertebrate and nematode MED28 homologues.

MATERIALS AND METHODS

Sequence analysis

The UniProtKB (http://www.uniprot.org) and NCBI (https://www.ncbi.nlm.nih.gov) databases were searched with BLAST, PSI-BLAST (*Altschul et al., 1997*), HHblits (*Remmert et al., 2011*), and HHpred (*Söding, Biegert & Lupas, 2005*) programs. The protein sequences were identified with their UniProtKB identifiers and the nucleotide sequences with their NCBI ones. The sequences were aligned with T-coffee (*Notredame, Higgins & Heringa, 2000*; *Di Tommaso et al., 2011*) and PROMALS (*Pei & Grishin, 2007*; *Pei et al., 2007*; *Pei, Kim & Grishin, 2008*). The secondary structure predictions were performed with PSIPRED (*Jones, 1999*; *Cuff & Barton, 2000*; *McGuffin, Bryson & Jones, 2000*). Multiple sequence alignments were displayed and analyzed with Jalview (*Clamp et al., 2004*).

RNA isolation and cDNA synthesis

RNA and cDNA were prepared as described (*Zima et al., 2015*) with modifications. Cultured nematodes were collected in water and pelleted by centrifugation for 5 min at 200 × g and 4 °C. The excess of water was removed and the pellet was frozen at −80 °C. For the isolation of RNA, the pellet was quickly melted and dissolved in 300 µl of resuspension buffer (10 mM Tris–HCl; 10 mM EDTA, 5% 2-mercaptoethanol; 0.5% SDS; pH 7.5). After adding 8 µl of proteinase K (20 mg/ml), the sample was mixed and incubated 1 h at 55 °C. RNA was isolated by phenol–chloroform extraction and ethanol precipitation. The obtained RNA was incubated with RQ1 DNase (Promega, Fitchburg, WI, USA) and purified again by phenol–chloroform extraction and ethanol precipitation. Complementary DNA (cDNA) was prepared with SuperScript III (Invitrogen, Carlsbad, CA, USA) using random hexamers.

Strains, transgenic lines and genome editing

The *Caenorhabditis elegans* Bristol N2 strain was used whenever not specifically stated and maintained as described (*Brenner, 1974*).

KV3: (8418)—heterozygous animals carrying one edited disrupted allele of *F28F8.5* ($P_{F28F8.5}$ *(V:15573749)::gfp::let858(stop)::SEC::F28F8.5*—edited *F28F8.5* disrupted by *gfp* and self-excising cassette (SEC)) and one WT allele of *F28F8.5*. This line segregates mutant animals.

KV4: (8419)—edited *F28F8.5* carrying *gfp::F28F8.5* in its normal genomic position (*$P_{F28F8.5}$(V:15573749)::gfp::F28F8.5* on both alleles.

Preparation of *$P_{F28F8.5(400\ bp)}$::F28F8.5::gfp*

For preparation of transgenic lines encoding F28F8.5::GFP from extrachromosomal arrays under regulation of endogenous promoter, we used the PCR fusion-based technique (*Hobert, 2002*). Primers 7886 and 7888 were used for amplification of the genomic sequence of *F28F8.5* (consisting of approximately 400 bp of the predicted promoter region preceding the coding region of *F28F8.5*). The gene encoding GFP was amplified from the pPD95.75 vector with primers 6232 and 6233. The complete construct was amplified with primers 7887 and 6234. The resulting fusion construct contains the 3′ UTR from pPD95.75 (originally from the *unc-54* gene). The PCR mixture was injected into the gonads of young adult hermaphrodite animals together with marker plasmid pRF4. The sequences of all primers used in the paper are in Supplemental Information.

Genome editing

Lines with edited genomes were prepared from wild type N2 animals using the CRISPR/Cas9 system as described (*Dickinson et al., 2013*, *2015*; *Ward, 2015*; *Dickinson & Goldstein, 2016*). Using this strategy, the *F28F8.5* gene was edited by insertion of a construct including the coding sequence of GFP and a SEC containing the *sqt-1(d)* gene (a visible selection marker leading to a Rol phenotype), *hs::Cre* (heat shock inducible Cre recombinase) and hygR (hygromycin resistance) genes. The sgRNA sequence was targeted near the start of the coding sequence for the *F28F8.5* gene using a modified pJW1219 plasmid (Addgene, Cambridge, MA, USA) as the Cas9 vector (pMA007); it was prepared by PCR with primers 8403A and 8333 and used in a concentration of 50 ng/µl for microinjections. The plasmid pMA007 was co-injected with the rescue repair template plasmid based upon modified pDD282 vector (pMA006) in a concentration of 10 ng/µl and with three markers (see below). The repair template plasmid pMA006 was prepared in two steps. First the plasmid pMA005 was prepared from gDNA of *F28F8.5* (containing both repair arms) and amplified by PCR with primers 8404 and 8405 and cloned into pCU19 backbone. The plasmid pMA005 was subsequently modified—the FP-SEC segment was added and the CRISPR/Cas9 site was altered to protect against Cas9 attack. The linear PCR product of pMA005 was prepared using primers 8406 and 8407 with overlapping regions for Gibson assembly (New England BioLabs, Ipswich, MA, USA). The primer 8406 was prepared with alternate codons for protection against CRISPR/Cas9 site. Linear insert of FP-SEC was prepared by PCR from pDD282 plasmid (Addgene, Cambridge, MA, USA) with primers 8408 and 8409. Primers were prepared with overlapping parts for cloning into linear pMA005 plasmid by Gibson assembly and the final rescue plasmid pMA006 was prepared. Plasmids pGH8 (10 ng/µl), pCFJ104 (5 ng/µl), and pCFJ90 (2.5 ng/µl) (Addgene, Cambridge, MA, USA) were used as fluorescent co-injection markers. After microinjections the population of nematodes were grown for three days at 25 °C and hygromycin (Invitrogen) was added in a final

concentration of 250 μg/ml. After three days integrated nematodes were selected according to the rolling phenotype and loss of extrachromosomal arrays.

Using this strategy, we obtained a heterozygous line (KV3) with a disrupted *F28F8.5* gene with an inserted *gfp* regulated by the endogenous promoter of *F28F8.5* in one allele and one WT allele. This line segregated homozygous animals for $P_{F28F8.5}$*:: F28F8.5::gfp* (edited *F28F8.5* with SEC—$P_{F28F8.5}$ *(V:15573749)::gfp::let858(stop)*::SEC::*F28F8.5*) with disrupted *F28F8.5* on both alleles and expressing GFP under the regulation of the endogenous promoter. Animals of this line were clearly distinguishable by their developmental phenotypes, weak expression of GFP in the cytoplasm and the presence of *rol* marker. These animals were sterile and had severe developmental defects (see Results). The genotypes were confirmed by single worm PCR of representative animals after their microscopic analysis (with primers 8398 and 8414).

The excision of the SEC was achieved by a 4 h heat shock at 34 °C. The line KV4 was obtained: animals with both alleles carrying the edited *F28F8.5* gene in the form of *gfp::F28F8.5* in its normal genomic position (edited *F28F8.5* with *gfp* tagged to the N—terminus—$P_{F28F8.5}$*(V:15573749)::gfp::F28F8.5*).

The presence of the knock-in of *gfp* was confirmed by single nematode PCR with primers 7887 and 8454, 8398 and 8454. The PCR products were purified and sequenced with primers 8455 and 8456. PCR was done by REDTaq ReadyMix PCR reaction (Sigma-Aldrich, St. Louis, Missouri, USA) or by Phusion High-Fidelity DNA Polymerase (New England Biolabs, Ipswich, MA, USA). During the maintenance of the heterozygous line KV3, animals with one edited disrupted *F28F8.5* allele and one allele with edited *F28F8.5* after self-excision of SEC were also generated (recognizable by the Rol phenotype, expression of *gfp* in nuclei and lack of developmental phenotypes). Schemes for genome editing are accessible in Files S4–S7.

Downregulation of gene expression by RNA interference

For RNAi done by microinjections, *F28F8.5* cDNA was prepared from total cDNA using primers 7889 and 7890. The plasmid pPCRII(Topo) (Invitrogen, Carlsbad, CA, USA) containing *F28F8.5b* cDNA was linearized using restriction enzymes *Not*I/*Sac*I. The dsRNA was prepared by in vitro transcription using SP6/T7 Riboprobe® in vitro Transcription Systems (Promega, Madison, WI, USA) from opposing promoters synthesizing complementary single stranded RNA (ssRNA) for both strands of *F28F8.5* cDNA and its complementary strand. After in vitro transcription (~2 h) equal volumes of sense and antisense RNA were mixed, incubated at 75 °C for 10 min and slowly cooled to room temperature during 30 min. Control RNAi was prepared from the promoter region of *nhr-60* as previously described (*Šimečková et al., 2007*) and repeated with dsRNA prepared using the vector L4440. Vectors used for preparation of dsRNA were linearized and transcribed using T7 RNA polymerase. The dsRNA concentration was measured using a UV spectrophotometer and diluted to the concentration of ~2 μg/μl that was used for injections (*Tabara et al., 1999*; *Timmons, Court & Fire, 2001*; *Vohanka et al., 2010*).

Microinjections

Microinjections of plasmids, DNA amplicons or dsRNA into gonads of young adult hermaphrodites were done using an Olympus IX70 microscope equipped with a Narishige microinjection system (Olympus, Tokyo, Japan). The plasmids were injected into the gonads of young adult hermaphrodites as described (*Tabara et al., 1999*; *Timmons, Court & Fire, 2001*; *Vohanka et al., 2010*).

Microscopy

Fluorescence microscopy and Nomarski optics microscopy were done using an Olympus BX60 microscope equipped with DP30BW CD camera (Olympus, Tokyo, Japan). Animals were analyzed on microscopic glass slides with a thin layer of 2% agarose and immobilized by 1 mM levamisole (Sigma-Aldrich, St. Louis, MO, USA). Confocal microscopy of live homozygous animals with edited *F28F8.5* expressing *gfp::F28F8.5* was performed using an inverted Leica SP8 TCS SMD FLIM system equipped with a 63 × 1.2 NA water immersion objective, a pulsed white light laser (470–670 nm), AOBS and two internal hybrid single photon counting detectors, and operated by Leica Application Suite X program (Leica Microsystems, Wetzlar, Germany). The GFP fluorescence was excited at a wavelength of 488 nm and the emitted light was simultaneously recorded in two spectral ranges (Channel 1—495 nm to 525 nm, Channel 2—525 nm to 580 nm; the two channel setup was used to help resolve between spectrally different autofluorescence and GFP fluorescence signals).

Fluorescence-lifetime imaging microscopy

For FLIM acquisitions the single photon counting signal from the internal hybrid detectors, acquired during confocal acquisitions, was simultaneously processed by HydraHarp400 TCSPC electronics (PicoQuant, Berlin, Germany) and information about the arrival times of all photons was stored to a hard-drive in TTTR data format. TTTR is freely accessible at https://www.picoquant.com/images/uploads/page/files/14528/technote_tttr.pdf. Data structure, program description and user instructions are also freely accessible at https://github.com/PicoQuant/PicoQuant-Time-Tagged-File-Format-Demos/blob/master/PTU/Matlab/Read_PTU.m. The signal from both time synchronized channels was added up. The false color scale (1–3 ns) is based on the average photon arrival time, with blue color representing short lifetime and red color long lifetime fluorescence.

Single nematode PCR

Single animal PCR was used for verification of all transgenic lines. Following the microscopy examination, selected animals were removed from microscopic slides and transferred into caps of PCR tubes with 4 μl of solution of Proteinase K (20 mg/ml) diluted 1:333 in Barstead Buffer (resulting in Barstead Lysis Buffer which consists of 50 mM KCl, 10 mM Tris pH 8.3, 2.5 mM $MgCl_2$, 0.45% (v/v) NP40 (Nonidet P-40), 0.45% (v/v) Tween-20, 0.01% (w/v)). Proteinase K was diluted immediately before use as a 20 mg/ml stock solution which was kept on ice and diluted to final working solution

at a concentration of 60 μg/ml. The tube was sealed in bottom-up position and the sample transferred to the bottom of the tube by centrifugation. The tube was frozen for 10 min at −70 °C. Next, the tube was heated for 1 h at 65 °C and additional 15 min at 95 °C. The resulting sample was used immediately for amplification of DNA by PCR or stored at −80 °C before further analysis. Similarly, genomic DNA was prepared from selected nematode culture plates and used for further screening by PCR and sequencing.

The resulting precipitated DNA was dissolved in 10 μl of deionized water and used for amplification by PCR using primers outside the edited genomic regions. Specificity of amplification was confirmed by DNA sequencing.

Similarly, homozygous animals with edited *F28F8.5* (with *gfp* inserted in front of the *F28F8.5* START codon) were analyzed by single worm PCR with primers 7887 (sense primer) and 7890 or 8454 (antisense primers).

Quantitative RT-PCR

For quantitative RT-PCR, the technique described by *Ly, Reid & Snell (2015)* was used with modifications. For assessment of the level of expression of *F28F8.5* from homozygous animals with the edited disrupted gene, five adult homozygous mutant animals recognized by the phenotype and the same number of young WT hermaphrodites with minimum number of formed embryos were manually harvested and collected in separate Eppendorf tubes. Reverse transcription was done using the Maxima H Minus cDNA synthesis kit (Thermo Fischer, Waltham, MA, USA) as recommended by manufacturer. Universal probe library and primers designed with the help of ProbeFinder Assay Design Software were used and qPCR was run on LightCycler 2.0 purchased from Roche (Roche, s.r.o. Prague, Czech Republic). An average of three sample cDNAs and three control cDNAs were analyzed (twice in duplicates and one time as single experiments), all containing the same amount of RNA for RT for each experiment. The expression of *F28F8.5* was normalized to *ama-1* and the values obtained in homozygous mutant animals with disrupted *F28F8.5* gene were compared to values obtained in control WT N2 animals.

Binding studies

Binding studies were done as described (*Kostrouch et al., 2014*) with modifications. The coding region of *mdt-6* was amplified using primers 8292 and 8293 from cDNA prepared from mixed stages *C. elegans* cultures and cloned into pTNT vector (Promega, Madison, WI, USA, amplified with primers 8277 and 8278) using the Quick Ligation Kit (New England Biolabs, Ipswich, MA, USA) and expressed in the rabbit reticulocyte TNT-system (Promega, Madison, WI, USA). The in vitro transcribed protein was labeled using ^{35}S Methionine (Institute of Isotopes, Budapest, Hungary). F28F8.5 coding sequence (amplified using 8255 and 8256 primers with 15 bp overhangs for insertion into the vector) was cloned into pGEX-2T vector ((Amersham Pharmacia Biotech, Amsterdam, UK), amplified with primers 8253 and 8254) using the GeneArt Seamless PLUS Cloning and Assembly Kit (Thermo Fisher Scientific, Waltham, MA, USA), transformed into BL21 *Escherichia coli* cells and the production of protein was induced by

isopropyl β-D-1-thiogalactopyranoside (IPTG) (Sigma-Aldrich, St. Louis, MO, USA). The Mediator subunit MDT-30 was amplified from mixed stages *C. elegans* cDNA with sense primer 8302 and reverse primer 8527 (containing FLAG sequence), cloned into pET28a(+) vector ((Addgene, Cambridge, MA, USA), amplified with primers 8519 and 8520) using the Quick Ligation Kit (New England Biolabs), transformed into BL21 *E. coli* cells and induced by IPTG. The lysate from bacteria producing His_6-MDT-30-FLAG was used directly or purified on HiTrap Chelating HP column (GE Healthcare, Chicago, IL, USA). Proteins produced by the TNT system or bacterial lysates of bacteria transformed with FLAG labeled Mediator subunits were incubated with glutathione–agarose (Sigma-Aldrich, St. Louis, MO, USA) adsorbed with equal amounts of GST or GST-F28F8.5. Radioactively labeled proteins were detected using TRI-CARB 1600TR, Liquid Scintillation Analyzer (Packard, Meriden, CT, USA).

The resulting samples (labeled proteins bound to GST- or GST-F28F8.5) were separated by polyacrylamide gel electrophoresis. ^{35}S-MDT-6 was visualized by autoradiography and subsequently, the gel containing radioactively labeled protein was localized using superimposed autoradiograms, excised and the radioactivity determined in the scintillation detector. FLAG-labeled MDT-30 was determined by Western blot using an anti-FLAG antibody (monoclonal anti-FLAG, M2 (Sigma-Aldrich)) and quantified densitometrically by ImageJ computer program (https://imagej.nih.gov/ij/download.html) (*Schneider, Rasband & Eliceiri, 2012*).

RESULTS

Identification of the closest homologue of vertebrate Mediator complex subunit 28 in *C. elegans*

To identify the *C. elegans* homologue of MED28, we queried protein databases with curated SwissProt sequences from UniProtKB. They comprised several mammalian and insect proteins (e.g., human MED28_HUMAN and *D. melanogaster* MED28_DROME). The more sensitive profile-to-profile HHblitz and HHpred algorithms provided hits to a *C. elegans* annotated protein F28F8.5a and b with highly significant *E*-values. According to Wormbase (WS248), two protein isoforms are produced from the *F28F8.5* gene, isoform a with the length of 200 amino acids and isoform b that has a two amino acid insertion at position 20 of the N-terminal evolutionarily non-conserved region. The best results were obtained when pre-aligned vertebrate and insect MED28 homologues were used as query in three iterations ($E < 10^{-48}$ and the probability of true positive >99.99%). When the pre-aligned nematode sequences homologues to F28F8.5 were used to query profiles of human or *Drosophila* sequences in reciprocal searches, MED28 proteins were obtained with equally significant scores. BLAST and PSI-BLAST searches in their standard settings were not able to reveal a significant hit ($E < 10^{-3}$); the only nematode hit was a *Trichinella spiralis* protein (E5RZQ1). However, when the searches in protein databases were limited to sequences from *Ecdysozoa* with *Insecta* excluded (conservative inclusion threshold $E < 10^{-6}$) in the first two iterations and then continued in the complete database of sequences from all species in the subsequent

Figure 1 A multiple sequence alignment of selected metazoan homologues of MED28 compared with F28F8.5. Aligned with PROMALS (http://prodata.swmed.edu/promals/promals.php), variable C- and N-termini not shown, amino acid residue types colored according to Clustal scheme in Jalview, red bars indicate consensus positions of predicted α-helices. Sequences from top to bottom (organism, identifier): *Caenorhabditis elegans*, O18692; *Trichinella spiralis*, E5RZQ1; *Wuchereria bancrofti*, EJW84794.1; *Pristionchus pacificus*, translated contig of CN657719.1 FG102945.1 CN657262.1 CN656622.1; *Ancylostoma ceylanicum*, A0A016SKV7; *Globodera pallida*, translated CV578368.1; *Panagrolaimus davidi*, translated JZ658977.1; *Ixodes scapularis*, B7PAW5; *Drosophila melanogaster*, MED28_DROME; *Homo sapiens*, MED28_HUMAN. Readers with specific color preferences may download the compared sequences from (File S1) and create the Clustal scheme with different color specifications using the Jalview program (http://www.jalview.org/).

iterations, the final hits of F28F8.5 included human and *Drosophila* MED28. PSI-BLAST with *T. spiralis* query sequence in database limited to *Ecdysozoa* in the first two iterations provided both human and *Drosophila* MED28 and F28F8.5 in one run ($E < 10^{-8}$). We concluded from these searches that F28F8.5 is a homologue of MED28 and very likely its previously unrecognized orthologue.

All PSI-BLAST MED28 homologues possess variable N- and C-termini of 3–80 amino acids showing no conservation across Metazoa. This conservation is loose even just within *Drosophilae* or *Caenorhabditae* sequences. Only the central core of about 110 amino acids is preserved in metazoan evolution. Figure 1 shows a sequence alignment of this conserved core of selected MED28 homologues. All sequences are predicted to fold into three helices forming a putative coiled coil fold (UniProt annotation). Submitting the alignment shown in Fig. 1 to HHpred for 3D structure recognition reveals a structural fold of yeast MED21 (PDB identifier 1ykh_B). It is indeed a three-helix coiled coil forming a heterodimer with MED7. It can be expected that MED28 forms a very similar fold interacting with a yet to be determined subunit of the MED complex.

F28F8.5 is a nuclear as well as a cytoplasmic protein

Information available in WormBase suggests that the *F28F8.5* gene can be expressed as both an individual and multigene transcript, located as the last gene in a four gene operon that is both SL-1 and SL-2 trans-spliced. To determine the intracellular localization of F28F8.5, we edited the *F28F8.5* gene using CRISPR/Cas9 technology. We inserted the gene coding for GFP directly in front of the first codon. The arrangement used in our

experiment (based on *Dickinson et al. (2013, 2015)*, *Ward (2015)* and *Dickinson & Goldstein (2016)*) employed a SEC that was added after *gfp*. This strategy initially created a disrupted *F28F8.5* gene and putative null allele that can be detected by expression of GFP alone regulated by the endogenous promoter elements of *F28F8.5*. We found that only heterozygous animals could be propagated due to the sterility of homozygotes tagged in this manner. Assuming this tag is not deleterious to the expression of other genes in the operon, this result suggests that *F28F8.5* is an essential gene.

After removal of the SEC from this edited *F28F8.5* gene induced by heat shock (visualized by continuous expression of GFP::F28F8.5 fusion protein and loss of the Rol phenotypic marker), the endogenous locus had an N-terminus GFP-tagged *F28F8.5* gene that we maintained as homozygous animals, demonstrating this edited allele is fully functional. Note that both known protein isoforms of F28F8.5 (a and b) would be tagged on their N-terminus with GFP by this method.

The GFP::F28F8.5 pattern was ubiquitous, both nuclear and cytoplasmic from embryos to adults (Fig. 2). Prominent nuclear localization was found in oocytes, zygotes, larvae, and adults. Cells with clear nuclear accumulation of GFP::F28F8.5 included epidermal, intestinal, pharyngeal, uterine and vulval muscle cells (Fig. 2). The gonad expressed *gfp::F28F8.5* and mitotic as well as meiotic nuclei accumulated GFP::F28F8.5 protein (Fig. 2).

Selected animals were analyzed by confocal microscopy for determination of subcellular distribution of GFP::F28F8.5. Scanning through several focal planes revealed signal in the GFP excitation/emission range in nuclei as well as in the cytoplasm of embryos, all larval stages and adults (Fig. 3). Structures resembling gut granules were also strongly positive in the GFP recording mode. In order to distinguish between GFP-specific fluorescence and autofluorescence, we applied FLIM with an expectation that autofluorescence (such as that from gut granules) is likely to produce a signal with a short fluorescence lifetime opposed to GFP-specific fluorescence. Structures such as gut granules were clearly detected (Fig. 3, panels O, Q, S, T and U, blue color) while fluorescence with a longer lifetime expected for GFP::F28F8.5 was detected in the germline, in oocytes and embryos and in most somatic nuclei of larvae as well as adult animals (Fig. 3, panels O, Q, S, T and U, red and yellow colors).

We also generated transgenic lines encoding F28F8.5::GFP from extrachromosomal arrays consisting of an endogenous internal *F28F8.5* promoter regulating a fusion gene with *gfp* attached to F28F8.5 on its C-terminal end. As with the N-terminally tagged F28F8.5, F28F8.5::GFP showed both nuclear and cytoplasmic localization. As expected for an extrachromosomal transgene, the expression of *F28F8.5::gfp* was not detected in the germline. This reporter was expressed in embryos starting at the twofold stage and continued throughout development (Fig. S1). We did notice that *F28F8.5::gfp* was expressed in the excretory canal cell (Figs. S1M, S1N, S1P and S1Q), a pattern not observed with the endogenously edited GFP-tagged gene.

F28F8.5 regulates development

To achieve loss-of-function, RNAi was used to downregulate *F28F8.5* expression. Analysis of 2,567 progeny of 17 young adult hermaphrodites inhibited for F28F8.5 function by

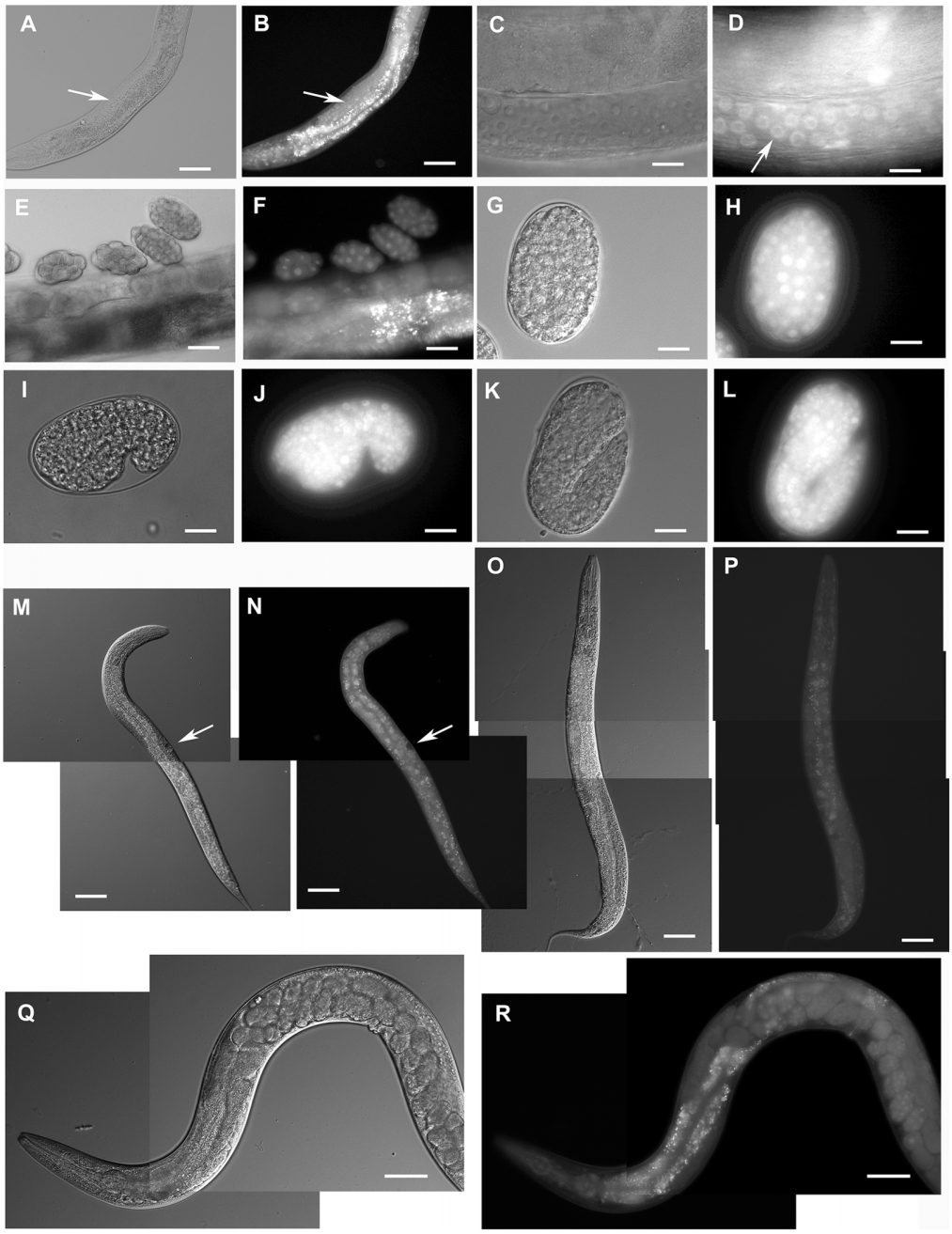

Figure 2 Expression pattern of GFP::F28F8.5 in homozygous animals with edited *F28F8.5* gene. GFP tagged to F28F8.5 at its N-terminus using CRISPR/Cas9 technology visualized the expression of F28F8.5 in the gonads (Panels B and D, arrows) in mitotic nuclei and continues throughout the embryonic development (Panels F, H, J, and L). The wide and likely ubiquitous expression of GFP::F28F8.5 continues during larval stages (larvae L3 and L4 are shown in panels M, N and O, P, respectively) as well as in adults (panels Q and R). Expression of the edited gene in the nuclei of the developing vulva is indicated by the arrows in panels M and N. Panels A, C, E, G, I, K, M, O, and Q show larvae in Nomarski optics and panels B, D, F, H, J, L, N, P, and R in GFP fluorescence. Bars represent 50 μm.

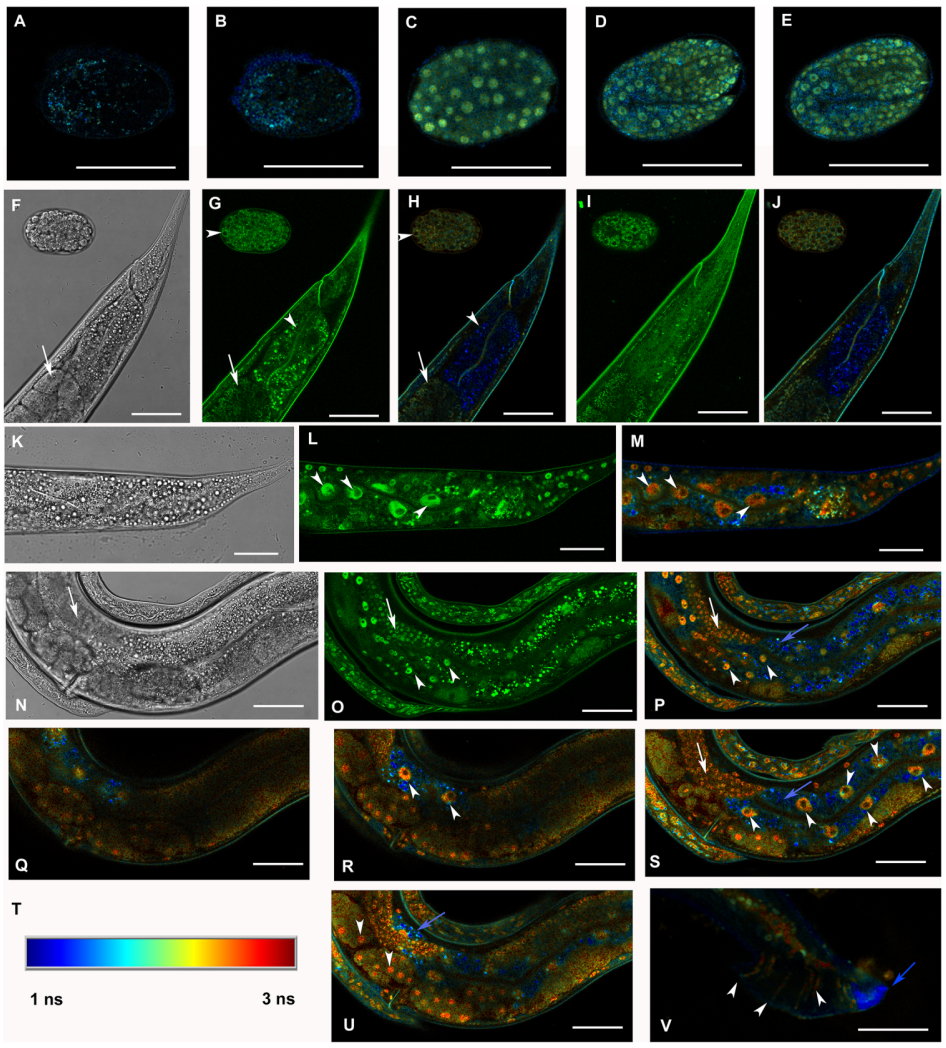

Figure 3 Analysis of GFP::F28F8.5 expression in homozygous animals with edited *F28F8.5* gene by confocal microscopy and fluorescence lifetime imaging microscopy (FLIM). All confocal images of GFP fluorescence are recorded in Channel 1 (495–525 nm). FLIM images (panels A to E, H, J, L, M, O to S, U, and V) are calculated from merged recordings in Channel 1 and Channel 2 (525–585 nm). Panels F, K, and N are images in Nomarski optics at the same optical focus as in corresponding confocal images of GFP fluorescence (panels G, I, L, O). Panels A and B show control images of WT embryos in bean and comma stages, respectively. No specific signal is detected in control embryos by FLIM. Panel C shows an embryo in bean stage expressing GFP::F28F8.5 from the edited gene. Two focal planes of an embryo expressing GFP::F28F8.5 in twofold stage are shown in panels D and E. FLIM detects GFP::F28F8.5 in most or all nuclei of developing embryos. Panels F to J show the distal part of a young adult control hermaphrodite animal and a control embryo in late bean stage. FLIM images in panels H and J show mostly short lifetime fluorescence in the cytoplasm of embryonic cells as well as cells and subcellular structures in the adult control animal (visualized by blue color). Arrowheads pointing at the embryo in panels G and H indicate weak autofluorescence in the cytoplasm of embryonic cells. Arrows in panels F, G and H indicate the turn of gonad and arrowheads indicate nuclei of an enterocyte which is devoid of almost all fluorescence (panels G and H). Panels K to S and U and V show animals with edited *F28F8.5* (*gfp::F28F8.5*). Panel M shows the distal part of an adult hermaphrodite animal expressing GFP::F28F8.5 from the edited gene at recording settings identical with that used in the control sample shown in panels A, B, H, and J. FLIM analysis shows a long lifetime fluorescence in nuclei and in the cytoplasm of most cells that contrasts with the low level of fluorescence seen in the control sample. Arrowheads indicate

Figure 3 ... **continued**
nuclei of enterocytes in panels L and M. Panels N to V show images of an adult animal and two L1 larvae with edited *F28F8.5*. Panels P to S, and U show selected focal planes in FLIM. Panel T shows the calibration table for FLIM in the range of 1–3 ns used in all panels presenting FLIM analysis. Blue areas shown in FLIM pictures represent short lifetime fluorescence presumably corresponding to autofluorescence (blue arrows in panels O, S, and U). Arrowheads in panels O, P, R, and S indicate nuclei of enterocytes and in panel U nuclei of early embryos with long lifetime fluorescence characteristic for GFP. Panel V shows the distal part of a male expressing GFP:F28F8.5 in male specific structures, in nuclei as well as in rays (marked by arrowheads) indicating that GFP::F28F8.5 is expressed not only in cell nuclei but also in the cytoplasmic structures. Bars represent 30 μm in panels A to E and 50 μm in panels F to S and U and V.

microinjection of dsRNA into the syncytial gonad revealed that F28F8.5 is essential for proper development (Fig. 4). From the total progeny, 1,127 animals were affected (44%) exhibiting embryonic and larval arrest and a range of less severe phenotypes, including defective molting, protruding vulvae that often burst, male tail ray defects (Fig. 4), and uncoordinated (Unc) movement. In contrast with this, control young adult N2 hermaphrodites injected with control dsRNA showed embryonic arrest in less than 2% of progeny (seven hermaphrodites injected, total progeny observed 1,066, embryonic arrest found in 19 embryos).

Complete loss of F28F8.5 that occurred in homozygous animals with both edited disrupted alleles of the *F28F8.5* gene (that are found among the progeny of heterozygous animals carrying one edited disrupted allele and one WT allele) resulted in defective development that was most pronounced in late larval stages. The phenotypes included a dumpy phenotype (Dpy) (Fig. 5C), irregular gut, severely defective growth of the gonad with signs of defect in directional growth (Figs. 5E and 5M) and Pvul phenotype (Figs. 5K and 5L). Most animals had darker gut cells than controls of the same age. The gonad did not develop fully in most animals (Figs. 5C–5L) and often contained empty spaces that were prevalent in some animals, leading to the formation of larvae with optically thin, empty-like tissue in the position of the gonad. The gonads contained foci of irregular tissue with an uncharacteristic appearance. Tissue defects were also visible in extragonadal locations, especially in the place of excretory canals. Body defects were also observed in the position of the uterus that was not properly formed and the spermatheca that was not identifiable in a large proportion of animals.

Estimation of the level of *F28F8.5* expression in homozygous mutant animals (originating from maternal load or from SEC self-excision (*Dickinson et al., 2015*)) from three experiments indicated that mutants with disrupted F28F8.5 had the level of expression about 17 times lower compared to the levels found in WT controls (File S8).

Heterozygous hermaphrodites carrying one edited disrupted allele of *F28F8.5* and one WT allele were grossly normal and produced viable embryos. Unlike in homozygous animals carrying the excised SEC allele, the GFP fluorescence was mostly cytoplasmic and most nuclei were not showing accumulation of GFP. In some embryos, however, the nuclei accumulated GFP indicating probable spontaneous SEC self-excision (Fig. 6).

Analysis of progeny of the heterozygous strain KV3 revealed differences compared to the expected Mendelian segregation of phenotypes. Animals with one edited disrupted

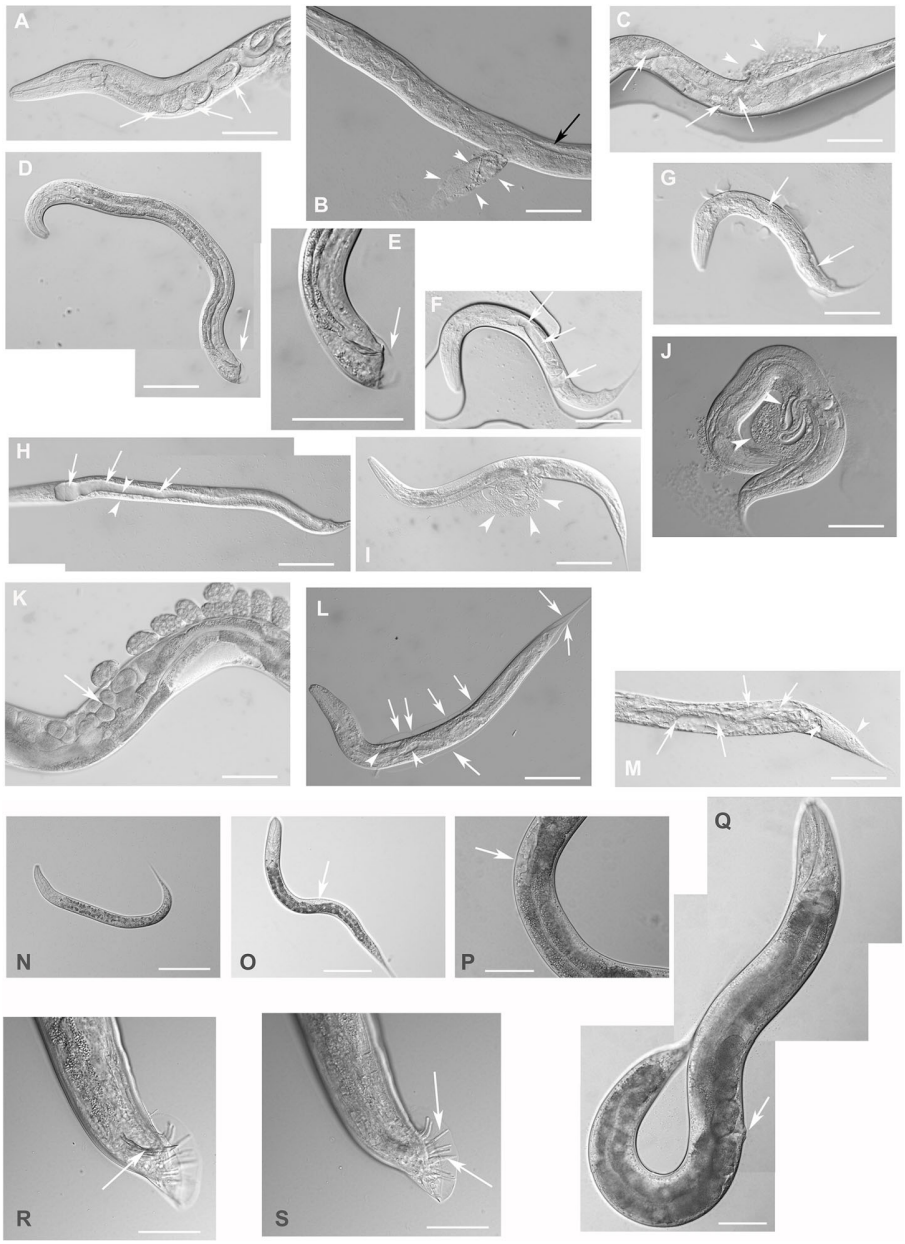

Figure 4 Downregulation of *F28F8.5* by RNAi induces developmental defects. Animals developed from parents injected with dsRNA specific for *F28F8.5* show retention of normal and malformed embryos (panels A and K, respectively), vacuoles (panels A and C, arrows), herniation and burst through the vulva (panels B, C, I, and J, arrowheads) and defective development of the gonad (panels J and M). Panel D shows a male nematode with defects of male specific structures—missing rays and fan and an abnormal distal part of the body (arrow). Panel E shows the magnified distal part of the male nematode in panel D and the defective male specific structures (arrow). Panels F and H show L3 larvae that were found atrophic, with thin enterocytes (arrowheads) and a dilated gut lumen (arrows). The dumpy phenotype with masses of tissue and vacuoles (panel G, arrows) were also common in the progeny of microinjected parents. Other phenotypes seen included molting defects indicated by arrows in panel L and cellular defects (indicated by arrowheads in panels L and M). Animals treated by control RNAi were morphologically normal and representative images are shown in panels N to Q. Panel N shows a L2

Figure 4 ... **continued**
larva, panel O shows a young L3 larva with developing germline (arrow). Panel P shows a young L4 Larva with developing vulva marked by an arrow. Panel Q shows a grossly normal adult hermaphrodite animal with few developing embryos and vulva (arrow). Panel R and S show the distal part of the body of a male animal with normal appearance of male specific structures. Arrow marks spicules (in panel R) and normal sensory rays (in panel S). All images are in Nomarski optics. Bars represent 50 μm.

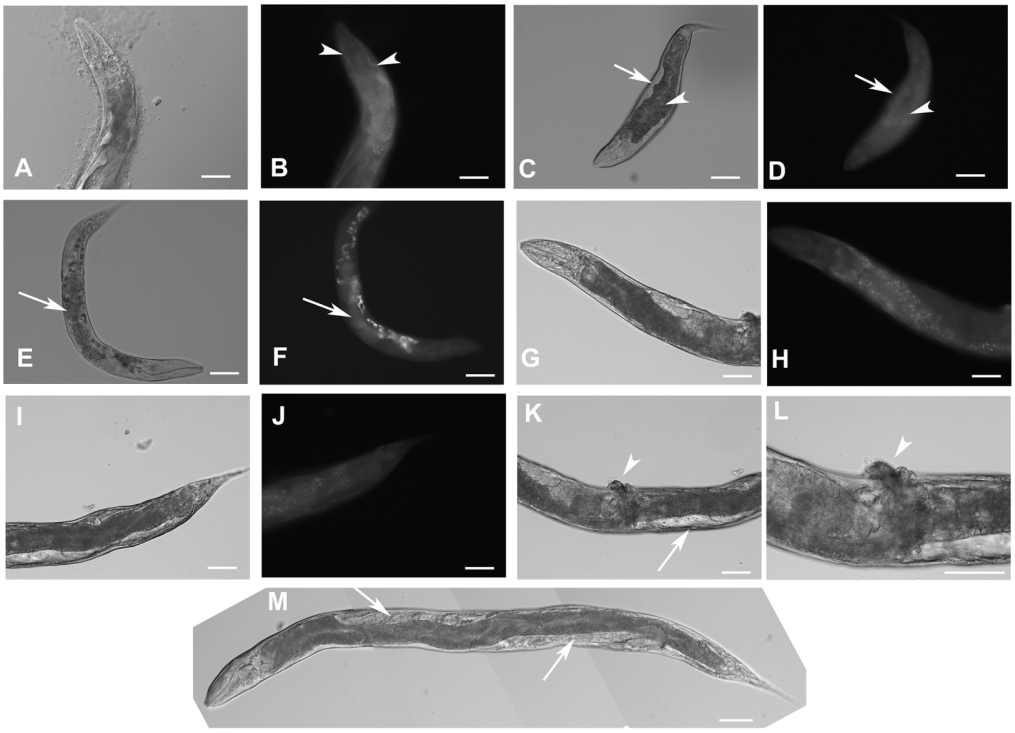

Figure 5 **Disruption of *F28F8.5* by CRISPR/Cas9 technique.** Animals with disrupted *F28F8.5* on both alleles express GFP under the regulation of *F28F8.5* promoter. Panels A to J show paired images of animals in Nomarski optics and in GFP fluorescence. Panels A and B show an adult hermaphrodite animal with diffuse fluorescence in cells in the head area including anterior arms of the excretory cell (arrowheads). Panels C and D show a malformed larva probably in L3 stage with a Dpy phenotype and diffuse fluorescence in a malformed gonad (arrows) and the intestine (arrowheads). Panels E and F show an adult hermaphrodite animal with diffuse fluorescence in gut, pharyngeal cells and severely malformed gonad containing irregular structures (arrows). Panels G, H, I, and J show an adult animal with a malformed gonad, Pvul phenotype, dense gut and diffuse GFP fluorescence throughout the body. Panels K and L show the central part of the body of a hermaphrodite with the Pvul phenotype (arrowhead) and malformation of gonad (arrow). Panel M is composed of three consecutive images showing an adult hermaphrodite animal with severely malformed gonad (arrows), and missing uterus and spermathecae. The fluorescence images show that unlike GFP::F28F8.5, GFP alone localizes diffusely in the cytoplasm and is not found in nuclei. Bars represent 50 μm.

F28F8.5 allele and one edited *F28F8.5* allele with excised SEC were detected. They were recognizable by the Rol phenotype, expression of GFP in nuclei and lack of developmental phenotypes. This genotype was supported by PCR amplification of genomic regions from single nematodes and obtained pattern of amplified DNA fragments. These lines were not stable and were not preserved.

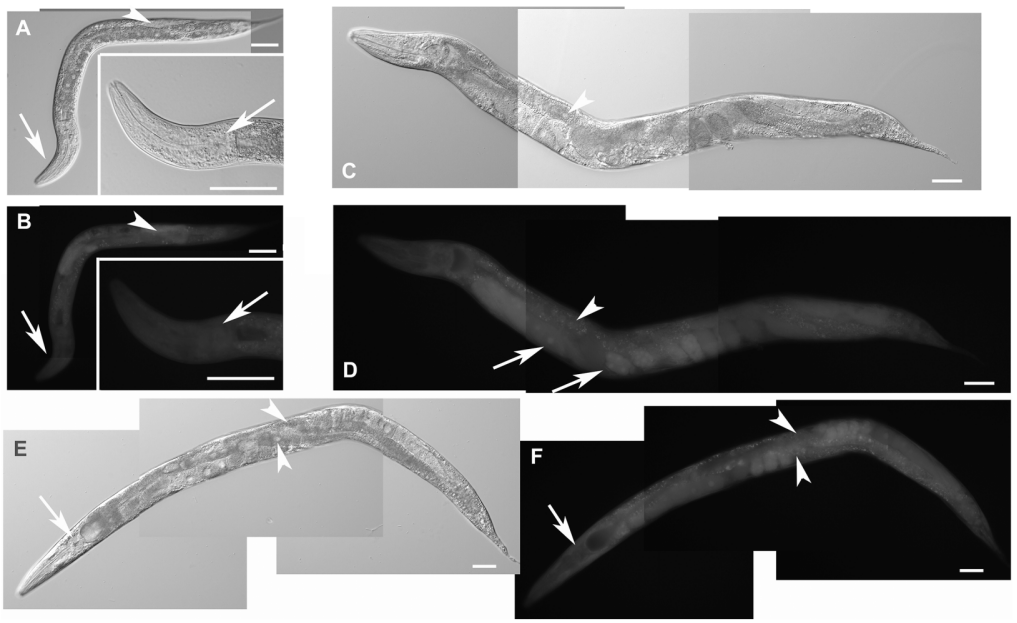

Figure 6 Heterozygous animals with one edited disrupted allele of *F28F8.5* and one WT allele. Heterozygous hermaphrodites carrying one edited allele of *F28F8.5* and one WT had grossly normal appearance and could be recognized by *rol* phenotype, presence of embryos, weak mostly cytoplasmic GFP fluorescence and absence of nuclear localization of GFP fluorescence. Panels A (Nomarski optics) and B (GFP fluorescence) show an L3 larva with weak fluorescence (panel B, arrowhead points at the gonad and arrows point at the head and pharynx). Inlets show head area at higher magnification (rotated 90° clockwise). Panels C and D show an adult hermaphrodite animal (C in Nomarski optics and D in GFP fluorescence) with weak cytoplasmic fluorescence in most cells. The arrowhead in panel D points at the nucleus of an enterocyte in focal plane that is devoid of GFP fluorescence. Arrows indicate two embryos with GFP fluorescence accumulated in nuclei which is most likely the result of spontaneous SEC self-excision. Panels E and F show an adult hermaphrodite in Nomarski optics (panel E) and GFP fluorescence (panel F). Arrows indicate the head area with diffuse intracellular fluorescence visible in panel F. Arrowheads point at two nuclei of enterocytes in focal plane that are also devoid of fluorescence. In contrast to the animal shown in panels C and D, the animal shown in the panel E and F contains embryos that have mostly diffuse cytoplasmic expression of GFP. Bars represent 50 μm.

F28F8.5 interacts with Mediator complex subunits

To determine if F28F8.5 could be part of the Mediator complex in *C. elegans*, we explored its ability to interact with previously identified Mediator subunits. We expressed ^{35}S-labeled MDT-6, part of the "head" module where MED28 is located, in rabbit reticulocyte lysate and assayed its binding to bacterially expressed GST-F28F8.5 or to GST only. As shown in Figs. 7A and 7B, a strong interaction (~7.7-fold enrichment) was detected between MDT-6 to F28F8.5 that exceeded that seen with GST alone. We also assayed for interaction between GST-F28F8.5 and MDT-30, but we were unable to obtain a satisfactory ^{35}S-Methionine labeled protein in the rabbit reticulocyte system. Therefore, we expressed MDT-30 containing a FLAG sequence inserted at the C-terminus and a His_6 sequence positioned at the N-terminus. After expression in bacteria and purification on a nickel column, we found that the MDT-30-FLAG bound F28F8.5 preferentially (~2.5-fold enrichment) in comparison to GST alone, as revealed by Western blot using an anti-FLAG antibody (Figs. 7C and 7D).

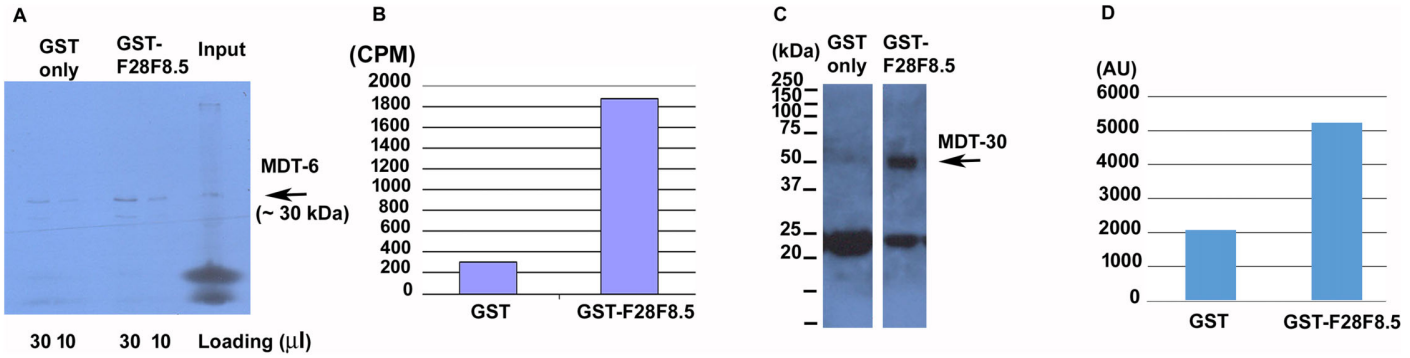

Figure 7 Binding of F28F8.5 to MDT-6 and MDT-30 in vitro. GST-F28F8.5 or GST alone were expressed in bacteria and purified using glutathione–agarose beads that were incubated with ^{35}S-Methionine-MDT-6 produced using rabbit reticulocyte lysate (A and B) or His_6-MDT-30-FLAG expressed in bacteria and purified using a nickel column (C and D). Panels A and C show fractions bound to glutathione–agarose beads resolved by polyacrylamide gel electrophoresis and visualized by autoradiography (panel A). For quantification, dried gel areas corresponding to proteins detected by radioactivity were excised and the radioactively labeled MDT-6 was determined using scintillation counter (panel B). Panels C and D show the interaction of FLAG-MDT-30 with GST-F28F8.5 or GST alone. FLAG-MDT-30 pulled down by GST or GST-F28F8.5 was determined by Western blot using an anti-FLAG antibody (panel C) and by densitometry (panel D). Both assayed Mediator subunits, MDT-6 and MDT-30 bind GST-F28F8.5 preferentially in comparison to GST only.

DISCUSSION

In this work, we identified an uncharacterized predicted protein F28F8.5 as the likely nematode homologue of MED28. This is supported by our findings that F28F8.5 interacts with nematode homologues of MED6 and MED30 (MDT-6, and MDT-30), the close sequence similarity of F28F8.5 to MED28 detected informatically in nematode genomes, a conserved dual nuclear and cytoplasmic expression pattern, and its involvement in a wide range of developmental processes. Thus we suggest F28F8.5 be identified as MDT-28, with the original gene for MDT-28 now recognized as the nematode homologue of perilipin, now named PLIN-1 (*Chughtai et al., 2015*).

The Mediator complex as a multiprotein structure is able to interact with a large number of additional proteins and integrate regulatory signals from several cell-signaling cascades (*Allen & Taatjes, 2015*). The Mediator complex possesses a high degree of structural flexibility and variable subunit composition (reviewed in *Poss, Ebmeier & Taatjes (2013)*). In yeast, a set of core subunits is important for a wide range of gene transcription (e.g., Med17 and Med22 (*Thompson & Young, 1995*; *Holstege et al., 1998*)), while others are non-essential in terms that single mutants can be maintained at laboratory conditions (Med1, Med2, Med3, Med5, Med9, Med15, Med16, Med18, Med19, Med20, Med31, and CDK module subunits Med12 (srb8), Med13 (srb9), srb10 (CDK8), and srb11 (CycC) (*Dettmann et al., 2010*)). Med31 and Srb9/Med13 Mediator subunits have different roles in gene selective transcription in *Saccharomyces cervisiae* and in *Candida albicans* (*Uwamahoro et al., 2012*). Mass spectrometry analyses indicate that many Mediator subunits are present in stoichiometric quantities but some subunits are over- or under-represented in budding and fission yeast and human HeLa cells (*Kulak et al., 2014*). Isolation of mammalian Mediator complexes lacking one or more of the 26 core subunits was reported for Med1 (TRAP220) (*Malik et al., 2004*), Med1 (Med220)

and Med26 (a.k.a. Med70 or CRSP70, or ARC70) (*Taatjes & Tjian, 2004*) (reviewed in *Allen & Taatjes (2015)*, the unified nomenclature can be found in (*Bourbon et al., 2004*) and for Med70 in *Rachez & Freedman (2001)*). While in cells with a stem cell like character, a broad spectrum of Mediator subunits was detected during; differentiation the expression of some Mediator subunits was markedly decreased (MED14, MED18, MED12, CDK8, MED26 in myotubes versus myoblasts) (*Deato et al., 2008*). In hepatocytes MED1, MED6, MED7, MED12, MED14, MED16, MED18, MED23, and CDK8 are decreased or even undetectable upon differentiation from hepatoblasts to hepatocytes (*D'Alessio et al., 2011*). Quantitative mass spectrometry analyses of Mediator complexes isolated by immunoprecipitation using four different Mediator subunits expressed as FLAG-tagged proteins in HeLa cells (Med10, Med26, Med28, Med29) identified most subunits of the Mediator complex in similar quantities with the exception of MED30, which was found in elevated ratios by Med28 pull-down experiments compared to other tested subunits. Med26 and Med29 precipitated more abundantly in their own pull-downs. Med31 was immunoprecipitated more efficiently in complexes with Med10 and Med25 was the least abundant subunit in all examined pull-downs (*Paoletti et al., 2006*). In-keeping with this, the abundance of individual Mediator subunits identified by quantitative proteomics indicate that some subunits are in similar abundance while others are under-represented or more numerous in yeast as well as in HeLa cells (*Kulak et al., 2014*). This suggests that Mediator complexes with specialized functions are likely to exist. A similar situation may be observed on ribosomes. Although the structure of ribosomal subunits is very firm and is given by the secondary structure of ribosomal RNAs and the presence of ribosomal proteins (*Ban et al., 2000*; *Schluenzen et al., 2000*; *Wimberly et al., 2000*), ribosome function during translation of mRNAs can be effectively regulated by viral proteins (*Diaz et al., 1993*, *1996*) which reveals the existence of a regulable "ribosomal code." The regulation of ribosome biogenesis and translation through the p53 pathway and methylation of ribosomal RNA by fibrillarin is leading to cancer specific ribosomes (*Marcel et al., 2013*). Cells infected with the viral oncogene v-erbA, the viral form of thyroid hormone receptor alpha, produce ribosomes with decreased levels of RPL11 which are translating more effectively Hsp70, a protein critical for tumorigenesis in avian erythroblastosis (*Nguyen-Lefebvre et al., 2014*). In comparison to ribosomal subunits, the Mediator complex possesses some analogies and differences.

The unit that is forming the structural backbone of Mediator is MED14 which is critical for both basal and activated transcription (*Cevher et al., 2014*). Mediator complexes bound to specific transcription factors (SREB Mediator, VP16-Mediator, TR-Mediator, VDR-Mediator, p53-Mediator) and the unliganded Mediator assume all distinct sterical conformations with fundamentally altered exposed protein surfaces (*Poss, Ebmeier & Taatjes, 2013*) that can be expected to form a multipotent basis for additional protein-protein interactions. This is possible because the fundamental features of the Mediator subunits are their intrinsically disordered regions that are to a certain degree positionally conserved between species, while others evolved in a phylum or species-specific way (*Nagulapalli et al., 2016*). In yeast, Med3 and Med15 form amyloid-like protein aggregates under H_2O_2 stress conditions. The amyloid formation can be

induced by overexpression of Med3 or glutamine-rich domain of Med15. This subsequently leads to the loss of Med15 module from Mediator and a change in the stress response (*Zhu et al., 2015*). The Mediator complexes contact a wide range of transcription factors using a fuzzy protein interface (*Brzovic et al., 2011*; *Warfield et al., 2014*). It can be therefore anticipated that additional proteins with a similar protein–protein interaction potential have the capability to interact with Mediator subunits if they are translocated into the nucleus.

Although individual Mediator complex subunits were shown to be associated with specific functions (reviewed in *Grants, Goh & Taubert (2015)*), the function of the nematode orthologue of MED28 could not be studied since it was not yet identified. MED28 has a special position in-between Mediator subunit proteins for its dual regulatory role, one as a Mediator subunit (*Sato et al., 2004*; *Beyer et al., 2007*) and the second, which is cytoplasmic, at the level of the cytoskeleton (*Wiederhold et al., 2004*; *Lee et al., 2006*; *Lu et al., 2006*; *Huang et al., 2012*). It can be anticipated that the interaction of primarily cytoplasmic proteins with MED28 if translocated to the nucleus may be able to bring cytoplasmic regulatory interactions towards the regulation of gene expression. In-between cytoplasmic proteins regulating gene expression, probably the most studied is beta-catenin, an adaptor of interaction between the cytoskeleton and cell adhesion molecules which critically regulates gene expression in the Wnt pathway. This connection is known in *C. elegans* to great detail (reviewed in *Grants, Goh & Taubert (2015)*). Interestingly, the phenotypes that we observed in F28F8.5 knock-down and loss of function experiments overlap with the EGFR regulatory cascade in *C. elegans*, especially the developmental defects of the vulva and of male specific structures, most obviously, male rays (*Grants, Goh & Taubert, 2015*; *Grants et al., 2016*). Our observation of the expression of *F28F8.5* in male rays and the defective development of male specific structures after *F28F8.5* RNAi support the cytoplasmic role of F28F8.5, that is in mammals mediated by Grb2 (*Wiederhold et al., 2004*). This cytoplasmic function of F28F8.5 is supported by the known involvement of the nematode homologue of Grb2, SEM-5, in the regulation of development of male rays. F28F8.5 protein contains a predicted SH2 binding site for Grb2 in the loop positioned in-between the two helices of F28F8.5, similarly as MED28 (identified using the site prediction tool Motif Scan http://scansite.mit.edu/motifscan_seq.phtml) (*Wiederhold et al., 2004*). Although, it has to be stressed that there are no close structures available for a high-probability prediction of the structure of F28F8.5. The burst through vulva phenotype is also likely to be connected to LET-60/Ras signaling (*Ecsedi, Rausch & Grosshans, 2015*) that also supports the conservation of the dual, nuclear and cytoplasmic functions, of MED28 homologues throughout the evolution of Metazoa.

We propose that MED28 is a candidate Mediator complex subunit linking cytoplasmic structural signals towards the core of transcription regulation. The connection between cytoplasmic events and regulation of gene expression can be seen frequently. Numerous transcription factors are regulated by their spatial restriction, binding or incorporation into cytoplasmic structures and organelles. Many proteins that have primarily cytoplasmic structural functions were shown to possess transcription regulating activity (e.g., proteins

interacting with steroid receptors (*George, Schiltz & Hager, 2009*), FOX transcription factors (*Gan et al., 2005*; *Wang et al., 2015*), and BIR-1/Survivin (*Kostrouch et al., 2014*)). In-between interactions of MDT-28 that we identified, the interaction with MDT-30 may suggest an additional link towards connection of structural signals with the regulation of gene expression. MED30 was shown to be pulled down by MED28 quantitatively with higher efficiency compared to other subunits, possibly suggesting that these two subunits may be present in some subpopulations of Mediator complexes that could lack other Mediator subunits. MED30 is similarly as MED28 a likely more recent Mediator subunit specific to Metazoa and absent in yeast and it is intriguing to speculate that the more recently evolved Mediator subunits are linked with the evolution of structurally differentiated cells and tissues. It can be anticipated that impairment of cellular structure sensing could be involved in cancer biology. In-keeping with this, MED30 was recently identified as an upregulated gene in stomach cancer connected with cancer proliferative properties (*Lee et al., 2015*) and in development of cardiomyopathy in mice carrying a missense mutation in the first exon (*Krebs et al., 2011*). MED28 was also connected with cancer behavior and migration of cancer cells (*Huang et al., 2012*, *2017*). Wormbase also lists phenotypes similar to F28F8.5 knock-down by RNAi for *mdt-30*, namely a Dpy, burst through vulva and locomotion defect but not a germline defect (Wormbase WS, accessed on March 11, 2017). The gene *mdt-30* is organized in an operon together with F44B9.8 which is an ortholog of human RFC5 (replication factor C subunit 5) and its inhibition by RNAi leads to embryonic defects. Similarly as F28F8.5, *mdt-30* is likely to be expressed independently from the operon since it is trans-spliced with both SL1 and SL2 splice leaders (Wormbase WS, accessed on March 11, 2017).

Our results demonstrated phenotypic differences comparing knock down versus knockout of F28F8.5 activity. For example, downregulation of *F28F8.5* by RNAi resulted in embryonic lethality and larval arrest whereas null mutants with a disrupted *F28F8.5* gene found in the progeny of heterozygous animals with one edited disrupted allele and one WT allele or one edited disrupted allele and one edited allele coding for GFP::F28F8.5 were able to reach adulthood. Morevoer, most phenotypes that we observed in our RNAi experiments have previously been reported in Wormbase (WS254) based on high throughput screens (*Kamath & Ahringer, 2003*; *Simmer et al., 2003*; *Frand, Russel & Ruvkun, 2005*; *Sönnichsen et al., 2005*). One explanation of the differences between knockdowns versus knockouts is that heterozygous animals with one functional allele of *F28F8.5* supply their embryos with maternal transcripts, while the embryos in the progeny of parents with *F28F8.5* downregulated by RNAi are devoid of this maternal load; maternal rescue of loss-of-function mutations is frequently observed in *C. elegans* early development. This model further predicts that the amount of *F28F8.5* product inherited maternally is not sufficient for normal development of the gonad and other post-embryonic developmental events such as male tail development. Alternatively, our F28F8.5 disruptions could be affecting other genes in the operon, although none have been reported to result in high level embryonic lethality when eliminated individually. The three other genes within this operon are *atx-3*, the orthologue of human ataxin-3,

F28F8.9, a non-characteristic predicted protein and F28F8.7, an orthologue of human ELMSAN1 (ELM2 and Myb/SANT domain containing 1) and TRERF1 (transcriptional regulating factor 1). RNAi experiments have been reported for *atx-3* and F28F8.9, of which only inhibition of *atx-3* produced embryonic arrest in 10–25% of embryos. This suggests that even if our gene disruption is affecting other genes in the operon (as reported in *Bosher et al. (1999)*), the severe larval changes reported here are most likely the consequence of inhibition of *F28F8.5*. In addition, *F28F8.5* is also expressed independently from its own promoter based on our translational fusions and reported SL1 splice leader (*Mounsey, Bauer & Hope, 2002*; *Matus et al., 2010*). Further studies will be required to sort out the potentially complex interactions among these genes in development.

The broad expression pattern and indispensability of F28F8.5 we find during embryonic development is similar to findings reported for Med28 in other systems ((*Li et al., 2015*); Mouse Genome Database (http://www.mousephenotype.org/data/genes/MGI:1914249) (*Eppig et al., 2015*); Human Protein Atlas (http://www.proteinatlas.org) (*Uhlén et al., 2015*)). F28F8.5 was also shown to have tissue-specific functions, as in the anchor cell where it is important for the regulation of anchor cell translocation across the basement membrane during the formation of the developing vulva (*Matus et al., 2010*).

Our experiments with transgenes fused to GFP also show the differences between the expression of N- or C-terminally labeled F28F8.5. The expression of fusion transgenes is not entirely without functional and developmental consequences. N-terminally labeled F28F8.5 is likely to be able to maintain the nuclear functions of F28F8.5. It is also able to support, at least partially the cytoplasmic functions of F28F8.5 in male rays, since they are formed but are not entirely normal and defects in some animals were observed. It seems likely that GFP-labeled subunits in viable lines may help localize the place of action of labeled proteins as well as their function in *C. elegans*. We did not observe elevated cytoplasmic expression of GFP::F28F8.5 in the anchor cell described by *Matus et al. (2010)*. This is probably dependent on the position of GFP in the fusion protein which was on the C-terminus, in the case of the study by *Matus et al. (2010)* as well as in the case of the data reported by Wormbase (both based on a clone originally prepared by Ian Hope). It has been suggested that proteins containing GFP at their C-terminus are more frequently properly intracellularly localized compared to proteins containing GFP at their N-terminus (*Palmer & Freeman, 2004*). GFP positioned at the N-terminus might also fold differently and fail to produce fluorescence in oxidizing compartments (*Aronson, Costantini & Snapp, 2011*).

The direct link between effector proteins and the regulation of transcription can be traced to Eubacteria and Archaea. Lrp/AsnC proteins, metabolic effectors in Archaea and related Lrs14 proteins are serving as multipotent (Lrp) and specific (Asn) regulators of gene expression. Lrs14 has a clear negative autoregulatory potential illustrating the ancient origin of the transcriptional function of effector proteins (*Bell & Jackson, 2000*; *Thaw et al., 2006*; *Orell et al., 2013*). Similarities between the core transcriptional machinery of Eukaryotes and Archaea can be clearly found (*Hirata & Murakami, 2009*).

While the archaeal transcriptional complex seems to be sufficiently dependent on two basal transcriptional regulators, TBP and TFB, Pol II dependent transcription in higher eukaryotes requires five or six general transcription factors (reviewed in *Burton et al. (2016)*) and the modular assembly of the Mediator complex at the promoters of regulated genes. This modular complex is capable of linking the informatic network necessary for cells differentiated to multiple cell types (or in other words multiple structural cell states) with gene expression. MED28 homologues are thus likely to be able to bring cytoplasmic proteins to the core of gene transcription. This may explain why MED28 evolved in multicellular eukaryotes containing structurally differentiated cells.

In conclusion, MED28 homologues in vertebrates, insects, and nematodes share similarities indicating their conserved roles in cytoplasmic and nuclear events. It can be hypothesized that many proteins that are primarily building blocks of cellular structures and structure-associated proteins are likely to be part of regulatory loops that regulate gene expression. Similarly, as is the case of evolution of operons in Rhabditida that are formed during evolution if they are biologically tolerated for the sake of other regulatory or energetic gains (*Qian & Zhang, 2008*; *Blumenthal, 2012*), regulation by structural proteins may also be evolving for a limited number of structural proteins leaving other structure-forming proteins available for evolution of other functions. The homologues of MED28 in mammals, insects and nematodes therefore may be a link between cellular structural states and regulation of gene expression.

ABBREVIATIONS

F28F8.5[1]	gene coding for protein F28F8.5
F28F8.5a	splice form a
F28F8.5a	protein form a
F28F8.5b	splice form b
F28F8.5b	protein form b
gDNA	genomic DNA
$\boldsymbol{P_{F28F8.5}}$***(V:15573749)::gfp::F28F8.5***	edited *F28F8.5* with *gfp* tagged to the N-terminus in the position *V:15573749* (allele named edited *gfp*::*F28F8.5*)
$\boldsymbol{P_{F28F8.5}}$ ***(V:15573749)::gfp::let858(stop)::SEC::F28F8.5***	edited *F28F8.5* disrupted by *gfp* and SEC (allele named edited disrupted *F28F8.5*)
$\boldsymbol{P_{F28F8.5(400\ bp)}}$***::F28F8.5::gfp***	*F28F8.5* tagged with *gfp* on its C-terminus regulated by its predicted internal promoter with the size of 400 bp upstream of the ATG
GFP::F28F8.5	protein F28F8.5 tagged on its N-terminus with GFP
F28F8.5::GFP	protein F28F8.5 tagged on its C-terminus with GFP

[1] *F28F8.5* is now renamed with WormBase approval to *mdt-28*.

MED28	vertebrate Mediator complex subunit 28 gene
MED28	vertebrate Mediator complex subunit 28 protein
Med28	Mediator complex subunit 28 in a general sense; this nomenclature is also used in *Drosophila* and mouse gene nomenclature

ACKNOWLEDGEMENTS

The authors thank WormBase and NCBI for accessibility of data and bioinformatic support and Caenorhabditis Genetics Center CGC for the N2 wild type strain. The authors thank Dr. Heather Etchevers, Dr. Stefan Taubert and the two anonymous reviewers for their very helpful comments, suggestions and corrections.

ADDITIONAL INFORMATION AND DECLARATIONS

Funding

This work was supported by the European Regional Development Fund "BIOCEV—Biotechnology and Biomedicine Centre of the Academy of Sciences and Charles University in Vestec" (CZ.1.05/1.1.00/02.0109) (The Start-Up Grant to the group Structure and Function of Cells in Their Normal State and in Pathology—Integrative Biology and Pathology (5.1.10)) and the LQ1604 National Sustainability Program II (Project BIOCEV-FAR) and the project Biocev (CZ.1.05/1.1.00/02.0109) from the Ministry of Education, Youth and Sports of Czech Republic; the grant PRVOUK-P27 and PROGRES Q26/LF1 from Charles University in Prague; the grant SVV 260377/2017, SVV 260257/2016, SVV 260149/2015 and SVV 260023/2014 from Charles University in Prague. This work was supported by the project OPPK No. CZ.2.16/3.1.00/24024, awarded by European Fund for Regional Development (Prague & EU—We invest for your future). MWK is supported by the Intramural Research Program of the National Institute of Diabetes and Digestive and Kidney Diseases (NIDDK) of the National Institutes of Health, USA. This work was supported in part by a monetary gift from MediCentrum Praha, Czech Republic. The imaging was done at the Imaging Methods Core Facility at BIOCEV, supported by the Czech-BioImaging large RI project (LM2015062 funded by MEYS CR). ZK and MK contributed with personal funds to this work. The funders (except authors) had no role in study design, data collection and analysis, decision to publish, or preparation of the manuscript.

Grant Disclosures

The following grant information was disclosed by the authors:
European Regional Development Fund "BIOCEV—Biotechnology and Biomedicine Centre of the Academy of Sciences and Charles University in Vestec":
CZ.1.05/1.1.00/02.0109.
The Start-Up Grant: 5.1.10.
Ministry of Education, Youth and Sports of Czech Republic: BIOCEV-FAR, CZ.1.05/1.1.00/02.0109.

Charles University in Prague: PRVOUK-P27, PROGRES Q26/LF1, SVV 260377/2017, SVV 260257/2016, SVV 260149/2015 and SVV 260023/2014.
European Fund for Regional Development: CZ.2.16/3.1.00/24024.
Intramural Research Program of the National Institute of Diabetes and Digestive and Kidney Diseases (NIDDK) of the National Institutes of Health, USA.
MediCentrum Praha, Czech Republic.
Czech-BioImaging large RI project (MEYS CR): LM2015062.

Competing Interests

Marta Kostrouchová is an Academic Editor for PeerJ. No other competing interests declared.

Author Contributions

- Markéta Kostrouchová conceived and designed the experiments, performed the experiments, analyzed the data, wrote the paper, prepared figures and/or tables, reviewed drafts of the paper.
- David Kostrouch conceived and designed the experiments, performed the experiments, analyzed the data, wrote the paper, prepared figures and/or tables, reviewed drafts of the paper.
- Ahmed A. Chughtai conceived and designed the experiments, performed the experiments, analyzed the data, wrote the paper, prepared figures and/or tables, reviewed drafts of the paper.
- Filip Kaššák conceived and designed the experiments, performed the experiments, analyzed the data, wrote the paper, prepared figures and/or tables, reviewed drafts of the paper.
- Jan P. Novotný conceived and designed the experiments, performed the experiments, analyzed the data, wrote the paper, prepared figures and/or tables, reviewed drafts of the paper.
- Veronika Kostrouchová performed the experiments, analyzed the data, wrote the paper, prepared figures and/or tables, reviewed drafts of the paper.
- Aleš Benda conceived and designed the experiments, performed the experiments, analyzed the data, wrote the paper, prepared figures and/or tables, reviewed drafts of the paper.
- Michael W. Krause conceived and designed the experiments, performed the experiments, analyzed the data, wrote the paper, prepared figures and/or tables, reviewed drafts of the paper.
- Vladimír Saudek conceived and designed the experiments, performed the experiments, analyzed the data, wrote the paper, prepared figures and/or tables, reviewed drafts of the paper.
- Marta Kostrouchová conceived and designed the experiments, performed the experiments, analyzed the data, contributed reagents/materials/analysis tools, wrote the paper, prepared figures and/or tables, reviewed drafts of the paper, contributed with personal funds.

- Zdeněk Kostrouch conceived and designed the experiments, performed the experiments, analyzed the data, contributed reagents/materials/analysis tools, wrote the paper, prepared figures and/or tables, reviewed drafts of the paper, contributed with personal funds.

Data Availability

The following information was supplied regarding data availability:

The raw data has been supplied as Supplemental Dataset Files.

Supplemental Information

Supplemental information for this article can be found online at http://dx.doi.org/10.7717/peerj.3390#supplemental-information.

REFERENCES

Allen BL, Taatjes DJ. 2015. The Mediator complex: a central integrator of transcription. *Nature Reviews Molecular Cell Biology* **16(3)**:155–166 DOI 10.1038/nrm3951.

Altschul SF, Madden TL, Schäffer AA, Zhang J, Zhang Z, Miller W, Lipman DJ. 1997. Gapped BLAST and PSI-BLAST: a new generation of protein database search programs. *Nucleic Acids Research* **25(17)**:3389–3402 DOI 10.1093/nar/25.17.3389.

Aronson DE, Costantini LM, Snapp EL. 2011. Superfolder GFP is fluorescent in oxidizing environments when targeted via the Sec translocon. *Traffic* **12(5)**:543–548 DOI 10.1111/j.1600-0854.2011.01168.x.

Ban N, Nissen P, Hansen J, Moore PB, Steitz TA. 2000. The complete atomic structure of the large ribosomal subunit at 2.4 Å resolution. *Science* **289(5481)**:905–920 DOI 10.1126/science.289.5481.905.

Bell SD, Jackson SP. 2000. Mechanism of autoregulation by an archaeal transcriptional repressor. *Journal of Biological Chemistry* **275**:31624–31629 DOI 10.1074/jbc.M005422200.

Beyer KS, Beauchamp RL, Lee MF, Gusella JF, Naar AM, Ramesh V. 2007. Mediator subunit MED28 (Magicin) is a repressor of smooth muscle cell differentiation. *Journal of Biological Chemistry* **282(44)**:32152–32157 DOI 10.1074/jbc.m706592200.

Blumenthal T. 2012. Trans-splicing and operons in *C. elegans*. In: Jane Mendel E, ed. *The C. elegans Research Community*. WormBook. *Available at http://www.wormbook.org*.

Bosher JM, Dufourcq P, Sookhareea S, Labouesse M. 1999. RNA interference can target pre-mRNA: consequences for gene expression in a *Caenorhabditis elegans* operon. *Genetics* **153(3)**:1245–1256.

Bourbon H-M. 2008. Comparative genomics supports a deep evolutionary origin for the large, four-module transcriptional Mediator complex. *Nucleic Acids Research* **36(12)**:3993–4008 DOI 10.1093/nar/gkn349.

Bourbon H-M, Aguilera A, Ansari AZ, Asturias FJ, Berk AJ, Bjorklund S, Blackwell TK, Borggrefe T, Carey M, Carlson M, Conaway JW, Conaway RC, Emmons SW, Fondell JD, Freedman LP, Fukasawa T, Gustafsson CM, Han M, He X, Herman PK, Hinnebusch AG, Holmberg S, Holstege FC, Jaehning JA, Kim Y-J, Kuras L, Leutz A, Lis JT, Meisterernest M, Naar AM, Nasmyth K, Parvin JD, Ptashne M, Reinberg D, Ronne H, Sadowski I, Sakurai H, Sipiczki M, Sternberg PW, Stillman DJ, Strich R, Struhl K, Svejstrup JQ, Tuck S, Winston F, Roeder RG, Kornberg RD. 2004. A unified nomenclature for protein subunits of Mediator complexes linking transcriptional regulators to RNA polymerase II. *Molecular Cell* **14**:553–557 DOI 10.1016/j.molcel.2004.05.011.

Brenner S. 1974. The genetics of *Caenorhabditis elegans*. *Genetics* **77(1)**:71–94.

Brzovic PS, Heikaus CC, Kisselev L, Vernon R, Herbig E, Pacheco D, Warfield L, Littlefield P, Baker D, Klevit RE, Hahn S. 2011. The acidic transcription activator Gcn4 binds the mediator subunit Gal11/Med15 using a simple protein interface forming a fuzzy complex. *Molecular Cell* **44(6)**:942–953 DOI 10.1016/j.molcel.2011.11.008.

Burton ZF, Opron K, Wei G, Geiger JH. 2016. A model for genesis of transcription systems. *Transcription* **7**:1–13 DOI 10.1080/21541264.2015.1128518.

Cevher MA, Shi Y, Li D, Chait BT, Malik S, Roeder RG. 2014. Reconstitution of active human core Mediator complex reveals a critical role of the MED14 subunit. *Nature Structural & Molecular Biology* **21(12)**:1028–1034 DOI 10.1038/nsmb.2914.

Chughtai AA, Kaššák F, Kostrouchová M, Novotný JP, Krause MW, Saudek V, Kostrouch Z, Kostrouchová M. 2015. Perilipin-related protein regulates lipid metabolism in *C. elegans*. *PeerJ* **3**:e1213 DOI 10.7717/peerj.1213.

Clamp M, Cuff J, Searle SM, Barton GJ. 2004. The Jalview Java alignment editor. *Bioinformatics* **20(3)**:426–427 DOI 10.1093/bioinformatics/btg430.

Cuff JA, Barton GJ. 2000. Application of multiple sequence alignment profiles to improve protein secondary structure prediction. *Proteins* **40(3)**:502–511 DOI 10.1002/1097-0134(20000815)40:3<502::aid-prot170>3.0.co;2-q.

D'Alessio JA, Ng R, Willenbring H, Tjian R. 2011. Core promoter recognition complex changes accompany liver development. *Proceedings of the National Academy of Sciences of the United States of America* **108(10)**:3906–3911 DOI 10.1073/pnas.1100640108.

Deato MDE, Marr MT, Sottero T, Inouye C, Hu P, Tjian R. 2008. MyoD targets TAF3/TRF3 to activate myogenin transcription. *Molecular Cell* **32(1)**:96–105 DOI 10.1016/j.molcel.2008.09.009.

Dettmann A, Jäschke Y, Triebel I, Bogs J, Schröder I, Schüller H-J. 2010. Mediator subunits and histone methyltransferase Set2 contribute to Ino2-dependent transcriptional activation of phospholipid biosynthesis in the yeast *Saccharomyces cerevisiae*. *Molecular Genetics and Genomics* **283(3)**:211–221 DOI 10.1007/s00438-009-0508-9.

Di Tommaso P, Moretti S, Xenarios I, Orobitg M, Montanyola A, Chang J-M, Taly J-F, Notredame C. 2011. T-Coffee: a web server for the multiple sequence alignment of protein and RNA sequences using structural information and homology extension. *Nucleic Acids Research* **39(Suppl_2)**:W13–W17 DOI 10.1093/nar/gkr245.

Diaz JJ, Dodon MD, Schaerer-Uthurralt N, Simonin D, Kindbeiter K, Gazzolo L, Madjar J-J. 1996. Post-transcriptional transactivation of human retroviral envelope glycoprotein expression by herpes simplex virus Us11 protein. *Nature* **379**:273–277 DOI 10.1038/379273a0.

Diaz JJ, Simonin D, Massé T, Deviller P, Kindbeiter K, Denoroy L, Madjar J-J. 1993. The herpes simplex virus type 1 US11 gene product is a phosphorylated protein found to be non-specifically associated with both ribosomal subunits. *Journal of General Virology* **74(Pt 3)**:397–406 DOI 10.1099/0022-1317-74-3-397.

Dickinson DJ, Goldstein B. 2016. CRISPR-based methods for *Caenorhabditis elegans* genome engineering. *Genetics* **202(3)**:885–901 DOI 10.1534/genetics.115.182162.

Dickinson DJ, Pani AM, Heppert JK, Higgins CD, Goldstein B. 2015. Streamlined genome engineering with a self-excising drug selection cassette. *Genetics* **200(4)**:1035–1049 DOI 10.1534/genetics.115.178335.

Dickinson DJ, Ward JD, Reiner DJ, Goldstein B. 2013. Engineering the *Caenorhabditis elegans* genome using Cas9-triggered homologous recombination. *Nature Methods* **10**:1028–1034 DOI 10.1038/nmeth.2641.

Ecsedi M, Rausch M, Grosshans H. 2015. The let-7 microRNA directs vulval development through a single target. *Developmental Cell* **32(3)**:335–344 DOI 10.1016/j.devcel.2014.12.018.

Eppig JT, Blake JA, Bult CJ, Kadin JA, Richardson JE, Mouse Genome Database Group. 2015. The mouse genome database (MGD): facilitating mouse as a model for human biology and disease. *Nucleic Acids Research* **43(D1)**:D726–D736 DOI 10.1093/nar/gku967.

Frand AR, Russel S, Ruvkun G. 2005. Functional genomic analysis of *C. elegans* molting. *PLoS Biology* **3(10)**:e312 DOI 10.1371/journal.pbio.0030312.

Gan L, Zheng W, Chabot JG, Unterman TG, Quirion R. 2005. Nuclear/cytoplasmic shuttling of the transcription factor FoxO1 is regulated by neurotrophic factors. *Journal of Neurochemistry* **93(5)**:1209–1219 DOI 10.1111/j.1471-4159.2005.03108.x.

George AA, Schiltz RL, Hager GL. 2009. Dynamic access of the glucocorticoid receptor to response elements in chromatin. *International Journal of Biochemistry & Cell Biology* **41(1)**:214–224 DOI 10.1016/j.biocel.2008.09.019.

Grants JM, Goh GYS, Taubert S. 2015. The Mediator complex of *Caenorhabditis elegans*: insights into the developmental and physiological roles of a conserved transcriptional coregulator. *Nucleic Acids Research* **43(4)**:2442–2453 DOI 10.1093/nar/gkv037.

Grants JM, Ying LTL, Yoda A, You CC, Okano H, Sawa H, Taubert S. 2016. The mediator kinase module restrains epidermal growth factor receptor signaling and represses vulval cell fate specification in *Caenorhabditis elegans*. *Genetics* **202(2)**:583–599 DOI 10.1534/genetics.115.180265.

Hirata A, Murakami KS. 2009. Archaeal RNA polymerase. *Current Opinion in Structural Biology* **19(6)**:724–731 DOI 10.1016/j.sbi.2009.10.006.

Hobert O. 2002. PCR fusion-based approach to create reporter gene constructs for expression analysis in transgenic *C. elegans*. *Biotechniques* **32**:728–730.

Holstege FCP, Jennings EG, Wyrick JJ, Lee TI, Hengartner CJ, Green MR, Golub TR, Lander ES, Young RA. 1998. Dissecting the regulatory circuitry of a eukaryotic genome. *Cell* **95(5)**:717–728 DOI 10.1016/s0092-8674(00)81641-4.

Huang C-Y, Chou Y-H, Hsieh N-T, Chen H-H, Lee M-F. 2012. MED28 regulates MEK1-dependent cellular migration in human breast cancer cells. *Journal of Cellular Physiology* **227(12)**:3820–3827 DOI 10.1002/jcp.24093.

Huang C-Y, Hsieh N-T, Li C-I, Weng Y-T, Liu H-S, Lee M-F. 2017. MED28 regulates epithelial-mesenchymal transition through NFκB in human breast cancer cells. *Journal of Cellular Physiology* **232(6)**:1337–1345 DOI 10.1002/jcp.25610.

Jones DT. 1999. Protein secondary structure prediction based on position-specific scoring matrices. *Journal of Molecular Biology* **292(2)**:195–202 DOI 10.1006/jmbi.1999.3091.

Kamath RS, Ahringer J. 2003. Genome-wide RNAi screening in *Caenorhabditis elegans*. *Methods* **30(4)**:313–321 DOI 10.1016/s1046-2023(03)00050-1.

Kim TW, Kwon YJ, Kim JM, Song YH, Kim SN, Kim YJ. 2004. MED16 and MED23 of mediator are coactivators of lipopolysaccharide- and heat-shock-induced transcriptional activators. *Proceedings of the National Academy of Sciences of the United States of America* **101(33)**:12153–12158 DOI 10.1073/pnas.0401985101.

Kostrouch D, Kostrouchová M, Yilma P, Chughtai AA, Novotný JP, Novák P, Kostrouchová V, Kostrouchová M, Kostrouch Z. 2014. SKIP and BIR-1/Survivin have potential to integrate proteome status with gene expression. *Journal of Proteomics* **110**:93–106 DOI 10.1016/j.jprot.2014.07.023.

Krebs P, Fan W, Chen Y-H, Tobita K, Downes MR, Wood MR, Sun L, Li X, Xia Y, Ding N, Spaeth JM, Moresco EMY, Boyer TG, Lo CW, Yen J, Evans RM, Beutler B. 2011. Lethal

mitochondrial cardiomyopathy in a hypomorphic *Med30* mouse mutant is ameliorated by ketogenic diet. *Proceedings of the National Academy of Sciences of the United States of America* **108(49)**:19678–19682 DOI 10.1073/pnas.1117835108.

Kulak NA, Pichler G, Paron I, Nagaraj N, Mann M. 2014. Minimal, encapsulated proteomic-sample processing applied to copy-number estimation in eukaryotic cells. *Nature Methods* **11(3)**:319–324 DOI 10.1038/nmeth.2834.

Lee M-F, Beauchamp RL, Beyer KS, Gusella JF, Ramesh V. 2006. Magicin associates with the Src-family kinases and is phosphorylated upon CD3 stimulation. *Biochemical and Biophysical Research Communications* **348(3)**:826–831 DOI 10.1016/j.bbrc.2006.07.126.

Lee YJ, Han M-E, Baek S-J, Kim S-Y, Oh S-O. 2015. MED30 regulates the proliferation and motility of gastric cancer cells. *PLoS ONE* **10(6)**:e0130826 DOI 10.1371/journal.pone.0130826.

Li L, Walsh RM, Wagh V, James MF, Beauchamp RL, Chang Y-S, Gusella JF, Hochedlinger K, Ramesh V. 2015. Mediator subunit Med28 is essential for mouse peri-implantation development and pluripotency. *PLoS ONE* **10(10)**:e0140192 DOI 10.1371/journal.pone.0140192.

Liu C, Zhang L, Shao Z-M, Beatty P, Sartippour M, Lane TF, Barsky SH, Livingston E, Nguyen M. 2002. Identification of a novel endothelial-derived gene EG-1. *Biochemical and Biophysical Research Communications* **290(1)**:602–612 DOI 10.1006/bbrc.2001.6119.

Lu M, Zhang L, Sartippour MR, Norris AJ, Brooks MN. 2006. EG-1 interacts with c-Src and activates its signaling pathway. *International Journal of Oncology* **29(4)**:1013–1018 DOI 10.3892/ijo.29.4.1013.

Ly K, Reid SJ, Snell RG. 2015. Rapid RNA analysis of individual *Caenorhabditis elegans*. *MethodsX* **2**:59–63 DOI 10.1016/j.mex.2015.02.002.

Malik S, Guermah M, Yuan CX, Wu W, Yamamura S, Roeder RG. 2004. Structural and functional organization of TRAP220, the TRAP/mediator subunit that is targeted by nuclear receptors. *Molecular and Cellular Biology* **24(18)**:8244–8254 DOI 10.1128/MCB.24.18.8244-8254.2004.

Marcel V, Ghayad SE, Belin S, Therizols G, Morel AP, Solano-Gonzàlez E, Vendrell JA, Hacot S, Mertani HC, Albaret MA, Bourdon JC, Jordan L, Thompson A, Tafer Y, Cong R, Bouvet P, Saurin J-C, Catez F, Prats A-C, Puisieux A, Diaz J-J. 2013. p53 acts as a safeguard of translational control by regulating fibrillarin and rRNA methylation in cancer. *Cancer Cell* **24(3)**:318–330 DOI 10.1016/j.ccr.2013.08.013.

Matus DQ, Li XY, Durbin S, Agarwal D, Chi Q, Weiss SJ, Sherwood DR. 2010. In vivo identification of regulators of cell invasion across basement membranes. *Science Signaling* **3(120)**:ra35 DOI 10.1126/scisignal.2000654.

McClatchey AI, Fehon RG. 2009. Merlin and the ERM proteins—regulators of receptor distribution and signaling at the cell cortex. *Trends in Cell Biology* **19(5)**:198–206 DOI 10.1016/j.tcb.2009.02.006.

McClatchey AI, Giovannini M. 2005. Membrane organization and tumorigenesis—the NF2 tumor suppressor, Merlin. *Genes & Development* **19(19)**:2265–2277.

McGuffin LJ, Bryson K, Jones DT. 2000. The PSIPRED protein structure prediction server. *Bioinformatics* **16(4)**:404–405 DOI 10.1093/bioinformatics/16.4.404.

Mounsey A, Bauer P, Hope IA. 2002. Evidence suggesting that a fifth of annotated *Caenorhabditis elegans* genes may be pseudogenes. *Genome Research* **12(5)**:770–775 DOI 10.1101/gr208802.

Nagulapalli M, Maji S, Dwivedi N, Dahiya P, Thakur JK. 2016. Evolution of disorder in Mediator complex and its functional relevance. *Nucleic Acids Research* **44(4)**:1591–1612 DOI 10.1093/nar/gkv1135.

Nguyen-Lefebvre AT, Leprun G, Morin V, Viñuelas J, Couté Y, Madjar J-J, Gandrillon O, Gonin-Giraud S. 2014. V-erbA generates ribosomes devoid of RPL11 and regulates translational activity in avian erythroid progenitors. *Oncogene* **33(12)**:1581–1589 DOI 10.1038/onc.2013.93.

Notredame C, Higgins DG, Heringa J. 2000. T-coffee: a novel method for fast and accurate multiple sequence alignment. *Journal of Molecular Biology* **302(1)**:205–217 DOI 10.1006/jmbi.2000.4042.

Orell A, Peeters E, Vassen V, Jachlewski S, Schalles S, Siebers B, Albers SV. 2013. Lrs14 transcriptional regulators influence biofilm formation and cell motility of Crenarchaea. *ISME Journal* **7(10)**:1886–1898 DOI 10.1038/ismej.2013.68.

Palmer E, Freeman T. 2004. Investigation into the use of C- and N-terminal GFP fusion proteins for subcellular localization studies using reverse transfection microarrays. *Comparative and Functional Genomics* **5(4)**:342–353 DOI 10.1002/cfg.405.

Paoletti AC, Parmely TJ, Tomomori-Sato C, Sato S, Zhu D, Conaway RC, Conaway JW, Florens L, Washburn MP. 2006. Quantitative proteomic analysis of distinct mammalian Mediator complexes using normalized spectral abundance factors. *Proceedings of the National Academy of Sciences of the United States of America* **103(50)**:18928–18933 DOI 10.1073/pnas.0606379103.

Pei J, Grishin NV. 2007. PROMALS: towards accurate multiple sequence alignments of distantly related proteins. *Bioinformatics* **23(7)**:802–808 DOI 10.1093/bioinformatics/btm017.

Pei J, Kim B-H, Grishin NV. 2008. PROMALS3D: a tool for multiple protein sequence and structure alignments. *Nucleic Acids Research* **36(7)**:2295–2300 DOI 10.1093/nar/gkn072.

Pei J, Kim B-H, Tang M, Grishin NV. 2007. PROMALS web server for accurate multiple protein sequence alignments. *Nucleic Acids Research* **35(Suppl_2)**:W649–W652 DOI 10.1093/nar/gkm227.

Poss ZC, Ebmeier CC, Taatjes DJ. 2013. The Mediator complex and transcription regulation. *Critical Reviews in Biochemistry and Molecular Biology* **48(6)**:575–608 DOI 10.3109/10409238.2013.840259.

Qian W, Zhang J. 2008. Evolutionary dynamics of nematode operons: easy come, slow go. *Genome Research* **18(3)**:412–421 DOI 10.1101/gr.7112608.

Rachez C, Freedman LP. 2001. Mediator complexes and transcription. *Current Opinion in Cell Biology* **13(3)**:274–280 DOI 10.1016/s0955-0674(00)00209-x.

Remmert M, Biegert A, Hauser A, Soding J. 2011. HHblits: lightning-fast iterative protein sequence searching by HMM-HMM alignment. *Nature Methods* **9(2)**:173–175 DOI 10.1038/nmeth.1818.

Sato S, Tomomori-Sato C, Parmely TJ, Florens L, Zybailov B, Swanson SK, Banks CA, Jin J, Cai Y, Washburn MP, Conaway JW, Conaway RC. 2004. A set of consensus mammalian mediator subunits identified by multidimensional protein identification technology. *Molecular Cell* **14(5)**:685–691 DOI 10.1016/j.molcel.2004.05.006.

Schluenzen F, Tocilj A, Zarivach R, Harms J, Gluehmann M, Janell D, Bashan A, Bartels H, Agmon I, Franceschi F, Yonath A. 2000. Structure of functionally activated small ribosomal subunit at 3.3 angstroms resolution. *Cell* **102**:615–623 DOI 10.2210/pdb1fka/pdb.

Schneider CA, Rasband WS, Eliceiri KW. 2012. NIH Image to ImageJ: 25 years of image analysis. *Nature Methods* **9(7)**:671–675 DOI 10.1038/nmeth.2089.

Šimečková K, Brožová E, Vohánka J, Pohludka M, Kostrouch Z, Krause MW, Rall JE, Kostrouchová M. 2007. Supplementary nuclear receptor NHR-60 is required for normal embryonic and early larval development of *Caenorhabditis elegans*. *Folia Biologica* **53**:85–96.

Simmer F, Moorman C, van der Linden AM, Kuijk E, van den Berghe PVE, Kamath RS, Fraser AG, Ahringer J, Plasterk RHA. 2003. Genome-wide RNAi of *C. elegans* using the hypersensitive rrf-3 strain reveals novel gene functions. *PLoS Biology* **1(1)**:e12 DOI 10.1371/journal.pbio.0000012.

Söding J, Biegert A, Lupas AN. 2005. The HHpred interactive server for protein homology detection and structure prediction. *Nucleic Acids Research* **33(Suppl_2)**:W244–W248 DOI 10.1093/nar/gki408.

Sönnichsen B, Koski LB, Walsh A, Marschall P, Neumann B, Brehm M, Alleaume AM, Artelt J, Bettencourt P, Cassin E, Hewitson M, Holz C, Khan M, Lazik S, Martin C, Nitzsche B, Ruer M, Stamford J, Winzi M, Heinkel R, Röder M, Finell J, Häntsch H, Jones SJ, Jones M, Piano F, Gunsalus KC, Oegema K, Gönczy P, Coulson A, Hyman AA, Echeverri CJ. 2005. Full-genome RNAi profiling of early embryogenesis in *Caenorhabditis elegans. Nature* **434(7032)**:462–469 DOI 10.1038/nature03353.

Taatjes DJ, Tjian R. 2004. Structure and function of CRSP/Med2; a promoter-selective transcriptional coactivator complex. *Molecular Cell* **14(5)**:675–683 DOI 10.1016/j.molcel.2004.05.014.

Tabara H, Sarkissian M, Kelly WG, Fleenor J, Grishok A, Timmons L, Fire A, Mello CC. 1999. The rde-1 gene, RNA interference, and transposon silencing in *C. elegans. Cell* **99(2)**:123–132 DOI 10.1016/s0092-8674(00)81644-x.

Thaw P, Sedelnikova SE, Muranova T, Wiese S, Ayora S, Alonso JC, Brinkman AB, Akerboom J, van der Oost J, Rafferty JB. 2006. Structural insight into gene transcriptional regulation and effector binding by the Lrp/AsnC family. *Nucleic Acids Research* **34(5)**:1439–1449 DOI 10.1093/nar/gkl009.

Thompson CM, Young RA. 1995. General requirement for RNA polymerase II holoenzymes in vivo. *Proceedings of the National Academy of Sciences of the United States of America* **92(10)**:4587–4590 DOI 10.1073/pnas.92.10.4587.

Timmons L, Court DL, Fire A. 2001. Ingestion of bacterially expressed dsRNAs can produce specific and potent genetic interference in *Caenorhabditis elegans. Gene* **263(1–2)**:103–112 DOI 10.1016/s0378-1119(00)00579-5.

Uhlén M, Fagerberg L, Hallstrom BM, Lindskog C, Oksvold P, Mardinoglu A, Sivertsson A, Kampf C, Sjöstedt E, Asplund A, Olsson I, Edlund K, Lundberg E, Navani S, Szigyarto CA, Odeberg J, Djureinovic D, Takanen JO, Hober S, Alm T, Edqvist P-H, Berling H, Tegel H, Mulder J, Rockberg J, Nilsson P, Schwenk JM, Hamsten M, von Feilitzen K, Forsberg M, Persson L, Johansson F, Zwahlen M, von Heijne G, Nielsen J, Pontén F. 2015. Tissue-based map of the human proteome. *Science* **347(6220)**:1260419 DOI 10.1126/science.1260419.

Uwamahoro N, Qu Y, Jelicic B, Lo TL, Beaurepaire C, Bantun F, Quenault T, Boag PR, Ramm G, Callaghan J, Beilharz TH, Nantel A, Peleg AY, Traven A. 2012. The functions of Mediator in *Candida albicans* support a role in shaping species-specific gene expression. *PLoS Genetics* **8(4)**:e1002613 DOI 10.1371/journal.pgen.1002613.

Vohanka J, Šimečková K, Machalová E, Behenský F, Krause MW, Kostrouch Z, Kostrouchová M. 2010. Diversification of fasting regulated transcription in a cluster of duplicated nuclear hormone receptors in *C. elegans. Gene Expression Patterns* **10(6)**:227–236 DOI 10.1016/j.gep.2010.05.001.

Wang W, Li X, Lee M, Jun S, Aziz KE, Feng L, Tran MK, Li N, McCrea PD, Park JI, Chen J. 2015. FOXKs promote Wnt/beta-catenin signaling by translocating DVL into the nucleus. *Developmental Cell* **32**:707–718 DOI 10.1016/j.devcel.2015.01.031.

Ward JD. 2015. Rapid and precise engineering of the *Caenorhabditis elegans* genome with lethal mutation co-conversion and inactivation of NHEJ repair. *Genetics* **199(2)**:363–377 DOI 10.1534/genetics.114.172361.

Warfield L, Tuttle LM, Pacheco D, Klevit RE, Hahn S. 2014. A sequence-specific transcription activator motif and powerful synthetic variants that bind Mediator using a fuzzy protein interface. *Proceedings of the National Academy of Sciences of the United States of America* **111(34)**:E3506–E3513 DOI 10.1073/pnas.1412088111.

Wiederhold T, Lee M-F, James M, Neujahr R, Smith N, Murthy A, Hartwig J, Gusella JF, Ramesh V. 2004. Magicin, a novel cytoskeletal protein associates with the NF2 tumor suppressor merlin and Grb2. *Oncogene* **23(54)**:8815–8825 DOI 10.1038/sj.onc.1208110.

Wimberly BT, Brodersen DE, Clemons WM Jr, Morgan-Warren RJ, Carter AP, Vonrhein C, Hartsch T, Ramakrishnan V. 2000. Structure of the 30S ribosomal subunit. *Nature* **407(6802)**:327–339 DOI 10.1038/35030006.

Zhu X, Chen L, Carlsten JOP, Liu Q, Yang J, Liu B, Gustafsson CM. 2015. Mediator tail subunits can form amyloid-like aggregates in vivo and affect stress response in yeast. *Nucleic Acids Research* **43(15)**:7306–7314 DOI 10.1093/nar/gkv629.

Zima V, Šebková K, Šimečková K, Dvořák T, Saudek V, Kostrouchová M. 2015. Prorenin receptor homologue VHA-20 is critical for intestinal pH regulation, ion and water management and larval development in *C. elegans*. *Folia Biologica* **61**:168–177.